The Application

of Aqueous Two Phase Systems

to the Analysis of Protein Isoforms of Importance

in Clinical Biochemistry and Biopharmaceutical Production

By

Rana Majeed Hameed

A thesis submitted in partial fulfilment for the degree of
Doctor of Philosophy

Advanced Bioprocessing Centre,

Institute of Environment Health and Societies

College of Engineering, Design and Physical Sciences

Brunel University London, UK.

December 2016

Dedication

الى أُمـي نـ بع الـحـنان

To My mother, the fountain of Love

الى أبـ ي شمـسي المُشرقة

To My father, the shining Sun

الى زوجي واولادي الـذي ن غمروذ يـ حـ بهم ومـساذدةّ هم

To My husband and my sons, who are so generous in their love and help

الى اخواتـ ي , ,اخواذ يـ والا صدقـاء ، الـذي ن دائـ ما شاركوذ يـ الـ سعاده

To My sisters, brothers and friends, for always sharing our happiness together

والـى بـ لدي الـ عراق ..❤

To Iraq, My Country

بـ كلـت وا ضـع اهـي لـهم هذا الـ جهد مع شـكري وإمـ ذـناذ ي

I am humbly dedicating my work to all of them with passion and gratitude.

Rana

Abstract

Aqueous Phase Partitioning has a long history of applications to the analytical characterisation of biomolecules. However process applications have attracted the most interest in biotechnology where it has become widely recognized as a cost-effective technique.

The main aim of this work was to explore the proposition that partition in Aqueous Two Phase Systems (ATPS) can be used as an analytical tool to detect protein isoforms and to assess the applicability of the method in clinical assays and for quality control in bioprocessing through examination of several analytical problems.

The work also examined the development of automated methods of system preparation and sampling techniques to determine the partition coefficient in ATPS. The study demonstrated that the geometrical form of the phase diagram co-existence curve was of crucial importance since this directly affected the accuracy with which systems of defined Tie Line Length and Mass Ratio could be constructed. The TLL %Bias (accuracy) of a theoretical system range in the PEG1000-$(NH_4)_2SO_4$ system at shorter TLL (12.2) was in the range +80.6% to -100% while at a longer TLL (53.1) the %Bias (accuracy) was reduced to +0.1% to -1.9%. At the same time the MR %Bias (accuracy) at shorter TLL (12.2) was in the range +59.5% to -21.3% while at the longer TLL (53.1) this was reduced to +2.7% to -2.6%. By contrast in the PEG8000-Dextran500 system the TLL %Bias (accuracy) at shorter TLL (13.1) was in the range +3.7% to -4.12%, while at a longer TLL (31.1) the range was +0.74% to -0.67%. The MR %Bias (accuracy) at the shorter TLL (13.1) was in the range +3.6% to -3% while at the longer TLL (31.1) the range was +1.1% to -1.4%. This illustrated that it is more difficult to work with a high degree of accuracy (e.g. %Bias <5%) close to the critical point in PEG-salt systems than in PEG-dextran systems.

Two different approaches were taken to examine analytical phase partitioning. In the first approach the structure of the isoforms of a model protein (ovalbumin) were altered enzymatically. Analytical methods involving Strong Anion-Exchange chromatography were developed and applied to the separation of the ovalbumin isoforms. Removal of the phosphorylated groups (dephosphorylation of ovalbumin) was undertaken using alkaline phosphatase and de-glycosylation was attempted using neuraminidase and Endo-glycosidase F. However, both enzymatic approaches to deglycosylation were unsuccessful. Dephosphorylated isoforms were successfully produced and

characterised. After partitioning in ATPS a clear difference was demonstrated between the behaviour of the native and dephosphorylated forms of ovalbumin. The mean % recovery in a PEG-salt ATPS was 99.8% (± 3.59) for the naive protein and 75.6% (± 4.03) for the dephosphorylated form. On the other hand, in a PEG3350-Dextran500 system, where solubility was maintained, a significant difference in the partition coefficient (K) of native and dephosphorylated ovalbumin was found. K for native ovalbumin was 0.85 while the partition coefficient of the dephosphorylated ovalbumin was 0.61. Analysis of covariance (ANCOVA) indicated that the regression coefficients of the respective partition isotherms were significantly different (p value < 0.05).

In a second approach to examine analytical phase partitioning, chemical modification of a specific target surface amino acid of another model protein (serum albumin) was used to determine the degree of conjugation of the protein and also to determine its oxidative state. The method examined the reactivity of a free surface thiol to a wide range of labels ((a) 2-methylsulfonyl-5-phenyl -1,3,4 oxidiazole reagent, (b) N-Ethylmaleimide (NEM) reagent, (c) 5, 5'-dithiobis (2-nitrobenzoate)(DTNB) (Ellman's reagent), (d) N-pyrenylmaleimide (NPM) reagent, (e) Fluorescein-5-maleimide (F-5-M) Reagent). Only DTNB was found to modify the surface free thiol of serum albumin in a highly specific and quantitative manner.

In the course of the development of a partitioning assay for surface free thiols of serum albumin significant oxidative properties were found to be associated with poly(ethylene glycol) PEG solutions and several attempts were made to find an oxidatively safe partitioning system by including antioxidants and by removal of contaminants by freeze drying. PEG3350-Dextran500 was found to provide an oxidatively safe environment for the development of a partitioning assay for the determination of albumin free thiols. A phase partitioning assay system capable of quantitatively resolving protein associated free thiols and low molecular weight thiols from a mixture of the two was developed. Correlation coefficients (R^2) for the regression of experimentally determined protein free thiols in the presence of different levels of added LMW free thiol on the known addition of protein ranged from 0.77 to 0.83. The results demonstrated that the assay could quantify and distinguish both types of thiol in a simple two-step procedure.

Table of Contents

Table of Figures

Table of Tables

Acknowledgments

Abbreviations

ACN	Acetonitrile
ALP	Alkaline phosphatase
ANCOVA	Analysis of covariance
ATP	Adenosine triphosphate
ATPE	Aqueous two phase extraction
ATPS	Aqueous two phase system
BCA assay	Bicinchoninic acid assay
BHT	Butylated hydroxytoluene
BSA	Bovine serum albumin
Cp	Critical point
Cv	Coefficient of variation
Cys.	Cysteine
DEA	Diethanolamine assay
DI water	Deionized water
DMF	Dimethylformamide
DMSO	Dimethyl sulfoxide
DTNB	5, 5'-dithiobis (2-nitrobenzoate)
DTT	Dithiothreitol
EDTA	(Ethylenedinitrilo) tetra acetic acid
ELISA	Enzyme-linked immunosorbent assay
Ellman's reagent	See DTNB
Endo-F1	Endoglycosidase F1

F3GA	Cibacron blue colour
F-5-M	Fluorescein-5-maleimide
IMAC	Immobilized metal affinity chromatography
IR	Infrared Spectroscopy
GSH	glutathione
K	Partition coefficient
kDa	Kilodalton
LHSP	Liquid handling sample processor
λ_{max}	Maximum absorbance
MBT	Methyl-benzene thiol
MeOH	Methanol
MPM-TBP	2,2'-methylene-bis(4-methyl-6-tert-butylphenol
MR	Mass ratio
mRNA	Messenger ribonucleic acid
MSPO	2-methylsulfonyl-5-phenyl -1,3,4 oxidiazole
Mw	Molecular weight
NEM	N-Ethylmaleimide
NMR	Nuclear magnetic resonance spectroscopy
NPM	N-(1-pyrenyl)maleimide
N-rHSA	Novozymes recombinant Albumin
Ova	Ovalbumin
pdb	Protein database

PEG	Polyethylene glycol
p-HSA	Purified human serum albumin
pI	Isoelectric point
PSA	Prostate specific antigen
PTM	Post- translation modification
Py	Pyrogallol
RFIC	Reagent free ion chromatography
rhGH	Human growth hormone
r-HSA	Recombinant human serum albumin
RP-HPLC	Reversed phase - High performance liquid chromatography
SAX-HPLC	Strong anion exchange HPLC
SD	Standard deviation
SDS-PAGE	Sodium dodecyl sulfate polyacrylamide gel electrophoresis
SEC	Size exclusion chromatography
SR	System range
STL	Slope of tie line
TFA	Trifluroacetic acid
TLL	Tie line length
TNB	2-nitro-5-thiobenzoic acid
Tris	Tris (Hydroxymethyl)aminomethane
WR	Working reagent

Chapter 1

1 Introduction and Literature Review

1.1 Post- translation Modifications of Proteins

Proteins are the most important biomolecules, playing an essential role in all biological processes. The genetic code, in the form of a sequence of nucleotides making up the chemical composition of DNA in any cell through a sequences of events termed transcription and translation is finally expressed as the amino acid sequence of proteins. Proteins are involved in all essential cellular processes as enzymes, structural components and so on. The encoded information in DNA is first transferred to RNA in the form of m-RNA (messenger RNA) in a process known as transcription by complementary base-pairing involving the enzyme RNA polymerase. Following transcription, the m-RNA is processed by ribosomes into the amino acid sequence comprising the protein backbone in a process known as translation. All proteins are made up of a sequence of amino acids linked together by peptide bonds. The unique sequence of the amino acid chain forms the primary structure of the protein. The unbranched polypeptide chains of amino acids are folded in a different patterns to form the secondary structure linked by hydrogen bonds between C=O and H-N as for instance in α-helical and β-sheet structures (1).

The protein three dimensional structures called (Tertiary structure) result from the folding of whole chains (secondary structure) into more compact structures driven by non-covalent interactions such as the burial of hydrophobic regions away from the aqueous environment (although membrane bound proteins differ in this respect) but also involving specific interactions such as salt bridges, hydrogen bonds and disulphide bonds. Quaternary Structures may be formed when the protein is made up of multiple polypeptide chains (which could be homo or heterodimer subunits) and/ or with an inorganic compound (such as a haem group). The life cycle of the proteins could be listed in Figure 1. Proteins have a diversity functions such as transport, storage and catalysis also it's have a multiple functional groups like thiols, amines, carboxyl and many others (1).
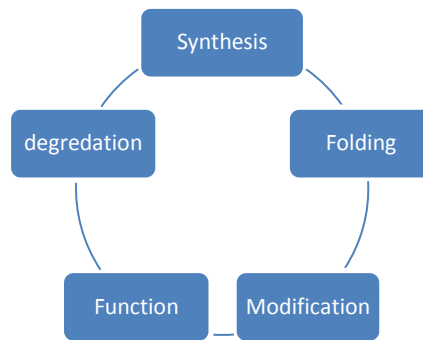
Figure 1- The synthesis cycle of the protein.

Post-translation Modifications of the basic protein structure outlined above can occur during and after the "synthesis cycle" of the protein, i.e. during and after translation; the synthesis of protein on the ribosome from the mRNA template. These modifications result in changes in the conformation of the final protein and in its structure, function and activity. Some proteins are modified shortly after translation, some are exposed to cleavage or addition of functional groups and other modifications occur during protein maturation, furthermore modifications may also arise during disease and during the manufacture of proteins, for instance in the manufacture of therapeutic proteins (1).

Post translational modifications of proteins are in general of two types involving either addition or cleavage of one or more groups at specific sites or links in the polypeptide chain. In addition, modifications may be reversible according to the nature of the modification such as in the catalytic activation or inactivation of the proteins e.g. phosphorylation or it could be irreversible such as in targeting for lysosomal destruction. Post translational modifications include N- and C-terminal modifications (acetylation, amidation and methylation) and modification of individual side chains (phosphorylation, glycosylation, carbonylation, hydroxylation, and nitration) (1)

Briefly, the importance of the former post translational modifications as biomarkers in disease can be summarized: acetylation is one of the most common modifications of proteins and involves the introduction of an acetyl group by modification of the lysine residue. Acetylation of histone proteins has a significant effect on the regulation of the transcription various factors and cellular metabolism. Acetylation normally occurs as N-terminal modifications and it has been linked to many cardiovascular and neurological diseases, while C-terminal modifications generally occur through amidation. Both acetylation and amidation have an impact on the overall charge of the peptide and

consequently on the solubility, stability and the biological activity of the proteins. Methylation of N-terminal amino groups is rare but it has a remarkable influence in some diseases such as in the inflammatory and immune system response (2).

In addition, modification by carbonylation and nitration has a tremendous impact on the formation of oxidative reactions and it's involved in many disorders for instance lung and cardiac diseases, cancer and neurodegenerative diseases. Similarly, hydroxylation also has a significant relevance to the cellular physiology properties. Modification of proline by hydroxylation has an important effect on the activation of antioxidant defense that responds to decreases in available oxygen in the cellular environment (2) .

In bioprocessing the PTMs have a vital role in biopharmaceutical manufacture, manufacture of drug therapies and additionally in drug response and in disease diagnostics where the PTM could be used as a disease biomarker (2). The common protein bioprocessing modifications include: proteins folding and aggregation. Protein folding is the most challenging in the production of therapeutic proteins. It results in accumulation of the protein or even folding to dimer, trimer or high molecular weight forms. Generally protein folding may occur during the overloading of processes. While the aggregation may result from reversible/irreversible reactions, hydrophobic interactions and the formation of covalent bonds between unpaired thiols. Another bioprocessing modification is the oxidation of some methionine residues which may be involved in loss of activity for instance oxidative damage in the case of α1-antitrypsin (which is used for the treatment of emphysema). In addition, the deamidation of asparagine residues is an isomerization modification which can result from long-term storage. This modification is involved in formation of iso-aspartate which has significant implications in reducing antibody reactivity and changing the activity of stem cell factors (3).

The existence of PTMs have wide ranging implications in many different sectors such as the development of cell based therapies, production of biotherapeutics, drug target proteins and for the optimization of the quality and efficacy of bioprocesses.

Significant post translational modifications include phosphorylation and glycosylation which play a crucial role in the regulation of protein activity, stability and function and may be strongly involved in biological processes and disease conditions (2).

Phosphorylation is one of the most common reversible protein modifications which have an important effect on the solubility of proteins and in the regulation of many cellular processes including cell cycle, growth and signal transduction pathways. The process of protein phosphorylation involves the donation of phosphate groups by ATP to specific amino acids having a hydroxylated side chain (serine, threonine or tyrosine). The process is controlled by a protein kinase while dephosphorylation (removal of the phosphate group) is mediated by a phosphatase.

Several methods have been used to assess the protein phosphorylation, according to the previous studies, acrylamide-pendant Phos-tagTM ligand has been successfully used for detection of phosphorylated proteins (4).

Another method for determination of the Phosphate Content of Phosphorylated Proteins is Reagent-Free Ion chromatography (RFIC). The method has been applied to the determination of phosphorylation of ovalbumin. (5)

A furthermore chromogenic method named GelCode has been used to analyse gel-separated proteins that are phosphorylated at serine and/or threonine residues. (6)

Other studies have been carried out to develop a fluoro-based phosphoprotein detection method for detecting phosphoproteins in poly-acrylamide gels. This is based on immobilized metal ion affinity chromatography (IMAC); it employs quercetin–aluminum (III)-appended complex as a fluoroprobe to selectively visualize phosphorylated proteins among total proteins. (7)

Glycosylation involves the modification of protein amino acid side chains by the addition of a Carbohydrates moiety. The effect of the glycosylation of proteins is considered to be one of the most significant modifications which are important in protein folding, conformation and stability (1). Glycosylation is of increasing significance in bioprocessing as the type and extent of glycosylation depends on the organism in which the protein is expressed during heterologous expression and the fidelity of glycosylation may be highly significant in determining efficacy and potency (8). On the other hand glycation although not strictly glycosylation involves the linkage of a reducing sugar residue to the amino side chains of the n-terminus and residues such as lysine and histidine. This modification mostly happens during hyperglycaemia in diabetes and results in various complications and the formation of less-functional biomolecules (9).

Glycosylation is classified according the amino acid to which the carbohydrate is attached. N-linked glycosylation refers to the attachment of the Carbohydrates moiety to the nitrogen atom of the imide group, usually the N- of an asparagine residue as shown in *Figure 2*. In bioprocessing if the glycosylation pattern does not match the human native glycosylation the therapeutic protein may be rejected by the immune system and fail to reach the target tissue or result in an undesirable immune response (8). N-linked glycosylation can be present as widely different structures resulting in several kinds of linkages for instance the N-Acetylneuraminic acid could be linked to either C3 or C6 of the galactose and produce a very different glycoprotein structure.

Other glycosylation classes are an O-linked glycosylation, which involves linkage to those amino acids containing a hydroxyl functional group that is linked to the additional carbohydrate, usually through the O- of the serine or threonine residue. Another form of glycosylation is C-linked glycosylation which refers to a different type of glycosylation since its represents the reaction of carbon-carbon bonds where the carbohydrate is usually linked to the C- of the indole ring of tryptophan.
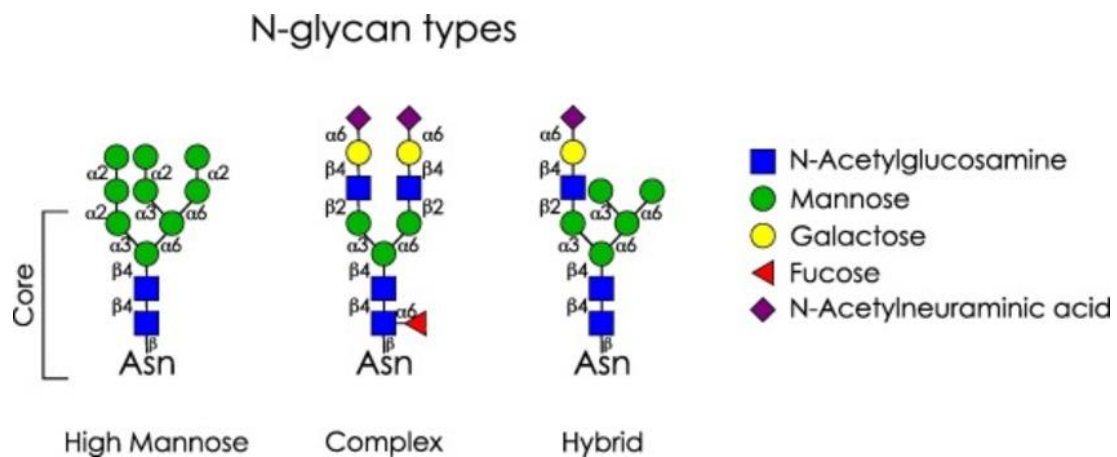
Figure 2- General types of N- glycan in mature glycoproteins (10).

Characterisation of glycosylation is very complex due to differences in the level of glycosylation for instance the variety in the number and type of glycan, the type of the glycosylation class and the site where the glycan is placed. In general analysis of protein glycosylation could be studied by different methods as summarized in *Figure 3*.
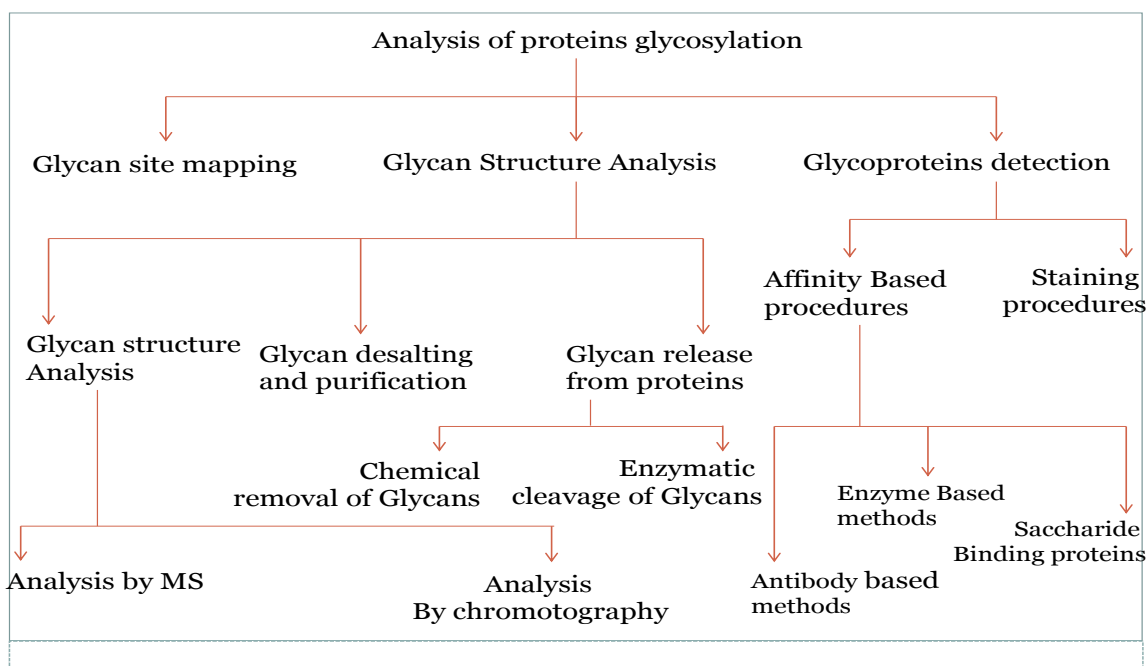
Figure 3 – Summary of methods for analysis of protein glycosylation (11).

Many methods are available to separate and detect protein structure relying on differences in their characteristic. These methods might maintain the native conformation of the protein or might not. However, there is no specific method which could be used to study the structure of all proteins.

The common methods employed in protein purification are concentrated salt solutions used in the salting-out of proteins, gel Electrophoresis is widely applied in the separation of proteins based on differences in charge and size, Adsorption chromatography is also a very important method to separate proteins base on their Polarity, Electrical Charge, Molecular Size or Binding Affinity, the separation could be performed using Specific Enzyme and Antibody Assays such as the ELISA system, furthermore Gene Sequences could be employed to determine the primary protein structure and the three-dimensional structures of proteins could be obtained by NMR spectroscopy, x-ray crystallography and cryoelectron microscopy (12).

It has been suggested that the difficult and complex task of characterising PTMs and bioprocess variants could be replaced by a simple assay involving partition in Aqueous two phase systems (ATPS). For some considerable time there has been continued interest in the application of ATPS in downstream purification of biomolecules (13). Partitioning in ATPS is generally deployed as a single-stage extraction process and has

been represented as a good alternative to the traditional methods involving solid phase adsorption steps in the separation, and purification of biomolecules (14).

Aqueous two phase systems have many distinctive features in comparison to traditional separations processes. The most important are the aqueous nature of both phases, few interactions with the substance to be separated and a non-denaturing environment allowing these biological substances to maintain their structure and functions (15).

Partitioning has frequently been employed as a large-scale separation, for analysis, and for the removal of contamination from chemical compounds, biological substance and biopolymers such as peptides, proteins, nucleic acid and the like with the advantage that it can rapidly effect an initial separation and purification procedure (15).

1.2   Introduction to Aqueous two phase systems

Aqueous two phase systems have been widely used as extraction and purification methods applied to the recovery of proteins and other biological macromolecules and particles (16). The first report of Aqueous two - phase systems (ATPS) was by the Dutch microbiologist Beijerinck, who observed the formation of two liquid phases when solutions of gelatine and starch were mixed together (17). Since the first discovery of these systems the field has developed widely and many studies have been performed in ATPS and in multiphasic systems. Albertson provided the first solid foundation for partitioning in ATPS and showed their potential for the separation of bio macromolecules, cells and organelles in a variety of ATPS including polymer/polymer and polymer salt systems (16).

ATPS are formed by aqueous mixtures of two or more polymers or of one polymer and a salt. Multi-phase systems can form when mixtures of more than two polymers are mixed together above defined concentrations (18).

When such components are mixed in water above certain concentrations two immiscible phases are formed. Separation of the phases into top and bottom phases depends on differences in the density of the polymer solutions and their viscosity, and this largely determines the time required to achieve complete phase separation (16).

Interactions between the substance to be analysed and the components of the ATPS create a highly efficient system for solute partitioning (16) (19).

The properties of the co-existing phases can be varied depending on the molecular weight, concentration and structure of the polymers. Additionally further chemical and physical factors may be varied through salt addition to control system charge and hydrophobicity. Differential partition of solutes having different phase preferences is based on their surface properties and the properties of the phase forming components. Partitioning in ATPS has been the subject of several books and review papers (20) (21) (22) (16) (23).

Walter (1977) also studied the factors which play an important role in affecting cell and particle partitioning. This early work showed the method to be well suited to the analytical and preparative separation of proteins (24).

1.3 Phase system composition

Phase separation in solutions containing a mixture of polymers is common, and phase separation has been attributed to the high molecular weight of the polymers combined with interactions occurring between segments of polymers; thus in high molecular weight polymers entropic contributions, which are dependent on the number of molecules, are small in comparison to enthalpic contributions which are dependent on the number of similar monomeric units. The separation system may also contain salts, which will have a significant effect on the behaviour of the system whose impact depends on both the type and concentration of salt (25).

Two types of aqueous two-phase systems are usually used:

1. Polymer-polymer two-phase systems

2. Polymer-salt two-phase systems

Polymer-polymer two-phase systems normally consist of Poly-ethylene-glycol (PEG) as one of the phase forming polymers in ATPS because it is widely and cheaply available and easily forms a two-phase system with other neutral polymers as well as salts. The other common polymer is Dextran which is a high molecular weight (MW) carbohydrate polymer consisting of alpha α-1,6 glycosidic linkages between glucose molecules, while branches begin from α-1,3 linkages.   The selection of ATPS depends on the nature of the biomolecule and preparatively on the relative cost of the different systems selected for the separation (25) (26). Salts can alter the physico-chemical properties of the systems through hydrophobicity differences between the upper and lower phases and

also by altering the distribution of ions between the phases, which consequently could affect the partitioning of analytes according to their molecular charge. Normally salt is added to increase the selectivity of protein partitioning in the aqueous two-phase methodology because it causes an uneven distribution in the system through the generation of a difference in electrical potential between the phases. The PEG/salt systems have mainly been used in large-scale enzyme extractions. (27) (28). PEG-salts systems have several advantages, including a greater difference in density between the phases, and a lower viscosity compared with PEG-dextran systems as well as a considerably lower cost.

The essence of partitioning relies on the equilibrium distribution of added solutes into different phases. The most important factors which can affect the distribution are the physical and chemical properties of the system (18).

Different ATPS have been found to be suitable and provide high partitioning sensitivity for the purification and extraction of different target biological materials. *Table 1* listed some examples of ATPS comprising both polymer/polymer and polymer/salt systems.

The composition of the phase system plays a crucial role in the partitioning process, because the wrong choice of phase composition could cause denaturation or aggregation of the partitioned substance. The goal of partitioning is to choose an appropriate phase system usually relatively close to the critical point to achieve the desired distribution and to be sensitive to the surface properties of the solute (35).

Numerous ways to manipulate the partition coefficient have been found including alteration to the molecular weight of one or both polymers and by the inclusion of various additives such as neutral salts (16) (36).

Table 1- Compositions of some of the early aqueous two phase systems

Phase –forming components	Reference
PEG/dextran	Albertsson 1986 (25)
PEG/phosphate	Albertsson1986 (25)
PEG/Ficoll	Albertsson1986 (25)
PEG/hydroxypropyl starch	Tjerneld et.al1986 (29)
PEG/polyvinyl alcohol	Tjerneld1986 (29)

Ethylhydroxyethylcellulose/ hydroxypropyl starch	Tjerneld1986 (29)
PEG/citrate	Vernau and Kule 1990 (30)
PEG/ hydroxypropyl starch	Tjerneld and Johansson 1985 (31)
PEG/maltodextrins	Sikdar et.al 1991 (32)
Hydroxyethylcellulose/polyethyleneimine	Dissing and Mattiasson 1994 (33)
Random copolymer of ethylene oxide-propylene oxide / hydroxypropyl starch	Planas et.al 1996 (34)

1.4   Phase diagram

Phase separation of polymer/polymer and polymer salt ATPS is characterised by the phase diagram in much the same way as conventional aqueous/organic systems used in conventional liquid-liquid extraction. The phase diagram defines the compositions at which the phase forming species separate into discrete phases.

In other words it is a map which indicates the phases present at a given temperature and composition. It is determined experimentally by recording and observing the cloud points over a range of compositions, the concentration of phase components in the top and bottom phases and the ratio of phase volumes necessary to form a system with two phases that are in equilibrium.

The phase diagram consists of a binodal curve which is constructed by determination of the compositions of top and bottom phases of a number of systems in which the polymer concentrations are varied (see *Figure 4*). The binodal of the system is influenced by the molecular weights of the polymers, the lower the molecular weight the higher are the concentrations required to form the two phases (16).

The binodal information is required to calculate the weight percent of each polymer in each phase and to define the models that predict partitioning of biomolecules. The binodal curve is determined by recording the weight of a series of systems prepared from stock solutions of known compositions and the critical points of these systems are

determined by the cloud point method. Finally, selected phase systems from within the biphasic region are constructed by selecting defined mixture compositions which are made up at convenient scale, mixed and allowed to settle. Upper and lower phase volumes are recorded and the density of the phases determined by pipetting numerous small samples of each phase and recording their weight. An empirical equation due to Merchuk (37) is often fitted to the binodal composition data by non-linear least squares regression to yield the parameters of an empirical equation delineating the binodal curve.

The composition of the individual phases generated can be obtained using tie-lines. The simplest way to find a phase system composition suitable for partition of the substance of interest is by making a number of systems which differ in polymer concentration, salt additive and pH (16).
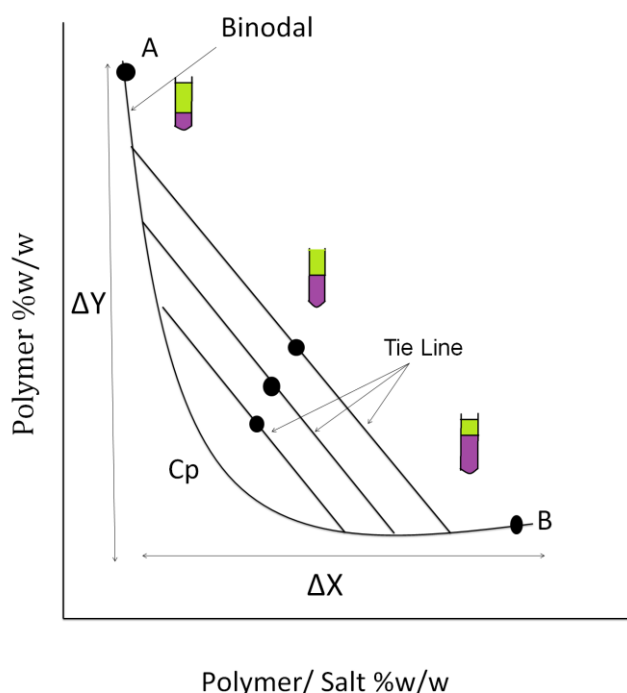
Figure 4- Binodal curve: A and B are ● Nodes which represent the final composition of the top and bottom phase, the points a1, a2 and a3 represent the total compositions of three systems lying on the same tie-line with different volume ratios. (Cp) The composition and volume of both phases are almost equal; Δx and Δy represent the difference in concentration of component X and Y between the two phases (19).

The tie-line length (TLL) is an important parameter allowing ordination of the partition coefficients of added solutes. The TLL reflects the solubility curve of the phase diagrams, and is proportional to the composition of the two phases that exist in

equilibrium with each other at this temperature. It also reflects the phase characteristics of a system and can be estimated by using the equation1:

$$\text{TLL} = \sqrt{\Delta X^2 + \Delta Y^2}$$ Equ. 1

Knowledge of the phase diagram enables specific systems to be made having selected values of TLL and volume ratio (16).

Phase composition is related to the polymers density difference between the phases and a linear dependence has been found. The density of the phase composition has a crucial impact on the settling rate by the gravitational force on the phase droplets, the friction between the drops and phase will be high, that leads to the separation time being longer (37). It is also the case that, whenever the TLL is increased, the difference between top and bottom composition become greater and the interfacial tension increases (38).

The critical point is found on the binodal where the TLL =0. Theoretically, at this point, phases have equal volume and composition and solutes are evenly distributed with a partition coefficient of one (19).

The properties of the phase systems are affected by many factors such as the temperature and the type of polymers used and their molecular weight. Very briefly, increasing the molecular weight of one polymer will tend to make the binodal more asymmetrical. The higher the molecular weight of the polymer, the lower concentration required for phase separation. On the other hand, the effect of the temperature depends on the type of the polymer and differs for different phase diagrams (16). Polymer-polymer systems represent a phase separation characterised by an upper critical solution temperature and polymer salt systems are in general characterised by a lower critical solution temperature.

The distribution of an analyte between the phases can be expressed in terms of the partition coefficient K which is to be calculated as a ratio of the analyte concentration in the upper and lower phases.

$$K = \frac{[\text{Analyte}]_{\text{Top}}}{[\text{Analyte}]_{\text{Bottom}}}$$

The partition of an analyte between the two aqueous phases depends on its physicochemical properties as well as those of the two polymers (16). The most important factors affecting protein partitioning in ATPS are analyte molecular weight, charge and surface properties while for the phase forming polymers these are the polymer molecular weight, phase composition, salt effects and affinity ligands attached to polymers, pH and temperature (16). To understand the mechanism of the aqueous two phase behaviour and the analyte partitioning, the fundamental theory of the system should be clarified. One force controlling the Phase Partition has been characterised as the free energy of transfer of the methylene group from the rich-salt lower phase to rich-PEG upper phase. This free energy represents just one contribution to the partition coefficient as the Hydrophobicity of the analyte surface Area.

Zaslavsky et.al (1981) has suggested a method to estimate the relative hydrophobicity of the analyte in ATPS by calculation of the free energy change (39). Based on the amino acids having different aliphatic side chains, the free energy was calculated using different partitioning systems

The free energy of transfer is dependent on the nature of the phase diagram and the relative composition of the phases (equation 2).

$$\Delta G = -RT \ln K \, (C - C_0) \qquad \text{Equ. 2}$$

Where ΔG is the free energy change, R is gas constant; T is absolute temperature, C-Concentration of system, C_0 –Concentration of critical point.

The proposed general relationship between the partition coefficient and methylene groups was considered in the equation 3

$$\ln K = C + E_{n \, (cH2)} \qquad \text{Equ. 3}$$

Where the K is the analyte partition coefficient, C is a constant related to the hydration properties of the phases, n is the number of carbons in chain and E is the slope of linear plot of ln K versus $n_{(CH2)}$ and the constant represents the contribution of polar group present in the partitioned analyte.

By the same principle, many relationships can be characterised from the calculation of the free energy change from simple thermodynamic relations (equation 4)

$$\Delta G^0 = -RT \ln K = \Delta H^0 - T\Delta S^0 \qquad \text{Equ. 4}$$

Where ln K is a rate constant or an equilibrium constant, R is the universal gas constant, ΔH is the Enthalpy; T is the temperature in Kelvin and ΔS is the entropy. Such processes can often be broken down into simple additive contributions.

The TLL relationship with free energy may be varied from zero at the critical point to increasing values as TLL increases. Generally the free energy is a small value for polymer-polymer systems but it is much larger for polymer salt systems and can be varied by altering the composition of the phases. Thus the chemical potential difference of the systems can be arranged to suit the surface potential of the added solute or particle. Since ΔG is a function characterising the phase behaviour and analyte partitioning, adjusting the phase composition by changing the phase components or increasing the TLL may result in achieving a desired separation.

Analytes in general are varied in the hydrophobicity which result in differences in the analyte- solvent interaction with the phase systems (40), these interactions could be described based by different properties of the analyte, and often can be broken down into simple additive contributions (equation 5).

$$\text{Some property} = \text{Cavity formation} + \text{ polarity terms} + \text{hydrogen bonding terms} + \text{constant} \quad \text{Equ. 5}$$

This equation represents a linear relationship to the free energy which is used widely in the several processes for instance partitioning in aqueous/organic systems and transport across biological membrane.

1.5   Analyte partitioning isotherm

The partition coefficient is defined as the ratio of the analyte concentration in the upper to its concentration in the lower phase. However the partition coefficient may be influenced by a number of factors which will result in concentration dependent behaviour. Analytes may associate or dissociate in a concentration dependent way or their solubility limits may be exceeded. This is analogous to the "overloaded condition" in analytical adsorption chromatography. In addition single determinations of the partition coefficient may be subject to a variable amount of error which may be minimised by multiple determinations of the distribution. However, this methodology does not reveal whether the partition isotherm is concentration dependent or subject to the effect of saturation or other non-idealities. Determination of the partition isotherm is a straight forward way of overcoming these problems or of revealing their existence. Ideally in attempting to make analytical measurements the isotherm should not be

concentration dependant. The method of determining the isotherm has been recommended in the ATPS literature but is very rarely applied. In almost all cases this method was adopted to determine the partition coefficient in the experimental parts of this work. The reliable method to measure the isotherm linearity is by using a range of concentrations of the solute and partitioning these separately in systems having identical compositions. The partition coefficient is then determined by the slope of a linear regression of the concentration in the upper phase against the concentration in the lower phase (23). Departures from linearity are then relatively easy to detect and indicate that there are problems in determining the partition coefficient which could lead to serious errors in any analytical application.

1.6   Advantages and limitations

Aqueous two-phase systems have received considerable attention in the development of biotechnological processes. Conventional techniques of purification and separation are often perceived to be inefficient, expensive and not fully scalable and this has led to a search for alternative process steps (41).

The application of ATPS that has attracted the most interest in biotechnology is its use in the isolation, extraction and purification of proteins and other biological materials such as enzymes/proteins, nucleic acids, viruses and cell organelles often from crude mixtures and homogenates. Suitably selected ATPS provide mild conditions which do not change or denature biomolecular structures. Partition and separation of added solutes occurs rapidly and the technique – as a form of liquid-liquid extraction is potentially fully scalable (22) (19).

However there still remain some drawbacks to the widespread application of ATPS (42). Mayolo-Deloisa (2011) reported that, there are two restrictions to limit the wide application of Aqueous Two-Phase Extraction (ATPE). Firstly, it is difficult to predict exactly the behaviour of target proteins in the ATPS system. Secondly, monitoring the characteristics of proteins is a basic requirement for assessment of bioprocesses, and many assay systems may be adversely affected by the presence of high concentrations of polymers or salts (43).

1.7   Factors determining by the partition coefficient

Any difference between the properties of the phases seems to convey the ability to discriminate between similar biomolecules. The analytical information which is provided

by partitioning process is completely related to the interactions between the phases and the solute and these interactions are known to be highly related to the solute structure, so the partition coefficient has emerged as a highly sensitive indicator of the characteristics of the solute.

In pathology many of the proteins, hormones, enzymes and peptides could be biological indicators or biomarkers of particular human diseases. This requires the analysis of protein compositions of samples from biological fluids or tissues by highly sensitive fractionation and analytical techniques. Many different approaches have been developed but some disadvantages exist such as the neglect of protein interactions and conformational change. Biphasic partitioning for a mixture could reflect the differences between components dependent on their structural and/or functional characteristics. Such differences could be used as a marker to determine the physiological condition of a biological system. Zaslavsky gives an example of the application of the partitioning method to what appears to be a complex situation. The method involved the partitioning of plasma from patients with post-traumatic stress disorder in comparison to similar samples from a control group. The results indicated a difference in the overall distribution of total plasma proteins between patient samples and healthy controls (44) (45) (46).

In another example, Apo-transferrin was used to prepare saturated solutions in the presence of a variety of ligands (Fe^{3+}, Cu^{2+}, Al^{3+}, Bi^{3+} and Ca^{2+}) which were then analysed in different aqueous two phase systems. Excess metal ions having been removed prior to partitioning using a centrifugal concentrator having a membrane characterised by a 3 KD molecular weight cut off. Protein concentrations were assayed by measuring the optical absorbance at 278nm by UV/VIS spectrophotometry. After that the partition coefficients for each solution were determined as the slope of the linear relationship for various dilutions of the transferrin samples representing the concentration in the upper phase versus the concentration in the lower phase.

The results were presented as a range of partition coefficients for the binding of different ligands. The conclusion of this example was stated to be that the partition coefficient determined following binding of the different ligands reflected the conformational state resulting from the binding of different ligands which provided a unique signature for each species (47) (48).

Another example of the application of ATPS partitioning as an analytical technique is provided by a method to determine the purity and homogeneity of recombinant human growth hormone (rhGH) again in a patent published by Zaslavsky et al (49). rhGH was characterised by measuring its relative distribution between the phases of an ATPS (the partition coefficient) and this was shown to be highly correlated with changes in the biological potency and purity of the product.

Further examples, also due to Zaslavsky, include the determination of the partition ratio of prostate specific antigen (PSA) as a biomarker for prostate cancer and the ratio of glycated haemoglobin to total haemoglobin as an indicator of diabetes status (50).

The k value may also represent an indicator for the purity of the solute similar to other physico-chemical characteristics such as melting point of a pure compound (51). Furthermore partitioning may provide quantitative information about changes in solute structure which is dependent upon the interaction between the solute and the co-existing phases (16) (52) (53).

The use of multiple systems to characterise partition has also been proposed – on the assumption that there are meaningful differences in K between different ATPS. This whilst more complicated than the use of a single K can statistically or graphically be used to produce a "signature" specific to a particular molecule (population of isoforms) which it is claimed can be used diagnostically in a technique termed solvent interaction analysis (15) .

On the other hand, the ratio of the amount of sub-populations of different molecules in a biphasic system can provide crucial information for medical diagnosis, quality control, pathology, toxicology, drug safety and other applications

Such biopolymers may differ by the number of certain isoforms such as phosphoforms and glycoforms. Many examples could be given of how the ratio of amounts of biomolecules or their sub-populations in a mixture could be considered clinically different from a reference sample. For example modified forms of transferrin have been proposed as a marker of long-term alcohol abuse (49).

In addition, Zaslavsky reported that classic fractionation techniques to separate or characterize biomolecules have neglected two important aspects. First generally, fractionation techniques cannot preserve protein-protein/ protein-ligand interactions and

are often unable to separate the mixture based on changes in conformation while ATPS may represent an advance in this field. The application of ATPS to quantify differences in the interactions of species using multiple biphasic systems has been claimed to enable identification of unique patterns of biomarkers for diagnostic applications (54).

Partition in ATPS can reflect the structural and functional characteristics of biomolecules through interactions with the co-existing phases. Often conformational changes in a biomolecule are associated with specific biological effects.

Such changes are often significant and may include changes to what other molecules may be bound by the biomolecule. Many biological processes are mediated by non-covalent interactions between a protein and another molecule, for instance in the interaction between cellular receptors and their binding partners. In some cases change in the binding partner can alter the function of the receptor, for example the effect of different estrogenic compounds on the estrogen receptor where the binding of different ligands results in conformational change and changed activity, so determination of ligand binding can also be used to determine the function of receptor. One example of this is the effect of different estrogenic compounds on the estrogen receptor. In this case, different compounds resulted in different, distinct conformational changes and these different changes result in different activity and/or function of the estrogen receptor (55).

1.8   *Detecting Protein Structural Modifications*

Since 1958, when Albertsson made his first publication on the partitioning of a set of proteins having different molecular weights (1.3×10^4 to 9×10^6) in an aqueous two phase system it has been followed by many studies attempting to understand the behaviour of proteins in these systems.

Albertsson (1960) began the development of a protein partitioning theory and outlines the basis of partitioning which may be summarized as some points: using low molecular weight of one polymer in the phase systems results in an increase in protein partitioning to the low molecular weight phase, dissociation of the protein may alter the partition of the protein. Partition is also strongly influenced by many factors such as the addition of salt where the partitioning changed dramatically with increasing concentration of salt from 1 to 5 M, polymer molecular weight, the pH and the net charge of the protein and

its concentration. In the following years, ATPs have become as an extremely attractive procedure to separate and purify biomolecules in large scale with maintaining the structure and has been a subject of several review papers (56) (57).

It has been claimed that partitioning can distinguish between protein isoforms so it can provide information about protein structural modifications. ATPS can reflect the differences between components dependent on their structure and the corresponding electrostatic interaction with the biphasic systems.

Structures of protein are usually associated with their function. X-Ray crystallography, NMR spectroscopy, Mass spectrometry (MS) are common methods used for determining structure. In addition, analytical techniques such as ELISA, whilst specific for particular species can only give quantitative information and information on structure is minimal or absent because the signal in ELISA is the sum of signals arising from all isoforms. Partition, determined by specific assay such as ELISA, however can give access to structural information since the partition coefficient contains information on the differential partition of the isoform population (15).

Partition in ATPS could be used as an index to provide information on the structural forms of proteins through the partition coefficient; this technique is based on differences in the interactions of proteins with the two phases mediated by differences in their properties. Differences in the nature of the two aqueous phases result in differences in distributions, enabling the detection of any changes in structure. Thus the partition coefficient might represent a sensitive detection method for changes in structure and conformation (58).

When combined with a suitable specific detection method partitioning can distinguish between protein isoforms and thus provide information about structural modifications. This method consists of two obvious steps (1) partitioning of the protein in a suitable biphasic systems, (2) Examination of protein concentration in the aqueous phases by a protein specific method (15).

Thus the technique can be used for classification and detection of changes to the structure of interest. This may represent a useful tool in various fields of biochemistry, molecular biology, cell biology and especially in the field of bio-technology and this represents the main goal in this work.

It has been clearly demonstrated that in a molecularly simple system the mixture composition of two different species can be determined from the measurement of the partition coefficient alone. Consider for example two species A & B having partition coefficients of 10 and 2 respectively. In a mixture comprising only A the partition coefficient will be determined as 10 and in a mixture comprising only B the partition coefficient will be determined as 2. Values intermediate between these two will be determined for all mixture compositions intermediate between these extremes. The resulting curve depends on the relative difference between the partition coefficients and the coefficient of determination of the assay. See Figure 5 where two proteins A & B are present in mixtures ranging from 100% B and 0% A to 100% and 0% B. In one plot of the overall partition coefficient the proteins are assumed to have the same coefficient of determination and in the other protein B is assumed to be determined with half the sensitivity of protein A.

For mixtures comprising many species the situation is much more complicated but the principle that differences in mixture composition can be determined by the partition coefficient seems the same. A detailed mathematical proof is given in analytical biochemistry (59).
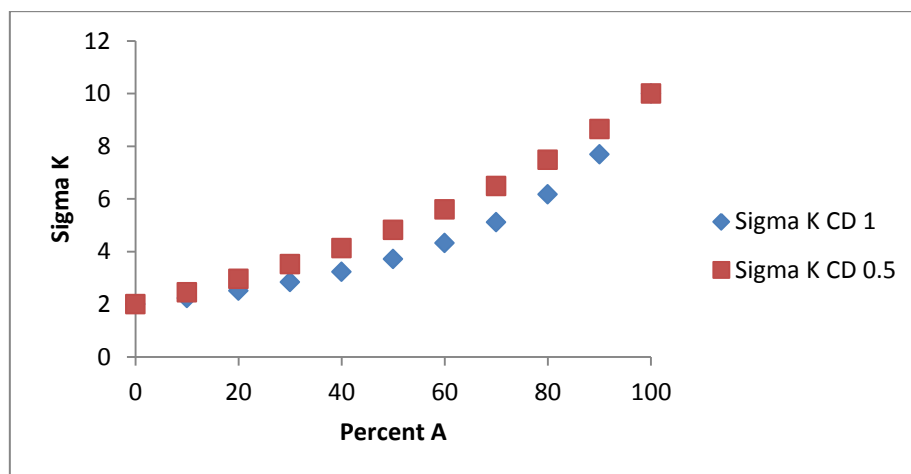
Figure 5- Total partition coefficient vs mixture composition for a hypothetical mixture of two proteins A & B having individual partition coefficient of 10 & 2. Red square, proteins have equal coefficient of determination and blue square coefficient of determination of B is half that of A.

Partitioning can distinguish between protein isoforms and combined with a specific detection assay seems capable of providing information about protein structural modifications since the partition coefficient represents the ratio of two different proteins such as the possibility of detecting the ratio of the carbohydrate deficient transferrin

(CDT) isoform from the total amount of the transferrin in a mixture. The separation of two sample populations depends on the difference in their K values and their relative abundance means the possibility of detecting the interactions of two isoforms. That will lead to the ability to quantify the amount of different isoforms in the mixture without initial separation (59).

On the other hand, determination of the concentration of the analyte from their distribution in the phases represents an analytical signal for that particular compound since it is related to the interaction with the phase components. The interactions between two different macromolecules or macromolecule and a particle can be applied to study the quantitation (60).

1.9   Highlighting the knowledge gap in the ATPS

Since their first discovery and development, ATPS have been used as a very powerful technique for the purification and separation of many biomolecules. On the other hand, there is increased demand for new, more rapid and more accurate bio-analytical techniques which can be exploited for studying the posttranslational modifications that may arise during the pathology of various disease conditions and to monitor product quality during biopharmaceutical production processes. Using ATPS as a Biotechnological method to achieve this goal may represent an attractive approach to this problem; however in ATPS the behaviour of the biomolecules is highly variable and many factors are involved in the partitioning process. This makes the prediction of the K values very complex, also studies of the partitioning of a modified protein using a protein model has rarely been undertaken. Finally the effect of the protein modification process and the properties of the ATPS used in terms of examination of analytical problems could result in new and interesting applications. This study was conceived of as taking two approaches to the examination of the problem of whether ATPS can usefully distinguish between different forms of a protein. One approach would consist in careful removal of parts of the post translational modifications of a model protein and to examine whether the system can distinguish between these native and non-native forms. The other approach would be to specifically modify the surface of a protein by targeting a particular residue with a chemical covalently linked modification.

1.10 Ovalbumin and Albumin as models for protein partitioning in the ATPS

Ovalbumin is a protein found in egg white, making up 60-65% of the total protein. Ovalbumin displays sequence and three-dimensional homology to the serpin superfamily of protease inhibitors. The function of ovalbumin is unknown, but it is believed to be a storage protein. (61). Table 2 summarised some literature review and molecular biological properties of ovalbumin.

Ovalbumin has importance in a number of research areas, particularly in studies of protein structure and properties, biochemical studies and in immunology experiments. Ovalbumin is a glycoprotein which has a variety of structures that vary in the degree and nature of their glycosylation and phosphorylation. For this reason, it has been chosen to outline the influence on partitioning of these isoforms. Since partitioning is sensitive to charge, hydrophobicity and size thus the study will focus on an examination of how these structural variations affect the partition coefficient. The effect of these structural modifications on the partition of various isoforms will be studied (62).

Table 2- Ovalbumin literature review and Molecular Biological Properties

Ovalbumin (OA)	References
Molecular Mass Mr 44.0-45.0 kDa 6 and 4 isoforms by mass spectrometry	(63)Kelly et al.1996 (64)Chakel et al.1997
Isoelectric Point pI 4.6	(65)Holen & Elsayed 1990
Amino Acid Sequence Amino acids 385 residues	(66)Nisbet et al. 1981
Physical and chemical properties	(67)Melvin S. Weintraub et.al.1970
Posttranslational Modifications*Acetylation: N-terminal acetylation Disulfide Bridges: disulfide bond: 73-120 , free Cys residues*Glycosylation of OA: -The carbohydrate of ovalbumin -Comparative study of chicken ovalbumin subfractions by high performance anion exchange chromatography. -carbohydrate composition by capillary gas chromatography/mass spectrometry -1 N-glycosylation site: Asn-292 -hydrazinolysis of sialyl-oligosaccharides and sialydase digestion -isolation and mass spectrometry of OA-glycans -purified glycopeptides characterized by sequential exoglycosidase digestion N-Acetylneuraminic acid were detected colorimetrically by periodate oxidation and reaction of the product with 2-thiobarbituric acid -study of N-linked Oligosaccharides from Ovalbumin	(68)Patrick C. Elwood, et.al.1988 (69)Henderson et al. 1981 (66)Nisbet et al. 1981 (70)Yamashita et al. 1984 (71) Chen et al. 1988 (72) Rago et al. 1992 (73) Ekman & Jäger 1993 (74) Suzuki et al. 1997 (75)Wei et al. 1998 (76)Steven M. Chamow, et.al.1988

- Simple fluorimetric method Refers to OA as having nonsialylated N-glycans(OA having nonsialylated N-glycans) - there are no N-Acetylneuraminic acid in OA *Phosphorylation of OA: -2 phosphorylation sites: Ser-68, Ser-344 -posphate content: 1.73 mol/mol OA -separation by capillary isoelectric focussing and mass spectrometry of mono- and diphospho-OA	(77)Yuan Chuan Lee et.al. 1961 (78)Hitoo Iwase et.al.1984 (79)Yukinobu Kato, et.al.1988 (80)Lattova et al (2004) (81) Matsuno and Suzuki (2008) (82)Yamamoto et al (2011) (83) Kanae Matsuno (2008)
Biological Function function unknown, OA belongs to serpin family of protease inhibitors active site: 352-353	(84) Burley & Vadehra (1989)

Serum albumin selected as another model, is a protein produced by the liver and characterized by a molecular mass of 66.5 kDa. It has 35 cysteines of which 34 participate in structure forming disulphide bonds leaving one as a surface free thiol and makes up about 60% of the total serum protein (85). Serum albumin is a multi-functional protein having biotechnological functions including: use as important nutrients in cell culture to cells (86), serum albumin is also used in drug delivery to transport pharmaceutical drugs like antibiotics and anti-inflammatories (87) and bioactive gas such as nitric oxide (NO) for treating ischemic/reperfusion injury (88). Albumin is also used as an excipient in pharmaceuticals due to its ability to stabilize other proteins in solution. in addition, it has a physiological functions including as a carrier for several hormones, fatty acids, trace element and many others molecules by non-specifically binding (89) (90).

Thiol groups have much importance in the modification of proteins and illustrated in many reactions especially when chemically modified by optical tags (91), affecting certain catalytic subunits relying on receptor/ligand interaction (92), and these roles of thiol can be used to covalently link and target therapeutic proteins.

Nowadays the most desirable way for creating a conjugated protein without altering the physicochemical properties is a site-specific method which is considered as an alternative method to create a covalent bond which is less likely to make any changes in the secondary or tertiary structure of proteins instead of amide bond plus the number of different species created can be controlled.

One of the most significant current discussions in biomolecules modifications is the covalent addition of a carbohydrate or polymers which could increase the thermodynamic stability of proteins (93) and recent developments have heightened the importance of this type of linkage to prevent denaturation of proteins and other functional molecules such as drug carriers by limiting conformational freedom (94).

Researchers have shown an increased interest in using HSA as a candidate to examine the albumin conjugate process with a number of chemical linker and their effect on for instance the solubilisation and cytotoxic activity of hydrophobic drugs (95), the examination of the binding affinity sites of albumin to a wide range of drugs (96). Different commercial Albumin with different chemical thiol labels could be used to examine an analytical problem by phase partitioning, including the determination of the

degree of conjugation of protein drug conjugates using appropriate model systems and determination of the oxidative state of human serum albumin utilising the reactivity of a surface free thiol group. Oxidative stress is clearly associated with a wide range of chronic and acute disease processes for instance heart disease, cancer, neuro-degenerative and many others (97). About 70 % of the serum antioxidant capacity accounts by the sulfhydryl group (thiol) of cysteine 34 in Albumin. Approximately two-thirds of serum albumin contains the thiol group of Cys-34 in the reduced form, which correspond to about 80 % of all serum thiol groups also corresponds to more than 50 % of all serum proteins (98). The approach will focus on the investigation of the reactivity of the labels towards the free thiol to prepare a stable and thiol specific conjugate which could be used as a probe for the determination of surface free thiols. Also examination of the analytical separation of a native and derivative albumin by ATPS will be dependent on the discovery of systems and derivatives which give optimum differences in their partition coefficients.

The argument has been made by Zaslavsky by analogy with simple protein mixtures that partition can be used to provide information on the isoforms present in a pure protein or a protein detected by a specific method. For two analytes with different partition coefficients measured by a single analytical technique (e.g. ELISA, A280 etc.) the partition coefficient will be a function of the mixture composition. The implication is that the K value for any protein which can exist in multiple forms is dependent on the overall ratio of those forms provided that the phase system (as distinct from the assay which must be specific for all of them) is able to distinguish between these isoforms. The aim of this thesis is to show that the production of differently modified proteins (isoforms) can be used to demonstrate that the method is feasible. The aim of the current study was to broadly explore this proposition and to determine whether partition in ATPS could be applied to analytical problems such as might be encountered in bioprocess quality control or in clinical studies of disease biomarkers for example.

Objectives and aims: The ability of ATPS to distinguish between the normal and disease conditions by determining the partition of protein isoforms has been little explored and what has been done is in the main restricted to workers associated with a single company. Thus exploration of aqueous phase systems in the context of the partitioning of PTMs and bioprocess variants represents a useful exercise

The project was looking for a strategy permitting a reproducible test to examine the separation conditions following two approach of the modification which were subtraction group and addition group or chemical labels and use it as an economical way to distinguish any conformational forms could be apply in any simple lab.

The economic benefits of the substance (ovalbumin) and method (HPLC) were selected as a convenient and economic approach. Ovalbumin has three sites of post synthetic modification in addition to the heterogeneous N-terminal acetyl group. One of the advantages of using it as a protein model is that the isoforms of this monomeric protein may easily be separated and thus the partition coefficient of each form can be accessed. Further information regarding the effect of the various post-translational medications may be made accessible by enzymatically removing some or all of these modifications. The study was gone some way towards enhancing our understanding of the properties of the PEG polymer used in ATPS to partition Albumin with a number of chemical labels

Understanding an aspect of the applications of Aqueous Two Phase Systems to the analysis of protein Isoforms and the importance in clinical Biochemistry and Biopharmaceutical production will increase the applicability in the characterizations of clinical samples (e.g. the detection of disease biomarkers) or product samples arising during biopharmaceutical manufacture (e.g. the detection of process derived variants).

Chapter 2

2   Materials and Methods

In this chapter materials and instruments have been described for a whole thesis; whereas methods have been described separately for each chapter.

2.1   Materials

The materials used in all chapters were: Polyethylene glycol (Lot 1356267) Mw=8000 (PEG 8000)(Lot SLBC9317V), Dextran 500 from Leuconostoc mesenteroides (Lot BCBJ7122V) weight-average molecular weight (Mw) 450,000-650,000, Ovalbumin from lyophilized powder, >98% (Lot SLBD2312V), Neuraminidase from Clostridium perfringens (C. welchii) type V from lyophilized powder 0.32 mg solid 7.9U/mg (N2876-2.5UN Lot SLBF5907V), Alkaline phosphatase (ALP) from bovine intestinal mucosa-BioUltra in buffered aqueous glycerol solution 2000-4000 DEA U/mg protein (DEA stands for Diethanolamine assay), Unit Definition is that one DEA unit will hydrolyze 1 µmole of 4-nitrophenyl phosphate per minute at pH 9.8 at 37 °C. Lot SLBF3716V, Cibacron Blue 3G-A (product No.C9534-25G), Polyethylene glycol Mw=600 (PEG 600) (Lot STBC5291V), Polyethylene glycol Mw=1000 (PEG 1000) (Lot A0319044), Polyethylene glycol Mw=4600 (PEG 4600) (Lot: 06621PH-418), Polyethylene glycol BioXtra powder Mw=3350 (PEG 3350) (Lot: SLBM1600V), Ammonium sulphate $(NH4)_2SO_4$, Sodium sulphate Na_2SO_4, Endoglycosidase F1 from Elizabethkingia miricola; recombinant, expressed in E.coli, ≥16U/mg buffered aqueous solution (Lot SLBK8022V), 2-(Methylsulfonyl)-5-phenyl-1, 3,4-oxadiazole (product No. L511757-50MG), Purified- Human serum albumin (p-HSA) (purified from lyophilized powder, ≥96% Lot# SLBG2676V) (Prod No. A1653-1G), Fluorescein-5-maleimide (F-5-M) $C_{24}H_{13}NO$ Mw. 427.4, Recombinant albumin human (rHSA) (expressed in Pichia pastoris, lyophilized powder, ≥90%) Lot# SLBM3404V (Prod No. A7736-1G), N-Ethylmaleimide (NEM) (Prod No. 389412-5G), Methylbenzenethiol (MBT) C_7H_8S Mw.124.2 g/mole ≥98% product No.T28525,

Dimethylformamide (DMF) $(CH_3)_2NC(O)H$ Mw. 73.09 g/mole product No.227056, Sodium borohydride $NaBH_4$ Mw. 37.83 product No. 71320, (Ethylenedinitrilo) tetra acetic acid (EDTA) Mw.292.24 Lot: SLBD0122V,Sodium metabisulphite $(Na_2O_5S_2)$, Ellman's reagent product No. D218200-1G Lot: STBD3094V, N-(1-Pyrenyl)maleimide(NPM) $C_{20}H_{11}NO_2$ product No.P7908 Fw. 297.31 g/mole Lot:

BGBB9393V, Butylated hydroxytoluenem [(BHT) $(CH_3)_3C]_2C_6H_2(CH_3)OH$ Mw. 220.35 product No.W218405 Lot:MKBV6032V, L-Ascorbic Acid Molecular Weight 176.12 g/mol product No. A0278-25G, purchased from Sigma-Aldrich (Dorset, UK).

Di-potassium hydrogen orthophosphate K_2HPO_4 Mw.174.18 (Lot: 1226885), Potassium di-hydrogen orthophosphate KH_2PO_4 Mw.136.09 (Lot: 1159924), Tris (Hydroxyethyl) amino methane (Tris) $C_4H_{11}NO_3$ Mw. 121.14 (Lot: 117137), Hydrochloric Acid (HCl) D=1.16 (32%) (CAS No.7647-01-0), potassium hydroxide(KOH) Mw.56.11 Lot: 1339716, Sodium Chloride NaCl Mw.58.44 (Lot: 1341160), Dextran average Mw. 500,000 (Lot: 126401), BCA protein assay kit (PRODUCT No.23227, Lot PH207175), Acetonitrile C_2H_3N Mw.41.04g/mole (HPLC grade), Trifluroacetic acid C_2HF_3 Batch 1001007 CAS 76-05-1, Dimethyl sulfoxide (DMSO) C_2H_6OS analytical reagent grade Mw.78.13g/mole Lot: 1414511 purchased from Thermo Fisher Scientific Leicester, Uk Novozymes recombinant Albumin (N-rHSA) batch No. PDP 130102 (recombinant Saccharomyces cerevisiae fermentation) was gifted from Abumedix Ltd.

2.2 Chapter 3 – Analytical method development for the partitioning of Ovalbumin in ATPS

2.2.1 Basic Column Operating Conditions for strong anion-exchange chromatography

Analytical HPLC was performed using a strong anion-exchange (SAX) column to separate ovalbumin isoforms on the basis of accessible surface charges and their corresponding electrostatic interaction with the column's stationary phase. A flow rate of 0.5 mL/min was used with a 100µL injection volume. Samples were eluted using a linear gradient.

Equilibration buffer: 20 mM Tris (pH 8.5) was prepared by weighing 6.05 g of Tris dissolved in 250 mL of 18.2 MΩ-cm deionized water. The pH was adjusted to 8.5 using concentrated (32%) hydrochloric acid. The buffer concentration was adjusted to 20mM using DI water and filtered through a 0.45 µm filter Lot: G9976559 (GE Healthcare, Germany) in order to prevent column fouling from any particulate material present.

Equilibration buffer: 20 mM phosphate buffer (pH 8.5) was prepared by weighing 17.41 g of di-potassium hydrogen orthophosphate dissolved in 500 mL of 18.2 MΩ-cm DI

water. The pH was adjusted to 8.5 using the same concentration of potassium di-hydrogen phosphate buffer and the solution was filtered through a 0.45 µm filter.

Tris elution buffer: 20 mM Tris, 500 mM Sodium Chloride (pH 8.5) was prepared by weighing 6.05 g of Tris and 14.6 g of sodium chloride into 500 mL of 18.2 MΩ-cm DI water. The pH was adjusted to 8.5 using concentrated (32%) hydrochloric acid and the solution was filtered through a 0.45 µm filter.

Phosphate Elution buffer: 20 mM phosphate buffer containing 500 mM Sodium Chloride (pH 8.5) was prepared by mixing 0.02 M (500ml) phosphate buffer (pH 8.5) with 14.6 g Sodium Chloride. Preparation of 1 mg/mL Ovalbumin Standard: 10 mg ovalbumin was dissolved into 10 mL 20 mM phosphate buffer (pH 8.5), the solution was filtered through a 0.45 µm filter to remove particulates.

Column wash solution: 1M Sodium Chloride was prepared by dissolving 29.22 g of sodium chloride in 500 mL of 18.2 MΩ-cm DI water. The pH was adjusted to 8.5 using concentrated (32%) hydrochloric acid and filtered through a 0.45 µm filter.

Operating Conditions: Strong anion-exchange (SAX) Column SOURCE 15Q 4.6/100 PE (code 17-5181-01, lot 10178855, ID 0008 GE Healthcare Life Sciences), flow rate: 0.5 mL/min. Temperature: 25 °C. Injection Volume: 100 µL. Detection: UV, 230 & 280 nm.

Eluents and Gradient Programs: for Tris running buffers: In this experiment Tris solution was run without any ovalbumin as a blank to monitor a baseline signal and the following gradient programmes outlined in Table 3 were used. Briefly the column was equilibrated for 2 minutes following sample injection using eluent A: 20 mM Tris buffer (pH 8.5). B: 20 mM Tris buffer, 500 mM Sodium Chloride (pH 8.5). And finally the column was washed using 1 M Sodium chloride (pH 8.5).

When phosphate buffer was used the gradient programme was adjusted as shown in Table 4 using the following solutions as eluent: A: 20 mM phosphate buffer (pH 8.5), B: 20 mM phosphate buffer, 1 M Sodium chloride (pH 8), C: 1M Sodium chloride (55 min Phosphate buffer gradient 0% NaCl pH 8.5).

Table 3- Conditions of SAX-HPLC of ovalbumin showing the time course and mobile phase composition for equilibration and elution steps when using Tris as running buffer.

Gradient started at 1% NaCl		
Time (min)	Solvent A (%)	Solvent B (%)
2.0	100	0
5.0	99	1
20.0	75	25
35.0	50	50
35.1	0	100

Gradient started at 5% NaCl		
Time (min)	Solvent A (%)	Solvent B (%)
2.0	100	0
5.0	95	5
20.0	70	30
35.0	50	50
35.1	0	100

Gradient started at 10% NaCl		
Time (min)	Solvent A (%)	Solvent B (%)
2.0	100	0
5.0	90	10
20.0	65	35
35.0	50	50
35.1	0	100

Table 4- Conditions of SAX-HPLC of ovalbumin showing the time course and mobile phase composition for equilibration, elution and wash steps when using phosphate as running buffer. The final column labelled "Curve" refers to the type of transition delivered by the gradient controller between chromatographic steps: curve 6 refers to a linear transition in composition usually used with binding and elution buffer, and curve 11 refers to an instantaneous increase or decrease in composition at the start of the time period.

Time (min)	Flow rate (mL/min)	Solvent A (%)	Solvent B (%)	Solvent C (%)	Curve
0.01	0.5	100.0	0.0	0.0	6
2.0	0.5	100.0	0.0	0.0	6
5.0	0.5	99.0	1.0	0.0	6
35.0	0.5	50.0	50.0	0.0	6
35.1	0.5	0.0	100.0	0.0	11
38.0	0.5	0.0	0.0	100.0	11
43.0	0.5	100.0	0.00	0.0	6
48.0	0.5	100.0	0.00	0.0	11
100	0.5	100.0	0.0	0.0	11

2.2.2 Method to Optimize the Resolution by Adjustment of Salt Gradient Profile

The gradient was changed in such a manner to study the effect of ionic strength; changing gradient percent is the most common way to improve selectivity and efficiency. Once a stable baseline had been obtained, increase in the concentration of gradient by 2% was performed, use a linear gradient from 0 to 10% buffer B over 35 min to elute the sample.

Table 5 shows the changes which were made to the concentration of the gradient using phosphate buffer.

Table 5- HPLC gradient programme flow and the compositions of mobile phase used to manipulate the resolution.

Phosphate gradient		
Time (min)	Solvent A (%)	Solvent B (%)
0.0	100.0	0.0
2.0	100.0	0.0
5.0	Start gradient compositions	
35.	Final gradient compositions	
35.1	0.0	100.0

Run No.	Start gradient compositions		Final gradient compositions	
	Solvent A (%)	Solvent B (%)	Solvent A (%)	Solvent B (%)
1	99.0	1.0	49.0	51.0
2	98.0	2.0	48.0	52.0
3	96.0	4.0	46.0	54.0
4	94.0	6.0	46.0	56.0
5	92.0	8.0	42.0	58.0
6	90.0	10.0	40.0	60.0

2.2.3 Method to Prepare Phase Diagrams

(A) Experimental technique: Turbidimetric titration was used to determine the form of the binodal curve which marks the lowest concentration of the components at which phase separation occurs. The procedure is briefly as follows. First an appropriate amount of PEG stock solution was placed in a test tube, weighed and recorded. Then Dextran was added drop wise with mixing until the cloud point was reached which was determined visually. The weight of Dextran added was determined and recorded. Then an arbitrary amount of buffer was added by weight and the weight recorded to move the system into the monophasic region of the bimodal removing the turbidity. The procedure was repeated to obtain a series of compositions denoting the location of the binodal curve as far as the inflexion point of the binodal. The same procedure was repeated from the Dextran side of the binodal by titrating Dextran stock solution with PEG.

The binodal information is required to calculate the weight percent of each polymer in each phase and to allow fitting of the tie lines and enabling the construction of systems of defined tie line length and volume ratio.

Following construction of the bimodal, selected phase systems from within the biphasic region were constructed by selecting defined mixture compositions which were made up at convenient scale, mixed and allowed to settle, then upper and lower phase volumes were recorded and the density of the phases was determined by pipetting numerous small samples of each phase and recording their weight. An empirical equation (Equ 6) due to Merchuk et al., (99) was fitted to the binodal composition data by non-linear least squares regression using Sigma plot version (12.5) to calculate the binodal curve.

$$Y_A = a \cdot \exp\left(bX_A^{0.5} - cX_A^{3}\right) \qquad \text{Equ. 6}$$

Y_A and X_A refer to the components plotted on the y & x axes e.g., PEG and Dextran. The equation is purely empirical – it appears to have no physical or chemical meaning,

Tie lines on the binodal curve connect coexisting equilibrium phases and denote the composition of these phases at the nodes; the lever rule was used to determine weight percentages of each phase of a binary equilibrium phase diagram and to find how much of each phase exists at the given temperature. The ratio of the two phases present can be found by using the lever rule.

Using the volume and density data relating to the phases of the selected systems a mass balance can be constructed such that, the sum of the mass of PEG and Dextran at each node equals the mass of PEG and Dextran at any point on the tie line. Using this relationship and the equation of the binodal a system of simultaneous equations can be established which lead by the application of numerical methods to the composition of the phase system at the nodes. These relations were determined using Mathcad version 15 (100).

In details, the experimental system compositions (% w/w of PEG and Dextran) were used along with the constants (a, b, c) of Merchuck equation to calculate the compositions of PEG and Dextran in each phase and also to calculate the TLL at the mass ratio one.

First of all, the mass of each phase was calculated from density and volume followed by calculation of the mass ratio in terms of the mass of the top divided by the total mass using equation

$$a = \frac{mt}{mt+mb} \qquad \text{Equ. 7}$$

Where mt is the mass of the top phase and mb is the mass of the bottom phase, and then using the following equations Equ. 8, 9 will result in calculation of the composition in each phase when set up as simultaneous equations.

$$\frac{Ym}{a} - \left[\frac{(1-a)}{a}\right] yb = yt \qquad \text{Equ. 8}$$

$$\frac{Xm}{a} - \left[\frac{(1-a)}{a}\right] xb = xt \qquad \text{Equ. 9}$$

Where Ym is the experimental mass in the Y axis (% w/w of PEG), Xm is the experimental mass in the X axis (% w/w of Dextran), yt and xt are the amount of PEG and Dextran in the top phase. Adjusting the constants for each binodal in both of these expressions result in:

$$a1* \exp(b1*Xt^{0.5} - c1* xt^3) = yt \qquad \text{Equ. 10}$$

$$a1* \exp(b1*Xb^{0.5} - c1* xb^3) = yb \qquad \text{Equ. 11}$$

yb is the amount of PEG in the bottom phase, after that delta PEG (the difference of the amount of PEG in the lower phase from the upper phase) and delta Dextran (the difference of the amount of Dextran in the upper phase from the lower phase) were calculated from:

$$\Delta PEG = yt - yb \qquad \text{Equ. 12}$$

$$\Delta Dex = xb - xt \qquad \text{Equ. 13}$$

To calculate the composition of the TLL at the mass ratio 1, the following equations were applied in

$$\left(yt + \left[\frac{(1-a)}{a} * yb\right]\right) * a = ym \qquad \text{Equ. 14}$$

$$\left(xt + \left[\frac{(1-a)}{a} * xb\right]\right) * a = xm \qquad \text{Equ. 15}$$

Then tie line length was calculated as below

$$TLL = \sqrt{(yt - yb)^2 + (xb - xt)^2} \qquad \text{Equ. 16}$$

(B) Preparation of Stock solutions

(B1) PEG8000 – Dextran500 ATPS

Concentrated 500mM Phosphate buffer stock solution was prepared as follows: 21.77 g K_2HPO_4 in 250mL of 18.2 MΩ-cm DI water, the pH was adjusted to 7.4 using the same concentration of potassium di-hydrogen orthophosphate buffer which was prepared by dissolving 6.8 g in 100mL of DI water. This was then diluted 10 times to give 50mM phosphate. Two different batches of Dextran, the Fisher and Sigma product (see detail in section 2.1) were used; a phase diagram was prepared for each of them. 25 % w/w of Dextran stock solution was prepared by dissolving 25g Dextran500 in 75g (50 mM)

phosphate buffer pH 7.4. PEG8000 was prepared at a concentration 20 % w/w by dissolving 20g PEG8000 in 80g (50 mM) phosphate buffer pH 7.4.

(B2) PEG600-Na$_2$SO$_4$ phase diagram

Stock solutions for the PEG600-Na$_2$SO$_4$ phase system were prepared, 100% w/w PEG600 used as supplied, Phosphate buffer stock solution was prepared as follows: 13.06 g K$_2$HPO$_4$ in 500mL of 18.2 MΩ-cm DI water and 4.08 g KH$_2$PO$_4$ in 200mL DI water to yield pH 7.4 and 14% w/w Na$_2$SO$_4$ by weighing 14g salt in 86g (0.15M) phosphate buffer (pH 7.4). The same experimental technique as described in paragraph (A) was used to create the phase diagram for the system.

(B3) PEG600 - (NH$_4$)$_2$SO$_4$ phase diagram

PEG600 and (NH$_4$)$_2$SO$_4$ stock solutions were prepared by weight to final compositions of 50% w/w PEG600 (50g PEG in 50g phosphate buffer) and 40% w/w salt (40g salt in 60g (150mM phosphate buffer pH 7.4)) and the same experimental technique as described in paragraph (A) was used to create a phase diagram for the system.

(B4) PEG1000 - (NH4)$_2$SO$_4$ phase diagram

PEG1000 and (NH$_4$)$_2$SO$_4$ stock solutions were prepared by weight to final compositions of 40% w/w PEG1000 (40g PEG in 60g buffer) and 40 % w/w salt (40g salt in 60g buffer (150mM potassium phosphate buffer pH 7.4)) and the same experimental technique as described in paragraph (A) was used to create a phase diagram for the system.

(B5) PEG4600 - Dextran500 phase diagram

PEG4600 and Dextran500 stock solutions were prepared by weight to final compositions of 25 % w/w PEG4600 (25g PEG in 75g 50mM phosphate buffer pH 7.4), concentrated 500mM Phosphate buffer stock solution was prepared as follows: 21.77 g K$_2$HPO$_4$ in 250mL of 18.2 MΩ-cm DI water and same concentration of KH$_2$PO$_4$ (6.8 g in 100mL) was used to yield pH 7.4. This was then diluted 10 fold to give 50mM phosphate. 30 % w/w Dextran was prepared by weighing 30g Dextran in 70g (50mM phosphate buffer pH 7.4). Determination of the compositions of upper and lower phases for the construction of the binodal and fitting of the tie lines was performed as described in paragraph (A).

2.2.4 General method of partitioning Ovalbumin in different phase systems

The partition isotherm experiments for all systems were performed using a set of different and increasing concentrations of protein added to a series of ATPS having the same overall polymer composition using a method outlined by Zaslavsky (23). Systems were dispensed into test tubes by a sample processor and vortexed using a digital mini vortexer for 10 sec, and centrifuged for 20 min at 5000 rpm to accelerate settling of the phases. After centrifugation, the upper and lower phases were separated and diluted in appropriate buffer for each system. Spectrophotometric absorbance at 280 nm (A280) was used to calculate protein concentration using an Extinction coefficient for ovalbumin of $30,590$ M^{-1} cm^{-1} and a Molar Mass of 42.7 kDa (101) and the partition was determined as the slope of the regression for a plot of concentration in the top phase versus concentration in the bottom phase

2.2.5 Method for Determination of Protein Concentration by BCA assay

The method combines the reduction of Cu^{2+} to Cu^+ by protein in an alkaline medium (the biuret reaction) with the highly sensitive and selective colorimetric detection of the cuprous cation (Cu^+) using a unique reagent containing bicinchoninic acid. (102)

The purple-coloured reaction product of this assay is formed by the chelation of two molecules of BCA with one cuprous ion. This water-soluble complex exhibits a strong absorbance at 562 nm that is linear with increasing protein concentrations over a broad working range of 20 µg/mL to 2,000 µg/mL. The macromolecular structure of protein, the number of peptide bonds and the presence of four amino acids (cysteine, cystine, tryptophan and tyrosine) are reported to be responsible for colour formation with BCA. (103)

The following reagents were used: bovine serum albumin (BCA) Reagent A, 1000mL (Product No. 23225) or 500mL (Product No. 23227), containing sodium carbonate, sodium bicarbonate, bicinchoninic acid and sodium tartrate in 0.1M sodium hydroxide. BCA Reagent B, 25mL, containing 4% cupric sulphate. Working reagent was prepared by mixing 50 parts of BCA Reagent A with 1 part of BCA Reagent B. Albumin Standard Ampules, 2mg/mL, 10 × 1mL ampules, containing BCA at 2mg/mL in 0.9% saline and 0.05% sodium azide.1 mg/mL protein ovalbumin standard, 50mM pH 7.4 phosphate buffers.

Preparation of Diluted BSA and ovalbumin standards: for each assay, standard curves were prepared using BSA and known protein (Ovalbumin). Table 6 was used to prepare a set of protein standards, in the range 0-2 mg/mL for BSA and 0-1 mg/mL Ovalbumin.

Table 6- Preparation of diluted BCA and Ovalbumin Standards (104).

		Dilution Scheme for standard Microplate Procedure		
Vial	Volume of diluent (µL)	Volume of stock protein solution added (µL)	Final BCA Concentration (µg/mL)	Final Ovalbumin Concentration (µg/mL)
A	0	300 of stock	2000	1000
B	125	375 of stock	1500	750
C	325	325 of stock	1000	500
D	175	175 of vial B dilution	750	375
E	325	325 of vial C dilution	500	250
F	325	325 of vial E dilution	250	125
G	325	325 of vial F dilution	125	62.5
H	400	100 of vial G dilution	25	12.5
I	400	0	0= blank	0

After Preparation of the standards according to the Table 6, 25µL of each standard or sample was added by pipette to tubes; 500µL of WR was added to each tube and mixed thoroughly for 10 seconds. Tubes were incubated for 30 min at 37∘C and the absorbance of samples was determined by spectroscopy at 562nm. Blank average standard replicates absorbance were subtracted from the measurements of all individual samples. A standard curve was prepared using the average blank-corrected 562nm measurement for each BSA or Ovalbumin standard vs. its concentration in mg/mL which was used to determine the protein concentration of each unknown sample.

Two assay procedures were performed: (1) the Test Tube Procedure requires a larger volume of protein sample; however, because it uses a sample to working reagent ratio of 1:20, the effect of interfering substances is minimized. (2) The microplate Procedure affords the sample handling ease of a microplate and requires a smaller volume (10-25µL) of protein sample; however, because the sample to working reagent ratio is 1:8, it

offers less flexibility in overcoming interfering substance concentrations and obtaining low levels of detection. The sensitivity of the assay was examined from the calibration curve using BSA. Then the performance of the assay with BSA was compared to its performance with ovalbumin.

2.2.6 Method to determine the protein partitioning isotherm using the BCA assay

Partitioning experiments were performed using a set of six different and increasing concentrations of protein added to a series of ATPS having the same overall polymer composition using a method outlined by Zaslavsky (23). Serial dilution of 10 mg/mL stock Ovalbumin (0.5, 0.75, 1, 1.5 and 2 mg /mL) were prepared in ATPS by a modified method, first a large blank ATPS without ovalbumin was prepared by mixing 15.709g of 20% w/w PEG, 30.42g of 25% w/w Dextran and 3.870 phosphate buffer pH 7.4. This blank system was left to settle overnight at 25°C to allow the phases to separate. The required ATPS were prepared according to Table 7.

After preparation of the individual ATPS with different ovalbumin concentrations, the phases were separated and 200 µL from upper and lower phase were taken. This step is probably the most critical in the whole experiment.

First, pipette was used to withdraw an aliquot from the upper phase which was transferred to a clean test tube. Then the tip was changed, and the lower phase was sampled by slowly pushing the tip through the interface down to the bottom of the test tube; wait 10 s before allowing the lower phase to enter the tip.

The pipet was slowly removed and soft paper tissue was used to remove any traces of solution on the outside of the tip to avoid any contamination with the upper phase. Samples of each phase were diluted 5 times by adding of 800 µL of the phosphate buffer in order to bring the protein concentration within the range of the BCA assay. Consequently, 25µL of each dilute phase replicate was transferred into microplate wells; 500µL of the working reagent (WR) was added to each well and mixed by pipette. All samples were incubated for 30 minutes at 37°C; the microplate was then cooled to room temperature. The absorbance was measured at 562nm on a micro- plate reader.

Table 7- A set of Two Phase System with different Ovalbumin concentration.

Prepare ATPS solutions					
[ovalbumin] (mg/mL)	Wt. Top (g)	Wt. Bottom (g)	Wt. Ovalbumin (g)	Wt. buffer (g)	Total system Wt. (g)
0	1	1	0	0.523	2.523
0.5	1	1	0.126	0.398	2.523
0.75	1	1	0.189	0.335	2.523
1.0	1	1	0.252	0.272	2.523
1.5	1	1	0.379	0.145	2.523
2.0	1	1	0.505 g	0.019	2.523

2.3 Chapter 4 – Examination of the partitioning of Ovalbumin isoforms in Aqueous Two Phase Systems

2.3.1 Method for the separation of protein isoforms (ovalbumin) using SAX-HPLC following partition in an ATPS

Two-phase systems were prepared from solid PEG 8000 (4.4%, w/w) and Dextran 500 (7 %, w/w). Aqueous two-phase systems (10 g total wt.) were made by combining 0.44 g PEG, 0.7 g Dextran solution, and 8.86 g of a solution of (20 mg protein (ovalbumin) in 10mL of 0.05 M Tris buffer pH 9 and 0.292 g/50ml NaCl). The resulting polymer compositions were 4.4% w/w PEG and 7.0% w/w Dextran. The mixture was shaken for 30 min and the phases were separated by centrifugation for 15 min at 1200 x g. Samples were withdrawn from each phase, mixed with an equal volume of distilled water and analysed by HPLC. Eluents and Gradient Program for partitioning Ovalbumin sample used 10% NaCl starting composition (see run No.6 Table 5) and the operating conditions were exactly as in section 2.2.1 using phosphate buffer and employing the optimized method in 2.2.2. The column was washed with starting buffer A until all non-bound components (e.g. Dextran and PEG) were eluted. A linear gradient of elution buffer B (10% NaCl) over 55 minutes was used, after that the column was washed with 100% elution buffer C to remove strongly bound material. The buffer used to equilibrate the column was 20mM phosphate buffer pH 8.5 to return to the initial conditions.

2.3.2 Method for studying the Ideal pH for partition of Ovalbumin isoforms

Phosphate buffer was prepared as in section 2.2.1 and adjusted to the required pH for analysis of the protein using the optimized method in 2.2.2. ATPS solutions were prepared by weighing 8.86 g of 20mM, pH 8.5 phosphate buffer to which was added 0.7 g of Dextran and 0.44 g of PEG as a solid. The solutions were vortexed until thoroughly mixed, 20mg of ovalbumin was added and after that the phase systems were vortexed using digital mini vortexer for 10 sec, and centrifuged for 20 min at 5000 rpm to accelerate settling of the phases. Upper and lower phases (0.7 mL each) were carefully pipetted from each phase system to a new vial and appropriately diluted two times for analysis by HPLC. The partition coefficient values were determined from the ratio of peak heights in the upper and lower phases as an average of duplicate experiments.

2.3.3 Methods of deglycosylation of Ovalbumin

The glycoforms of Ovalbumin were examined by two different methods. Neuraminidase was used in an attempt to prepare ovalbumin depleted in neuraminic acid residues to examine the effect of neuraminidase treatment on the partitioning and analysis of ovalbumin.

To examine potential differences in glycosylation in ovalbumin: Neuraminidase treatment: 20mg of ovalbumin was dissolved in 10 mL of 10mM phosphate buffer pH 6 to which 100μL neuraminidase stock solution was added and the mixture was incubated at room temperature. Then samples were taken approximately every hour and analysed by SAX-HPLC. Neuraminidase stock solution was made up as follows: 0.32 mg neuraminidase in 1 mL 100mM sodium acetate buffer pH 6, with 20 mM $CaCl_2$. The optimised method established in 2.2.2 was used for chromatographic analysis.

In addition, gel electrophoresis was used as qualitative analyses to study distinguish between native and modified Ovalbumin following treatment with the enzyme Endoglycosidase F1 (Endo-F1).

For the Endo-F1 treatment, stock ovalbumin was prepared at a concentration of 5.3mg/mL in 25mM Tris-HCl pH 9 containing 50mM NaCL. Enzymatic deglycosylation by Endo-F1 was attempted by incubating 2 μL Endo F1 with 37.5 μL stock ovalbumin in 10 μL of reaction buffer (provided with the enzyme kit (Endoglycosidase F1 from Elizabethkingia miricola)) at 37 °C overnight. Treated and non-treated Ovalbumin was prepared by mixing 37.5 μL stock ovalbumin in 12 μL of reaction buffer and another

solution with 12 µL DI water. The treated and non-treated ovalbumin was diluted twice and heated for 10 min at 70 °C.

Electrophoretic procedure: stock running buffer TruPAGE TEA-Tricine SDS was diluted 20-folds and used to fill the Bio-RAD running tank, the TruPAGA Precast 10% Gel was used for loading samples which were washed with deionized water very carefully to eliminate the preservative and bubbles, after that duplicate 10 µL from each samples (with one and two times dilution) and 7 µL from sigma marker (wide range molecular weight) were loaded.

Once the samples were loaded into the wells and the buffer chamber was filled, electrophoresis was started at a constant voltage (180 v) until reached the bottom of the gel within 60 min. Depending on the gel percentage and running buffer, run time can range from 30-70 min.

For gel staining, the electrophoresis gel (SDS-PAGE) was placed in a plate filled with water and washed three times, then simply Blue safe stain (Lot 1237898) was used to make the proteins bands visible.

2.3.4 Method to Identify the Phosphoforms of ovalbumin using alkaline phosphatase (ALP)

Enzymatic dephosphorylation was performed by incubating ovalbumin with ALP. Tris 50 mM containing 100mM NaCl was prepared by weighing 0.303 g of Tris and 0.292g NaCl dissolved in 50 mL of 18.2 MΩ-cm DI water. The pH was adjusted to 9 using concentrated (32%) hydrochloric acid.

700 units /mL (0.7 units/ µL) working solution of alkaline phosphatase was prepared by: adding 500 µL of 50 mM Tris buffer (pH 9) into a vial containing 13 mg protein /mL alkaline phosphatase, bovine intestinal mucosa (3285 units /mg protein) and then 1.5mL of deionized water 18.2 (MΩ-cm) was added and gently swirled until thoroughly mixed, 400 µL aliquots were dispensed into separate micro-tubes and frozen at -20 °C.

Ovalbumin treatment was performed by adding of 400 µL of 0.7 units/ µL ALP to 5 mL of protein at a concentration of 10 mg/mL in 50 mM Tris buffer (pH9) at 23°C overnight.

Partitioning experiment: ATPS were prepared as in 2.3.1 using un-treated and treated ovalbumin solution. The mixture was shaken for 30 min and the phases were separated by centrifugation for 15 min at 1200 x g. Samples were withdrawn from each phase and

mixed with an equal volume of distilled water. Samples were analysed during the time course (every hour) of the treatment under the optimized conditions established in 2.2.2.

2.3.5 Method of Size exclusion chromatography (SEC) for examining the effect of dephosphorylation of Ovalbumin

SEC was used to assess the effect of dephosphorylation on the molecular integrity and degree of aggregation of ovalbumin. 50mM phosphate buffer pH 7 with and without 150mM NaCl was used as the elution buffer. The SEC column (TSKgel G2000SW) was calibrated from the retention times of a Bio-Rad Gel Filtration Standard (Catalog 151-1901) having molecular weight markers ranging from 1,350 to 670,000 Da.

Concentrated (500mM) phosphate buffer was prepared by weighing 8.709 g of di-potassium hydrogen orthophosphate dissolved in 100 mL of 18.2 MΩ-cm DI water. The pH was adjusted to 7 using the same concentration of potassium di-hydrogen orthophosphate buffer which was prepared by weighing 6.804 g in 100mL DI water. The solution was diluted 10 times to give 50mM phosphate, and 4.383g salt was added to 500 mL of this buffer and filtered. This buffer used to equilibrate the column at a flow rate of 0.4 mL/min with UV detection at 280 & 260 nm. ALP treated and non-treated ovalbumin with ALP was prepared as in section 2.3.4.

2.3.6 Method of using PEG3350-Dextran500 system for partitioning treated and non-treated Ovalbumin

A new phase system was chosen from the phase diagrams given by Zaslavsky (23) composed of PEG3350-Dextran500, in a screening programme to monitor the partitioning behaviour in PEG3350 Dextran500 system using different pH and salt, which was performed by comparing the partition coefficient values of Ovalbumin calculated from the concentration of the protein in each phase using the absorbance at 280nm measured by the spectrophotometry. PEG3350 - Dextran500 system was prepared in 10mM phosphate buffer but differing in pH (4.6, 5.5, 7.4, and 9). Selected pH values ranged from the isoelectric point (pI) of the protein (when the Ovalbumin carries no net electrical charge in the statistical mean, pI Ovalbumin 4.5. (66)) to 4 pH units above the pI with respect to different added salts (100mM $NaClO_4$, 100mM KCl, 50mM K_2SO_4) for each pH individually. The partition coefficient value of the protein was determined using the concentration obtained in each phase from absorbance measurements at 280nm.

Potassium phosphate buffer 10mM was prepared from stock 100mM potassium phosphate diluted 10 times. The concentrated stocks were prepared by dissolving 8.709g K_2HPO_4 in 500mL of 18.2 MΩ-cm DI water and 100mM KH_2PO_4 (1.36 g KH_2PO_4 in to yield the different pH values selected.

Then a weighed amount of different salts was added separately to buffers prepared at each pH, e.g. for phosphate buffer pH9, either 100mM $NaClO_4$ (1.224g $NaClO_4$ was added to 100mL phosphate buffer pH9), or 100mM KCl (0.745g KCl was added) or 50mM K_2SO_4 (0.873g K2SO4 was added).

2.4 Chapter 5 – Robotic method development for the partitioning of Ovalbumin in ATPS

2.4.1 Introduction to the preparation of performance files for each solution

A Perkin Elmer Multi-probes II plus Liquid Handling Sample Processor (LHSP) was used to prepare ATPS samples and to study the accuracy of the delivery gravimetrically either a Sartorius Mechatronics analytical balance or a Denver balance instruments both having a readability of 0.1mg was used.

Stock 20% w/w PEG8000, 25% w/w Dextran500 was prepared in 50mM phosphate buffer pH 7.4 as described previously in section 2.2.3**.** For each stock solution of the ATPS, the relationship between demanded volume and delivered mass was measured gravimetrically. Delivery of a range of volumes between 50 µL and 2 mL was examined for each stock solution (without any volume compensation being applied by the LHSP). The amounts dispensed were determined by weight. The weights were determined so that the correct volume can be requested which gives the desired weight. The procedure simply conforms to the traditional w/w relations used to prepare ATPS. The regression relationship between the volume of polymer stocks demanded and the weight delivered by the LHSP was used to establish the required volumes for the delivery of a given weight of polymer stock.

$$y = ax - y_0 \qquad \text{Equ. 17}$$

The parameters of the regression equations were used to convert this weight to volume because the robotics system operates on a volume basis.

$$x = \frac{[y - y_0]}{a} \qquad \text{Equ. 18}$$

Where (y) represents the mass delivered, (x) represents the volume demanded, (a) is the slope and (y0) is the intercept value. The third TLL (2nd phase diagram) of the system given in Table 31 was selected which is composed of 5.67 % w/w PEG8000 and 10.85 % w/w Dextran500 (see Figure 9) and used to prepare ATPS for the partitioning of ovalbumin. Since the LHSP functions on the basis of the transfer of a known volume of solution, the required weights were converted to volume using the regression equations (above) for PEG and Dextran, as shown in Table 8.

Table 8- Composition of ATPS in µL volume for preparation by robotics system.

Volume of stock PEG (µL)	Volume of stock Dextran (µL)	Volume of stock Buffer (µL)	Total Volume (µL)
462	885	524	1871

In a similar way a system volume table to be used by the LHSP for delivering different concentrations of ovalbumin was created as shown in Table 9, the amount of Ovalbumin and buffer to be added were calculated depending on the available room for samples in the compositions of the TLL used.

Table 9- The amounts of ovalbumin and buffer to be added to the third TLL of PEG8000-Dextran500 system to give a range of Ovalbumin concentrations.

Demanded [ova]mg/mL	Buffer wt.(g)	Ovalbumin(mg) (10mg/mL)	Ovalbumin volume(µL)	Buffer volume (µL)
0	0.524	0	0	524
0.5	0.424	0.10	100	424
0.75	0.374	0.15	150	374
1.0	0.324	0.20	200	324
1.25	0.274	0.25	250	274
1.5	0.224	0.30	300	224
1.75	0.174	0.35	350	174
2.0	0.124	0.40	400	124

2.4.2 Method to study the Accuracy of delivery of ATPS solutions (PEG, Dextran, phosphate buffer and ovalbumin) by LHSP

2.4.2.1 Introduction to the preparation of performance files for each solution

Performance files are employed by the LHSP to produce accurate and precise pipetting by defining system parameter values specific to a tip type, mode of operation, syringe size, and liquid type.

The parameters controlling the aspiration and dispensing steps, each performance file has the same fundamental structure, there are three pages of information within each performance file including: Performance Set, Global parameters and Selection criteria.

Performance Set: The performance characteristics of liquids depend on the volume of liquid being aspirated and dispensed. In order to optimize the performance of the system at any given liquid volume it is important to optimize the control parameters in the performance files, The performance file contains a table of pump speeds, pump delays ,waste volumes and air gaps that are assigned to given ranges of liquid volumes. The method focused on delivering different volumes of ATPS contents cover the range of demanded composition (50 - 2000 µL).

The performance files were calibrated and prepared for all solutions and sampling regimes. It is important that when adjustments are made to the performance files to provide accurate delivery of particular solutions the file must be saved with a unique name to ensure the correct performance characteristics are associated with the correct dispensing steps for each solution.

2.4.2.2 Method for studying the accuracy of delivery using Blowout and Dispense back mode

Modes of operation (Blowout and Dispense back), which could affect the accuracy and precision of the delivery for different volumes, were examined. Stock 20 % w/w PEG8000 and 25 % w/w Dextran500 were prepared in 50mM phosphate buffer pH 7.4 as described previously in section 2.2.3 paragraph (B1). For each stock solution of the ATPS, the method consisted of aspirating a range of volumes of 20 % w/w PEG8000; 25 % w/w Dextran500, protein and buffer solutions using two different modes. The performance was assessed gravimetrically for each aspiration mode.

2.4.2.3 Method for calibration of the LHSP

Stock solutions of the ATPS were prepared (as described previously in section 2.2.3 paragraph (B1) to examine the accuracy of delivering.

Delivery of a range of volumes between 50 µL and 1.4 mL were examined for each stock solution without any volume compensation. The relationship between demanded volume and delivered mass was measured gravimetrically. Thus at this stage a linear relationship between delivered mass and demanded volume was assumed having a slope of 1 and offset value of 0 as defined in Eq. Below

$$W = V.x + C \quad \text{Equ. 19}$$

Where W is the mass delivered, V is the volume demanded, x is the slope and C is the intercept value. The true relationship between the volume demanded and the weight delivered was determined from gravimetric determinations of the delivered mass and a new slope and offset calculated. These values were then used to set the volume compensation of the LHSP. Note that this is equivalent to a determination of the density of the stock solutions and that a similar procedure could be implemented through performance files in the absence of a volume compensation parameter.

2.5 Chapter 6 – Developing the method of modifying Human serum albumin and measuring the amount of free thiol by partitioning in ATPS

2.5.1 Methods of site specific derivatisation of Human serum albumin

2.5.1.1 Method of Modification of surface free-thiol with 2-methylsulfonyl-5-phenyl -1,3,4 oxidiazole (MSPO) Reagent

Reaction buffer: 20mM potassium phosphate buffer was prepared from stock 200mM potassium phosphate buffer diluted 10 fold. Concentrated stock solutions of K_2HPO_4 and KH_2PO_4 were prepared by dissolving 1.741g K_2HPO_4 in 50mL of 18.2 MΩ-cm DI water and the same concentration of KH_2PO_4 (1.36 g KH_2PO_4 in 50mL) was used to yield pH 7.4, then 4.383g NaCl to 500mL buffer was added to give 150mM NaCl.

A solution of 2mg/mL purified-albumin (p-HSA) in 20mM phosphate buffer pH 7.4 containing 150mM NaCl was prepared , A stock solution of 5mg/mL 2-methylsulfonyl-5-phenyl -1,3,4 oxidiazole in DMSO was prepared. Reaction mixtures of protein and label reagent differing in molar ratio were prepared by mixing (1mL) protein and a label solution of (34, 17 and 7 µL) to give molar ratios of label: protein (25:1, 12.5:1 and 5:1).

Mixtures were incubated for 2h at room temperature to afford Human Serum Albumin (HSA) conjugated to the thiol label, after that the samples were analysed by RP-HPLC. For each mixture of protein-label reagent blanks were prepared in the same concentration of label and protein used in the mixture to monitor any changes in the HPLC-chromatogram after reaction.

The maximal wavelength of absorbance of the MSPO was determined by scanning UV-visible spectrophotometry. RP-HPLC analysis was done with C18 YMC-pack ODS-AQ (5.0 μm, 150 × 4.6 mm). Gradient elution used buffer A 10% CAN containing 0.1% Trifluoroacetic acid (TFA) pH1.7, Buffer B 90% ACN containing 0.1% TFA pH 0.9 with gradient elution of 25 to 50% of solution B in 15 minutes (105). This method was developed to meet the requirements of the separation by testing several mobile phase compositions and changing the slope of the gradient for the separation of the protein, linker and albumin conjugate. The final eluent and gradient flow program is shown in Table 10.

Table 10– RP-HPLC gradient programme flow and the compositions of mobile phase under the conditions: solvent A was 10% v/v ACN (0.1%) TFA pH1.7 and solvent B 90% v/v ACN containing (0.1%) TFA pH 0.9, the conditions were used to analyse the reaction mixture of the protein (Albumin) and different thiol labels.

Time (min)	Flow (mL/min)	Solvent A (%)	Solvent B (%)	Curve
3	0.8	100	0	6
8	0.8	75	25	6
13	0.8	50	50	6
18	0.8	50	50	6
18.1	0.8	100	0	11
23	0.8	100	0	11
28	0	100	0	11

2.5.1.2 Method of Modification of Cysteine thiol with N-Ethylmaleimide (NEM) Reagent

(A) Reaction of N-Ethylmaleimide (NEM) with cysteine-thiol employed NEM stock 20mg/mL and Cysteine stock 20mg/mL in 100mM phosphate buffer pH 7. Each stock was diluted 10 fold and then used to prepare a series of dilutions as shown in Table 11. The absorbance of NEM at 300nm was measured by spectrophotometer to monitor the reaction.

Concentrated stock phosphate buffer (100mM) was prepared by dissolving 1.741g K_2HPO_4 in 100mL of 18.2 MΩ-cm DI water and KH_2PO_4 (1.36 g KH_2PO_4 in 100mL) was used to yield pH 7, then 0.876g NaCl to 100ml buffer was added to give 150mM NaCl.

Table 11- The volume composition of the reaction mixture samples of NEM and Cysteine.

Dilution times of Cys	Vol NEM (µL)	Vol Cys (µL)	Vol Buffer (µL)	[Cys] (mg/mL)
100	150	150	1200	0.2
200	150	75	1275	0.1
250	150	60	1290	0.08
500	150	30	1320	0.04
1000	150	15	1335	0.02

(B) Reactivity with other electrophilic reagents namely Methylbenzenethiol (MBT) was performed to confirm whether the reaction took place at the free thiol or the amine group exactly under the same conditions describe above for the cysteine experiment.

20mg/mL MBT was dissolved in ethanol, the reaction mixtures were prepared using the compositions in Table 11.

(C) Assessment of the reactivity of NEM towards protein-thiol was performed using BSA. The stock solutions of BSA and NEM were prepared at a concentration of 30 and 20mg/mL respectively in 100mM phosphate buffer at pH 7 containing 150mM NaCl.

The following concentrations of BSA were prepared: 1, 3, 6, 15 and 30 mg/mL using phosphate buffer as a diluent. The reaction solutions were prepared by mixing 1000µL protein at different concentrations with 25 µL (2mg/mL) NEM.

Solutions were incubated at room temperature for 30min, after which the samples were analysed by HPLC and UV-visible spectrophotometry at 300nm. For protein thiol-labelling with NEM adjustment to the HPLC method was required to achieve a baseline separation for the peaks, the flow program followed the elution profile in the Table 12.

Table 12- The adjustment in the HPLC gradient programme flow and the mobile phase composition for the analysis of the reaction mixture of the protein (Albumin) and different thiol labels under the conditions: solvent A was 10% v/v ACN containing (0.1%) TFA pH1.7 and solvent B 90% v/v ACN containing (0.1%) TFA pH 0.9

Time (min)	Flow (mL/min)	Solvent A (%)	Solvent B (%)	Curve
3	0.7	100	0	6
8	0.7	50	50	6
14	0.7	50	50	6
15	0.7	100	0	11
25	0	100	0	11

2.5.1.3   Method of Modification of albumin with 5, 5'-dithiobis (2-nitrobenzoate)

This section descries a method of albumin modification with 5, 5'-dithiobis (2-nitrobenzoate), often referred to as Ellman's reagent or DTNB.

(A) Procedure for Quantitating Sulfhydryl Groups Using a Cysteine Standard: phosphate buffer 100mM pH8 containing 1mM EDTA (included in the reaction buffer to protect SH-groups from oxidation and to prevent metal-catalysed formation of disulphide bonds). This was prepared from 1M phosphate buffer prepared as follows: 17.418 g K_2HPO_4 in 100mL of 18.2 MΩ-cm DI water and 1M KH_2PO_4 (13.608 g in 100ml) was used to yield pH 8. This was then diluted 10 times to give 100mM phosphate, to which 0.146g of EDTA was added to 500 mL phosphate buffer.

Ellman's reagent stock solution was prepared by dissolving 12 mg DTNB in 3 mL of reaction buffer. L-Cysteine stock Solution was prepared at a concentration 0.26mg/mL by dissolving 26 mg Cysteine in 100mL of reaction buffer, and then several dilutions were made following Table 13. Reaction of cysteine with Ellman's reagent was performed by preparing a set of test tubes, each containing 25 µL of DTNB solution and 2.5 mL of reaction buffer, after which 250 µL of each Cysteine standard was added separately. Absorbance was measured by UV-visible scanning spectrophotometry between 200 and 500 nm. Total thiol concentration was determined by the amount of TNB, calculated from its extinction coefficient (E 14150 M^{-1} cm^{-1}) (106), released after reaction with Cysteine

Table 13- The volume composition of the Cysteine standard at the indicated concentrations.

Standard	Volume of reaction buffer (mL)	Amount of Cysteine	Final concentration (mM)
A	100	26mg	2.15
B	5	25 mL of standard A	1.79
C	10	20 mL of standard A	1.43
D	15	15 mL of standard A	1.07
E	20	10 mL of standard A	0.72
F	25	5 mL of standard A	0.35
G	30	0	0.00

(B) The reaction of DTNB with protein (purified HSA) was performed using stock protein which was prepared at a concentration 30mg/mL and filtered through a 0.45 µm filter, and then several dilutions were made as shown in Table 14.

Table 14- The volume composition of the reaction mixture samples of DTNB and protein (purified HSA).

Samples	Volume of reaction buffer	Amount of Protein	Final concentration of protein (mM)	Molar ratio DTNB : protein
A	0	1mL	4.028×10^{-5}	4.5
B	167 µL	833µL of stock A	3.357×10^{-5}	5.4
C	333 µL	667µL of stock A	2.685×10^{-5}	6.7
D	500 µL	500µL of stock A	2.014×10^{-5}	9.0
E	667 µL	33µL of stock A	1.343×10^{-5}	13.5

The reaction mixture of Ellman's reagent and protein was prepared by mixing 50 µL Ellman's reagent (4mg/mL), 250 µL from each protein sample and 2.5mL reaction buffer. The resulting solutions were incubated at room temperature for 30min.

(C) Reaction of Ellman's reagent (DTNB) with recombinant-HSA (rHSA) were performed using the protein stock solution at a concentration of 50mg/mL, which was prepared by dissolving 350mg rHSA in 7mL reaction buffer, and DTNB stock at a concentration of

4mg/mL. Serial dilutions were made following Table 15 to prepare different molar ratios of DTNB to protein which were used later to study its partitioning.

Table 15- The volume composition of the reaction mixture samples of DTNB and protein (rHSA).

Samples	rHSA (µL) (50mg/mL)	DTNB (µL) (4mg/mL)	Reaction Buffer (µL)	Molar ratio DTNB : rHSA
A	560	7	2233	0.2
B	560	14	2226	0.3
C	560	21	2219	0.5
D	560	28	2212	0.7
E	560	42	2198	1.0
F	560	210	2030	5.0
G	560	420	1820	10.1

In this context, a calibration curve for DTNB was obtained by making several dilutions of the stock solution to yield the same concentration as in the samples as shown in Table 16. Quartz matched cuvettes were used for the spectrophotometry, and the readings were made against buffer. The concentrations of the standard solutions were obtained through the reading of the absorbance by spectrophotometer at their maximal absorbance (λ_{max}). A linear relationship for calibration was determined by plotting the absorbance (y) versus the corresponding concentration (x).

All samples were diluted 10 fold to measure the absorbance by spectrophotometry and the reaction was monitored by the changing in the absorbance at 324 and 412nm.

Table 16- The volume composition of the DTNB standard for the quantitation of the amount of DTNB after reaction with free thiol groups.

DTNB standard	DTNB (µL) (4mg/mL)	Reaction buffer (µL)
A	7	2793
B	14	2786
C	21	2779
D	28	2772
E	42	2758
F	210	2590
G	420	2380

(D) The ATPS PEG3350 - Dextran500 phase system with 10mM phosphate buffer pH 9 containing 50mM K_2SO_4 was prepared as in section 2.3.6. The system was used to study the partitioning of protein after reaction with DTNB.

The LHSP was used to prepare ATPS having a final mass of 2.5 g, the mixture containing (0.84g) 8.4% w/w PEG3350, (0.7g) 8.4 % w/w Dextran500, the remaining liquid in the system was made up of protein in (0.96g). Phases were separated and diluted 5 fold and the analysis was carried out by UV/visible spectrophotometry.

(E) The PEG3350–K_2HSO_4 stock solutions were prepared at a concentration of 25 and 30 % w/w respectively. Ellman's reaction buffer was used to prepare DTNB stock at 4mg/mL and stock r-HSA of 50mg/mL.

Single phase reaction solutions for rHSA and DTNB were prepared following Table 17, and a calibration curve for DTNB was obtained by dilution from the stock solution as shown in Table 18.

The LHSP was used to prepare ATPS having a final mass of 2.5 g, the mixture contained (1g) 10% w/w PEG3350, (0.84g) 10.08 % w/w K_2HPO_4, the remaining mass in the system (0.66g) was made up of the protein- Ellman's reaction mixtures. Phases were separated and diluted 5 fold and the analysis was carried out by spectrophotometry as previously described.

Table 17- The volume composition of the single phase reaction mixture samples of Ellman's reagent and rHSA protein which were used in the partitioning experiment in the PEG 3350– K_2HSO_4 system.

Samples	rHSA µL (50mg/mL)	DTNB (µL) (4mg/mL)	Buffer (µL)	Molar ratio DTNB :rHSA
A	560	7	2233	0.2
B	560	10.5	2229.5	0.25
C	560	21	2219	0.50
D	560	42	2198	1.0
E	560	84	2156	2.0
F	560	168	2072	4.0
G	560	336	1904	8.1

Table 18- The volume composition of the DTNB standard for the quantitation of the amount of DTNB after reaction with free thiol groups.

DTNB standard	DTNB (µL) (4mg/mL)	Reaction buffer (µL)
A	7	2793
B	10.5	2789.5
C	21	2779
D	42	2758
E	84	2716
F	168	2632
G	336	2464

(F) The PEG1000–K_2HSO_4 stock solutions were prepared at a concentration 25 and 40 % w/w respectively. Ellman's reaction buffer was used to prepare DTNB stock at 4mg/mL and stock rHSA at a concentration of 50mg/mL.

Single phase reaction solutions for rHSA and DTNB for the samples (c, d, e, and f) were prepared in a total volume of 2.8mL following Table 17, and a calibration curve for initial DTNB concentration was obtained by dilution from the stock solution as shown in Table 18. All samples were diluted 10 fold and measured by spectrophotometry as previously described.

The LHSP was used to prepare ATPS having a final mass of 2.5 g, the mixture contained of (1.47g) 14.7 % w/w PEG1000, (0.72g) 11.55 % w/w salt, the remaining mass in the system (0.308g) contained the samples consisting of protein and DTNB. Phases were separated and diluted 2.5 fold and the analysis was carried out by spectrophotometry.

2.5.1.4 Method of conjugation of albumin with N-pyrenylmaleimide (NPM) reagent

(A) Method of calculation of the molar extinction coefficient of NPM in DMSO by calibration with a solution dissolved in MeOH.

NPM stock solution 5mg/mL was prepared in DMSO, and then diluted 50 fold to give 0.1mg/mL. After which number of dilutions were made using pure DMSO to get the following concentrations: 0.0005, 0.001, 0.0015, 0.003 and 0.005 mg/mL the solutions were mixed and the spectrophotometry readings were made against DMSO.

In addition, NPM stock 1mg/mL in methanol was prepared by mixing 200µL (5mg/mL NPM in DMSO) with 800µL Methanol and then further diluted to 0.1mg/mL in methanol. Exactly the same dilutions as used for DMSO were made with methanol. The absorbance was measured in order to determine the molar extinction coefficient of NPM in DMSO from the known value in methanol (107).

(B) The reaction mixture solutions of NPM with recombinant HSA (rHSA) were made using freshly prepared rHSA at a concentration of 5mg/ml in 18.2 MΩ-cm DI water and 0.5mg/mL NPM in 60 % v/v DMSO and these were used to prepare several dilutions as single phase samples at different molar ratios of NPM: rHSA as shown in Table 19 in a total volume of 1125 µL and a final concentration of DMSO (6.67 % v/v) in the protein mixtures. A standard calibration curve for NPM was obtained by dilution from the stock solution as shown in Table 20.

Table 19- The volume composition of the single phase reaction mixture samples of NPM and rHSA protein.

Samples	rHSA (µL) (5mg/mL)	NPM (µL) (0.5mg/mL)	Molar ratio NPM:rHSA
A	1000	125	2.80
B	1000	100	2.24
C	1000	75	1.68
D	1000	50	1.12
E	1000	25	0.56

Table 20- The volume composition of the Standard NPM for the quantitation of the amount of NPM after reaction with free thiol groups.

NPM Standard	NPM (µL) (0.5mg/mL)	60% DMSO (µL)	Water (µL)
A	125	0	1000
B	100	25	1000
C	75	50	1000
D	50	75	1000
E	25	100	1000

(C) To study the solubility of NPM in a mixture of DMSO/buffer, phosphate reaction buffer 20mM pH7.5 was prepared from 0.2M stock as follows: 1.74 g K_2HPO_4 in 50mL of 18.2 MΩ-cm DI water and 0.2M KH_2PO_4 (1.36 g in 50mL) were mixed to yield pH 7.5. This was then diluted 10 times to give 20mM phosphate. NPM was prepared in pure DMSO at a concentration of 5mg/mL, and then standard samples were prepared by dilution whilst keeping the 60% v/v DMSO constant in all samples as shown in Table 21. Then the following dilutions; 5, 10 and 20 fold were made for each concentration and the absorbance was measured spectrophotometrically.

Table 21- *The volume composition of the standard NPM samples prepared in 60 % v/v DMSO and the phosphate reaction buffer 20mM pH7.5.*

NPM (µL) from stock (5mg/mL)	New conc. of NPM (mg/mL)	Pure DMSO to keep the 60% (µL)	Buffer (µL)
400	1	800	800
320	0.8	880	800
160	0.4	1040	800
80	0.2	1120	800
40	0.1	1160	800
20	0.05	1180	800

(D) Preparation of reaction mixture of NPM and protein: stock solutions of NPM 0.5mg/mL in 60 % v/v DMSO/buffer and 5mg/mL rHSA in phosphate buffer 20mM pH7.5 were prepared whilst maintaining the consistency of % v/v DMSO in all samples. The reaction mixture solutions in 1200 µL total volume were prepared as shown in Table 22.

Table 22- *The volume composition of the reaction mixture samples of NPM and protein (rHSA) in 60% v/v DMSO and the phosphate reaction buffer of 20mM pH7.5.*

Samples	rHSA (µL) (5mg/mL)	NPM (µL) (0.5mg/mL)	60% DMSO solution (µL)	Molar ratio NPM:rHSA
A	1000	12.5	187.5	0.28
B	1000	25	175	0.56
C	1000	50	150	1.12
D	1000	100	100	2.24

E	1000	200	0	4.47

(E) Calculation of the extinction coefficient of NPM in ACN: a stock solution of 5mg/mL NPM was prepared in DMSO, and then diluted to give 0.1mg/mL using ACN, after that a number of dilutions were made using pure ACN to get the following concentrations: 0.02, 0.08, 0.01, 0.005 and 0.0025 mg/mL, the solutions were mixed and the spectrophotometer readings were made against pure ACN.

(F) Study of the solubility of NPM in ACN/buffer: NPM was prepared in pure DMSO at a concentration of 5mg/mL, and then diluted 10 fold in 60 % v/v ACN to give 0.5mg/mL. Stock rHSA was prepared at a concentration 5mg/mL in 20mM phosphate buffer pH 8.7. A reaction mixture solution containing rHSA in 1200 µL total volume was prepared by dilution whilst keeping the concentration of ACN constant in all samples (10% v/v ACN in protein mixture) as shown in Table 23. Standard NPM was obtained by dilution from the stock solution to get the same concentration as in the samples following Table 24.

Table 23- The volume composition of the reaction mixture samples of NPM and protein (rHSA) in the condition 60 % v/v ACN and 20mM phosphate buffer pH 8.7

Samples	rHSA (µL) (5mg/mL)	NPM (µL) (0.5mg/mL)	60% ACN Solution (µL)	Molar ratio NPM:rHSA
M1	1000	200	0	4.47
M2	1000	100	100	2.24
M3	1000	50	150	1.12
M4	1000	25	175	0.56
M5	1000	12.5	187.5	0.28

Table 24- The volume composition of the Standard NPM in the % v/v ACN and phosphate buffer 20mM pH 8.7

NPM Standard	0.5mg/mL NPM in 60% v/v ACN (µL)	60% v/v ACN (µL)	Buffer (µL)
St.1	200	0	1000
St.2	100	100	1000
St.3	50	150	1000

St.4	25	175	1000
St.5	12.5	187.5	1000

2.5.1.5 Method of conjugation of albumin with Fluorescein-5-maleimide reagent

The reaction mixture of the Fluorescein-5-maleimide (F-5-M) and protein was made by preparing phosphate reaction buffer 20mM pH 7.2 containing 150mM NaCl and 5mM EDTA. Buffer was prepared from stock concentration of 0.2M of K_2HPO_4 as follows: 1.74 g K_2HPO_4, 4.38 g NaCl and 0.75 g EDTA in 50mL of 18.2 MΩ-cm DI water. 1M KOH was used to yield pH 7.2. This was then diluted 10 times to give 20mM phosphate 150mM NaCl and 5mM EDTA.

Stock 5mg/mL Fluorescein-5-maleimide was dissolve in pure Dimethylformamide (DMF) and aliquots of 400 μL were frozen at -20 ^{o}C. One aliquot was diluted using pure DMF to prepare the following concentration (1, 0.5, 0.25 and 0.125 mg/mL).

Freshly prepared rHSA at a concentration of 5mg/mL in reaction buffer was used to prepare several different molar ratios of F-5-M: rHSA. The reaction was begun by mixing 1mL of protein with 100 μL of the stock F-5-M in a total volume of 1100 μL and a final concentration of 5.45 % v/v DMF. A standard calibration curve for F-5-M was prepared using the same concentration of F-5-M as in the samples using reaction buffer instead of protein solution. All samples were diluted 5 fold to measure the absorbance at 494nm.

2.6 Chapter 7 – Method of development the specificity of DTNB toward protein free-thiols in a partitioning assays for free thiols

(A) Fresh DTNB phosphate reaction buffer 100mM pH8 containing 1mM EDTA (as in section 2.5.1.3 paragraph A) was used to prepare the stock solutions of DTNB at 4 mg/mL and protein at a concentration of 100 mg/mL. Protein samples were filtered through 0.45 μm filter. Each stock solution of the protein was used to prepared several dilutions as shown in Table 25 using reaction buffer as a diluent

The reaction was begun by mixing 250μL protein, 50μL DTNB and 2.5 mL of buffer in a total volume of 2.8mL. All samples were analysed by spectrophotometry and numerical methods were used (with the Mathcad as a tool) to calculate the concentrations of free

DTNB, protein and TNB released from the reaction, which will be described in the results and discussion.

Table 25- The volume composition of the diluted protein stock solutions

100mg/mL Albumin stock (µL)	Buffer (µL)	[c] protein mM
997.5	2.5	1.5
665	335	1
332.5	667.5	0.5
166.25	833.75	0.25
83.125	916.88	0.125
41.56	958.44	0.0625
0(blank)	1000	0

(B) Stock solutions of the ATPS components were prepared at a concentration 40 % w/w K_2HPO_4 and 50 % w/w PEG1400. ATPS system was used to partition the albumin after reacted with DTNB.

Single phase reactions were prepared using 10mg/mL protein (N-rHSA) stock, 4mg/mL DTNB stock, the latter was diluted in buffer to yield concentrations of (1, 0.5, 0.25, and 0.125 mg/mL). The reaction mixture consisted of 1mL protein mixed with 250µL DTNB diluted stock in a total of 1250 µL, DTNB standards at the same concentrations were prepared to monitor any changes after reaction and to study the partitioning performance in the ATPS. The mixtures were incubated at room temperature for 15min then all samples were diluted 10 fold to measure the absorbance by spectrophotometry.

The LHSP was used to prepare PEG1400- K_2HPO_4 ATPS having a final mass of 2.5 g. Partitioning of rHSA was performed by weighing out the appropriate amount of the stock solutions using the robotic system. A mixture containing (0.556g) 11.125 % w/w PEG1400, (0.867g) 13.875 % w/w K_2HPO_4, and the remaining mass (1.077g) was made up with buffer. The amount of protein mixture with DTNB was 0.625g in order to keep the protein concentration fixed at 2mg/mL in the ATPS; the remaining volume was completed with buffer. This experiment was repeated twice before and after adjustment

of the pH of the salt phase to pH8 which was prepared by mixing 35g K_2HPO_4 with 5g KH_2PO_4 in 60g DI water.

(C) A further experiment was designed for the reaction of Novo-HSA (N-rHSA) and DTNB. The stock solutions of the protein (50mg/mL) and reagent (4mg/mL) were prepared using as reaction buffer 100mM potassium phosphate pH8 containing 1mM EDTA. Serial dilutions were made as shown in Table 26 to prepare different molar ratios of DTNB to protein. The ratio was chosen to start well below the saturated condition (to allow monitoring of the change in partition of free DTNB) to a ratio 4 times greater than the saturated condition. A calibration curve for DTNB was prepared by dilution from the stock solution to cover the same concentration range in the samples as shown in the Table 27. All samples were incubated for 15 min, diluted with buffer 5 fold and analysed by spectrophotometry.

Table 26- The volume composition of the reaction mixture samples of DTNB and N-rHSA in the phosphate reaction buffer 100mM potassium phosphate pH8 containing 1mM EDTA.

Samples	N-rHSA (µL) (50mg/mL)	DTNB (µL) (4mg/mL)	Reaction buffer (µL)	Molar ration DTNB : rHSA
M1	560	0	2240	0.0
M2	560	10.5	2229.5	0.3
M3	560	28	2212	0.7
M4	560	42	2198	1.0
M5	560	84	2156	2.0
M6	560	168	2072	4.0

Table 27- The volume composition of the standard samples of DTNB and N-rHSA in the phosphate reaction buffer of 100mM potassium phosphate buffer pH8 containing 1mM EDTA.

DTNB Standard	DTNB (µL) (4mg/mL)	Reaction buffer (µL)
A	0	2800
B	10.5	2789.5
C	28	2772
D	42	2758
E	84	2716
F	168	2632

2.7 Instruments

1.   Analytical HPLC was performed on an Alliance 2695 HPLC system (Waters Corporation, Milford, USA) equipped with a 2996 PDA detector. Three types of HPLC columns used were: strong anion-exchange SOURCE 15Q 4.6/100 PE, (code 17-5181-01, lot 10178855, ID 0008, GE Healthcare Life Sciences, UK) and C_{18} column YMC-pack ODS-AQ 5.0 µm, 150 × 4.6 mm (YMC, Japan).

2.   Digital mini vortexer , CAT No. 128103 (3300rpm/sec, Fisher, USA).

3.   66411 ST. NAZAIRE Centrifuged 5000 rpm (Jouan DBV, France).

4.   UV-1800 Shimadzu (UV/Visible) Scanning Spectrophotometer (Shimadzu Corporation, Analytical Instrument Division, Kyoto, Japan).

5.   pH meter (0-14) (Denver instrument, USA).

6.   Thermo Scientific Barnstead D4641 E-Pure Ultrapure Water Purification System, serial No. 10900306, 18.2 Megohm-cm Resistivity, <10 ppb TOC, 2.5 LPM, 120V (Thame, UK).

7.   Gel electrophoresis consist of Bio-RAD running tank (chamber invitrogen Novex Mini-Cell with Voltage supply Model No. power Pac, Max power 150AV, frequency 50/60Hz (Singapore).

8.   Size Exclusion Chromatography was performed using a Shimadzu Isocratic HPLC system consisting of SCL-10A VP system controller, SPD-10A pump and LC-10AT UV-VIS detector with data collection by Shimadzu EZStart chromatography software version 7.3 (Shimadzu Corporation, Analytical Instrument Division, Kyoto, Japan). the SEC column was TSKgel G2000SW (7.8mml I.D. x 30.cm) 5µm.

9.   Sartorius Mechatronics analytical balance 1601A MP8-1 (Epsom, UK) and a Denver instruments M-220D balance (USA) both having a readability of 0.1mg.

10.   Perkin Elmer Multi-probes II plus Liquid Handling Sample Processor, fitted with a 4 tip pipetting arm, controlled by WinPREP® software (PerkinElmer Life and Analytical Sciences, USA).

11.   Eppendorf centrifuge 22331-Hamburg, Max speed 14500 rpm (Germany).

12.   IsoTemp -water bath serial 302N0060 (Fisher Scientific, UK).

13.   IsoTemp- incubator 600 series-Model : 625F (Fisher Scientific, UK).

14.   IsoTemp- Magnetic Stirrer- serial 401N0060 (Fisher Scientific, UK).

15.   Microplate Reader BioTek Instrument 210657 (BioTek, USA).

16. Thermo Scientific Heto Power Dry LL3000 Freeze Dryer, Electron Corporation, Model RV12, code No. A655-01-903 (Electron Corporation, USA).

Chapter 3

3 Analytic method development for the partitioning of Ovalbumin in ATPS

Introduction:

The partitioning of proteins and other biomolecules in Aqueous Two phase Systems (ATPS) has been applied to the analytical characterisation of biomolecules and to large scale biomolecule purification schemes, including a number of industrial applications, with in some cases reasonable separation efficiencies and recoveries (22). The technique has also been successfully used for the separation of virus and virus-like particles and to monitor the post-translational modifications of proteins as biomarkers of disease processes. In Bioprocessing the technique seems readily adaptable to continuous processing and in analytical applications to automated high-throughput modes. In addition partitioning may be used to determine ligand binding, molecular association, critical quality attributes and the presence of molecular variants (22). ATPS partitioning is simple to implement; and although normally thought of as purely quantitative can potentially yield significant structural information through the interactions between the analyte and the aqueous environment of the ATPS (21).

Analytically, the optimum K value for the analyte should be neither too high nor too low. A high or low partitioning coefficient could lead to large variations in the measurement of the partition coefficient since low concentrations of the analyte will be present in one phase perhaps approaching detection limits compared to very large concentrations in the other phase whose determination may involve considerable dilution leading to large uncertainties in the measured K value. On the other hand, close to the critical point the analyte will almost partition equally between the phases. Thus a reasonable choice might be to select an ATPS having a modest K value. In general, the partition of the analyte between the phases depends upon its surface properties. Since the Partition Coefficient represents a thermodynamic constant under the specific conditions of the experiment, the logarithm of the K value may be considered to be a function of several interacting properties encapsulated by:

$$ln\,K = lnK_0 + lnK_{charge} + lnK_{hydrophobicity} + lnK_{affinity} + lnK_{size} + lnK_{conformation}$$

Where charge, hydrophobicity, affinity, size and conformation are a factors contributing to the partition coefficient and K^0 is a constant including all other factors (22).

The contents this chapter gives details of the development and optimization of the methods required to support the analysis and characterization of the partitioning of model proteins in ATPS and to reduce the time and effort required for the analysis.

Aims and Objectives

The aims and objectives of this chapter were:

1. To establish analytical methods and operating conditions for the separation and quantification of ovalbumin isoforms using Strong Anion Exchange Chromatography.
2. To establish laboratory procedures and mathematical methods for the construction of ATPS coexistence curves based on cloud point titration and to fit the tie lines to these curves using the mathematical methods of Merchuk (99) to yield a graphical and mathematical representation of ATPS binodal curves.
3. To establish working protein assay methods applicable to the determination of protein concentrations to enable the quantification of protein concentrations in the phases of the ATPS used.
4. To establish and examine the use of a protein partitioning isotherm method (23) to determine the partition coefficient and its relationship with concentration and solubility.

3.1   Anion Exchange Chromatography of Ovalbumin isoforms

3.1.1 Background:

Appropriate separation conditions and methods were required to resolve the partitioning of the different isoforms present in commercial ovalbumin preparations. Chromatography on a strong anion exchange resin was selected.

Strong Anion-exchange chromatography (SAX) separates proteins on the basis of accessible surface charges and their corresponding electrostatic interaction with the column's stationary phase (108). This approach required the establishment of the appropriate chromatographic regime including selection of an appropriate running buffer, sample loading conditions and elution conditions. In the first step an appropriate running buffer (column equilibration buffer) was selected so that an appropriate baseline could be established, substantially free of interferences and contaminants.

Ranges of operating parameters that can be changed in order to manipulate the resolution have been examined. Different eluents have been used for improving the resolution of HPLC and to get better separation as described in section 2.2.1 Careful consideration for analysis would seem to be fundamentally valid for all chromatographic techniques as requirements of successful method development.

To demonstrate how the type of eluent is important, different eluents and gradient were used to get a good baseline for the model protein, using different gradients to modulate the interaction of the analyte with the column.

3.1.2 Results and discussion

Obviously, there are several possible protocols for optimizing resolution. Sodium chloride is the most commonly used eluent for protein separation by ion-exchange chromatography; it has no significant effect on protein structure.

Tris buffer was used as an eluent for the ion exchange column, being used to separate the negatively charged protein and their isoforms on a positively charged surface.

A good baseline must be established for the analyte which will be displaced with a mobile phase containing ions that are more strongly attracted to the stationary phase sites reducing the interaction of the analyte with the column surface.

Modification of the gradient program of the mobile phase can lead to improvements in the selectivity of the column. Buffer A 20mM Tris pH 8.5 was used to equilibrate the

column for 2min, then buffer B 20mM Tris containing 500mM NaCl was used with a different gradient program flow for 15min (following the Table 3 in section 2.2.1) to examine whether a good baseline could be achieved.

The chromatograms shown in Figure 6 indicated that Tris as an eluent was a poor choice regardless of gradient or control method. There are several reasons why the baseline absorbance may be poor.

It could be that the gradient slope is too steep or the column is poorly packed, or it might be that the buffer has precipitated on the column or the column is contaminated, or the column has been overloaded. However, in the case of Tris as eluent it seems here that the extraneous peaks that were seen during elution without any sample present may relate to the presence of impurities in the Tris buffer which showed a high interaction with the column stationary phase up to a salt concentration of 10% NaCl.

Another attempt was made to enhance the baseline absorbance by using phosphate buffer as an eluent which was prepared in section 2.2.1 and following the experimental conditions in Table 4. Using this buffer improved the baseline performance during elution; the chromatogram appeared as a smooth baseline showing fewer major contaminants which appeared to be suitable for the analysis of ovalbumin isoforms.

From replicated runs of phosphate buffer without protein sample through the anion exchange column a smooth baseline was achieved.

It should be mentioned that these results are representative of many runs that were attempted in order to optimise the performance.

In spite of the fact that Tris is a good eluent for many biomolecules unfortunately it was not found suitable under these experimental conditions. In addition, Tris is an organic compound which may contain many impurities.
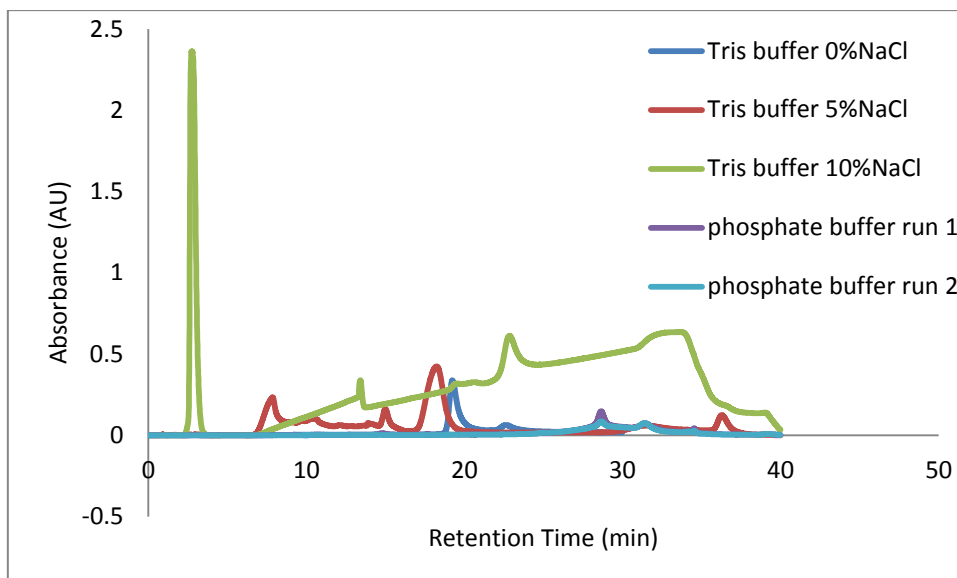
Figure 6- HPLC chromatograms for the analytical profile of Tris and phosphate buffers under the operating conditions: Strong anion-exchange (SAX) Column SOURCE 15Q 4.6/100 PE, flow rate: 0.5 mL/min. Temperature: 25 °C. Injection Volume: 100 µL. Detection: UV, 230 & 280 nm.

3.2 Optimisation of Resolution by Adjustment of Salt Gradient Profile

3.2.1 Background:

Having established suitable operating conditions in terms of employing a suitable running buffer giving a stable baseline, further experiments were performed following the experimental procedure in section 2.2.2 to optimise the resolution of ovalbumin isoforms by adjusting the loading conditions and the salt gradient profile. The shape and duration of the salt gradient was adjusted in order to modulate the interaction of the protein with the column to improve the protein's adsorption and separation efficiency.

3.2.2 Results and discussion:

Manipulation of the duration and final eluent concentration of a linear gradient (continuous elution) is the method of choice for the optimization of column chromatography to achieve higher resolution of the loaded analytes and to show the ability of the chromatographic system to distinguish between the two components of interest and/or one component and their population. Ovalbumin protein samples were prepared and applied to the SAX column whilst using different compositions of the phosphate buffer gradient following the flow program shown in Table 5 section 2.2.2
All runs had an identical elution profile but differed in the starting and ending concentration of the gradient.

Adjusting the slope and final concentration of the initial salt gradient by increasing the concentration of the gradient by 2% with a linear gradient from 0 to 10% buffer B lead to earlier elution of the all protein isoforms and this was advantageous in shortening the analysis time as shown in Figure 7 .
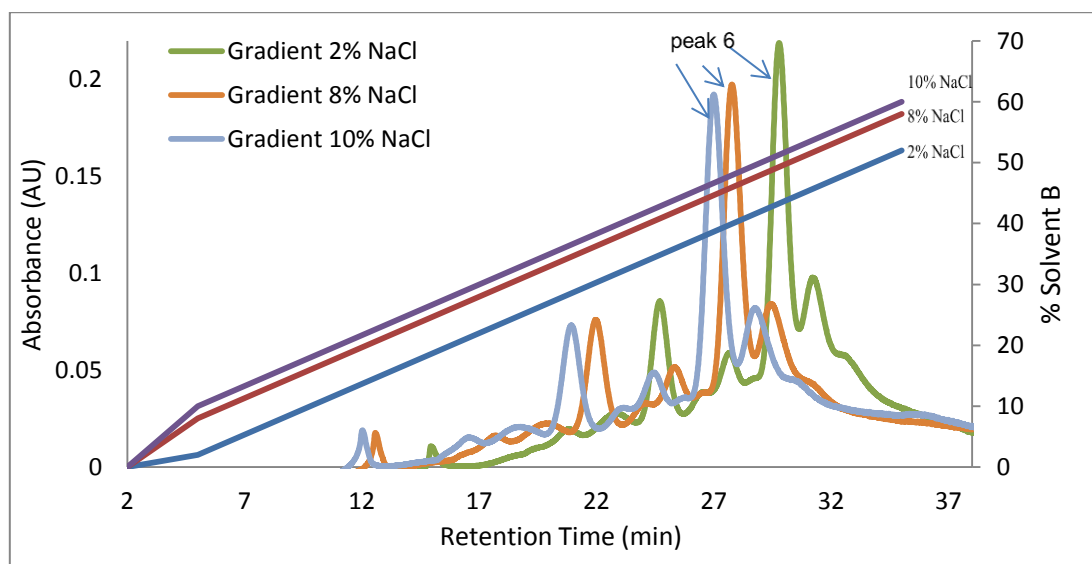
Figure 7- Comparison of the results of salt gradient from 0 to 35 minutes, by 20mM /min of Elution buffer B for the analysis of ovalbumin isoforms using different initial concentrations of NaCl and under the operating conditions: Strong anion-exchange (SAX) Column SOURCE 15Q 4.6/100 PE, flow rate: 0.5 mL/min. Temperature: 25 °C. Injection Volume: 100 µL. Detection: UV, 230 & 280 nm.

As the ionic strength of the mobile phase increases, the rate of analyte migration along with the column will accelerate. 10% (50mM) gradient NaCl represented the starting gradient concentration with 60% (300mM) as an ending gradient concentration which was enough to give effective separation and earlier eluting peaks.

The steepness gradient as controlled by the mobile phase starting and ending composition improved the retention time of the protein elution and resulted in isoforms eluting from the column in order of increasing charge.

Apparently, increased solvent composition by changing the gradient during the run has advantages in elution pattern, NaCl is an anionic compound which competes with analyte ions for sites on the resin, so increasing the concentration of salt decreased the time required (see Table 28) to elute the protein isoforms whilst maintaining the resolution of the peaks. Thus the 10% NaCl gradient was selected as the optimized elution method in all later experiments.

Table 28- HPLC gradient elution programme and the compositions of mobile phase showing the time course and mobile phase composition for equilibration and elution buffers when using phosphate as running buffer.

No. of samples	Start gradient compositions		Final gradient compositions		Retention time for the peak No.6
	Solvent A (%)	Solvent B (%)	Solvent A (%)	Solvent B (%)	
1	99.0	1.0	49.0	51.0	30.02
2	98.0	2.0	48.0	52.0	29.78
3	96.0	4.0	46.0	54.0	29.17
4	94.0	6.0	46.0	56.0	28.53
5	92.0	8.0	42.0	58.0	27.77
6	90.0	10.0	40.0	60.0	26.99

3.3 Preparation Phase Diagram of the polymer-polymer and polymer-salt systems

3.3.1 Background

A phase diagram is a graphical representation which summarizes all experimental data (composition of the two phases) to study and understand the partitioning process. It describes the equilibrium conditions (more information about the phase diagram can be found in the introduction). There are potentially hundreds of different phase systems that form at different concentrations depending on the salt used, the polymers used, and the pH of the systems. By defining the binodal and constructing the tie-lines to describe the phase diagram the position and composition of individual systems can be accurately located within the phase diagram. The main aim in this experiment was to prepare a phase diagrams to be the key to understanding solute partition in that the TLL represents the chemical potential difference between the phases. The partition coefficient is completely dependent on this factor, thus it is necessary when comparing K values, to know that they were obtained at the same tie line length. Knowledge of the phase diagram enables specific systems to be made having selected values of TLL and volume ratio (16). All phase diagrams were prepared following the experimental procedure as described in section 2.2.3

3.3.2 Results and discussion

Initial phase diagrams were determined utilizing PEG8000 and Dextran500 from two different suppliers, stock solution of the polymers were prepared following paragraph (B1) in section 2.2.3 the constructed phase diagram was used in the manual and automatic preparation of aqueous biphasic systems for protein characterization, and supported the development of the modelling and prediction of protein partitioning in aqueous two-phase systems. The composition of phases offers a range of physical and chemical environments in which to study the partitioning of solutes.

Fisher Dextran product (Lot126401) was used to prepare the phase diagram of PEG8000 - Dextran500 system; Table 29 shows the compositions of the total system and the % w/w of both PEG and Dextran in the upper and lower phases.

Table 29- Experimental Composition of selected Tie Lines in the system PEG8000 – Dextran500 (using Dextran500 supplied by Fisher).

Tie line No.	Total System			Bottom Phase			Top Phase		
	Dextran % w/w	PEG %w/w	Buffer % w/w	Dextran % w/w	PEG %w/w	buffer % w/w	Dextran % w/w	PEG %w/w	buffer % w/w
1	4.79	5.04	90.18	11.27	1.19	87.53	1.96	6.71	91.32
2	5.99	6.00	88.01	16.54	0.79	82.66	1.38	8.27	90.33
3	7.01	7.02	85.97	23.22	0.75	76.01	1.10	9.29	89.59
4	7.98	8.01	84.01	24.82	0.81	74.36	0.74	11.10	88.14
5	8.99	9.00	82.00	27.42	0.99	71.57	0.52	12.68	86.79

The binodal curve shown in Figure 8 was determined by fitting the Merchuk equation to the experimental data. The equilibrium polymer concentrations are expressed in terms of % w/w and the binodal curve reflects the critical concentration of polymers in the two phases. The two phase diagrams were almost identical but a difficulty was encountered in fitting the tie lines to the binodal since the empirical equation used contains a constant, a, which represents y when x=0. Tie lines could not be fitted beyond the extent of the binodal on the ordinate because of this.

In order to do so the axes were reversed (as shown in the second phase diagram). In addition the Dextran used in this experiment proved to be highly coloured (yellow)

through the presence of contaminants. Thus a second phase diagram using higher quality Dextran was prepared.
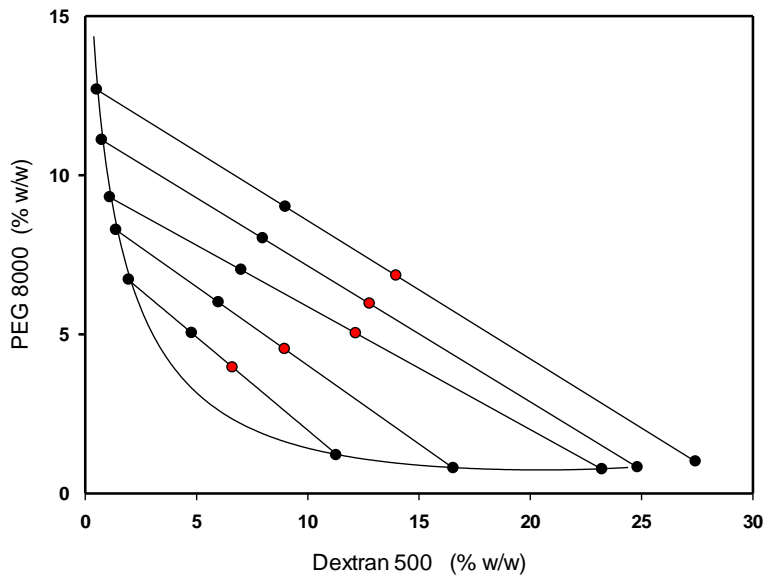
Figure 8- Experimentally determined first phase diagram for the PEG 8000 – Dextran 500 system showing tie lines, ● represents actual system compositions prepared, ● represents the calculated systems compositions at mass ratio = 1.

A second phase diagram was prepared using same procedure using Dextran which was purchased from Sigma-Aldrich. Table 30 illustrates the experimental total system compositions.

Phase diagram shown in Figure 9 obviously indicates that the empirical equation gives a rather good fit to the data using the Merchuk equation following reversal of the axes.
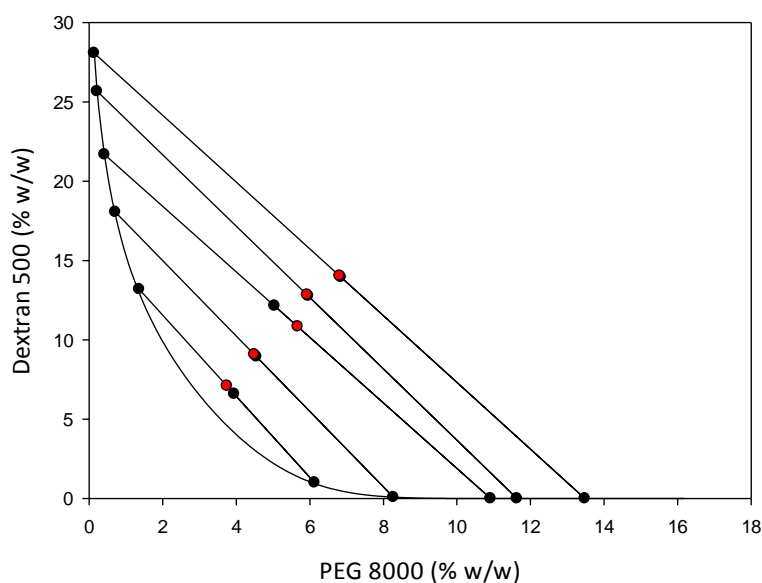
Figure 9- Binodal curve for (PEG8000 – Dextran500) aqueous two-phase system, binodal curve determined by cloud point titration and ● the compositions of several fitted tie lines with ● total system composition when mass ratio = 1.

Table 30 - Experimental Composition of selected Tie Lines in the system PEG8000 – Dextran500 (using Dextran500 supplied by sigma-Aldrich)

Tie line No.	Total System			Bottom Phase			Top Phase		
	Dextran % w/w	PEG %w/w	buffer %w/w	Dextran % w/w	PEG %w/w	buffer %w/w	Dextran % w/w	PEG %w/w	buffer %w/w
1	6.59	3.94	89.47	1.00	6.13	92.87	13.19	1.36	85.45
2	8.95	4.54	86.51	0.09	8.27	91.64	18.07	0.71	81.23
3	12.15	5.04	82.82	$7.55e^{-4}$	10.92	89.08	21.69	0.42	77.90
4	12.78	5.95	81.27	$1.32e^{-4}$	11.64	88.37	25.68	0.21	74.11
5	13.96	6.84	79.19	$5.53e^{-7}$	13.48	86.52	28.08	0.13	71.78

This table represents potential experimental systems of increasing tie line length but with equal mass of phases (for the PEG-Dextran system these will also be nearly volume ratio one systems since densities are close to one and differ by only a small amount). Since the phases are of equal mass, sampling is made easier and any concentration effects of varied volume ratio are eliminated. However, by making a comparison between the two phase diagrams, slight differences in TLL can be seen

under the effect of the different commercial Dextrans and the Table 31 illustrates the results.

Table 31- Phase compositions of the PEG8000 – Dextran500 system at different TLL under the effect of the different Dextran supplier

No. of Tie line	First phase diagram Total composition mass ratio1			No. of Tie line	Second phase diagram Total composition mass ratio1		
	PEG (%w/w)	Dextran (%w/w)	TLL		PEG (%w/w)	Dextran (%w/w)	TLL
TL1	3.95	6.62	10.82	TL1	3.74	7.097	13.08
TL2	4.53	8.97	16.91	TL2	4.49	9.08	19.50
TL3	5.03	12.17	23.71	TL3	5.67	10.85	24.10
TL4	5.96	12.79	26.18	TL4	5.93	12.84	28.11
TL5	6.84	13.98	29.34	TL5	6.81	14.04	31.09

Selection of a suitable phase system is a crucial and the most important step in the development of systems for ATPS partitioning. In general the properties of PEG/ salt systems such as economical cost and low viscosity are thought to be important in downstream recovery operations (28). In order to study the ability of the partitioning technique to act as a probe for protein modifications it was necessary to construct more phase diagrams and these were PEG600- Na_2SO_4, PEG600-$(NH_4)_2SO_4$ and PEG1000-$(NH_4)_2SO_4$.

Preparation of the PEG600-Na_2SO_4 system

Following the methods for the preparation of the stock solutions as described in paragraph (B2) section 2.2.3 and the experimental technique given in paragraph (A) in the same section, the binodal of the PEG600-Na_2SO_4 system was determined by cloud-point titration. The solution undergoes phase separation at a total polymer weight fraction above several weight percent. Tie lines connecting coexisting equilibrium `following the method of Merchuk et al. The slope of the tie line (STL) was determined as the ratio STL = (Δ PEG)/ (Δ salt) where Δ represents the difference in the concentration of polymer and salt in the two coexisting phases.

After defining the binodal and constructing the tie-lines to describe the phase diagram the position and composition of individual systems can be accurately located within the phase diagram as shown in Table 32.

Table 32– Experimental phase composition of the PEG 600- Na$_2$SO$_4$ system.

Tie line No.	Total System			Top Phase			Bottom Phase		
	Salt (%w/w)	PEG (%w/w)	buffer (%w/w)	Salt (%w/w)	PEG (%w/w)	buffer (%w/w)	Salt (%w/w)	PEG (%w/w)	buffer (%w/w)
1	8.00	19.98	72.01	3.50	28.4	68.09	13.24	10.18	76.58
2	9.00	20.99	70.00	1.98	34.36	63.65	16.91	5.928	77.16
3	9.99	21.99	68.01	1.44	37.36	61.19	18.74	4.254	77.0

The tie lines were determined for the system Table 33 Shows the TLL phase equilibrium compositions (Mass ratio 1) by % w/w and Figure 10 Shows the phase diagram for the system PEG600-Na$_2$SO$_4$.

Table 33- Experimental Composition of selected Tie Lines of the PEG600-Na$_2$SO$_4$ system.

No. of Tie line	TLL composition of PEG600/Na$_2$SO$_4$ phase diagram		
	(% w/w) PEG-600 (100% stock)	(% w/w) Na$_2$SO$_4$ (14% stock)	TLL
TL1	20.22	7.98	20.66
TL2	21.21	8.97	32.12
TL3	22.34	10.00	37.35
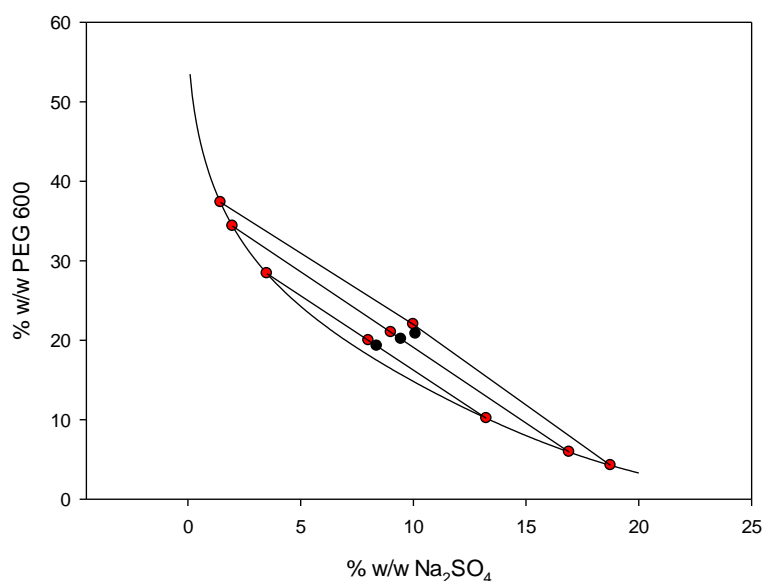
Figure 10- Binodal curve for the phase diagram of the PEG600-Na$_2$SO$_4$ system showing the tie lines, ● represents actual system compositions prepared, ● total system composition when mass ratio = 1.

Certain practical difficulties were found in implementing the PEG600-Na$_2$SO$_4$ system these were the maximum solubility of the salt which was found to be 14%, thus to prepare the phase diagram the amount of salt in the stock solution cannot be increased beyond this point which left little available volume for the addition of sample. Density difference between the polymer and salt will raise and that will lead to increase in the interfacial tension.

Preparation of PEG600- (NH$_4$)$_2$SO$_4$ system

Due to the difficulties in preparing a working PEG600-(NH$_4$)$_2$SO$_4$ system, another PEG-salt system was selected namely a PEG600- (NH$_4$)$_2$SO$_4$ system. Following the preparation of the stock solution in paragraph (B3) section 2.2.3 several defined two-phase system compositions were made, the binodal was determined and the Tie lines were constructed.

The experimental results for the phase diagram composition of PEG600- (NH$_4$)$_2$SO$_4$ system is shown in Table 34 and Figure 11

Tie-lines constructed across the two phase region of the phase diagram are shown in Table 35 and representing the compositions having a mass ratio of one.

Table 34- Experimental phase compositions of PEG600- $(NH_4)_2SO_4$ system at a different TLL.

Tie line No.	Total System			Top Phase			Bottom Phase		
	Salt % w/w	PEG % w/w	buffer % w/w	Salt % w/w	PEG % w/w	buffer % w/w	Salt % w/w	PEG % w/w	buffer % w/w
1	17.00	17.04	65.96	6.27	30.87	62.86	27.67	3.301	69.02
2	18.90	19.13	61.97	3.43	37.79	58.78	34.11	0.78	65.11
3	21.02	20.90	58.10	2.07	42.64	55.29	39.06	0.18	60.76
4	22.0	22.0	56.01	1.55	45.14	53.31	41.37	0.08	58.56
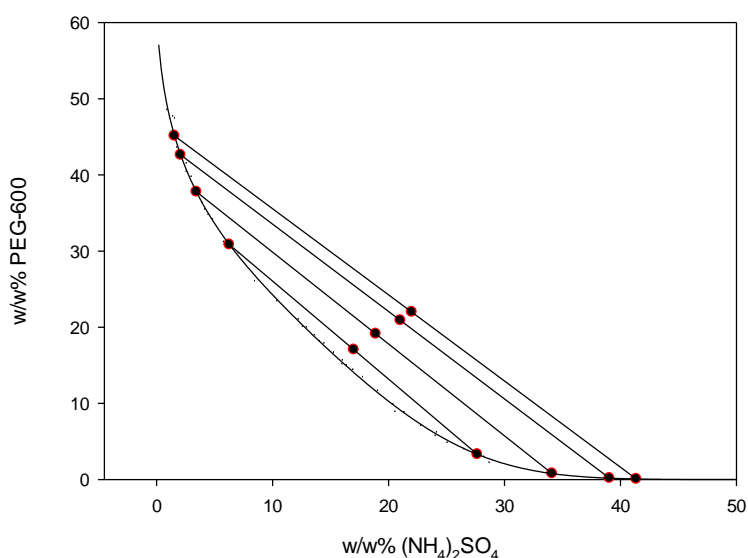
Figure 11- Binodal curve for the phase diagram of the PEG600 - $(NH_4)_2SO_4$ system showing the tie lines, ● represents actual system compositions prepared, ● total system composition when mass ratio = 1

Table 35- Experimental phase composition of selected Tie Lines in the PEG600-$(NH_4)_2SO_4$ system at a mass ratio = 1.

No. of Tie line	PEG600-$(NH_4)_2SO_4$ phase diagram TLL		
	% w/w PEG-600 (50% stock)	% w/w $(NH_4)_2SO_4$ (40% stock)	TLL
TL1	17.09	16.97	34.89
TL2	19.29	18.77	48.07
TL3	21.41	20.57	56.31
TL4	22.61	21.46	60.14

Preparation of PEG1000-(NH$_4$)$_2$SO$_4$ system

In a further attempt to find a suitable analytical PEG-salt system the PEG1000-(NH$_4$)$_2$SO$_4$ was selected. Since increasing the PEG molecular weight and decreasing the concentration of salt in the system would be expected to affect the partition coefficient of the biomolecule and to increase its solubility.

The phase diagram of this system was prepared following the preparation of stock solutions as described in paragraph (B4) section 2.2.3 and the experimental technique given in paragraph (A) in the same section.

The phase diagram was constructed using PEG1000 and Ammonium Sulphate.

Table *36* Shows the experimental composition of the PEG1000-(NH$_4$)$_2$SO$_4$ ATPS for each component in each phase, Table 37 shows the phase equilibrium compositions by % w/w for a range of TLL at mass ratio one and *Figure 12* shows the phase diagram of the system.

Table 36- Experimental phase composition of PEG1000-(NH$_4$)$_2$SO$_4$ system at a different Tie lines.

Tie line No.	Total System			Top Phase			Bottom Phase		
	Salt % w/w	PEG % w/w	buffer % w/w	Salt % w/w	PEG % w/w	buffer % w/w	Salt % w/w	PEG % w/w	buffer % w/w
1	14.98	15.03	69.99	11.42	20.30	68.28	18.24	10.19	71.57
2	14.69	16.42	68.89	7.30	27.26	65.43	21.70	6.14	72.16
3	15.07	16.96	67.97	5.55	30.67	63.78	24.07	4.01	71.93
4	16.92	16.88	66.20	5.25	31.30	63.44	29.73	1.05	69.22
5	18.02	17.84	64.15	3.33	36.05	60.63	31.97	0.54	67.49
6	19.11	18.71	62.19	2.69	38.03	59.29	34.84	0.20	64.96
7	20.10	19.9	60.00	2.43	38.91	58.66	38.53	0.04	61.43

Table 37- Experimental Composition of selected Tie Lines in the PEG1000-(NH₄)₂SO₄ system at a mass ratio = 1.

No. of Tie line	PEG1000/(NH₄)₂SO₄ phase diagram TLL		
	(% w/w)PEG1000 (40% stock)	(% w/w)(NH₄)₂SO₄ (40% stock)	TLL
TL1	15.03	14.98	12.19
TL2	16.42	14.69	25.56
TL3	16.96	15.07	32.46
TL4	16.17	17.49	38.91
TL5	17.84	18.02	45.62
TL6	19.11	18.76	49.64
TL7	20.47	19.47	53.04
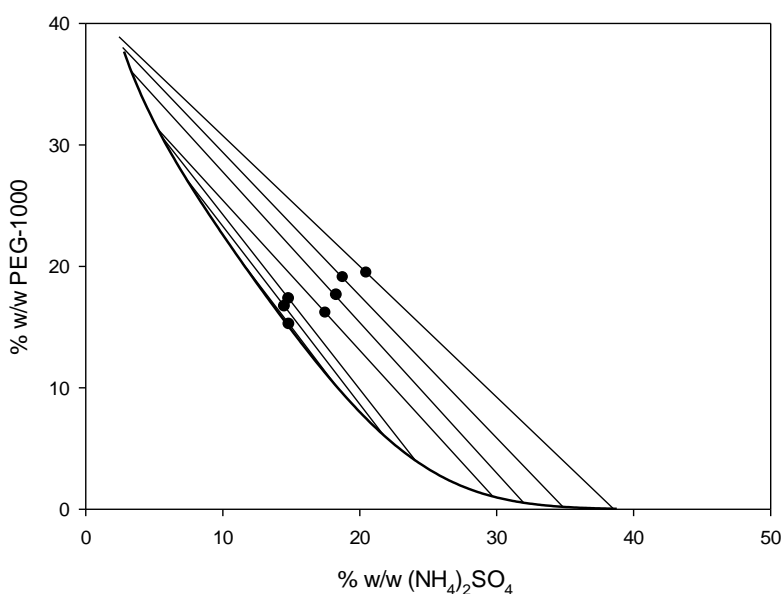
Figure 12- Phase diagram for a PEG1000 and ammonium sulphate (NH₄)₂SO₄ system, ● represents the system compositions when mass ratio = 1.

Preparation of a PEG4600-Dextran500 system

Following the basic rules of partitioning in aqueous two phase systems, the partition coefficient is strongly affected by the molecular weight of the polymers. Replacing the polymer with one of a different molecular weight is useful in selecting a phase system having some desired partition coefficient for the analyte (16). The binodal of the PEG4600-Dextran500 system was determined manually by the cloud point method as

described in paragraph (A) section 2.2.3 after preparation the stock solution as in paragraph (B4) in the same section. The experiment was followed by the determination of the compositions of the upper and lower phases. The system was used to examine the partition coefficient of ovalbumin in its native state and after treatment with ALP.

The data from the construction of the phase diagram of the PEG4600-Dextran500 system is shown in Table 38 including the composition of the equilibrium phases and the overall system composition in % w/w at each TLL, while Table 39 shows the Tie-lines which were constructed across the binodal region as shown in the phase diagram in Figure 13.

Table 38- Composition of selected compositions in the PEG4600 –Dextran500 ATPS.

Tie line No.	Total System			Top Phase			Bottom Phase		
	Dex500 % w/w	PEG4600 % w/w	buffer % w/w	Dex500 % w/w	PEG4600 % w/w	buffer % w/w	Dex500 % w/w	PEG4600 % w/w	buffer % w/w
1	10.5	10.5	79.0	8.23	13.26	78.51	14.44	5.73	79.83
2	11.5	11.5	77.0	6.91	16.35	76.74	19.54	3.1	77.36
3	12.0	12.0	76.0	6.5	17.48	76.02	21.52	2.45	76.03
4	13.0	13.0	74.0	5.82	19.7	74.48	25.35	1.55	7301

Table 39- Experimental Composition of selected Tie Lines in the PEG4600-Dextran500 system.

No. of Tie line	TLL composition of PEG4600/Dextran500 phase diagram		
	(% w/w) PEG4600 (25% stock)	(% w/w) Dextran500 (30% stock)	TLL
TL1	9.5	11.33	9.75
TL2	9.73	13.22	18.31
TL3	9.96	14.015	21.24
TL4	10.62	15.58	26.66
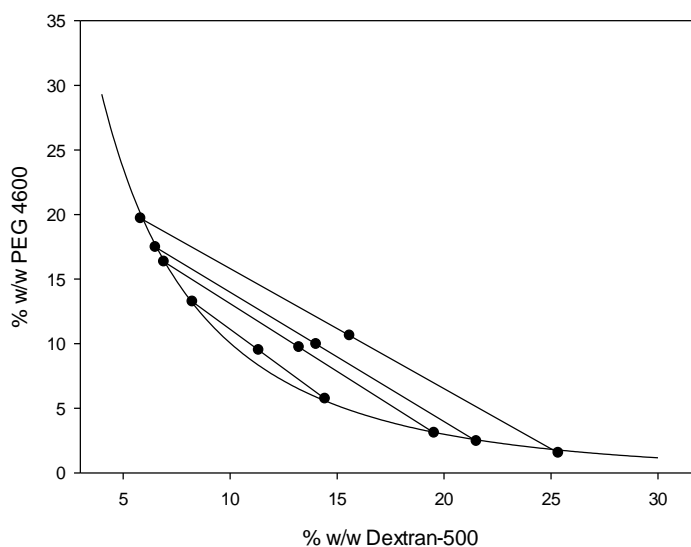
Figure 13- Phase diagram for PEG4600 –Dextran500 system, ● represents the system compositions when mass ratio = 1.

3.4 Determination of Protein Concentration by BCA assay

3.4.1 Background:

The BCA Protein Assay was introduced by Smith, et al. in 1985. BCA Protein Assay is based on bicinchoninic acid (BCA) for the colorimetric detection and quantitation of total protein. The main aim of this experiment was to establish a reliable assay applicable to the quantitation of any "pure" protein in the aqueous two phase systems following the experimental procedure in section 2.2.5

3.4.2 Results and discussion:

Selection of a reliable, quantitative and accurate protein assay is essential for a given sample and also for correctly evaluating results. Clearly, accuracy and precision of specific measurements depend as much on accurate calculation of protein concentration. In order to measure protein concentration and consequently the partition coefficient, the BCA assay has been used. The sensitivity of the BCA assay is dependent upon the ratio of working reagent to the sample concentration. These different protocols were examined, the first in which the WR: Sample ratio was 8: 1 and the second in which this ratio was 20:1. The results are shown in Figure 14 going with the most sensitive version might be a mistake as greater sensitivity might imply greater sensitivity to interference (104). The figure below shows the sensitivity of each reagent ratio.
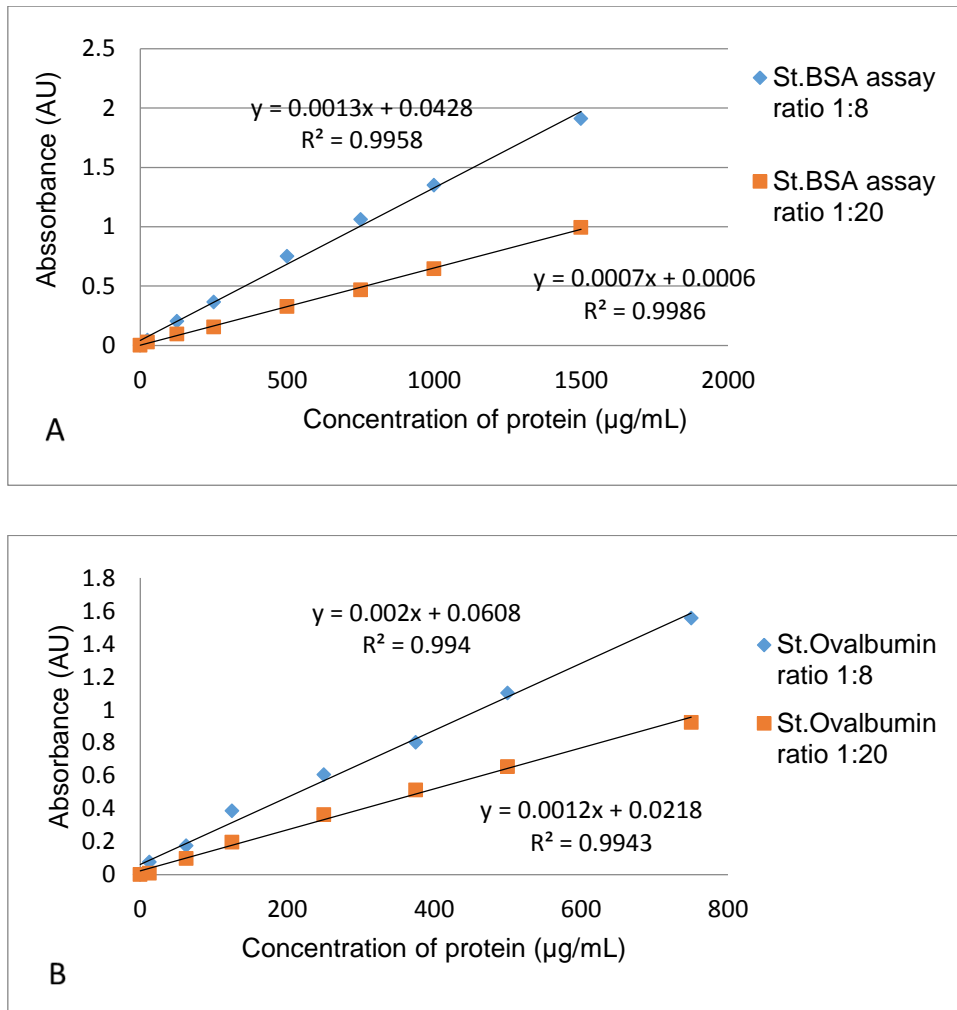
Figure 14- Sensitivity of (A) standard BSA and (B) standard Ovalbumin in the BCA assay using differing ratios of WR: sample (1:8 Microplate Procedure, 1:20 Test-tube Procedure).

A standard curve was prepared using the average blank-corrected 562nm measurement for each BSA standard vs. its concentration in µg/mL which was used to determine the protein concentration of each unknown sample.

Two assay procedures were performed : (1) the Test Tube Procedure requires a larger volume of protein sample; however, because it uses a sample to working reagent ratio of 1:20, the effect of interfering substances is minimized. (2) The microplate Procedure affords the sample handling ease of a microplate and requires a smaller volume (10-25µL) of protein sample; however, because the sample to working reagent ratio is 1:8, it offers less flexibility in overcoming interfering substance concentrations and obtaining low levels of detection. The sensitivity of the assay was examined from the calibration curve using BSA.

3.5 Application of the BCA assay to the construction of a protein partitioning isotherm

3.5.1 Background:

The equilibrium between the concentrations in upper phase and the concentration in lower phase is expected to be linear at low concentrations. In column chromatography this is the region used for analytical determinations whenever possible. At high concentrations there may be departure from linearity, this would often be the case for capture chromatography and for ATPS extractions optimised for productivity.

Other conditions that may affect linearity would be association/ dissociation of the solute and aggregation through low solubility. Effect of the concentration and the solubility of ovalbumin in the ATPS were examined following the experimental procedure in 2.2.6

3.5.2 Results and discussion:

Aqueous two phase systems were prepared with increasing ovalbumin concentration. This method (23) is reported to be sensitive to any concentration dependence of partitioned species as might occur during aggregation. It is also an examination of the linearity of the partition isotherm for un-filtered samples.

At low concentrations of protein K would be expected to be linear with concentration. However at high concentration partition may be influenced by non-idealities, solubility may become limiting and 2nd order protein–protein interactions may become important. Analytically, it prefers that the isotherm to be linear.

Preparatively non-linear isotherms are perhaps inevitable; nevertheless knowledge of the isotherm is still important for its predictive value and the initial experimental results shown in Figure 15
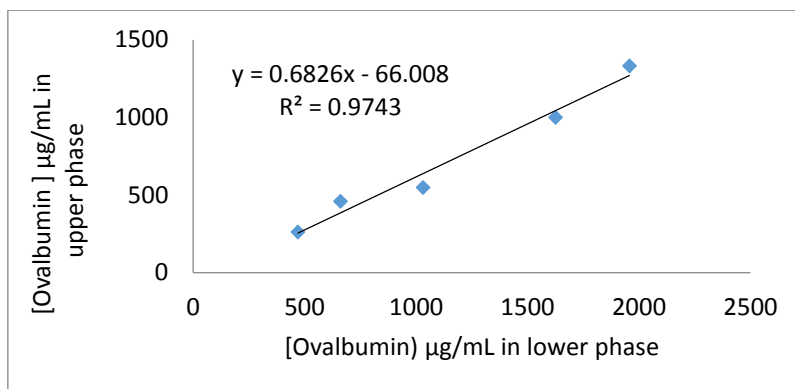
Figure 15- The correlation between the ovalbumin concentration in each phase plotted as a partition isotherm. The partition experiment was performed using increasing concentrations (0.5, 0.75, 1 and 2mg/mL) of ovalbumin.

In order to optimize further experiments on the partitioning of proteins, a study of aggregation was performed; aggregates may be present in commercial samples of ovalbumin and could affect the partition coefficient. Indeed, according to Yoshio (1965) the rate of change in the turbidity of protein solutions increases with increasing protein concentration, temperature, and ionic strength but decreases rapidly with increase in pH above the isoelectric point. (109)

For various reasons, not least their characteristic hydrophobicity proteins to self-associate resulting in populations of monomeric, dimeric and higher order structures (110).

To show if there is a dynamic equilibrium between aggregated and un-aggregated forms filtered and unfiltered ovalbumin samples were partitioned in the ATPS following the experimental procedure in section 2.2.6. The method outlined by Zaslavsky (23) was used which relies on using different concentrations of the analyte prepared and partitioned separately under same ATPS composition, the method also validates the partition measurement and the reproducibility of the experiment. Linear partitioning over a range of concentrations indicates that the coefficient was independent of the concentrations.

Partitioning of filtered and unfiltered ovalbumin samples in PEG8000-Dextran500 system were used to examine the deviation of the protein concentration in the upper and lower phases with the effect of the aggregation

The results show that there was alteration in the concentrations of protein when used filtered and un-filtered solutions, the presence of low concentrations of aggregated

protein can impact protein partitioning and can create defects with partition coefficient measurements, Figure 16   show the concentration of the protein in the upper and lower phases in both cases.

A

B
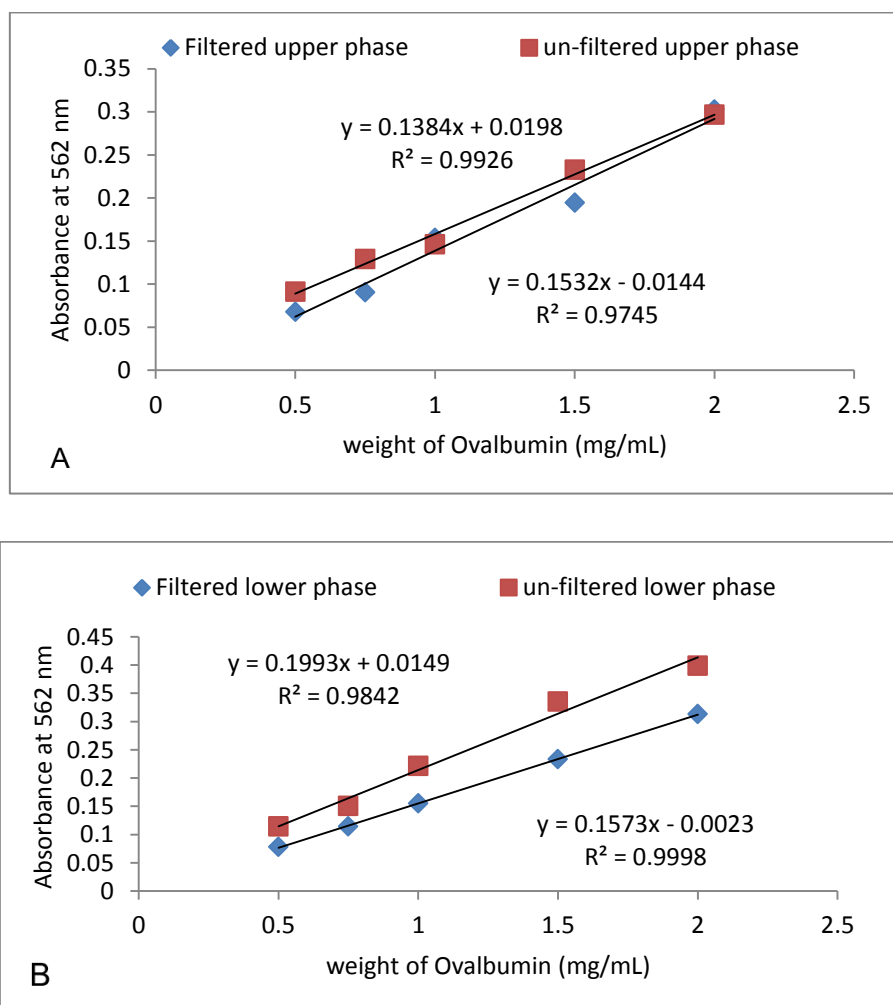
Figure 16- Concentration of Ovalbumin (A) in the upper and (B) lower phases using un-filtered and filtered samples partitioned in PEG8000-Dextran500 system.

Figure 16 shows different behaviour of the protein in the phases comparing filtered and unfiltered samples. The amount of aggregation could be very low, but have a direct influence on the partitioning. Analytically, we looking for linear regression related to their importance in the accurate calculation of the partitioning value of the protein, presence of aggregation could considerably effect the partitioning of the analyte due to their interaction with the system compositions or with the analyte itself   (26). Many efforts have been made to study this phenomenon and the simplest way could be by determining the partition of filtered and unfiltered samples. Figure 17 demonstrates that partitioning in ATPS is a sensitive method to detect self-association and aggregation
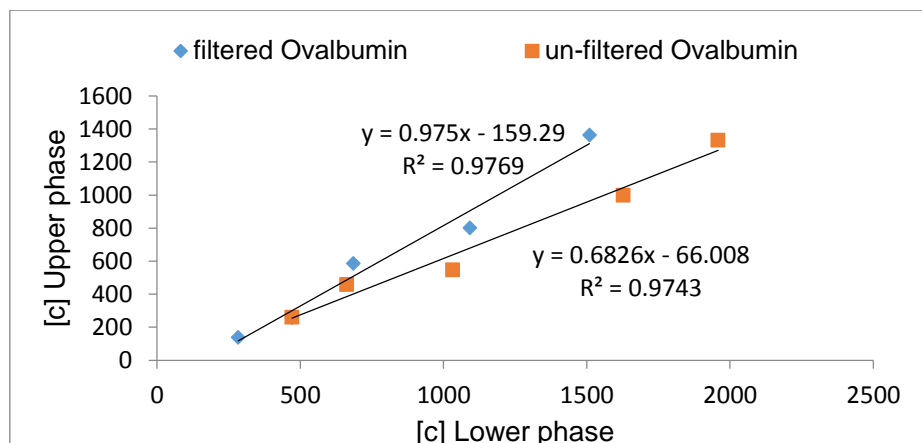
Figure 17- Partitioning of filtered and unfiltered ovalbumin in the PEG8000 - Dextran500 system at the TLL composition 5.67 % w/w PEG8000, 10.85 % w/w Dextran500.

Measurement of K as a non-linear isotherm could imply that aggregation is concentration dependent and actively promoted by the increasing protein concentration and / or the presence of the phase forming components. However there is a difference in the partition of filtered and unfiltered samples this has no effect on the linearity of the plot as concentration increases. However the difference between samples containing aggregates and samples not containing them are clearly detected. This implies that the aggregates present in these samples arose during processing (purification) or during formulation (freeze drying) or upon storage. If there is a dynamic equilibrium present it is hardly detectable under these conditions.

Conclusions:

Initial work concentrated on finding an appropriate chromatographic regime to separate and quantify the variants of a model protein. Ovalbumin was selected as a model protein to begin this study since it is widely and cheaply available and consists of a number of different isoforms with differing glycosylation patterns and degrees of phosphorylation.

The selected method (Strong Anion-Exchange HPLC – SAX-HPLC) was relied upon to characterise subsequent partitioning experiments. A simultaneous measurement of the distribution of ovalbumin isoforms by HPLC and by partitioning was performed. The method was applied to the separation of the ovalbumin isoforms after partitioning in ATPS and it was developed successfully.

Following established of several analytical phase partitioning systems, the behaviour of the protein and their isoforms in different environment of ATPS was examined. Several phase diagrams were successfully prepared allowing informed construction and characterisation (TLL) of analytical ATPS.

Attention was also directed toward investigation of reliable assays for measuring the partition coefficient. A quantitative chemical method (BCA assay) was used to determine the partition coefficient and some difficulties were found in making this accurate and reproducible. This should be reconsidered since the introduction of the different analytical methods to determine the partitioning can be a valuable tool, especially in determining the purity and perhaps in quantifying variants since different methods are based on different aspects of protein structure. It was proved that the absorbance at 280 nm techniques was reliable and easy to implement.

In addition, the importance of the application of the partition isotherm in the partitioning experiment was examined. It showed the ability to detect differences in aggregation which is potentially applicable for instance in examining protein fractions arising during bioprocessing. Also it was examined as an indicator to determine the protein solubility in ATPS. The partitioning isotherm has importance in the limitation of the errors which may result in analytical applications due to overloaded conditions.

Chapter 4

4   Examination of the Partitioning of ovalbumin isoforms in Aqueous Two-Phase Systems

Introduction:

Since the early 1970s, a considerable amount of work on the correlations between the structural characteristics of proteins and their distribution in ATPS has been conducted (16). Understanding the behaviour of proteins based upon their molecular structure should lead to improvement in the design of extraction, fractionation and analytical processes, particularly in the detection and quantitation of protein isoforms and variants (111). Modelling of protein partitioning behaviour centres around the examination of the partition coefficient in relation to molecular structure and has been suggested as a method to distinguish the effects of post-translational modifications on partition behaviour of selected macromolecular analytes (23). Understanding the effects of post-translational modifications should aid in the prediction of protein partition coefficients to the benefit of bioprocessing regimes and in the application of ATPS as an analytical tool for the detection of protein variants in the form of disease biomarkers and in bioprocess quality control. The objective of this chapter was to examine the partition coefficient of Ovalbumin and to distinguish the effects of posttranslational modifications on its partition behaviour using different phase systems.

The practical application of protein partitioning in ATPS has been demonstrated in many cases, including a number of industrial applications, with excellent levels of purity and yield. The technique has also been successfully used for the separation of virus and virus-like particles and to monitor the post-translational modifications of proteins as biomarkers of disease processes (16). In Bioprocessing the technique is readily adaptable to continuous processing and in analytical applications to automated high-throughput modes (112) permitting increased adoption of ATPS based processes and increases the accuracy and reproducibility of the experiments. However, the wider application of this technology is diminished by a lack of a clear understanding of the factors and mechanisms that govern the behaviour of proteins in these systems which has slowed the development of analytical models to aid the rational design of these systems (43). Prediction of protein partition coefficients from structure has yet to be

convincingly demonstrated, this is because protein crystal structures only partially represent the range of isoforms present in the native protein and some post-translational modifications such as glycosylation are poorly represented in crystal structures and only by inference form the amino acid sequence or codon sequences of proteins in structure databases. In order to develop this modelling, an analytical approach was used. Ovalbumin was selected as a model protein for this study since it is readily and cheaply available and comprises several post- translationally modified isoforms differing in degree of phosphorylation and glycosylation. This study aims to begin to outline the structural basis of the partitioning of ovalbumin isoforms.

Enzymatic cleavage of phosphorylation and glycosylation sites will be used to access partially or completely deglycosylated and dephosphorylated ovalbumin isoforms. These novel isoforms will be used to study the influence of phosphorylation and glycosylation on ovalbumin partitioning and to select systems showing greatest contrast in the partitioning of the different isoforms in order to develop sensitive analytical partitioning systems.

Aims and Objectives

The aims and objectives of this chapter were:

1. To study and quantify the partitioning behaviour of ovalbumin isoforms in different ATPS environments including systems based on polymer/polymer and polymer salt phase separation.
2. To define ATPS conditions giving rise to partition coefficients suitable for the analytical discrimination of ovalbumin isoforms.
3. To study the effect of ovalbumin PTMs on the partition coefficient in selected ATPS by enzymatic removal of the phosphate groups using alkaline phosphatase and by enzymatic modification of the glycoforms using neuraminidase and Endo-glycosidase F.
4. To examine the sensitivity of selected ATPS to the altered protein isoforms resulting from the enzymatic modification.

4.1 Separation and partitioning of Ovalbumin isoforms Using Strong Anion Exchange Chromatography

4.1.1 Background:

The study of protein modification by phosphorylation and glycosylation and their roles in biochemical pathways could be employed as an index to enable the interpretation of differences in partition of unknown proteins. Once the effect of such modifications has been identified, it might be possible to use this interpretation to develop quantitative biomarkers for clinical and bioprocessing applications.

The initial aim of this experiment was to analyse ovalbumin isoforms by HPLC, and then to use the partition coefficient as a structural descriptor of the protein for development of a quantitative structure –isoforms relationship. Development of the method for the separation of isoforms will apply later to the examination of the effect of these modifications on the protein partition coefficient in ATPS.

4.1.2 Results and discussion:

The previously established conditions were employed with Strong anion-exchange HPLC to separate ovalbumin isoforms following the experimental procedure **in** section 2.3.1 on the basis of accessible surface charges and their corresponding electrostatic interaction with the column's stationary phase. There are many published studies describing the structure of ovalbumin as a glycoprotein that has a range of structures which differ in the degree and nature of their glycosylation (difference in oligosaccharide profile) and phosphorylation (113) (114) (115) (61)

Ovalbumin samples were analysed by HPLC to identify its isoforms, and the results are shown in Figure 18 which illustrates a typical chromatogram of the protein fractions resolved and the separation of the isoforms achieved.
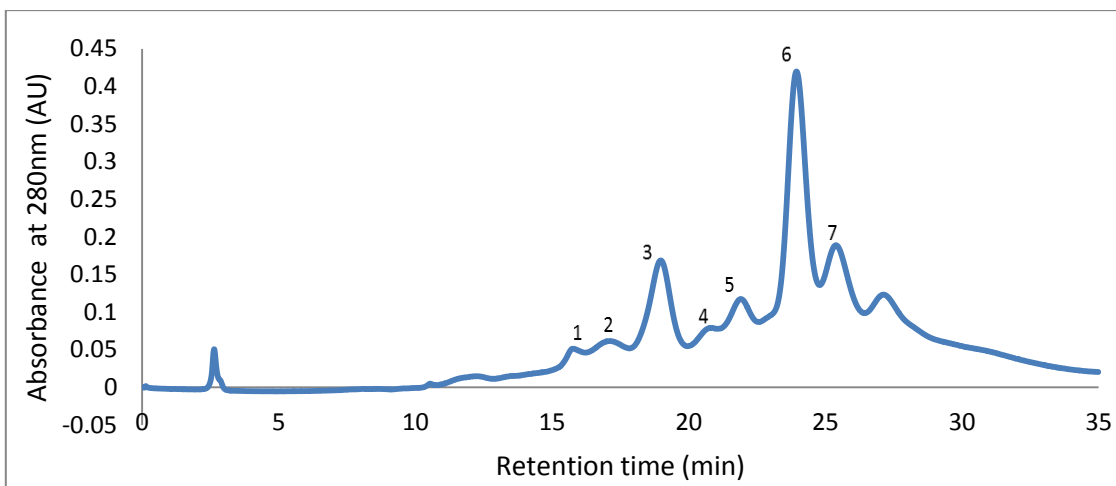
Figure 18- HPLC chromatogram of the separation of Ovalbumin isoforms using operating conditions: Strong Anion-exchange column SOURCE 15Q 4.6/100 PE, Flow Rate: 0.5 mL/min. Temperature: 25 °C .Inj. Volume: 100 µL Detection: UV, 280,230 nm.

The peaks shown in Figure 18 and labelled as peaks 1, 2 and 3 were designated (P0G1), (P0G2) and (P0G3) respectively under the assumption that P0 is an isoform having zero phosphorylation and G1, G2 and G3 represent glycoforms differing in charge. Peaks 4(P1G1) and 5(P1G2) represent ovalbumin with one site phosphorylated and similar glycan variants conveying additional negative charge, while peak 6(P2G1) and peak 7(P2G2) may represent ovalbumin having both phosphorylation sites modified but again with various glycan structures conveying additional negative charge (116). The detailed reasoning behind this characterization of ovalbumin isomers will be discussed in more detail in section 4.4
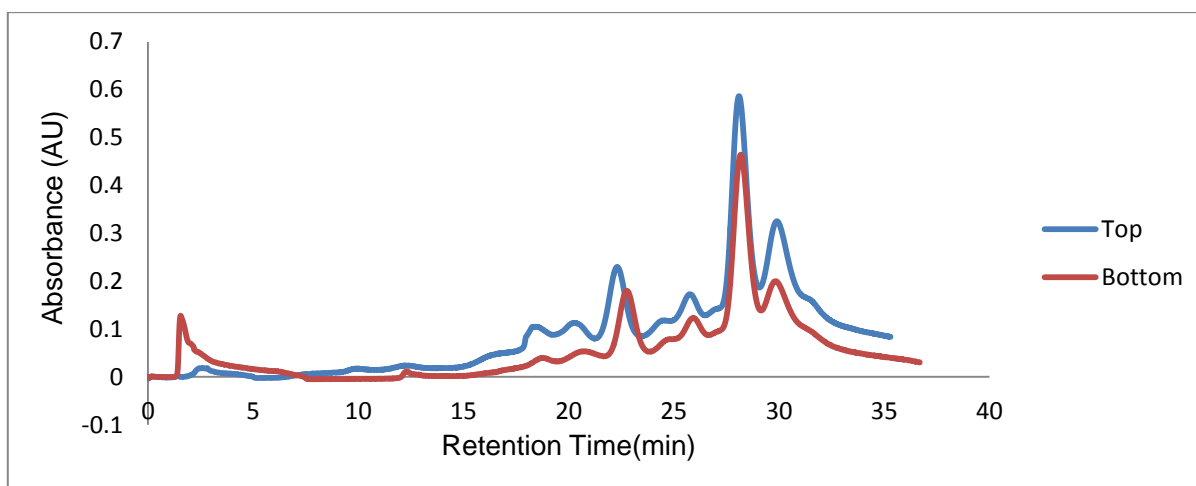
Figure 19- Partitioning of ovalbumin isoforms using Strong anion-exchange (SAX) Conditions: SOURCE 15Q 4.6/100 PE, Flow Rate: 0.5 mL/min. Temperature: 25 °C .Inj. Volume: 100 µL Detection: UV, 230 nm.

117

Ovalbumin is being used as a MODEL protein for the detection of isoforms by phase partitioning. The partitioning of ovalbumin was carried out in a simple way by preparing the ATPS system from solid polymers (PEG and Dextran) and pipetting the protein solution directly into the phase system which was then mixed and the phases allowed to settle and separate prior to sampling. The partitioning of ovalbumin in the ATPS showing identical isoforms in the upper and lower phases. This suggests that interaction between the protein population present and the ATPS environment did not affect the gross structure which had such been apparent might have invalidated this approach as illustrated in Figure 19. In a later experiment where the protein was dephosphorylated using alkaline phosphatase it was possible to tentatively identify the nature of the isoforms separated by this method.

4.2 Study of the effect of pH on the partitioning of ovalbumin isoforms in ATPS and their subsequent analysis

4.2.1 Background:

Charge on the surface of the ovalbumin can be controlled by adjusting the pH of the elution buffer. The isoelectric point, pI, is the pH at which the net charge of the protein is neutral (the number of positive charges is equal to the number of negative charges). If the pH is above the pI, the protein will be negatively charged overall and can be retained on an anion-exchange sorbent. The effects of changing pH on the analysis of ovalbumin isoforms after partitioning in the ATPS were examined following the experimental procedure in section 2.3.2

4.2.2 Results and discussion:

The pH of the ATPS is one of the important factors influencing protein partitioning due to the effect on the surface net charge of the solute. The experiment was designed to study the effect of pH on the partitioning behaviour of the ovalbumin isoforms.

Aqueous two-phase systems differing in pH were used to study the partition conditions in terms of pH. Systems were screened in regard to the partition behaviour of individual isoforms at different pH (5.5, 7, and 8.5). The pH of the partitioning system resulted in a change in distribution through affecting the net charge of the partitioned species. The effect of pH on the partition coefficient was varied; the partition coefficient of ovalbumin was calculated form the peak height at pH 5.5, 7.0 and 8.5 as illustrated in Table 40.

Table 40- Partition coefficient values of the identified ovalbumin isoforms obtained by SAX-HPLC for ATPS of different pH, K values were measured from the ratio of the peak height in the upper and lower phases.

partition coefficient (K)	No. of peak	K at pH 8.5	K at pH 7	K at pH 5.5
	1	1.74	1.13	0.86
	2	1.56	1.21	0.92
	3	1.20	1.10	0.79
	4	1.22	1.12	0.81
	5	1.22	1.08	0.77
	6	1.21	1.08	0.76
	7	1.38	1.10	0.77

Over this pH range the protein has a negative net molecular charge since the pI of ovalbumin is 4.6 (65), at pH 5.5 the protein is partially negatively charged. At pH 7 and 8.5 the protein is fully negatively charged.

Depending on the pH, the ovalbumin was found to favour partition into the upper phase at pH 8.5 under these conditions. The results were shown that there was a variation in the partition coefficient as a result of the influence of pH (see Table 40) Partition at pH 8.5 showed the highest partition coefficient which decreased at lower pH with decrease in the net negative charge of the protein. There was little difference in the partition of the different isoforms except for a suggestion that the least phophorylated forms had a higher partition coefficient than the phosphorylated forms. Compare peaks 1 and 2 to later eluting species. This suggests that in the pH which represents differences in the H$^+$ ion activity might be useful as a tool in the analytical partitioning process when there are present a variety of charged and uncharged structures for the same solute (23).

As a conclusion, each isoform shows an increase in K with increase in partitioning pH. However increasing phosphorylation as distinct from overall charge shows a decrease in K

4.3 Deglycosylation of Ovalbumin for the production of modified ovalbumin isoforms.

4.3.1 Background

Neuraminidase enzymes are sialic acid hydrolase enzymes that cleave the glycosidic linkages of neuraminic acids. It catalyses enzymic hydrolysis of terminal N-acetylneuraminic acid residues from glycoproteins and oligosaccharides. N-linked glycosylation as in ovalbumin occurs when glycans are attached to asparagine residues of the protein amino acid backbone. The method is much gentler than chemical deglycosylation. Removal of Neuraminic acid residues of ovalbumin may be expected to result in a change in the net charge of the protein. Negatively charged neuraminic acid residue is found in complex glycans (see Figure 20).
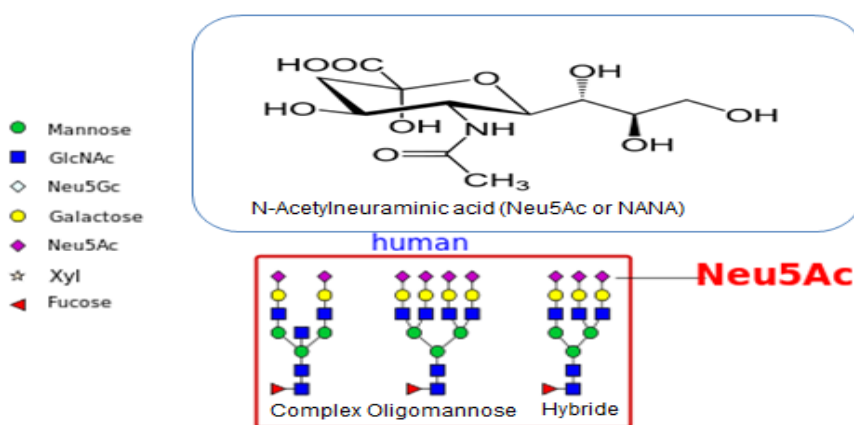
Figure 20- Glycan variation and structure of N-Acetylneuraminic acid (10)

Glycoproteins exist as a heterogeneous population of glycoforms with a single protein backbone. In view of this heterogeneity and the presence of branched structures, the analysis of glycan is much more complicated than protein structure analysis. The importance of studying profiles of glycoproteins is to compare finding in normal and diseased states and in the characterisation of biopharmaceuticals where differences in glycoforms may influence efficacy (8). Neuraminidase could be used for monitoring the modifications of ovalbumin and the actual protein structure without terminal sialic acids with the expectation of seeing differences in elution pattern during SAX and differences in partition coefficient following partition in ATPS.

4.3.2 Results and discussion

Ovalbumin is a glycoprotein that has a range of structures which differ in the degree and nature of their glycosylation, it has been reported that ovalbumin has a four sites of postsynthetic modification; an acetylated N terminus, a carbohydrate moiety which is located at Asn-292 (as shown in Figure 21), and up to two phosphorylated serines (66).
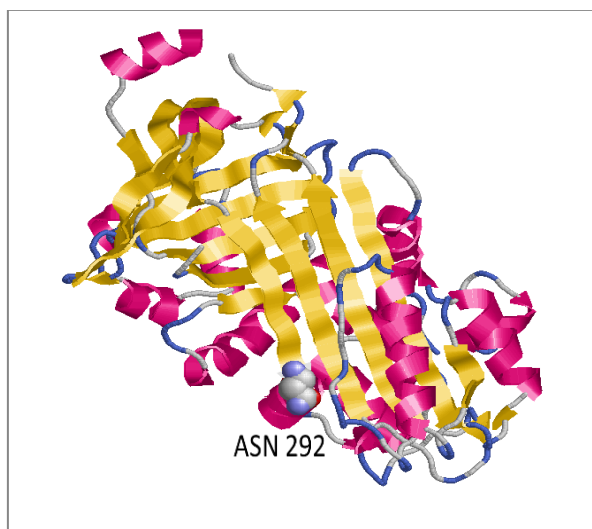
Figure 21- Model Ovalbumin structure showing the amino acid Asparagine 292, the site of carbohydrate moiety (117)

Enzymatic removal of terminal neuraminic acid residues from glycosylated ovalbumin isoforms was attempted using neuraminidase and following the experimental procedure in section 2.3.3. Since each neuraminic acid residue should add one unit of negative charge to glycosylated ovalbumin changes in the number of neuraminic acid residues as a result of enzymatic cleavage should result in changed behaviour during SAX-chromatography and under appropriate conditions during partition in ATPS. In this study the effect of neuraminidase addition on the SAX chromatography of ovalbumin was examined.

Following application of neuraminidase, treated samples of ovalbumin at increasing reaction times failed to show any change in their SAX elution behaviour even after 24 hours (Figure 22). This indicates that the neuraminidase treatment was ineffective in changing the charge distribution of ovalbumin isoforms.

It could be there is a resistance to the action of neuraminidase or the enzyme could not physically access the glycan linkage. Surveys such as that conducted by the National Institute of General Medical Sciences, have shown that in the glycoprotein, there are

two types of linkages between these residues and the carbohydrate moiety: one of these bonds is cleaved readily, while the other is split very slowly (118). However the experiment reported here indicates that neuraminic acid residues if present are inaccessible or unreactive to neuraminidase under the conditions used. Alternatively, Endoglycosidases might represent an alternative strategy for deglycosylation without denaturing the protein. Such a strategy would cleave glycan from a different structural location compared to neuraminidase for instance Endoglycosidase F3 and F2 can remove glycan from biantennary and triantennary structures, while Endoglycosidase F1 can remove Oligomannose and hybrid structures (119).
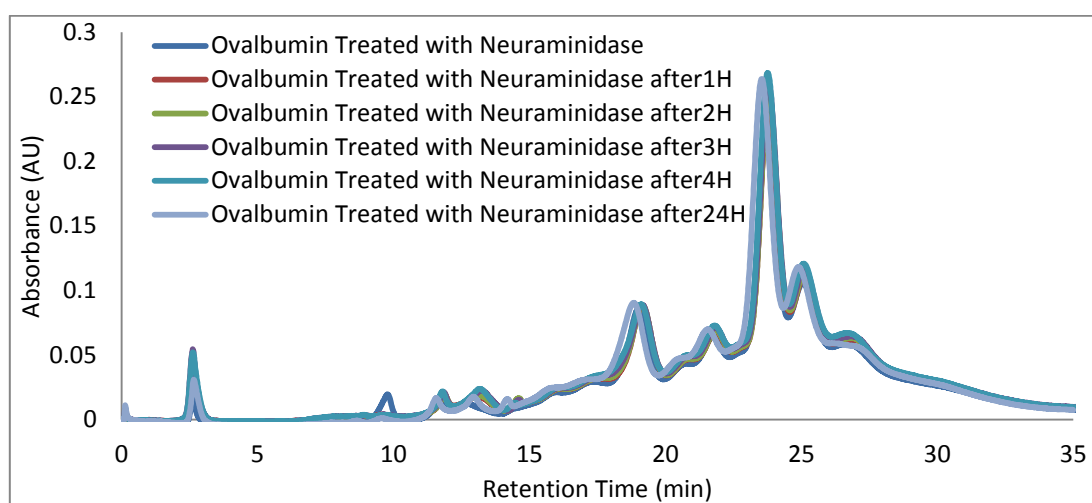
Figure 22- Time course of HPLC elution pattern chromatogram for ovalbumin after treatment with neuraminidase under the operating conditions: Strong anion-exchange (SAX) Column SOURCE 15Q 4.6/100 PE, flow rate: 0.5 mL/min. Temperature: 25 °C. Injection Volume: 100 µL. Detection: UV, 230 & 280 nm.

The goal in developing this approach was to produce different protein isoforms and to see whether these modifications had any influence on the partition coefficient of the protein. An electrophoretic method for detecting changes in the glycosylation state of ovalbumin by electrophoretic separation was performed.

Following the experimental procedure in section 2.3.3, the reaction solutions of the native ovalbumin, ovalbumin treated with Endo-F were examined following SDS-PAGE electrophoresis with subsequent blue-staining.

The protein was observed as a single migration band for each reaction solution, a protein band could be seen in the blue-stained images with almost no changes marked

for the treated and non-treated protein. However conditions used were inefficient for separation ovalbumin isoforms as indicated by the protein band remaining in the gel.

4.4 Alkaline phosphatase for the production of modified ovalbumin isoforms

4.4.1 Background:

Phosphorylated modifications play an influential role on the solubility and stability of many proteins and act as a switch to control biological activity which regulates the function, localization, and binding specificity of target proteins (120). Reportedly, Ovalbumin contains two phosphorylation sites at Ser-68 and Ser-344 (66) as shown in Figure 23.
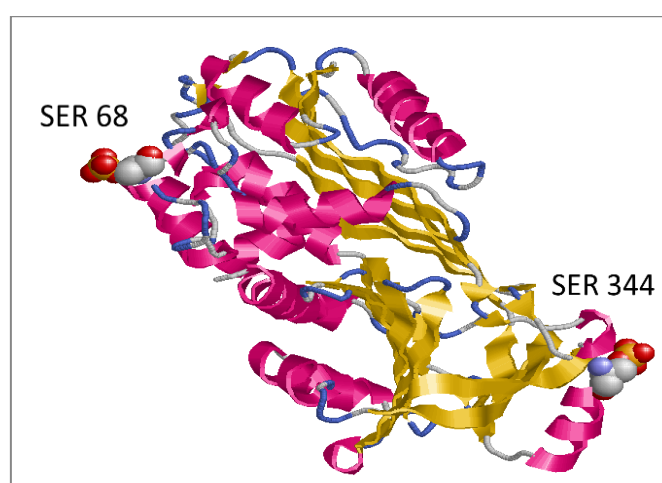
Figure 23- Model protein Ovalbumin with the sites of postsynthetic modification (phosphorylation) of serine 68 and 344 residues (121).

Previous work indicates that Ovalbumin has two phosphorylation sites resulting in two phosphorylated peptides following tryptic digestion (121). Depending on the method specificity and the recovery yield, many methods have been reported for detection of phosphorylated proteins (5) (4). (7) Ion-exchange is a reliable technique and used extensively for separation, quantification and identification of the charge of ovalbumin phosphoisoforms. (122) It was elected to study the ovalbumin phosphoforms following enzymatic cleavage by SAX-HPLC with studies involving partitioning in ATPS.

The main aim of this experiment was to attempt the enzymatic cleavage of phosphate from ovalbumin to prepare dephosphorylated forms of ovalbumin following the experimental procedure in section 2.3.4. SAX chromatography was applied to study the effect of alkaline phosphatase on the distribution of phosphoforms resulting from this treatment. The RSCB protein structure database (123) for any potentially

phosphorylated protein (pdb) shows the phosphorylation as it existed in the protein crystal following the preparation procedure and specific to the particular sample used and is hardly relevant to the analysis of structure occurring in nature or during process production. This reveals a difficulty to accurately predict the partition coefficient from published protein structures. The ability to do this opens up the possibility of finding ATPS which can resolve by difference in partition the degree of phosphorylation of a given ovalbumin sample.

4.4.2 Results and discussion:

Enzymatic dephosphorylation was performed by incubation of ovalbumin with ALP and the sample was analysed before and after treatment with ALP over time. SAX-HPLC was employed for the determination of the degree of phosphorylation of the model protein ovalbumin.

The initial HPLC chromatogram mapping experiments served to identify the ovalbumin phosphoforms in a single phase. Alkaline phosphatase was used to remove the phosphate groups from serine residues. The de-phosphorylated isoforms were analysed by HPLC and then compared to the corresponding peaks in the original ovalbumin chromatogram every one hour (see Figure 24).
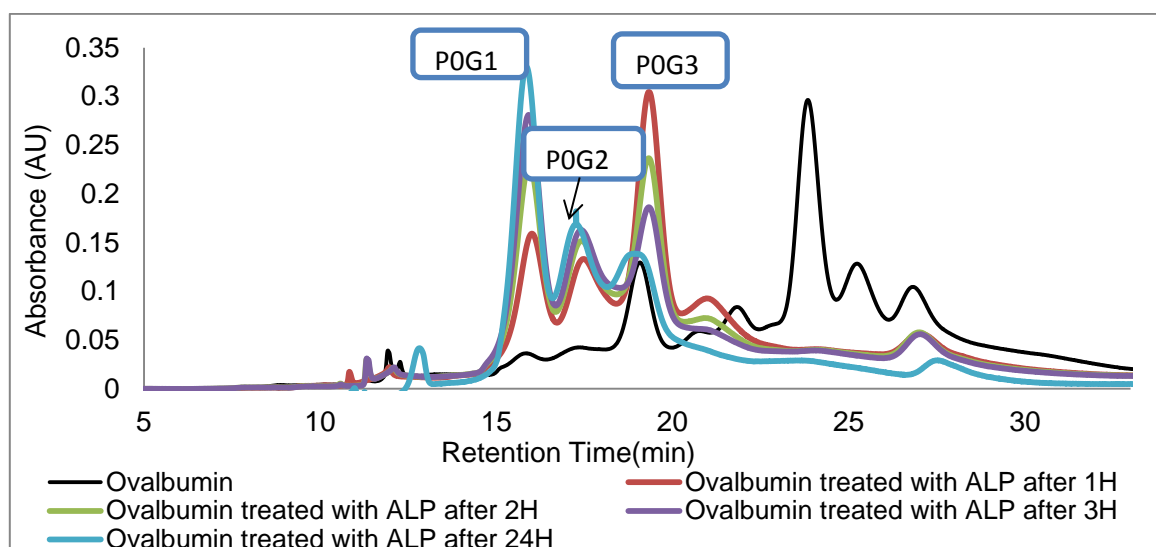
Figure 24- Time course of the HPLC-chromatogram to identify the phosphorylated sites in ovalbumin using the alkaline phosphatase strategy and under the operating conditions: Strong anion-exchange (SAX) Column SOURCE 15Q 4.6/100 PE, flow rate: 0.5 mL/min. Temperature: 25 °C. Injection Volume: 100 µL. Detection: UV, 280 nm, the ALP concentration in the reaction mixture was 0.052 units/µL.

Ovalbumin with and without treatment gave different elution profiles. Treated ovalbumin showed a decrease in the original number of peaks and the process led to almost complete de-phosphorylation revealing the remaining presence of only the heterogenous ovalbumin glycoforms separated on the basis of increasing net charge. The chromatogram of native ovalbumin as shown in Figure 18 indicated a variety of phosphate isoforms: peaks P0 represented dephosphorylated forms consisting of 3 different glycoforms (P0G1, P0G2, and P0G3). From which the remaining isoforms can be tentatively assigned as singly and doubly phosphorylated forms associated with similar glycoforms (PIG1, P2G1 etc). While (Figure 25) shows how much the peak height of each isoform has changed as a result of the effect of ALP over the time course of the experiment. The changes indicate the gradual shift from later eluting (more charged isoforms) to earlier eluting (less charged isoforms).
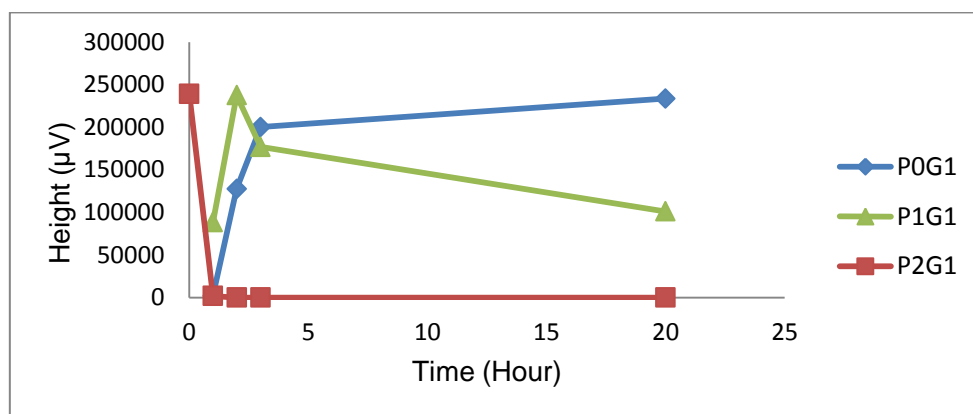
Figure 25- The change in the peak height of ovalbumin isoforms as a result of the dephosphorylation by ALP calculated from the chromatogram shown in fig 24.

After treatment with ALP only glycosylated species remained at the end of the dephosphorylating process. During the time-course of ALP treatment SAX chromatography showed a reduction of the peaks; P2G1 was rapidly removed due to its relatively high concentration, while P0G1 gradually increased to maximal due to the addition of the glycoforms of P1G1 and P2G1. The majority of the dephosphorylated peaks were shifted earlier due to the removal of phosphate through the reduction in the negative charges of the proteins. These findings enabled identification of the isoforms as reported in a previous section. Ovalbumin appears to have three isoforms with varying phosphate content, one with zero, two with one and one with two phosphates which may occur as three glycororms differeing in charge (116)

Both treated and non-treated ovalbumin samples were partitioned in an ATPS. The partition coefficient was calculated from the ratio of the average peak height of the various isoforms found in the upper and lower phases, also the ratio of phosphorylated isoforms in both case (before and after treatment with ALP) was calculated. A PEG8000-Dextran500 system was used to partition the protein, ovalbumin was separated using the SAX-HPLC methods previously developed; Figure 26 shows an overlay of the separation of ovalbumin in upper and lower phases following de-phosphorylation using alkaline phosphatase.
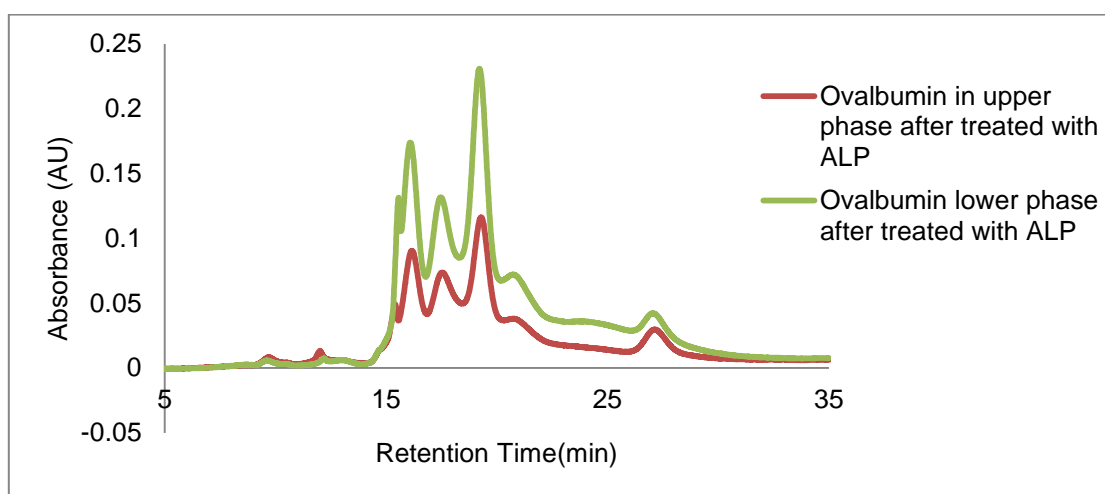
Figure 26- HPLC chromatogram showing the partitioning of ovalbumin as a phosphate free fraction in the PEG - Dextran system at the TLL composition 5.67 % w/w PEG8000, 10.85 % w/w Dextran500. The operating conditions: Strong anion-exchange (SAX) Column SOURCE 15Q 4.6/100 PE, flow rate: 0.5 mL/min. Temperature: 25 °C. Injection Volume: 100 µL. Detection: UV, 280 nm

The partition coefficient values in aqueous two phase system were calculated from the average of height peaks for two replicates and the phosphorylation ratio was identified through interpreting the elution results from HPLC in order to get complete examination of phosphorylation in such proteins.

Quantitation of the phosphorylation ratio was achieved following partition of the treated ovalbumin in the aqueous two phase system by calculation of the peak area ratios as illustrated in Table 41.

A visual representation of the information in Table 41 could be constructed by the K values obtained from the treatment of ovalbumin by alkaline phosphatase, the result indicates that overall distribution of ovalbumin differs between phospho and dephospho forms so ATPS system has succeeded in identifying unique patterns of markers for

analytical applications. The dephosphorylated form has a reduced partition coefficient compared to the phosphoforms due to the removal of the phospho groups.

In addition, the K for the glycoforms should not be changed before and after dephosphorylation however ovalbumin has a variety of structures that vary in the degree and nature of their glycosylation and since the partitioning is sensitive to charge, hydrophobicity and size thus the K values may differ due to the heterogeneity of Isoforms of the protein

Table 41- The ratios of the peak areas for the ovalbumin isoforms and the partition coefficient values before and after treatment with ALP.

Peak name	Area % for phosphorylation Isoform	Partition coefficient for dephosphorylated	Partition coefficient for phosphorylated
P0 G1	3.64	0.49	0.94
P0 G2		0.56	0.97
P1G1	24.89	0.50	0.49
P1G2		-	0.49
P1G3		-	0.44
P2 G1	71.47	-	0.39
P2 G2		-	0.38

4.5   Study of the modification of Ovalbumin and Ovalbumin isoforms using Size exclusion chromatography (SEC)

4.5.1   Background:

Size exclusion chromatography (SEC) also called gel filtration chromatography (GFC), employs a hydrophilic packing material and an aqueous mobile phase to separate, molecules soluble in the chosen mobile phase on the basis of their molecular size. For water soluble hydrophilic biomolecules the mobile phase is normally water containing buffer to control the pH and added salt to suppress charge interactions with the stationary phase.

Protein characterisation may require complementary techniques. SEC was used as an analytical method to provide further information about the enzymatic modification of Ovalbumin and in particular to show whether the resulting de-phosphorylated ovalbumin was in other respects identical to the native form for instance in the amount of multimeric or aggregated species present. The main aim of this work was to assess the differences in the molecular weight of ovalbumin resulting from the previous work

(section 2.3.4) and to assess the effect of dephosphorylation on the molecular integrity of ovalbumin following the experimental procedure in section 2.3.5.

4.5.2 *Results and discussion:*

Phosphorylation affects the surface charge and charge density of proteins and may induce conformational change and changes in hydrophobicity which could be reflected in changed interaction parameters with the ATPS components and hence in the partition coefficient. SAX-HPLC was used to investigate that ovalbumin was substantially dephosphorylated by the action of ALP and SEC was used to confirm that ALP-treatment did not induce any other gross changes such as degradation or aggregation. Using the principle of SEC, the column used is filled with material containing many pores. When dissolved molecules of various sizes flow into the column, smaller dissolved molecules flow more slowly through the column because they penetrate deep into the pores, whereas large dissolved molecules flow quickly through the column because they do not enter the pores. Consequently, larger molecules elute from the column sooner and smaller molecules later, which effectively sorts the molecules by size. This is the separation principle of size exclusion chromatography.

SEC retention times were normalised as $Ve/V0$; where Ve is the elution volume and $V0$ is the void volume. Figure 27 shows the chromatogram of a series of standards which was best suited to the analytical range of molecule weights to be measured which is a function of the porosity of the column packing material. The SEC column was calibrated from the retention times of a Bio-Rad Gel Filtration Standard (Catalog 151-1901) having molecular weight markers ranging from 1,350 to 670,000 Da. Ovalbumin de-phosphorylation was evaluated as demonstrated in Figure 28 which shows peaks having different elution times for de-phosphorylated ovalbumin over the time course of in vitro de-phosphorylation with ALP in duplicate test.
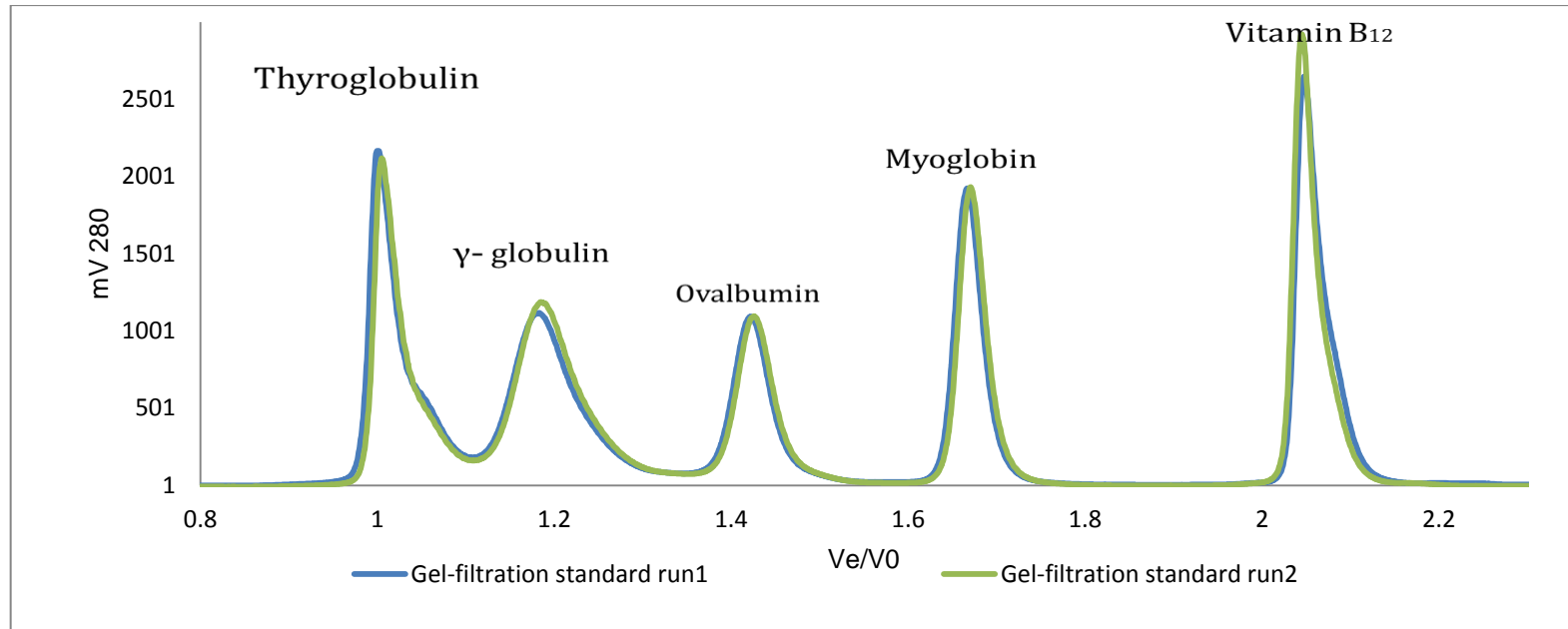
Figure 27- Separation of Bio-Rad standard during Size exclusion chromatography under the conditions: Buffer 0.05 M potassium phosphate ,0.3 M NaCl, pH 7,Column TSKgel G2000SW 300 x 7.8 mm, Flow rate 0.4 ml/min, Sample Treated & Non-Treated Ovalbumin 2mg/mL, Detection UV @ 280nm.
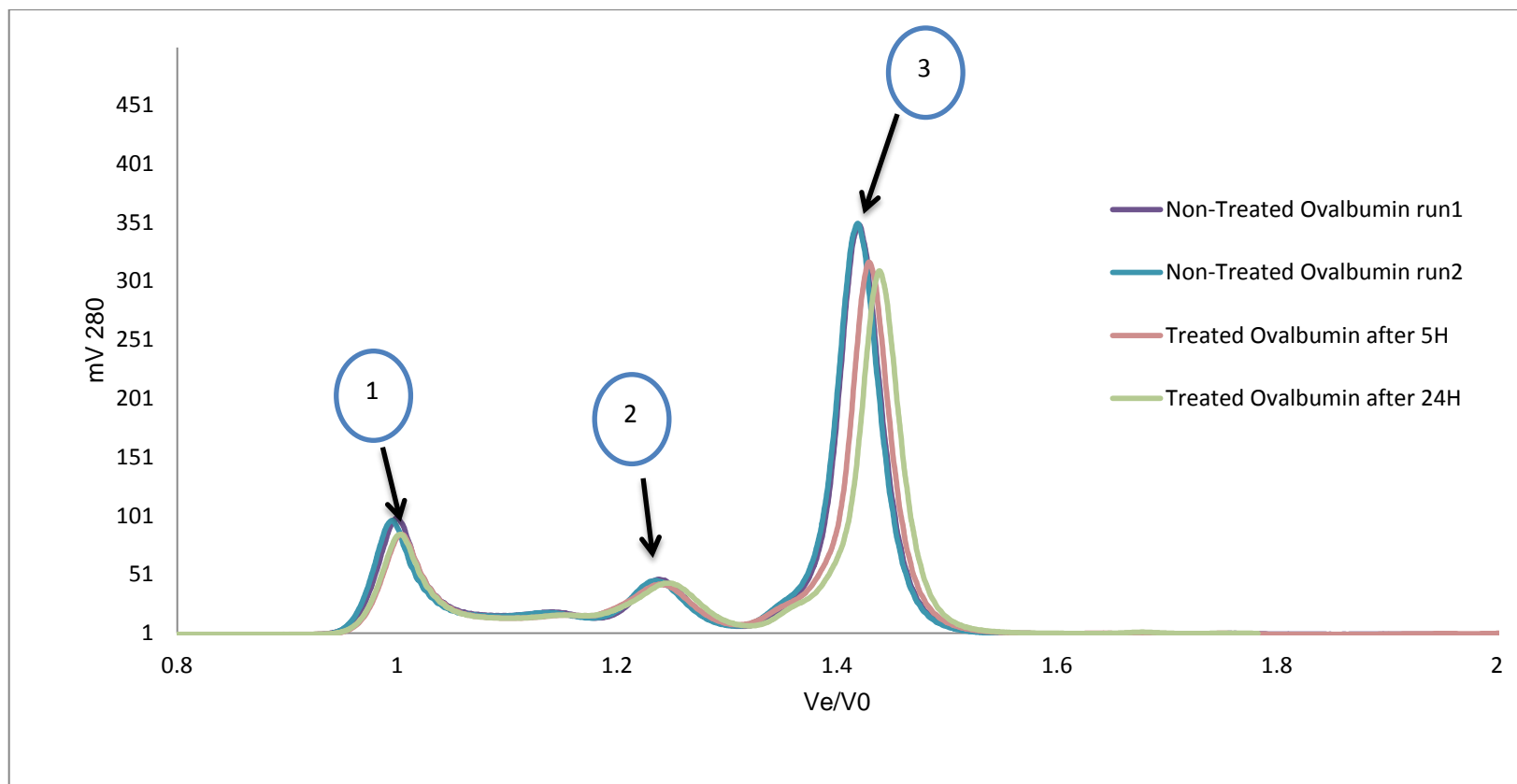
Figure 28- Separation of Ovalbumin samples (treaded and non-treaded) on Size exclusion chromatography under the conditions: Buffer 0.05 M KP,0.3 M NaCl, pH 7,Column 300 x 7.8 mm, Flow rate 0.4 ml/min, Sample Treated & Non-Treated Ovalbumin 2mg/ml, Detection UV @ 280nm.

Following dephosphorylation with ALP, SEC shows an increase in elution time of the main monomeric ovalbumin peak As a result of de-phosphorylation which can be interpreted as a change in molecular size of ALP-treated ovalbumin having an apparent molar mass of 40.9 KDa compared to 43.6 KDa of the native state.

It was important to show that the size exclusion chromatograms contain no increase in the % area of the higher order aggregates in both non-treated and treated ovalbumin with ALP, which is also demonstrated in Figure 28. The figure shows that the peak No.1 and 2 which represent higher order aggregates and multimers respectively were not significantly affect by the dephosphorylation process while the monomer form of the protein as a treated and non-treated has showed different peaks.

Since the protein was separated base on their size, the SEC chromatogram shows two different peaks for the native and modified Ovalbumin. Removal of phosphate groups was found to produce a change in molecular size but no other significant changes were seen such as proteolysis and the extent of aggregation and presence of multimeric species remained the same, Table 42 shows the calculated molecular weight of Ovalbumin before and after treated with ALP.

Table 42- Molecular weight of the ovalbumin species as determined by SEC and shown in Figure 28

	Non-treated ovalbumin			Treated ovalbumin		
Peak replicate	Peak 1 Mwt. (KDa)	Peak 2 Mwt. (KDa)	Peak 3 Mwt. (KDa)	Peak 1 Mwt. (KDa)	Peak 2 Mwt. (KDa)	Peak 3 Mwt. (KDa)
1	346.30	105.0	43.7	346.3	104.0	40.5
2	346.07	107.0	43.5	346.3	106.0	41.01

4.6   Study of the partitioning of Ovalbumin using different ATPS systems

For analytically purposes ATPS systems were examined with a view to finding a suitable partition coefficient for the analysis of native and modified Ovalbumin. Since the enzymatic method of dephosphorylation was developed for the preparation of dephosphorylated ovalbumin. This allowed for a comparison between the partitioning of phosphorylated and dephosphorylated isoforms of ovalbumin in various different ATPS.

Measurement the concentration of ovalbumin in the phases was performed by spectrophotometry at 280nm. Absorbance assays are fast and convenient, since no additional reagents or incubations are required; also the assay does not consume the protein.

Proteins in solution absorb ultraviolet light with absorbance maxima at 280, Amino acids with aromatic rings are the primary reason for the absorbance peak at this wavelength.

The phase preference of the analyte normally changes depending on the molecular weight of the polymer, the partitioned molecules show a preference for the phase containing the lower molecular weight polymer. Manipulating the partitioning by varying the molecular weight of the polymer can be useful in giving a partition coefficient suited to the aims of the process (16).

PEG600- Na_2SO_4 system had been highlighted by Zaslavsky (23) was used to examine the partitioning of Ovalbumin. Stock solutions of polymers and salt were dispensed from the liquid handling sample processer (LHSP) by volume and weighed on an analytical balance at each stage to provide calibration and performance data. Final compositions were achieved by addition of appropriate amounts of buffer or buffer containing analyte (Ovalbumin) and weighed as before.

The LHSP was used to prepare ATPS having a final mass of 3 g for the PEG600-Na_2SO_4 ATPS. Partitioning of Ovalbumin was performed by weighing out appropriate amount of the stock solutions using the LHSP. A mixture containing (0.58g) 19.28% w/w PEG600, (1.79g) 8.37 % w/w Na_2SO_4, and the remaining mass of the system (0.627g) was used to accommodate the protein sample and buffer. Partitioning experiments were performed using a set of different and increasing concentrations of protein added to a series of ATPS having the same overall polymer composition using the theory which was described in section 2.2.4**.** Determination of the partition coefficient of the protein was performed by carefully dispensing 200 µL of upper phase and 200 µL of lower phase, and these were then diluted with 800 µL of the ATPS buffer. The solutions were mixed and the protein concentration was determined by spectrophotometric absorbance at 280nm against blank buffer.

The K value of Ovalbumin in the system was determined from the slope of the regression which was 6.06 as shown in *Figure 29*.
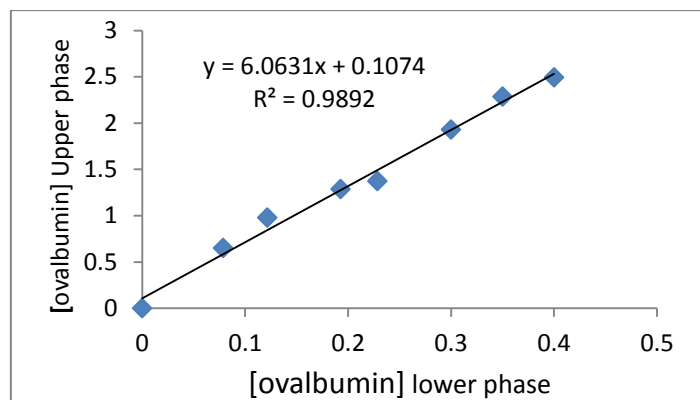
Figure 29- The isotherm partitioning of ovalbumin in PEG600-Na$_2$SO$_4$ system, the composition of the TLL was 19.28% w/w PEG600 and 8.37 % w/w Na$_2$SO$_4$. Partitioning experiments were performed using a set of different and increasing concentrations of protein added to a series of ATPS having the same overall polymer composition.

Apparently, the limited solubility can be problematic in terms of restricted the available amount of the sample in the system, increasing the concentration of salt and made the protein easily precipitate by salting out process.

PEG600-(NH$_4$)$_2$SO$_4$ was selected to overcome the solubility limits of Na$_2$SO$_4$ and to examine the system environment in the partitioning of ovalbumin.

The first tie-line length composition of this system which is illustrated in section 3.3, Figure 11 and Table 35 was implemented on the LHSP to prepare the ATPS and the general isothermal partitioning procedure which described in section 2.2.4 was used. The partitioning of ovalbumin was examined in a system having a total mass of 2g comprising (0.68g) 17% w/w PEG600, (0.85g) 16.97 % w/w (NH$_4$)$_2$SO$_4$. The remaining mass of the system (0.47g) was used to accommodate the protein sample and buffer. Ovalbumin was partitioned using increasing concentrations of ovalbumin (0-2mg/mL) from 10mg/mL stock solution.

Experimentally, the composition of the first TLL (34.89) was very sensitive resulting in an un- stable system (no phases were formed). At this TLL composition, constructing stable phases becomes difficult to manage. Small variations in phase composition are likely to occur close to the critical point which will lead to changes in the physical and chemical characteristics of the system and uncontrolled changes in distribution.

Therefore, systems will differ in stability and be more sensitive to salt critical concentration and the result of an individual change, or a combination of changes will

give a corresponding deviation in the tie-line length and consequently, in the composition and volume of the phases.

A new phase composition was selected which was a further from the critical point (TLL2). Here the polymer weight was 1.157g (19.287 % w/w) and the corresponding salt weight was 1.4076g (18.769% w/w) and buffer 0.435g in a total system weight of 3g. The system was prepared using the LHSP. However the lower molecular weight of PEG-600 and the high concentration of salt increased the partitioning value of Ovalbumin (K=8.53) and resulted in low recovery as shown in Table 43. This may be ascribed to the salting out effect of the higher concentration of salt and the small excluded volume of low molecular weight of PEG (124). High partition coefficient value may make distinguishing between native and modified protein more difficult because of this preference of protein for the upper phase in addition the precipitation of the protein seems analytically undesirable.

Table 43- Comparison the recovery of native Ovalbumin in PEG600-Na₂SO₄ and PEG600-(NH4)₂SO₄ systems

Systems % Recovery of Native Ovalbumin in	
PEG600-Na$_2$SO$_4$ 19.28% w/w PEG600 and 8.37 % w/w Na$_2$SO$_4$	PEG600-(NH$_4$)$_2$SO$_4$ 19.29 % w/w PEG 600 and 18.769% w/w (NH$_4$)$_2$SO$_4$
72.8	50.7
73.3	49.5
74.1	50.4
64.4	49.9
74.3	49.8
75.4	46.8
72.8	46.4

The PEG600-salt systems were found to have severe shortcomings in addition to low recovery due to the protein salting out as shown in Table 43. Thus, these results did not encourage further work with these systems and attention was directed toward the development of alternative partitioning systems.

Partitioning of ovalbumin was next examined in a PEG1000-(NH$_4$)$_2$SO$_4$ system. The fourth tie-line length composition (TLL 38.91) was prepared using the LHSP, the ATPS

having a final mass of 3.5 g, the mixture containing (1.415g) 16.17% w/w PEG1000, (1.53g) 17.49 % w/w $(NH_4)_2SO_4$, the amount available for protein and buffer was (0.554g). ATPS systems were prepared using increasing concentrations (0-2mg/ml) of ovalbumin from 14mg/mL stock protein solution following the partitioning procedure in section 2.2.4.

The partitioning of native ovalbumin was compared to the partitioning of dephosphorylated forms prepared enzymatically in vitro. However in the PEG1000-$(NH_4)_2SO_4$ system Ovalbumin dephosphorylated using ALP (see section 4.4) was found to have greatly reduced solubility compared to the native form which led to accumulation at the interface and a failure to close the mass balance since only material in the bulk phases was quantified. This is clearly illustrated in Figure 30 A & B. This partitioning system showed low recovery for ALP-treated Ovalbumin at that TLL which was exacerbated when the TLL was reduced (second TLL) see Table 44. Calculation of the mass balance of the ATPS is an important consideration when systems approach the analyte solubility limit or where molecular association occurs; these findings stimulated the examination of the performance of the LHSP and its accuracy in relation to variation on TLL.

In spite of the failure to analytically partition ovalbumin in this system due to the precipitation of the dephosphorylated form the experiment does demonstrate that the solution behaviour of dephosphorylated from is considerably altered in relation to the native form showing considerably reduced solubility. Such a result indicates changing in the surface net charge or a reduction in conformational stability due to the removal of phosphate. PEG1000-$(NH_4)_2SO_4$ reveals that removing phosphate groups effect the partitioning performance of the protein which showed a tendency to precipitate at the interface of the upper and lower phases following dephosphorylation.

Figure 30 - A
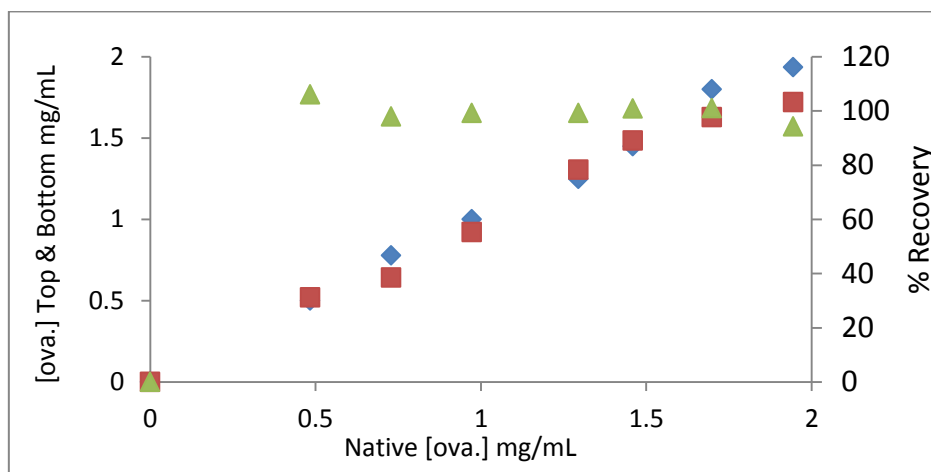
Figure 30– B
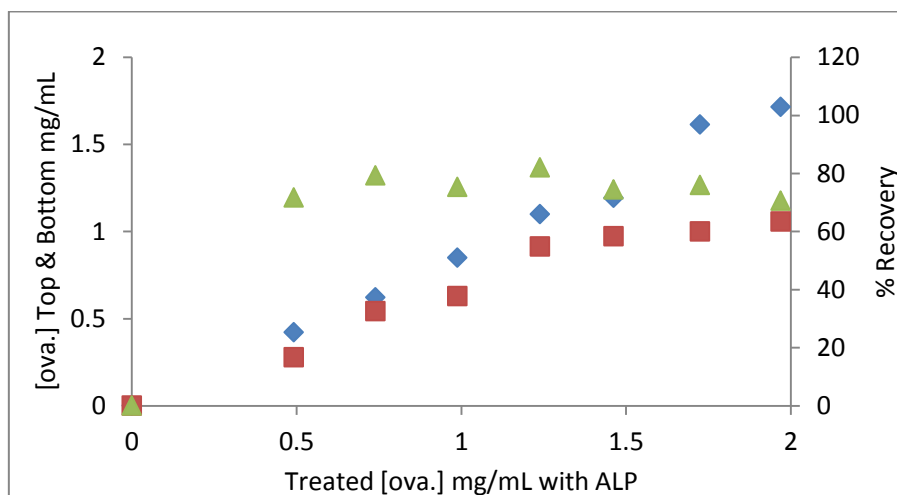
Figure 30- Partition of (A) native and (B) ALP treated ovalbumin in the PEG 1000/ $(NH_4)_2SO_4$ system at the TLL composition (16.17 % w/w PEG1000 and 17.49 % w/w $(NH_4)_2SO_4$ showing the concentration in the top (◆) and bottom (■) phases and the overall recovery from both phases (▲).

The partitioning method was sensitive enough to the modification of the protein and showed radically altered behaviour. This demonstrated in a graphic way the ability of partition to distinguish between phospho and dephosphoforms

The effect of the dephosphorylation on the protein solubility was reflected by the different behaviour of the protein before and after treatment with ALP, on the other hand recovery and low solubility of dephosphorylated ovalbumin made the PEG1000-$(NH_4)_2SO_4$ system not suitable for the main aim of the study.

136

Table 44- Comparison of the recovery of Ovalbumin in PEG1000-$(NH_4)_2SO_4$ system at different TLL.

Systems % Recovery of Ovalbumin in PEG1000-$(NH_4)_2SO_4$		
(TLL2) 16.42 %w/w PEG- 14.69 % w/w salt	(TLL4) 16.71 % w/w PEG- 17.49 % w/w $(NH_4)_2SO_4$	
Native Ovalbumin	Native Ovalbumin	Treated Ovalbumin by ALP
61.5	106.2	71.7
61.6	97.9	79.3
61.8	99.3	75.4
56.5	99.3	82.0
56.8	100.9	74.4
56.9	101.0	76.0
52.3	94.3	70.5

Subsequently a PEG4600-Dextran500 system was used for the partition ovalbumin, the second TLL shown in section 3.3, Table 39 and Figure 13 was prepared using the LHSP system. The ATPS had a final mass of 2.5 g and the mixture contained (0.973g) 9.73 % w/w PEG4600, (1.102g) 13.22 % w/w Dextran500, the amount available for protein and buffer was (0.425g). ATPS systems were prepared using increasing concentrations (0-2mg/mL) of ovalbumin from 15mg/ml stock protein solution following the partitioning procedure in section 2.2.4. Ovalbumin was partitioned as the native form and following treatment with ALP; samples were analysed by measuring the absorbance at 280nm. Different systems for the partitioning of Ovalbumin had already been examined and so this system was selected to avoid precipitation, system instability and also to find a K value suited to the analytical application.

Using this PEG4600-Dextran500 system, the K value for the native protein was 0.266 as calculated from the slope of regression of the concentration in upper and lower phases with increasing concentration of the protein (isothermal partitioning method as outlined in section 3.5) whilst the K value for protein treated with ALP was 0.29.

Analysis of covariance (ANCOVA - IBM SPSS statistics version 20) was used to compare the two regression coefficients in this system to determine whether they were

significantly different by calculation of a common regression slope for the whole set of the concentration data in the upper and lower phases (treaded and non-treated ovalbumin). The method determines whether changes in the partition coefficient differ significantly with respect to the independent variable while considering the possible effects of the covariate, the result reveals that there was no significant difference in the partition coefficient value with a p-value of 0.479.

4.7 Study of the partitioning of Ovalbumin using PEG3350-Dextran500

4.7.1 Background

The type of salt included in an ATPS has a direct effect on the partition phase efficiency and recovery of the solutes. Manipulation of the electrostatic interfacial potential of the partitioning systems by altering the system pH and by inclusion of neutral salts is an important method of controlling partitioning behaviour of the protein in an ATPS system. This may be due to differences in the electrostatic potential generated between the coexisting phases and to changes in the phase properties (16).

Inorganic salt ions partition differently between the phases and this alters the distribution of the analyte in the system which has been attributed to the changes in the electrostatic potential between the phases (22).

While k values depend on the ionic composition of the phase system and the pH, any change will affect the protein partitioning due to changes in protein solvation caused by protonization and deprotonization (22).

It has been shown that for various inorganic salts included in the system the partitioning of all negatively charged proteins increased according to the following order of included ions:

$$SO_4^{-2} > CL^{-1} > CLO_4^{-1}$$
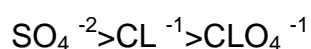
Addition of neutral salts has been shown to influence the distribution of biomolecules in ATPS, for instance the influence of different alkali and ammonium salts on the partitioning of positively charged proteins has been reported (22). Partition coefficients values decreased linearly when the system included different K^+ salts due to differences in the electrostatic potential between the phases.

4.7.2 Results and discussion

Following the experimental procedure in section 2.3.6 and in order to study the steering effect of salts and pH on the negatively charged protein (ovalbumin) and its effect on the

K value of the protein following dephosphorylation with (ALP) K values were compared in systems differing in the relative concentration and type of salts added.

A PEG3350 / Dextran 500 system containing 10mM phosphate buffer but differing in pH (4.6, 5.5, 7.4, and 9) was used.

The pH was selected to cover a range from the protein pI to 4 pH units above pI. Each system contained different added salts (100mM $NaClO_4$, 100mM KCl, 50mM K_2SO_4) for each pH condition, the K value for the protein was determined from the equilibrium phase concentration determined by spectrophotometric absorbance at 280nm

Over this limited survey of the influence of the ionic strength and the net charge on the partitioning, the best results were obtained from the system containing 10mM phosphate buffer pH9 and containing 50mM potassium sulphate salt which resulted in a K value suitable for analytical application. The results are shown in (Figure 31 Figure 32)
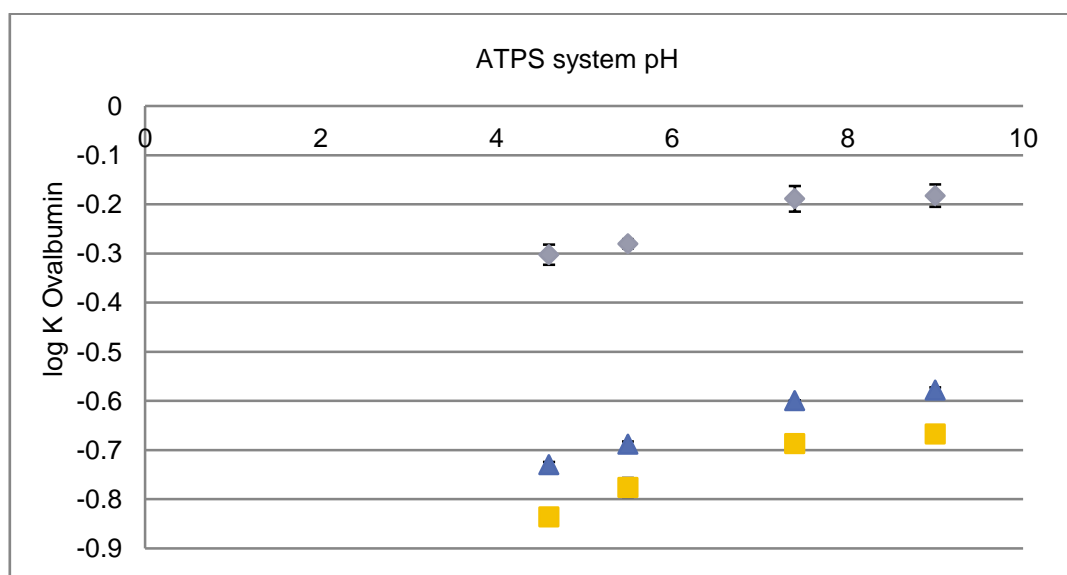
Figure 31- Log K of Ovalbumin partitioned in the PEG3350-Dextran 500 system at the TLL composition 8.4 % w/w PEG and 8.4 % w/w Dextran in systems containing different salts (■, 100mM KCl, ▲, 100mM $NaClO_4$, ◆, 50mM K_2SO_4) plotted as a function of system pH.
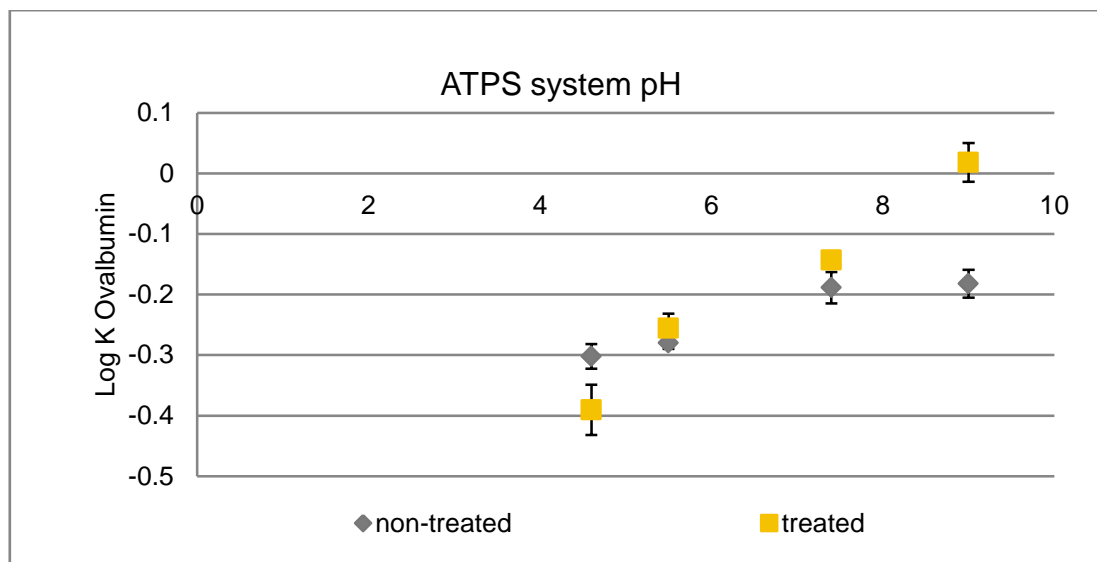
Figure 32- The difference between log K in terms of native ovalbumin and ovalbumin treated with ALP in a PEG3350-Dextran500 phase system at the TLL composition 8.4 % w/w PEG and 8.4 % w/w Dextran containing 50mM K_2SO_4 plotted as a function of pH.

The PEG3350-Dextran 500 phase system containing 50mM K_2SO_4 was examined for any significant difference between the partitioning of ALP treated and non-treated ovalbumin. The differences in the electrical potential due to presence of salt cause a difference in the distribution of the ovalbumin. The partition coefficient of the native ovalbumin under these conditions was 0.847 while the partition coefficient of the dephosphorylated ovalbumin was 0.606. Analysis of covariance (ANCOVA) was used to compare the two regression coefficients of the ovalbumin in the PEG 3350 / Dextran 500 system and the P values were found to be well below the 0.05 probability level as shown in Table 45

PEG3350-Dextran500 system showed significant difference in partition when comparing ALP treated (dephosphorylated) and non-treated (native) ovalbumin. This might be ascribed to the addition of inorganic salt (K_2SO_4) changing the hydrophobic character and the ionic composition of the phases. On the other hand the effect of the pH on the partitioning by altering the surface net charge of the protein resulted in an increasing difference in the behaviour of the ovalbumin isoforms. Both salt and pH represented significant factors affecting the protein partitioning.

able 45- Analysis of covariance (ANCOVA - IBM SPSS statistics version 20) was used to compare the two regression coefficients for the PEG 3350 - Dextran 500 system

Tests of Between-Subjects Effects Dependant Variable :Cb					
Source	Type III sum of squares	df	Mean square	F	Sig.
Corrected Model	8.826a	2	4.413	137.568	.000
intercept	0.041	1	0.041	1.265	0.281
Ct	8.582	1	8.582	267.509	.000
sample	0.407	1	0.407	12.680	.003
error	0.417	13	0.032		
Total	33.411	16			
Corrected Total	9.243	15			

[1] df - the number of values in the final calculation of the F statistic that are free to vary.

[2] F - the distribution of ratios of two independent estimators of the population variances.

Conclusions:

Progress in Analytic separation by ATPS depends upon the development of a suitable partitioning method. Since the partitioning method can only give an indication of the mixture composition of the analytical sample (see introduction) in terms of a single variable (the partition coefficient) the applicability of the method requires confirmation by another technique capable of resolving the isoforms present. Given a suitable phase system the properties of protein as influenced by the separation phase environment may be accessed. This chapter utilized the ATPS method to probe the robustness of constructed systems to compositional variability, location within the phase diagram and analyte k value and their ability to highlight differences in partition as a result of differences in the isoform composition of the analyte.

Many systems were screened in this chapter and some were judged unsuitable for application to the particular analytical problem either because of precipitation, instability, difficulties in formulation, or in producing a measurable K value.

For instance the PEG600-Na_2SO_4 system was found to be problematic in terms of a restriction in the amount of sample which could be added to the system due to the limited solubility of the phase forming.

Working close to the critical point in the PEG600- $(NH_4)_2SO_4$ system gave rise to deviations in the tie-line length and consequently in the composition and volume of the

phases. Also the system was found to give rise to the precipitation of the protein which analytically is undesirable.

In addition PEG1000-$(NH_4)_2SO_4$ system proved very sensitive to the modification of the protein by dephosphorylation. This resulted in a reduction the solubility of dephosphorylated ovalbumin compared to the native leading to accumulation at the interface and a failure to close the mass balance. Although the protein precipitated in several PEG salt systems a clear difference was demonstrated between the behaviour of the protein isoforms. Whilst the native form was distributed between the phases without noticeable precipitation and the mass balance could be closed, the dephosphorylated form proved much less soluble and protein was lost to the interface and the mass balance could not be closed. Many of these findings concerning the stability of the systems stimulated the examination of the performance of the LHSP and its accuracy in relation to variation on TLL which will be discussed more extensively in chapter 5.

PEG4600-Dextran500 system was not able to show changes in the partition coefficient differ significantly.

It was shown that PEG3350 - Dextran500 system containing 10mM phosphate buffer pH9 and 50mM K_2SO_4 was able to clearly distinguish between the phosphorylated and dephosphorylated forms through the demonstration of a statistically difference in the partition coefficient for the Ovalbumin as a native protein and after modification (removing phosphate groups by ALP). The detection of the protein isoforms modification was achieved by showing differences in the partition coefficient in the ATPS and confirmed by specific detection methods such as the spectrophotometer and Size exclusion chromatography.

Chapter 5

5 Robotics method development for the partitioning of Ovalbumin in ATPS.

Introduction:

The most significant limitation of the extensive using of ATPS is time. Significant empirical experimental work is required to develop the process. Since the partitioning method involves analyte distribution between completely liquid phases the method potentially can be adapted to conventional automated liquid handling techniques available in many laboratories. This approach has been taken in a number of studies, for instance in the screening of conditions for preparative process design employing ATPS (112) (125) and for the automated preparation of analytical phase partitioning systems (47) (48) (54) (15)

A number of studies have applied automated ATPS preparation such as the evaluation of automated mixing efficiency by determining the protein fraction as a function of time or utilized dispensing cycles without studying the accuracy of the transfer of the solutions or phases; also this study showed that the degree of automation might have a crucial role in the designing of the ATPS processes in an integrated manner in both the industry and research (112). However several areas still need further study.

Using ATPS systems have many limitations resulting from the lack of ability to predict the variables involved which are governing the operation and the large number of parameters that affect the partitioning result, since many parameters are interrelated in designing phase systems and have an impact on the partitioning, and consequently on applications.

Additionally, an alternative approach for estimating protein solubility using a robotic liquid handling station has been suggested since solubility is criteria in the design of biological manufacturing processes to establish a valid application could be apply in pharmaceutical industries and biotechnology purifications (125).

The use of automation for the preparation of ATPS is an encouraging approach which may lead to more frequent use of ATPS in research. The use of rapid methods, including improved technologies for the preparation of ATPS will accelerate determination of partition coefficients. Manual methods are often time-consuming while LHSP have the capability of improving reproducibility; perform the task accurately and in

less time than manual methods. The importance of accuracy in the development of automated processes has been described in (126) in order to achieve good results and avoid the overloading of expensive /rare samples which has a significant impact to the loosing of the material. Authors studied the correlation between the delivered volumes of each Aspiration and dispense step with the rate of delivery and the authors discuss the few proven methods, among these were using a colorimetric calibrating method (127), or by using the measurement of the optical path length by spectrophotometer (128) (129).

However, few details have been reported of the practical development of automated methods for the preparation of ATPS which involve the handling of relatively concentrated and viscous solutions of polymers and salts, nor is there much detail on the accuracy and reproducibility of their delivery. Accurate and reproducible phase system construction and subsequent sampling is a sine qua non for both analytical applications and screening for process development. Pipetting accuracy and precision of automated liquid handling systems is essential for data quality and integrity. Robotics system delivering data has been used to investigate limitations of processing, instrumental complexity and the relationship between behaviour of the robot and its ability to deliver solutions having different physical properties (130).

Aims and Objectives

The aims and objectives of this chapter were:

1. To develop a robust strategy for the application of an automated Liquid handling Sample Processor (LHSP) to the preparation and sampling of selected ATPS including polymer/polymer and polymer/salt systems.

2. To develop gravimetric methods for the calibration of the LHSP reflecting the mass fraction relationships of ATPS phase diagrams.

3. To examine the accuracy (%bias/accuracy) of the delivery of the individual system components (polymers, salts, buffer and sample).

4. To examine the accuracy of the delivery of the total system composition in relation to the demanded system composition.

5.1 Study of the Accuracy of delivering ATPS solutions (PEG- Dextran system) using a Liquid Handling Sample Processor (LHSP)

5.1.1 Creation of performance files for each solution

5.1.1.1 Background

Development of automated liquid handling is an essential step toward improving the throughput of ATPS sample preparation. Programming of all liquid-handling steps begins with the creation of a performance file which can be adjusted to calibrate the instrument for the delivery of a range of volumes. The performance can be monitored for the preparation of specific fixed compositions. Each performance file has the same fundamental structure, there are two tables of information within each performance file including: Performance Set and Global parameters which should be carefully studied. In order to optimize the performance of the system at any given liquid volume it is important to control the performance file parameters since it contains a table of pump speeds, pump delays, waste volumes and air gaps.

The aim of this study was to examine and enhance the understanding of the variables that affect the performance of automatic liquid handling to provide assurance that the performance of the instrument can be reliably assessed following the experimental procedure in section 2.4.1. To achieve this, it was necessary to study several factors individually.

5.1.1.2 Results and discussion

First attempts focused on trying different values for these contents, and by studying the results to develop a delivery system capable of handling solutions with a wide range of viscosities. The method focused on delivering different volumes of ATPS solutions covering the range of compositions demanded. Many experiments dealing with the performance file parameters were performed; for instance the speed and the delay time of dispensing and aspirating because these factors often affect volume accuracy especially with high viscosity solutions. Consequently, a good experimental structure was conducted and the optimum performance conditions for each solution and sampling ATPS are described in the APPENDIX (A).

Table 46 shows an example of the structure of the performance file and the parameters that should be adjusted.

The LHSP performance is controlled by many adjustable parameters governing aspiration and dispensing steps. The performance of all liquid-handling steps of the LHSP are controlled by an instrumental performance file which is used to adjust a wide range of parameters such as the speed and the delay time of dispensing and aspirating as well as the height of the probe tips. The results indicated that the most important parameters to be controlled were the speed of the delivery and the time delay during both aspiration and dispense. for instance, the aspiration rate for the PEG8000 stock solutions (20% w/w) for the volume range 250 - 2000 µL was set at 10 µL/s, while for the Dextran stock solution (25% w/w) for volumes of >100, >250, >400, and 900-2000 µL) the aspiration speed was set at 5, 10, 12.5 and 15 µL/s respectively. The speed of dispense was also reduced, for PEG8000 the dispense speed over the volume range >100, and 250-2000 µL was set at 400 and 300 µL/s while for Dextran 500 this was set at 100 and 30 µL/s over the same range of volumes.

Finally the time delays between the end of aspiration and dispense and tip withdrawal was extended to ensure that the procedure was complete. The aspiration delay for PEG8000 stock solution for volumes in the range > 400 µL was set at 200ms. Whilst for volumes of 400-2000 µL this was set at 300ms. For Dextran500 stock solutions this was further extended to 800 ms. also it was also found necessary to adjust LHSP performance parameters and to calibrate the sampling procedure for phase sampling in the same way as previously described for system preparation.

A performance file was created for each ATPS component to reduce the effect of the variability of the volume transferred however this was not enough to an accurate delivered volume and the decision was made to the calibrate of the instrument for each componen

Table 46- The performance file for the delivery of PEG 8000 after optimization of the performance parameters of the LHSP.

PEG performance file (slope :1.041 offset :-3.943)										
Volume (µL)	Asp. speed (µL/s)	Asp. Delay (msec)	Dis. speed (µL/s)	Dis. Delay (msec)	Waste volume (µL)	Waste volume% (%of Asp.)	Blowout Volume (µL)	Blowout Delay (msec)	Transport Air Gap (µL)	System AirGap (µL)
5	1.7	200	500	300	5	100	0	0	3	8
30	2.5	200	500	300	15	50	0	0	3	8
50	5	200	400	300	25	50	0	0	3	8
100	8	200	400	300	30	30	0	0	3	8
250	10	200	300	300	75	30	0	0	3	8
400	10	300	300	300	120	30	0	0	3	8
900	10	300	300	300	270	30	0	0	3	8
2000	10	300	300	300	600	30	0	0	3	8

5.1.2 Study of the accuracy of delivery using Blowout and Dispense back mode for Aspiration mode:

5.1.2.1 Background

In order to get a high degree of accuracy and precision during sample pipetting, the pipetting performance of different modes was studied.

Pipetting accuracy and precision of automated liquid handling systems is essential for data quality and integrity as was mentioned before, pipetting performance being dependent upon liquid type, volume ranges and dispense mode.

Performance Files contain optimized settings for various parameters which affect the variability of the volume transferred. These allow the user to optimize pipetting accuracy for their specific instrument and for specific liquids; the experiment was preformed following the method in section 2.4.2.2.

Blowout and Dispense back volume modes were tested to measure the performance of LHSP system to aspirate and dispense a requested volume for ATPS systems. [1] Blowout mode means a volume of air is aspirated prior to the requested transfer volume. The total volume (sample + air) is expelled during the dispense step. The air volume is used to force any remaining sample from the tip. [2] Dispense back volume mode means a volume is aspirated with the sample and then dispensed back into the source location before moving to the next step in the test outline.

5.1.2.2 Results and discussion

From assay development to high throughput screening, scientists seek to improve throughput and reduce reagent/sample consumption, while maintaining a high level of data integrity.

The LHSP offered two different modes of delivering samples which could be examined to see the mode efficiency in terms of saving materials. The method was performed by dispensing the demanded volume of the PEG8000 and Dextran500 solutions for four replicates using different each mode into tubes. Protein and buffer solutions were added using a range of volume to cover the demanded volume each tube was then weighed to make the calibration based on the performance of the mode. The %Bias was determined from the actual mass dispensed relative to the intended mass.

$$\%\text{Bias (accuracy)} = \left(\frac{(M_A - M_0)}{M_0}\right) * 100 \qquad \text{Equ. 20}$$

Where M_A is the actual mass dispensed and M_0 is the intended mass. Table 47 shows the experimental results of the Mean %Bias of the accuracy for dispensing stock solutions of the two phase components using different modes of aspiration.

Table 47- Comparison of the %Bias (accuracy) in the delivery of ATPS solutions using different modes of Aspiration.

Requested PEG8000 Volume (µL)	Dispense Mode	Mean Dispense Weight (g)	Mean %Bias
	Blowout	0.496	-1.39
503	Dispense back volume	0.497	-1.158

Requested Dextran500 Volume (µL)	Dispense Mode	Mean Dispense Weight (g)	Mean %Bias
	Blowout	0.963	-1.046
973	Dispense back volume	0.971	-0.203

Requested Buffer Volume (µL)	Dispense Mode	Dispense Weight (g)	%Bias
524	Blowout	0.524	0
424		0.4247	0.165
374		0.3751	0.294
324		0.3254	0.432
524	Dispense back volume	0.5305	1.240
424		0.4302	1.462
374		0.3836	2.567
324		0.334	3.086

Requested Ovalbumin Volume (µL)	Dispense Mode	Dispense Volume (µL)	%Bias
0	Blowout	0	0
100		98.3	-1.7
150		145.7	-2.867
200		197.1	-1.450
0	Dispense back volume	0	0
100		93.3	-6.700
150		144.2	-3.867
200		195.8	-2.100

The data in the Table 47 demonstrated that the pipetting performance for the mode selected can affect the accuracy of the delivering.

Each mode was added to the aspiration step individually, the ATPS solutions were classified into high viscous like PEG and Dextran and low viscous like protein and buffer solutions. The blowout mode was more accurate than dispense back mode when used with low viscous solutions as can be seen from the % Bias which was showed low error in the blowout mode. The problem with the dispense back volume was that a drop may stick at the end of the probes during dispense back the demand volume in the aspiration step, which may cause the increasing in the volume delivered in buffer and ovalbumin solutions.

On the other hand, high viscous solutions namely Dextran showed improved delivery in dispense back mode, which may be because that mode gave a chance and time for the probe to aspirate enough sample and then adjusted the demanded amount by the dispense back the extra solution. The time was very important in the aspiration of high viscous solution due to their density and low velocity as investigated earlier when the time delay for aspiration and dispense was examined during the creation of the performance file.

The blowout mode seems preferable when transferring non-high density solutions or when it is undesirable to waste the solutions such as buffer, ovalbumin and any other expensive materials, but it is not recommended for viscous liquids. However, blowout mode reduces reagent waste and can lower assay cost per sample.

Further conclusions by repetition, depending on the nature of the procedure the flush/wash step which washes the exterior and interior of the sample tips can be

optimised. This step may be initiated per procedure or per transfer group. Where there is no risk of cross contamination time can be saved by selecting the per transfer group option.

- Under normal circumstances, pipetting operates according to the Well Map order. Lab ware is associated with liquid handling steps. Mapping lab ware affords greater control over exactly which wells are associated with a particular step. If ignore dispense Well Map order is not selected, reagent addition will follow the Well Map exactly and the reagent procedure will be completed slowly. Each of 4 tips will dance across the plate to dispense liquid in the appropriate numerical order. While if ignore dispense well map order is selected, reagent addition will start from the origin well (A1) and dispense down the column. The first four wells to be filled are A1, B1, C1 and D1, followed by E1, F1, G1 and H1.Same thing will happen if numbering starts from the end of the plate (or rack) to reverse the Well Map within the Map Room tab.

- The lab ware used can also affect the overall performance time. By using reagent troughs rather than sample vials all four sample tips can aspirate sample at the same time rather than sequentially offering a considerable saving in time.

- Control the height of aspirate and dispense by making the tips enter about 2-5 mm below liquid surface to avoided any air entering when aspiration sample, and the same thing applies when dispensing high viscous solutions. Ensure that the tips are1-2 mm below the liquid surface or at least at 5-10 % above well bottom to avoid any drops sticking at the end of tips and causing inaccuracy in volume delivered especially with highly viscous solutions.

- The performance for each solution may need to be different depending on the speed of aspiration and dispense and the waste volume may play a significant role in the accuracy of the robotic delivery. The aspirate/ dispense speed of the robot has to be considerably reduced to handle highly viscous solutions.

5.1.3 Calibration the LHSP through the global parameters set.

5.1.3.1 Background

One of the objectives of using a LHSP system was to develop the delivery of different solutions accurately and reproducibly. For this purpose, the delivery of the ATPS components was optimized through the creation of accurate procedure and steps by

monitoring the behaviour and performance of the LHSP system in delivering the required quantities of components.

Initial study was performed to monitor the relation between the densities of the solutions to the accuracy of delivering and then calibrate the robot with the demanded volume.

The second table of performance set is global parameters, this parameter control motor speeds and tip heights that may depend on the viscosity or other characteristics of the solutions to be processed. The volume compensation parameter was controlled the volume delivered dependent on the slope and offset values.

The slope and offset values are calculated from a linear relationship between measuring the requested versus actual dispense weights over a range of volumes following the experimental procedure in section 2.4.2.3 and then determining the linear regression line that fits those points. The study of slope and intercept value was performed in two steps. First step was by starting with 1, 0 slope and intercept value and preparing a standard curve over a range of volumes. Second step was performed by redefining the volume compensation parameters using the new input corresponding to the slope and offset values determined in the first step the checking the calibration. The actual relationship in terms of the new slope and offset over a range of volumes represents the real linear regression line that fits each range.

5.1.3.2 Results and discussion

Pipetting accuracy and precision of automated liquid handling systems is essential for data quality and integrity. The density of the stock solutions used by LHSP has to be considered in order to control the volume that robot should deliver to prepare a two phase system. Delivery of a range of volumes between 50 µL and 2 mL was examined for each stock solution and liquid handling robot was used to study the relationship between the volume demand and the delivered weight.

This step was performed to examine the LHSP system accuracy when transfer different viscosity solutions. Figure 33 showed a high variability in the delivering specially with high viscous solution like Dextran, the residuals of the PEG was 28µL while for the Dextran was about 80µL since its more viscous. The handling of relatively concentrated and viscous solutions of polymers is affected the phase system construction.
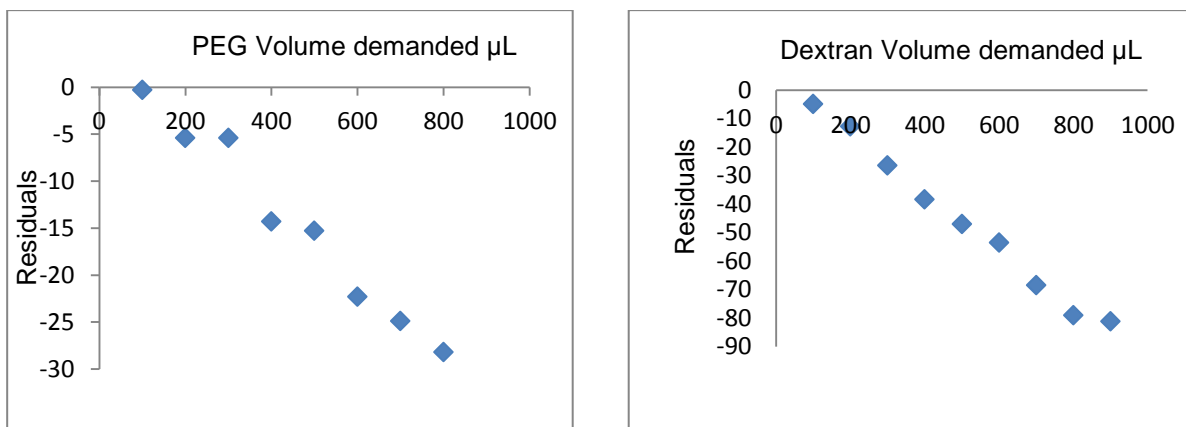
Figure 33- The variability in the transfer of PEG8000 and Dextran500 solutions by automated liquid handling processer using a residual plot to illustrate the accuracy of the automated preparation.

In order to define the relationship between demanded volume and the response of the robot, a calibration curve was constructed. The calibration was for the solutions properties and the performance of the robot. Delivery of a range of volumes was examined for each stock solution used. Sigma plot was used for regression analysis. Gravimetric procedure in section 2.4.2.2 was used but without using volume compensation to pre-calibrate the LHSP for the delivery of ATPS solutions. For each stock solution the relationship between demanded volume and delivered mass was measured gravimetrically. This procedure was repeated for the delivery of all stock solutions required to form the ATPS as shown in Table 48.

Statistical analysis of the delivery was performed and this is shown in the APPENDIX (B)**.** Total system error and residual values defined as the difference between the demanded volumes and those delivered was measured to provide a quantitative assessment of overall volume system performance. The residual was used as an estimate of the uncertainty in predicted volume values, rather than carrying out the standard error of prediction calculation.

In addition, the coefficient of variation (CV) is defined as the ratio of the standard deviation to the mean. The absolute value of the CV is sometimes known as relative standard deviation (RSD), which is expressed as a percentage. %Bias (accuracy) also gives an idea about the delivery errors.

Table 48- Generalised LHSP pre-calibration procedure for aspirating and dispensing ATPS components.

1	• Dispense first component without volume compensation.
2	• Gravimetric determination of delivered mass.
3	• Calibration of LHSP with delivered vs demanded relationship.
4	• Confirm the accuracy of the calibration.
5	• Repeat for each additional component.
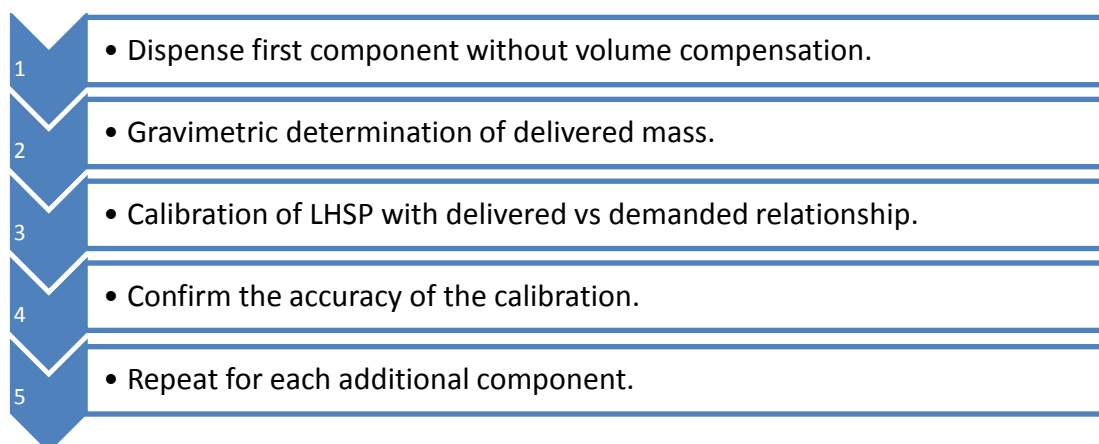
The appendix (B) shows how this was achieved. Details were given of the dispensing of stock solutions with no instrumental adjustment to delivered volumes (slope, offset; 1, 0) followed by a performance file in which the determined values of slope and offset are adjusted to give the required delivered volumes. The procedure was carried out on a range of volumes and a specific value.

For example: Dispensing files and Statistical analysis which describe the accuracy of the experiments during delivery of PEG 8000 is illustrated in the following Table 49 Table 50 which clearly show the accuracy through the residuals which was improved from 30 μL to few microliters after adjusting the slope and offset values as shown in Figure 34. In order to validate the calibration step statistical relevant to the errors was made to examine the improvement in the process. To do so, residuals plots which represent the residual versus predicted value was used to assess the sufficiency of the functional part of the model and indicate if the form of the function can be improved in some way. The systematic pattern of the data distribution has a meaning with respect to the variability. If random pattern could be described from the distribution of the data which drawn from a normal distribution, the reason behind that is the normal distribution often describes the actual distribution of the random errors in real-world processes reasonably well. Also it's used because the mathematical theory behind it is well-developed and supports a broad array of inferences on functions of the data relevant to different types of questions about the process (131). On the other hand, for the non-normally errors distributions any inferences made about the process may be incorrect such that the distribution shifted away from the true mean value. In the non-

normally distributed case, a significant curvature may be visible in the relationship between the residuals and the quantiles from the standard normal distribution, or there would be residuals at the upper and/or lower ends of the line that clearly did not fit the linear relationship followed by the bulk of the data (131)
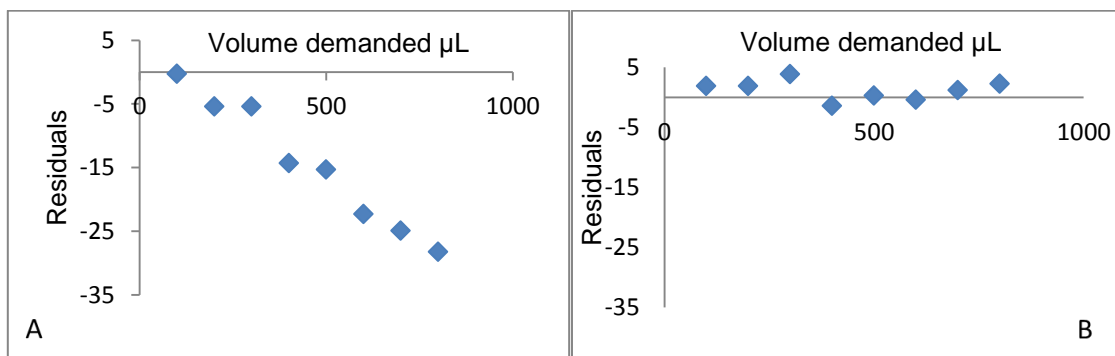
Figure 34- Residual plots for dispensing stock PEG solution (A) Using PEG performance file (slope 1, offset 0) (B) Using PEG performance file (slope 1.041, offset -3.943).

Table 49- A- Dispensing of PEG Stock Solution [PEG performance file slope 1, offset 0]

Dispensing of PEG Solution (PEG performance file slope 1 offset 0)					
Tubes No.	Mass of Empty Tubes(g)	Mass Tubes + PEG (g)	Mass of PEG(g)	Volume Demanded (µL)	Volume delivered (µg)
1	2.3761	2.4764	0.1003	100	100.3
2	2.3349	2.5403	0.2054	200	205.4
3	2.3614	2.6668	0.3054	300	305.4
4	2.3256	2.7399	0.4143	400	414.3
5	2.3425	2.8578	0.5153	500	515.3
6	2.3363	2.9586	0.6223	600	622.3
7	2.3664	3.0913	0.7249	700	724.9
8	2.3977	3.2259	0.8282	800	828.2

B- Statistical regression analysis for dispensing stock PEG Solution using Excel

Residuals	Std. Dev.	Mean	CV	RSD %	%Bias Accuracy
-0.3	0.255	0.4645	0.549	54.8962	0.300
-5.4					2.700
-5.4					1.800
-14.3					3.575
-15.3					3.060
-22.3					3.720
-24.9					3.557
-28.2					3.525

Table 50- A- Dispensing of PEG Stock Solution range of volumes using PEG performance file (slope 1.041, offset -3.943)

Tubes No.	Mass of Empty Tubes (g)	Mass Tubes + PEG (g)	Mass of PEG (g)	Volume Demanded (μL)	Volume delivered (μg)
Dispensing of PEG Stock Solution (PEG performance file slope 1.041　offset -3.943)					
1	2.476	2.575	0.098	100	98.1
2	2.540	2.738	0.198	200	198.1
3	2.667	2.963	0.296	300	296.1
4	2.74	3.141	0.401	400	401.4
5	2.858	3.356	0.499	500	499.7
6	2.959	3.559	0.600	600	600.4
7	3.091	3.790	0.699	700	698.8
8	3.226	4.024	0.798	800	797.7

B- Statistical regression analysis for dispensing stock PEG Solution (slope 1.041, offset -3.943) using Excel

Residuals	Std. Dev.	Mean	CV	RSD %	%Bias Accuracy
1.9	0.2453	0.4488	0.5466	54.659	-1.9
1.9					-0.95
3.9					-1.3
-1.4					0.35
0.3					-0.06
-0.4					0.067
1.2					-0.17
2.3					-0.29

It's worth mentioning that the performance files should be specific to the test procedure conditions. Modification of performance values is important, so for some applications the user may require to make adjustment to the default values, sometimes changes may be made to the new performance file without marring the integrity of the original/factory Performance File.

For example, to transfer PEG stock solution or a diluted PEG solution essentially the same performance file may be used but with each having its own optimised slope and intercept values to control the Volume Compensation parameter in the Global Settings table. Delivering viscous solution like Dextran required specific conditions and the most important was decreasing the speed and time delay of dispensing and aspirating. By doing so, it will avoid any air gap could be in tube might causes inaccuracy in volume delivered. The appendixes (A) illustrated the performance files for dispensing each

component and step of ATPS after optimization of the robotic system as well as the statistical analysis to describe the accuracy of the experiments.

Through the study of the sampling upper and lower phases, the contamination of the sampling of the lower phase by the upper phase was examined since the probe had to pass through the upper phase. The test was performed using a simple method in which a dye (Cibacron Blue F3GA) was added to the PEG phase. ATPS were prepared by dispensing appropriate the appropriate amount of the stock solutions into eight test tubes using the LHSP. The processor then withdrew a range of volumes [100, 200, 300, 400, 500, 600, 700 and 800µL] from each phase.

The dye showed almost complete preference for the upper phase and when sampling lower phase contamination with upper phase was easily visible as shown in Figure 35. With increase in the demand volumes, it was observed that the dispensed volumes contained some blue colour which indicates contamination with the upper phase. The cross-contamination of the phases was found to be problematic during phase sampling and could be related to the part of the variability in the delivery since the probe had to pass through the upper phase in order to sample the lower phase. To overcome this problem, an extra step was created in the sampling procedure (as shown in Table 51) by aspirating 400µL from each phase in clean tubes and then transfer 200µL which required for analysis. By doing so, no more contamination was noted.
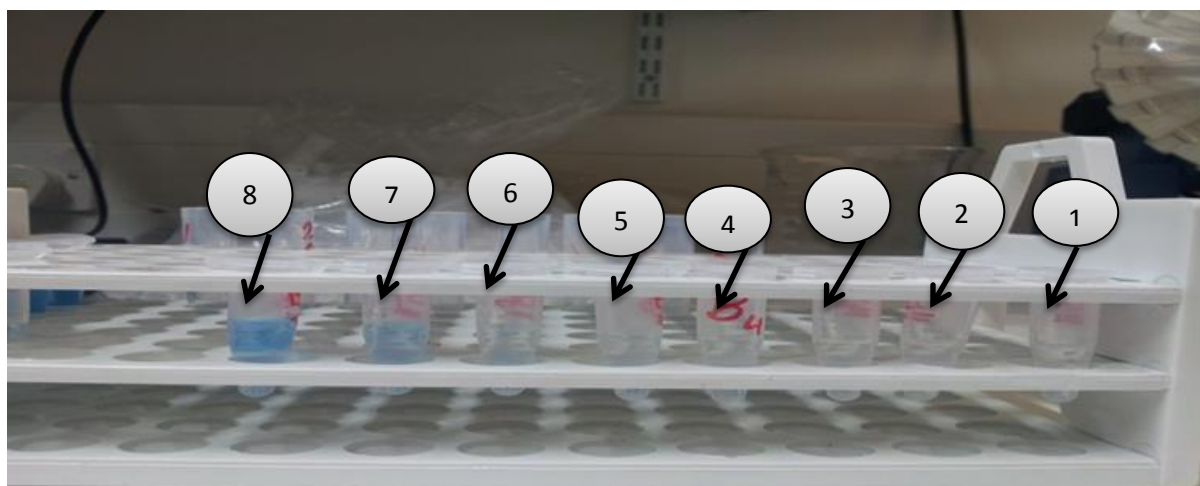
Figure 35- Using dye in PEG phase to study the contamination when sampling bottom phases: eight bottom phases with volume ranges of sample (1) 100, (2) 200, (3) 300, (4) 400, (5) 500, (6) 600, (7) 700 and (8) 800µL were aspirating from the bottom of two phases and monitoring the results

Table 51- Modified three-step phase sampling procedure to avoid cross-contamination of ATPS phases.

- Sample 400µL of each top and bottom phase

- Centrifuge to separate any residual contaminating phase

- Re-sample 200µL from each separated phase
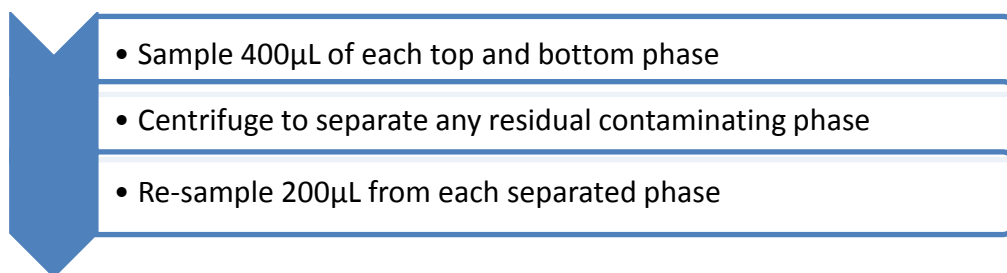
The conclusion of setting up the accuracy of the LHSP delivery and programming the liquid-handling steps begins with the creation of a performance file which can be adjusted to calibrate the instrument for the delivery a range of volumes. Performance was monitored for the preparation of fixed compositions and consisted of examined the robot behaviour by studying the result of the delivering of ATPS component. Individual liquid handlers have to be pre-calibrated to determine the specific input corresponding (slope and offset values) to a particular dispenses volume by using the nominal volumes when preparing ATPS during the optimization procedure.

5.1.4 Study the post calibration

5.1.4.1 Background

The first calibration relationship would reflect the values for the desired quantity as a function of values output in X and Y. Once the pre-calibration had been completed for all components of the ATPS. The performance of the LHSP in delivering a specific ATPS composition of defined Tie Line Length (TLL) was examined.

Experimentally, robotic pre-calibration was not enough to get accurate delivering volume in spite of it was improved the accuracy. However, in some case errors might be made due to interactions, interferences, noise, contaminations and other sources of bias. In an attempt to correct the systematic deviations, the mean of %Bias was chosen as a correction factor applied to the demanded volume of the ATPS solutions in a step called post-calibration.

5.1.4.2 Results and discussion

In order to reduce the effect of the variability in the volume transferred, the mean % Bias for a selected component covering the range of interests was measured. Then added to the volume demanded to eliminate the over or under delivery. The calibration factor was adjusted to attain the desired target volume. This procedure was repeated for all ATPS components until the dispensed or aspirated volume error is ≤ 1% of the nominal volume. To give a specific example, 8 replicates of a PEG1000-$(NH_4)_2SO_4$ system (TLL: 38.9 % w/w composed of 16.18 % w/w PEG1000 and 17.48 % w/w $(NH_4)_2SO_4$) and a PEG8000-Dextran500 system (TLL: 24.1 % w/w composed of 5.67 % w/w PEG8000 and 10.84 % w/w Dextran500) were constructed using the volume compensations previously established for each component. The appropriate amount of each component required to give the final composition was dispensed in turn and the results examined gravimetrically. For multiple trials of the same experiment with some condition or parameter changing each time. Boxplots illustrate the distribution of data in a sample across trials and how values are spaced out in different sets of data by comparing pre and post – calibration. The whole procedure was replicated three times. The results are shown in Figure 36 for PEG1000 – Ammonium sulphate system and in Figure 37 for PEG8000 – Dextran500 system.

Figure 36 - A
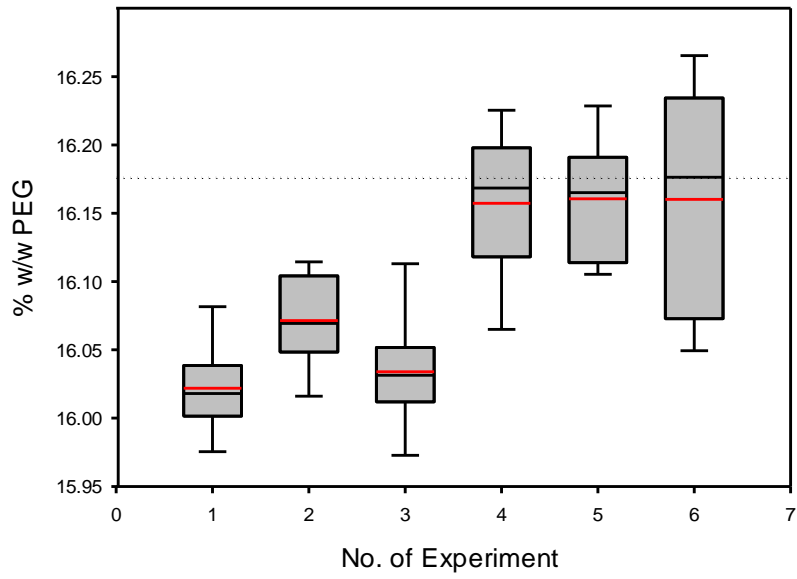
Figure 36- B
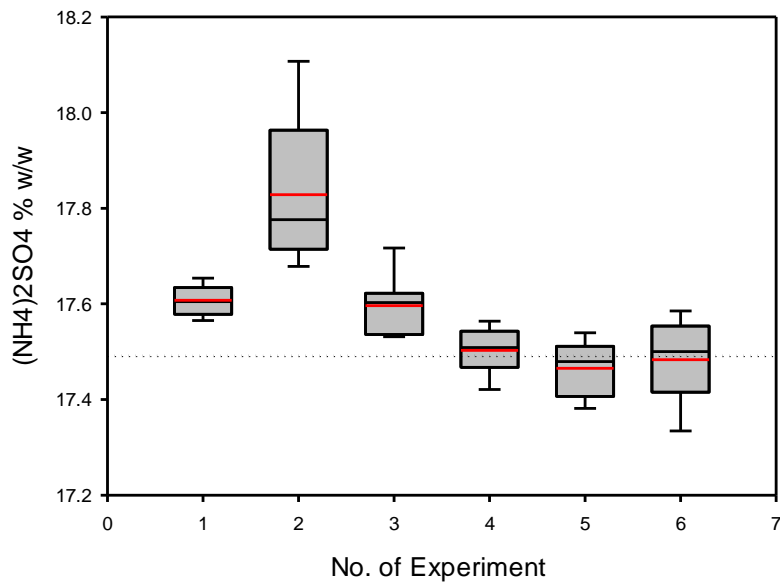
Figure 36 - Box Plots of the Phase compositions of PEG1000 – (NH₄)₂ SO₄ system in terms of (A) % w/w PEG1000 and (B) % w/w (NH₄)₂ SO₄, following a pre-calibration procedure (No. 1-3) and a post calibration adjustment (No. 4-6).The black Line within the box represents the mean of data; The red line represents the median.

Figure 37- A
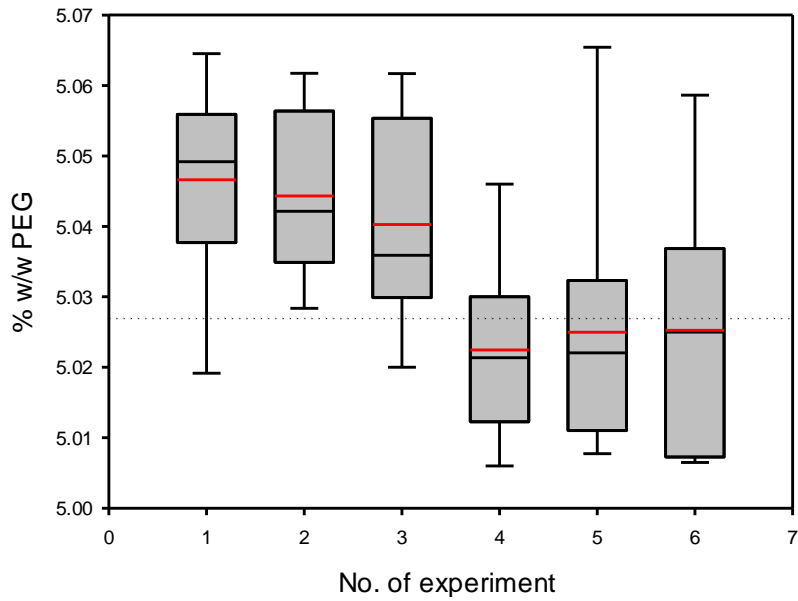
Figure 37- B
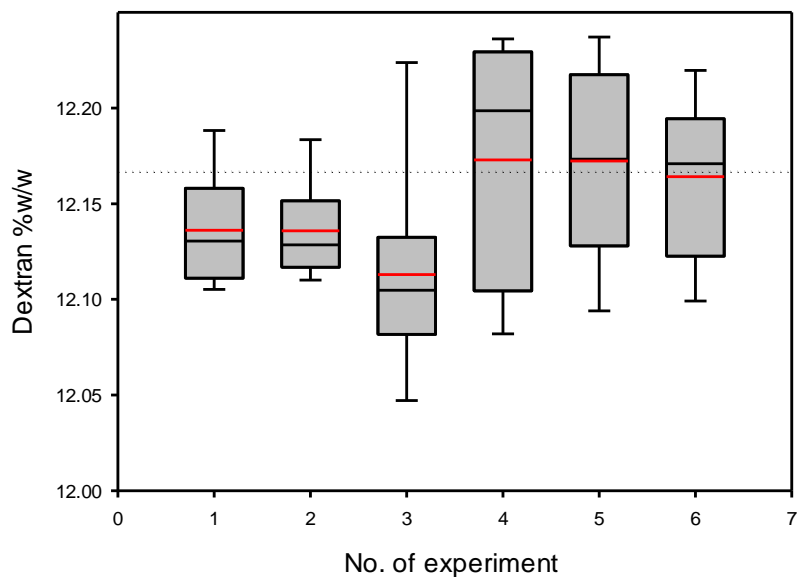
Figure 37 - Box Plots of the Phase compositions of PEG8000 – Dextran500 system in terms of (A) % w/w PEG8000 and (B) % w/w Dextran500, following a pre-calibration procedure (No. 1-3) and a post calibration adjustment (No. 4-6)

Each box represents the Range of 8 delivering systems by LHSP at the particular TLL, while the dotted line represents the demanded composition. For the PEG /salt system, the PEG concentration was lower than required and vice versa for the salt, while for the PEG/Dextran system the PEG concentration was higher than required and the Dextran concentration varied above and below the target. Several reasons may be adduced for this; first the regression in the volume compensation parameter is the best fit through the calibration data and may not perfectly describe all individual compositions within the range. Secondly, the final fractional composition of the system is a function of each added component, since:

$$T_m = X_m + Y_m + Z_m \quad \text{Equ. 21}$$

$$X_F = \frac{X_m}{T_m} \quad \text{Equ. 22}$$

$$Y_F = \frac{Y_m}{T_m} \quad \text{Equ. 23}$$

Where T_m is the total system mass, X_m, Y_m, Z_m are the mass of the three major components of the ATPS (salt or Dextran, PEG, and buffer respectively) and X_F, Y_F are the mass fractions of each component.

Although the composition of each component of each system under the pre- calibration conditions was within 2 % of the target composition, there was systematic deviation from the target.

As a result of applying this correction, the mean composition of the systems was brought much closer to the target value; however the range was not generally improved. %Bias (accuracy) was found to be a calibration factor for the robotic system; the results were improved throughput and achieved a high level of data integrity.

5.1.5 Study the variability of the LHSP delivery on the TLL and mass ratio.

5.1.5.1   Background

Robotics system delivering date has been used to investigate limitations of processing, instrumental complexity and the relationship between behaviour of the robot and delivering solutions having different properties as a step toward improving the throughput of ATPS sample preparation.

Different TLL behaviour and phases properties of aqueous solutions have been the subject of a number of works, a wide range of experimental techniques, including the investigation and determination of the mathematical relationship between Tie Line Length and the mass ratio of the dispensed systems.

The study of the variability consists of examined the robot behaviour through the results of the delivering of ATPS component. Also to see how this affects TLL and mass ratio, the idea was to compare the %Bias within same system on a different TLL and delivered mass ratio.

5.1.5.2   Results and discussion

A PEG1000-$(NH_4)_2SO_4$ system was selected to compare the error in the delivered TLL and MR at two different tie lines lengths; A PEG/salt systems (8 replicates as before) were constructed at a reduced TLL (25.57 % w/w compared to the previous TLL of 38.9% w/w).

These tie lines were chosen to examine the effect of their length on the % Bias (accuracy) within same phase diagram. The actual TLL and mass ratio of the practical delivered systems were calculated from their gravimetric compositions. Under the assumption that the slope of each tie line (STL) is the same for all tie lines laying very close together, the STL was calculated from the equation

$$STL = \frac{\Delta PEG}{-\Delta \, salt} \qquad \text{Equ. 24}$$

Where ΔPEG is the difference between the PEG in the upper and lower phases, and the Δ salt is the difference between the salt in the lower and upper phases.

The gravimetric compositions of each delivered system (% w/w PEG and %w/w salt) were used to calculate the constant y= mx+c for the slope using the equation

$$Cs = ym1 - STL. xm1 \qquad \text{Equ. 25}$$

Where the Cs is the constant of the slope, ym1 is the experimental mass in the Y axis (%w/w of PEG), and xm1 is the experimental mass in the X axis (% w/w of salt).

The TLL for each constructed system was calculated by numerical methods (see section 2.2.3) from its slope and intersection with the binodal curve, the STL was used to estimate the upper and lower compositions following the equations

$$STL. xt + Cs = yt \qquad \text{Equ. 26}$$

$$\frac{yb - Cs}{STL} = xb \qquad \text{Equ. 27}$$

$$a1 * \exp(b1 * Xt^{0.5} - c1 * xt^3) = yt \qquad \text{Equ. 28}$$

$$a1 * \exp(b1 * Xb^{0.5} - c1 * xb^3) = yb \qquad \text{Equ. 29}$$

The yt and xt are the amount of PEG and salt in the upper phase, the yb and xb are the amount of PEG and salt in the lower phase while the a,b,c are the constant of the Merchuk equation. From the compositions of the delivered system, the TLL was calculated following the equations Equ.1

From this estimate of the TLL and the system composition, the mass ratio (MR) of the each of the practical eight systems could be obtained along with the % Bias of both TLL and MR. The MR was calculated form the system position on Tie line using the following equations

$$TL_B \text{ PEG} = ym1 - yb \qquad \text{Equ. 30}$$

$$TL_B \text{ Salt} = xb - xm1 \qquad \text{Equ. 31}$$

$$TL_T \text{ PEG} = yt - ym1 \qquad \text{Equ. 32}$$

$$TL_T \text{ Salt} = xm1 - xt \qquad \text{Equ. 33}$$

$$TL_B = \sqrt{(TL_B \text{ PEG})^2 + (TL_B \text{ Salt})^2} \qquad \text{Equ. 34}$$

$$TL_T = \sqrt{(TL_T \text{ PEG})^2 + (TL_T \text{ Salt})^2} \qquad \text{Equ. 35}$$

$$MR = \frac{TL_B}{TL_T} \qquad \text{Equ. 36}$$

where the TL $_{T,B}$ is the Tie Line position in Top ($_T$) and Bottom ($_B$), the calculated TLL and MR for each system was compared to the demanded value in the original data then the %Bias was calculated, the mean of %Bias of the eight replicate was used in Table 52 to compare the two different TLL.

Table 52 - Mean % bias (accuracy) of system component composition, TLL and MR for two different TLLs of the PEG 1000-(NH4)$_2$SO$_4$ system.

Mean	PEG 1000-(NH$_4$)$_2$SO$_4$ TLL4=38.91		PEG 1000-(NH$_4$)$_2$SO$_4$ TLL2=25.56	
	PEG	(NH$_4$)$_2$SO$_4$	PEG	(NH$_4$)$_2$SO$_4$
Delivered %w/w	16.16	17.50	16.41	14.76
%Bias %w/w	-0.12	0.07	-0.15	0.43
Delivered system TLL	38.89		26.27	
Delivered system Mass Ratio	0.998		0.93	
TLL %Bias	-0.05		2.75	
Mass Ratio %Bias	-0.19		-7.08	

The mean % Bias of the mass ratio (MR) and TLL was found to be greater at shorter TLL. This must affect the variability (error in determination) of the partition coefficient (K) of added solutes at shorter TLL since K is a function of TLL (16). In addition the increase in % Bias (accuracy) of MR of systems lying closer to the critical point will similarly compromise the calculation of the mass balance of the ATPS. This variability in MR is an important consideration when systems approach the analyte solubility limit or where molecular association occurs. The consequences of this effect of variation of TLL and mass ratio should not go unconsidered.

5.1.6 Theoretical implications Robotic accuracy on TLL and mass ratio

5.1.6.1 Background

A range of 8 PEG1000-(NH$_4$)$_2$SO$_4$ and PEG8000 –Dextran500 systems of known TLL were used to illustrate the mathematical relationship between Tie Line Length and the %Bias (accuracy).

The strategy was performed by using the system range (SR) of the phase compositions from a set of 8 replicates delivered this range was then applied to the calculation of the new compositions of each TLL within the same phase diagram. Same Mathcad structure (as in section 5.1.5.2) has been applied to compute the new TLL and mass ratio for each system range. Consequently, %Bias (accuracy) was calculated. These attempts have been made to utilize this technique to understand the TLL variation of a different ATPS systems were prepared by robotics and to define the limits of detection to analytical ATPS and to be able to make recommendations for the method of system preparation and the design of analytical partitioning experiments.

5.1.6.2   Results and discussion

The LHSP accuracy of aspiration and dispense on the TLL and mass ratio was studied using two different systems, the compositions of four hypothetical ATPS systems were calculated. The composition of the modelled systems range were assigned such that they lay two standard deviations (SD) (based on the distribution of the data already found for the PEG-salt system (TLL 38.9% w/w) and the PEG-Dextran system (TLL 24.1% w/w)) above and below the phase compositions of a system having mass ratio of 1 at each TLL, thus encompassing 95% of the previously determined experimental variability.

The compositions of these hypothetical systems may be expressed as X+2SD Salt, Y+2SD PEG; X-2SD Salt, Y-2SD PEG; X+2SD Salt, Y-2SD PEG; X-2SD Salt, Y+2SD PEG; and similarly for the PEG-Dextran system. Note that these systems form a rectangle surrounding the selected target composition with one pair (X-2SD Salt or Dextran, Y+2SD PEG and X+2SD Salt or Dextran, Y-2SD PEG) lying approximately parallel to the slope of the TLs and the opposite pair lying approximately orthogonal to this slope.

On the basis of the finding in section 5.1.5.2 the range in system compositions was used to estimate the %Bias of TLL and MR for a series of tie lines chosen to lie increasingly close to the critical point for each PEG-salt and PEG-Dextran ATPS (see Table 53 and Table 54)

Table 53 - Systems selected for analysis of the effect of variability in construction on the TLL and MR of the PEG-1000 -(NH$_4$)$_2$ SO$_4$ ATPS.
*STL- Tie Line Slope defined as the ratio STL= (Δ PEG) / (Δ salt) where Δ PEG is the difference between the concentration of PEG and Δ salt the difference between the (NH$_4$)$_2$SO$_4$ in the coexisting phases.

No. of Tie line	PEG1000-(NH$_4$)$_2$SO$_4$ system			
	(% w/w) PEG-1000	(% w/w) (NH$_4$)$_2$SO$_4$	TLL	STL*
TL1	15.03	14.98	12.19	-1.482
TL2	16.42	14.69	25.56	-1.467
TL3	16.96	15.07	32.46	-1.44
TL4	16.17	17.49	38.91	-1.236
TL5	17.84	18.02	45.62	-1.24
TL6	19.11	18.76	49.64	-1.176
TL7	20.47	19.47	53.04	-1.077

Table 54 - Systems selected for analysis of the effect of variability in construction on the TLL and MR of the PEG 8000-Dextran 500 ATPS.

No. of Tie line	PEG8000 –Dextran 500 system having Mass Ratio 1			
	(% w/w) Dextran500	(% w/w) PEG8000	TLL	STL*
TL1	7.097	3.74	13.08	-2.557
TL2	9.08	4.49	19.50	-2.377
TL3	10.85	5.67	24.10	-2.066
TL4	12.84	5.93	28.11	-2.249
TL5	14.04	6.81	31.09	-2.105

For each TLL, statistical range of four systems was calculated, and then the TLL and MR were calculated for each system range as described in section 5.1.5.2. After that the mathematical relationship between Tie Line Length, MR and %Bias in the system range was examined. The effect of the variability in the system range composition on the % bias in TLL and MR for the PEG-Dextran system is shown in Figure 38 A&B.

Figure 38 -A
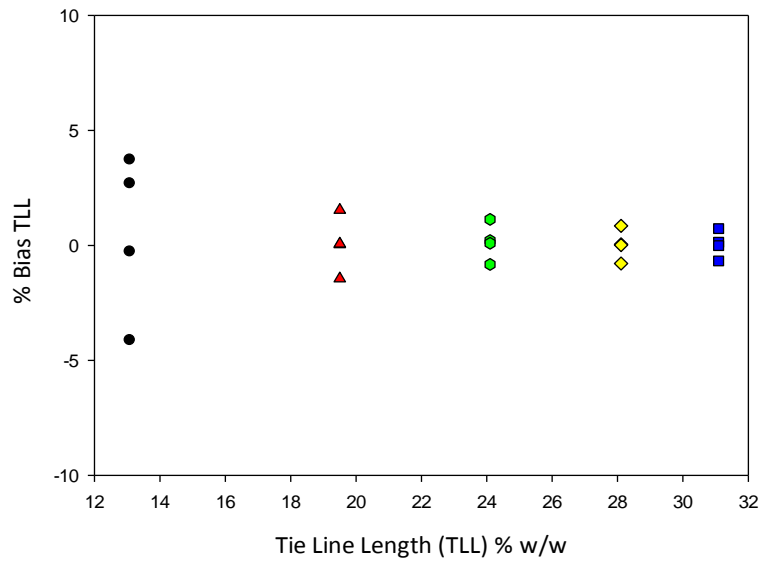
Figure 38 -B
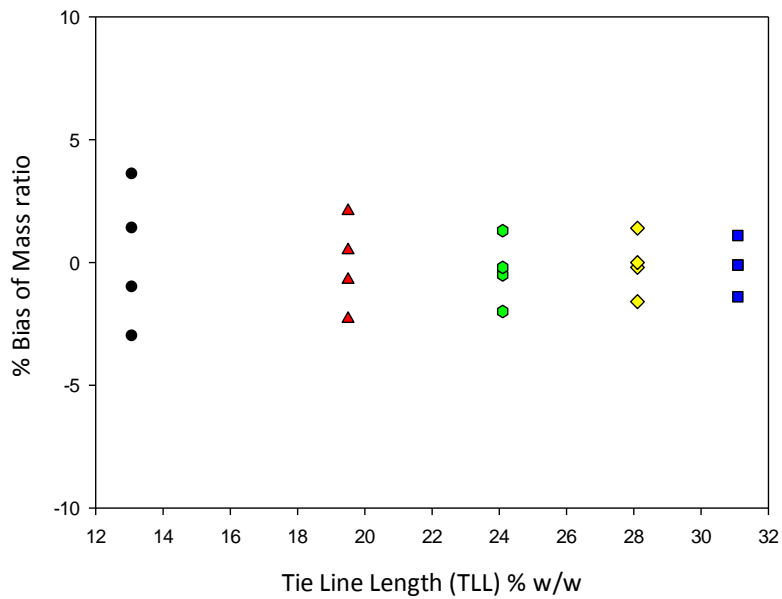
Figure 38 - Modelled variability in the composition of a PEG 8000-Dextran500 system in terms of (A) the %Bias (accuracy) of the TLL (See Table 54) and (B) the %Bias (accuracy) of the MR. Each symbol represents the modelled system range of known TLL (●) TLL1   (▲) TLL2 (●) TLL3 (◆) TLL4   (■) TLL5, illustrating the effect of TLL on the % Bias accuracy in TLL and MR in the construction of ATPS.

The % Bias (accuracy) of TLL length is within ±1% of the target value at long TLL and even at the shortest TLL examined only increases to about ± 4%. Similar results were found for the effect of variability in system composition on the % Bias (accuracy) of MR in this system. These results seem quite acceptable in the context of automated system preparation; erroneous results due to excessive variability of TLL and its effect on the partition coefficient or due to large changes in MR and its effect on mass balance calculations are unlikely at any but the very shortest tie line lengths say below 13 % w/w.

It seems to be accepted that for automated sample preparation in analytical applications % Bias should be within 5% (132), although this criterion appears to be more relaxed for very high throughput minimal volume systems such as may be used in pharmaceutical lead analysis (133).

On the other hand, when the same procedure was repeated a range of TLL of the PEG1000 - $(NH_4)_2SO_4$ system. Similar results showing the effect of % Bias (accuracy) on TLL and MR in the preparation of the PEG1000 -$(NH_4)_2SO_4$ system using parameters derived from the LHSP performance data for the target range of TLLs given in Table 53 are shown in Figure 39 – A&B.

Figure 39 shows the relation between the statistical range of the four modelled systems at each TLL in the PEG1000 - $(NH_4)_2SO_4$ system and (a) the calculated %Bias in the TLL and (b) the calculated %Bias in the MR. The % Bias in TLL of the shortest TLL examined (12.2 % w/w) for systems lying orthogonal to the TLs were found to be very much greater than 5% (+42% and -100%). The latter because this TL composition lies outside the co-existence curve and would fail to form a biphasic system.

As above the errors associated with decreasing TLL, % Bias (accuracy) in MR is in excess of 10% and the % Bias of one system reported as 0% is meaningless as it again lies outside the binodal curve (see Figure 39- B). Increase in TLL to 25% w/w results in a reduction in % Bias (accuracy) of both TLL and MR; however % Bias (accuracy) of TLL is close to ±10% and greater than 5% for MR.

Figure 39 -A
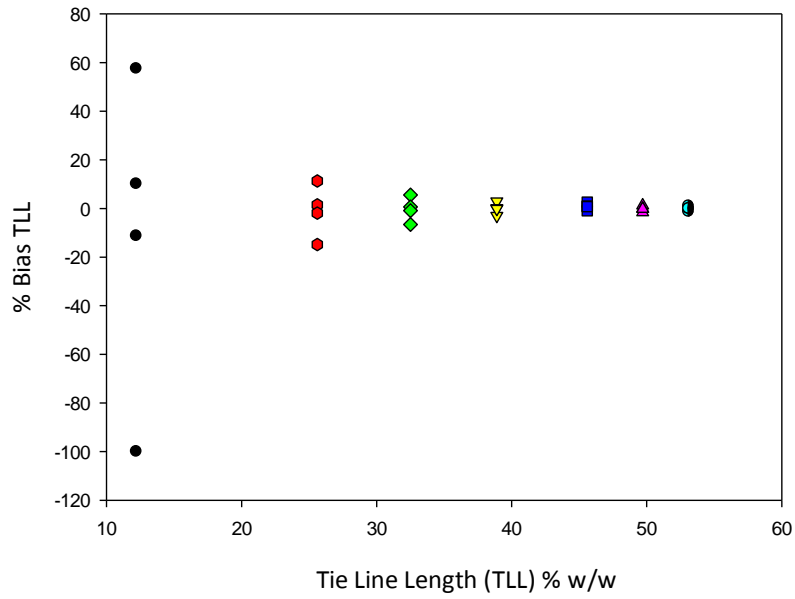
Figure 39 -B
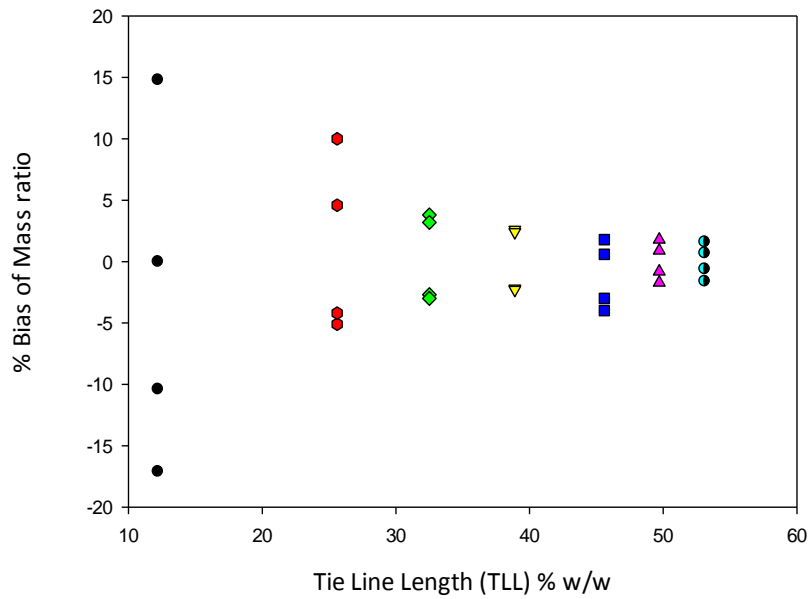
Figure 39 - Modelled variability in the composition of a PEG1000 -(NH₄)₂SO₄ system in terms of the (A) %Bias (accuracy) of the TLL (See Table 53) and (B) %Bias (accuracy) of the MR. Each symbol represents the modelled system range of known TLL (●) TLL1 (⬢) TLL2 (◆) TLL3 (▽) TLL4 (■) TLL5 (▲) TLL6 (◐) TLL7, illustrating the effect of TLL on the % Bias accuracy in TLL and MR in the construction of ATPS.

Note that system pairs lying approximately parallel to the target tie line lead to the greatest error in MR and for those lying orthogonal to the Tie line to the greatest error in TLL. By 32% w/w TLL the error associated with TLL and MR is only marginally acceptable being still somewhat greater than 5% at 2SD from the mean. At longer tie line lengths % bias accuracy is reduced to more acceptable levels

In systems where % Bias (accuracy) is much greater than 10 %, partitioning measurements could only be accurately made with complete knowledge of system composition obtained gravimetrically or photometrically (125) or perhaps by the exhaustive determination of numerous replicates.

The % Bias accuracy of TLL and MR increases more rapidly in PEG-salt systems than in PEG-Dextran systems as tie line length is reduced. The reasons behind this difference are related to differences in the form of the co-existence curve for these systems.

In the PEG-salt system the curvature of the co-existence curve is very low and the TLs run almost parallel to the co-existence curve with the result that the TLL increases rapidly with distance from the critical point. Figure 40 A & B shows the phase diagrams for the systems used here along with the instantaneous radius of curvature of the binodal curve which may be calculated from the curvature defined as:

$$\kappa = \frac{|y''|}{[1+(y')^2]^{\frac{3}{2}}} \qquad \text{Equ. 37}$$

Where y represents a function which describes the binodal curve (134). It is immediately apparent that the curvature of the PEG-salt system is very low and the radius is consequently very high in comparison to the PEG-Dextran system.

This is likely to be true for many, but perhaps not all, relatively high Mw. PEG-salt systems. In some PEG-salt systems in the region of the critical point the curvature of the co-existence curve approaches zero i.e. is almost a straight line see for instance the many phase diagrams given in (16).

Figure 40 -A

Dextran 500 / PEG 8000

Figure 40 -B

PEG 1000 / Ammonium Sulphate
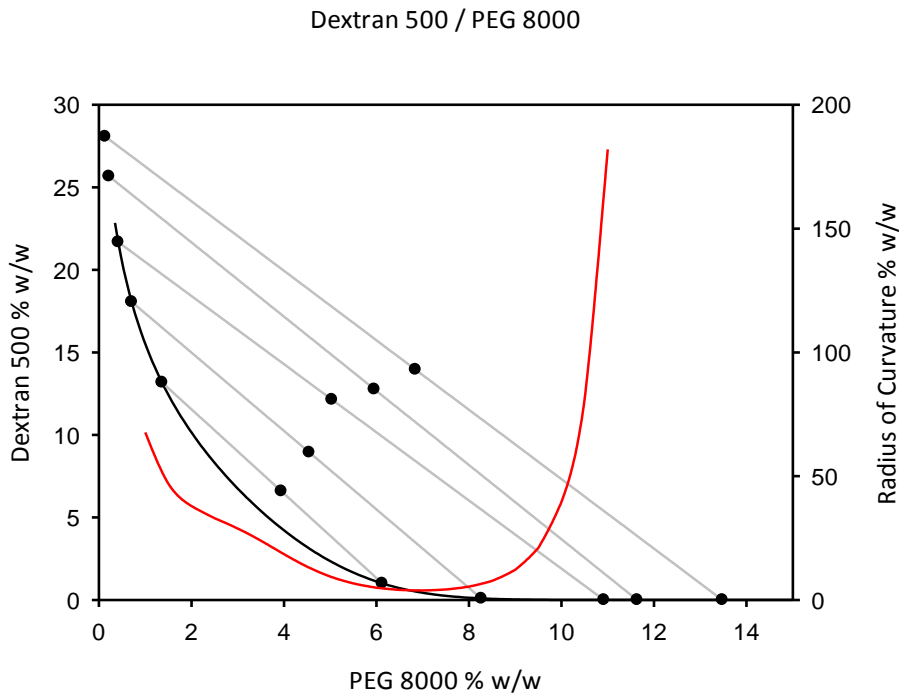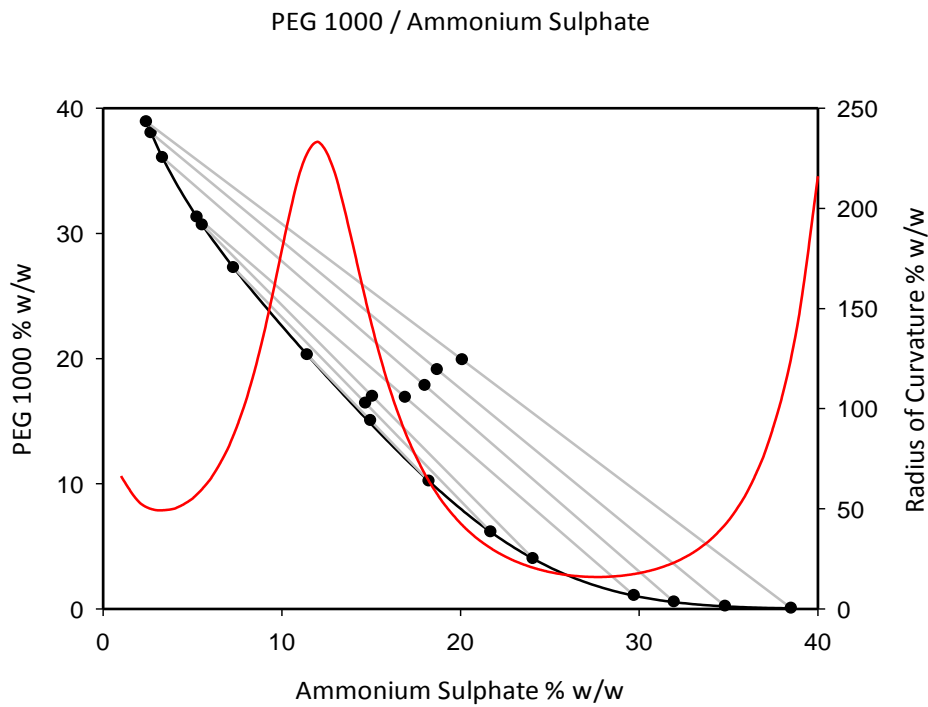
Figure 40 - Phase diagrams of (A) the PEG8000 – Dextran500 system and (B) the PEG1000-(NH₄)₂SO₄ system showing the coexistence curves and disposition of the tie lines and illustrating the considerable difference in curvature of their co-existence curves, the red line represents the instantaneous radius of curvature of the binodal curve which was calculated by equation No. 37

On the other hand in the PEG-Dextran system examined here, this effect is much less pronounced and the co-existence curve has by comparison considerable curvature; this is likely to be the case for many, but not all, polymer-polymer systems. As a consequence the relative increase in TLL (equivalent to the chord length) is more modest as the distance from the critical point increases and the impact of error in system preparation is consequently much reduced. In establishing robotic sample handling systems for the preparation of ATPS attention to the curvature and disposition of the tie lines of the system is important for their accurate preparation particularly when attempting to work close to the critical point.

Conclusion:

Preparative methods and sampling techniques were created for the preparation and sampling of ATPS to enable more accurate determination of the partition coefficient on an automated robotic platform. During the course of this work generic gravimetric methods were developed for establishing accurate and reproducible preparation and sampling of polymer/polymer and polymer/salt ATPS which should be applicable to a wide range of different ATPS.

These methods and particularly the development methodology, and optimization seems to be applicable in general to prepare ATPS of any composition. It was found that for the accurate preparation of ATPS close to the critical point the geometrical form of the phase diagram co-existence curve has a crucial importance since this directly affected the accuracy with which systems of defined TLL and MR could be constructed.

The rate of the change %Bias of TLL and MR in relation to system composition of PEG 8000-Dextran 500 was less than in the PEG 1000-$(NH_4)_2SO_4$ which was found to be dependent on the shape of the phase diagram. In the PEG 8000-Dextran 500 system increased curvature was found in comparison to the PEG 1000-$(NH_4)_2SO_4$ system which was found to be almost flat close to the critical point. As a result the PEG 8000-Dextran 500 system was found to be more robust than the PEG-Salt system in terms of accurately reproducing the demanded TLL and MR. This was found to be increasingly the case the nearer the critical point was approahed.

For systems with a very low degree of curvature, PEG-salt systems in this example, increases in bias (accuracy) are appreciable at relatively long tie line lengths. Where the degree of curvature is more pronounced, PEG-Dextran systems here, closer approach to the critical point is possible without major effect on bias/accuracy.

Chapter 6

6 Method development for the partitioning of specifically labelled Human serum albumin in ATPS

Introduction:

Serum albumin is one of the multifunctional proteins with a number of binding sites and transport properties (85). The importance of the thiol or sulfhydryl group is due to its widespread use in the detection of conformational changes and ligand-binding processes (135) interactions with nitric oxide, binding with several metal cations and it has an importance as scavengers of reactive oxygen species (ROS)

In general, as observed from prior studies (136) (95) (137) there was a performance enhancement in albumin- drug delivery taking advantage of the natural properties of albumin such as the solubility of hydrophobic drugs, selectivity for active tumours, active transportation across the endothelium of blood vessels and facilitation of the diffusion of lipophilic drugs across cell membranes.

For the successful therapeutic development of albumin conjugate process a number of chemical labels were used with a variety of preparation conditions in order to introduce reliable conjugate properties which could be employed for a direct interaction with many conditions, site-specific modification was particularly important for labelling small proteins in applications where the activity or binding affinity of the conjugate is paramount (138).

Aims and Objectives

The aims and objectives of this chapter were:

1. To examine an analytical problem by phase partitioning, including the determination of the degree of conjugation of a protein drug conjugate using an appropriate model system (recombinant HSA) and the determination of the oxidative state of albumin utilising the reactivity of a surface free thiol group.

2. To define the solubility and stability of the chemical label and the protein conjugate, and investigate the reactivity of the label towards the free thiol group.

3. To define the limitations of the modifications and to examine the sensitivity of partition in selected ATPS to the altered protein isoforms resulting from the chemical modification.

4. To develop quantitative methods for monitoring the effectiveness of the conjugation reactions and partitioning procedures such as UV-vis spectroscopy, RP-HPLC and size exclusion chromatography (SEC).

5. To examine a number of chemical labels under a variety of conditions in order to develop a reliable method to prepare a stable and thiol specific conjugate for use as a probe to quantify surface free thiols.

During the course of this work the reagents used for protein conjugation to human and bovine serum albumin were;

(a) 2-methylsulfonyl-5-phenyl -1,3,4 oxidiazole (MSPO), (b) N-Ethylmaleimide (NEM), (c) 5, 5'-dithiobis (2-nitrobenzoate)(DTNB) (Ellman's reagent), (d) N-pyrenylmaleimide (NPM), (e) Fluorescein-5-maleimide (F-5-M).

6.1 Modification of HSA with 2-methylsulfonyl-5-phenyl -1,3,4 oxidiazole Reagent:

6.1.1 Background:

To form a covalently linked protein–label conjugate, 2-methylsulfonyl-5-phenyl -1,3,4 oxidiazole (Molecular structure shown in Figure 41) has been reported as thiol-linking to produce an Albumin-conjugate. The recent work suggested the possibility of using MSPO as a label for modifying human serum albumin (139) following the reaction scheme in Figure 42. Protein conjugation means joining a chemical or biological molecule to a protein exploiting a specific site or, in this case, by making a covalent bond to a free surface Cys-thiol, which is considered a good nucleophile. In order to explore the effectiveness of the 2-methylsulfonyl-5-phenyl -1,3,4 oxidiazole reagent and the stability of any thiol conjugate formed a variety of conditions were examined in order to develop a reliable method to prepare a stable and thiol specific conjugate, which could be used as a probe for the determination of protein surface free thiols by partitioning following the experimental procedure which is described in section 2.5.1.1
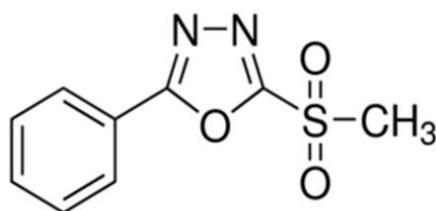
Figure 41- Molecular structure of 2-methylsulfonyl-5-phenyl -1,3,4 oxidiazole
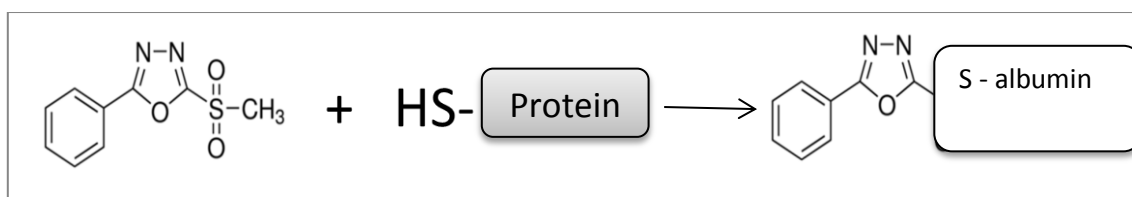
Figure 42- Reaction scheme for modification of Albumin with 2-methylsulfonyl-5-phenyl -1,3,4 oxidiazole (139)

6.1.2 Results and discussion

Several different concentrations of the label in buffer covering the range 0.16, 0.38 and 0.76 μM were used to determine the absorbance in the range 200-400nm. The maximum absorbance was recorded at 268nm and identified as the wavelength of maximal absorption ($λ_{max}$) for the label.

To initially identify the label–HSA derivative, RP-HPLC was used. The separation peak of albumin, label and the modified HSA after derivatization were determined using a C18 column to separate the protein and the chemical label based upon surface hydrophobicity. The HPLC chromatogram (Figure 43) showed a separate peak for the protein and label with almost no change in the peak height of the label and protein. There is no evidence of any appreciable reaction. Under the assumption that no free thiol was present in the purified human serum albumin or that it had become oxidized during the purification process or it was buried inside the protein structure and therefore only partially accessible to reagents a second attempt to examine the reactivity of the MSPO label was made using recombinant-HSA (rHSA) following the procedure as outlined in section 2.5.1.1. In order to estimate the extent of the reaction, the ratio of 268/280nm for the label and label**:** protein was calculated utilizing the peak height of the blank linker and the peak height of the linker in presence of the protein from the results of RP-HPLC.

The HPLC results indicate there is no evidence of appreciable reaction since there was no change in the peaks height for both the protein and label before and after reaction using two different sources of albumin as illustrated in the Table 55 A&B
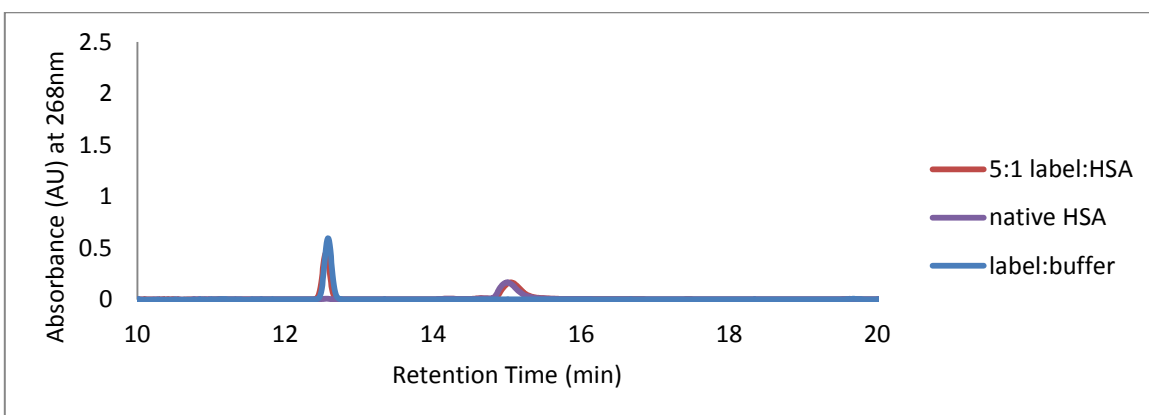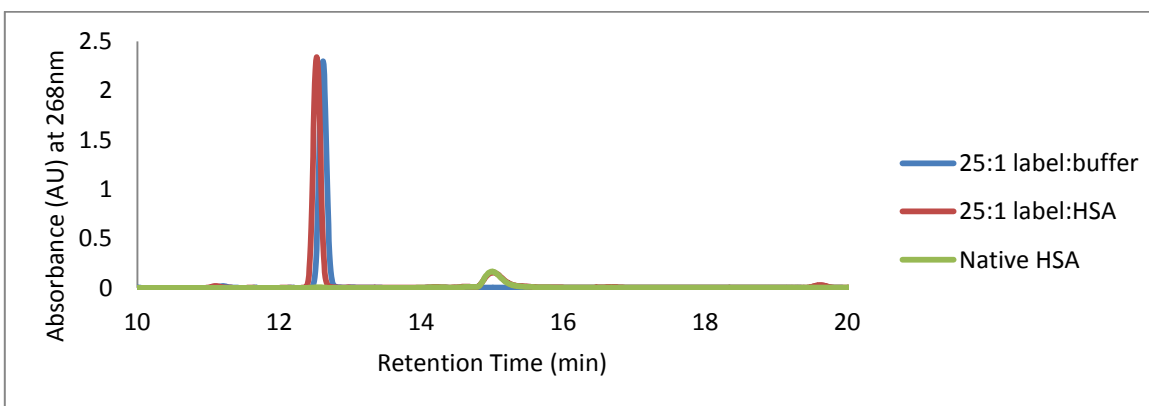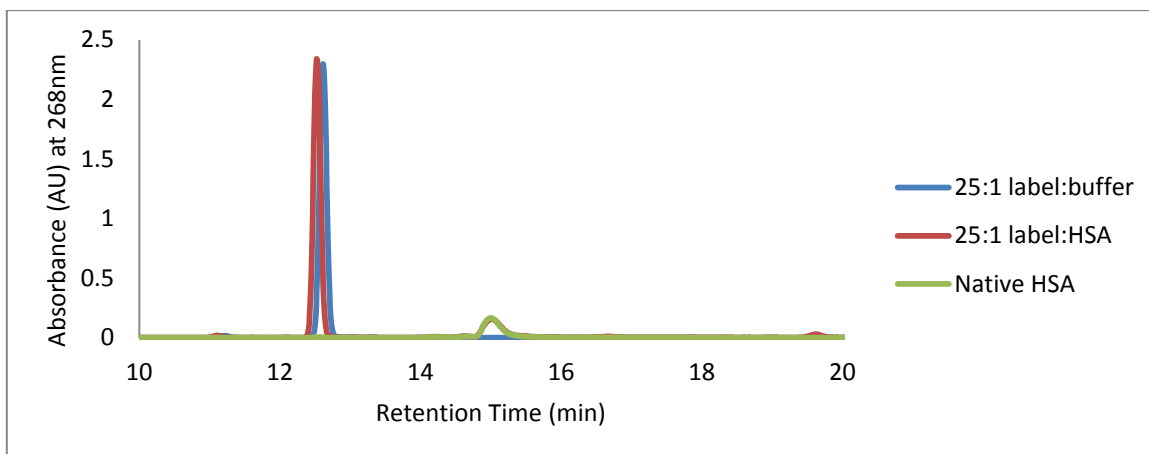
Figure 43- HPLC chromatogram using C$_{18}$ column (YMC-pack ODS-AQ 5.0 µm, 150 × 4.6 cm) for the analysis of a reaction mixture containing 2-(Methylsulfonyl)-5-phenyl-1, 3, 4-oxidiazole (label) and purified-HSA at a different molar ratio label: HSA 25:1, 12.5:1 and 5:1.

Table 55- The experimental calculation of the absorbance ratio of 280/268 for the standard MSPO and the ratio after treatment with (A) purified albumin and (B) recombinant albumin at different molar reaction ratios.

-A-	A280nm	purified albumin			
Molar ratio Label: protein	Label	protein	Label: protein	280/268 Label	280/268 Label: protein
5:1	0.540	0.156	0.408: 0.158	0.44	0.44
12.5:1	1.14		1.145: 0.153	0.47	0.48
25:1	2.174		2.197: 0.149	0.74	0.74
A268nm					
5:1	1.227	0.150	0.931: 0.149		
12.5:1	2.426		2.385: 0.146		
25:1	2.937		2.979: 0.141		

-B-	A280nm	Recombinant albumin			
Molar ratio Label: protein	Label	protein	Label: protein	280/268 Label	280/268 Label: protein
5:1	0.468	0.213	0.417: 0.192	0.44	0.44
12.5:1	1.045		1.061: 0.189	0.46	0.46
25:1	1.886		2.123: 0.193	0.65	0.67
A268nm					
5:1	1.068	0.210	0.95: 0.181		
12.5:1	2.258		2.32: 0.177		
25:1	2.90		3.17: 0.178		

L-Cysteine (Mw. 121.15) was used to further examine the reaction since the number of free thiols in the cysteine is absolutely known and is also known to be accessible. A 2mg/mL solution of L-cysteine was prepared in 50mM potassium phosphate buffer pH 7.4 containing 150 mM NaCl. A range of dilutions were prepared (0.01, 0.05, 0.1, 0.25 and 0.5 mg/mL) in a final volume of 1 mL to which was added a constant amount of MSPO (10μL) at a concentration of 5mg/mL.

However, HPLC could not achieve any separation for Cysteine mixture due to the solubility in the aqueous solution buffer and that caused a rapid elution of Cysteine without interaction with the C18 column. There was no visible change in the height of the MSPO label peak following a 2 hour reaction time as illustrated in Figure 44.
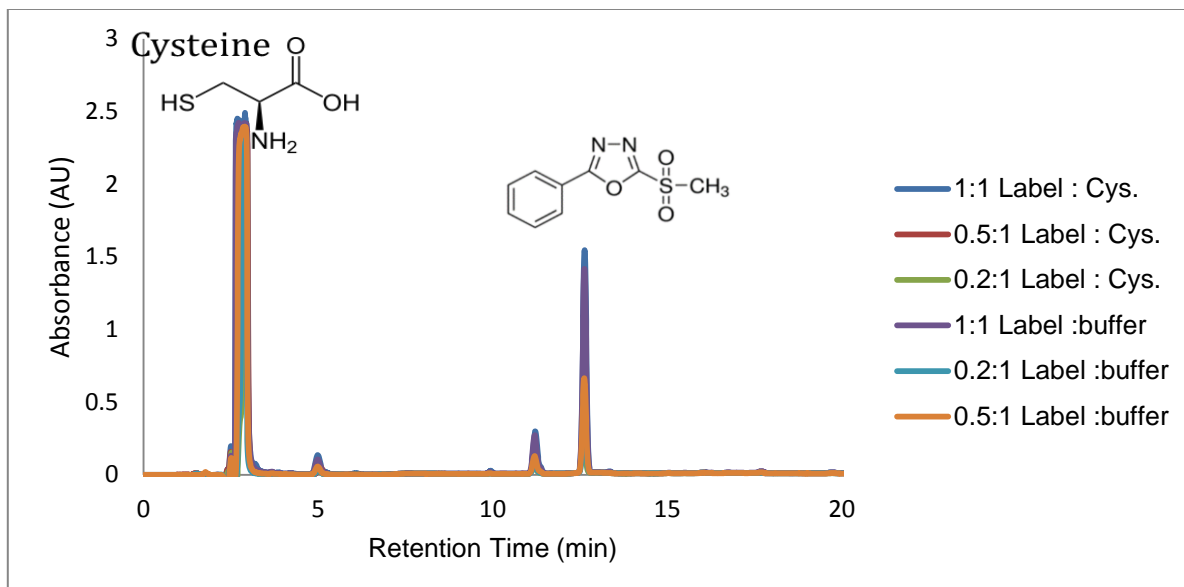
Figure 44- HPLC chromatogram for the reaction of MSPO (label) with Cysteine using a molar ratio label : Cysteine (1:1, 0.5:1 and 0.2:1), C18 YMC-pack ODS-AQ (5.0 µm, 150 × 4.6 mm), Buffer A 10% v/v ACN containing 0.1% TFA pH1.7, Buffer B 90% v/v ACN containing 0.1% TFA pH 0.9.

A final attempt to induce this reaction was made using methyl-benzene thiol (MBT) (Mw. 124.2 g/mole and the molecular structure shown in Figure 45) under exactly the same conditions as given above for L-cysteine. This attempt was made to examine the reaction with other source of thiol.
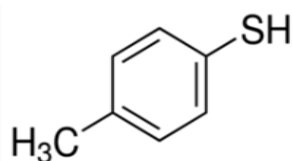
Figure 45- Molecular structure Methyl-Benzene Thiol (MBT)

Analysis by RP-HPLC showed no change in MBT peak height (see Figure 46).

Final conclusion: MSPO was employed as a thiol specific ligand in reaction with free thiol groups of albumin, cysteine and methylbenzenthiol. However the reagent proved unreactive under all tested conditions. The results of RP-HPLC analysis showed

separation of protein and label with almost no change in the peak height of the label with proteins, cysteine or MBT before and after the reaction.
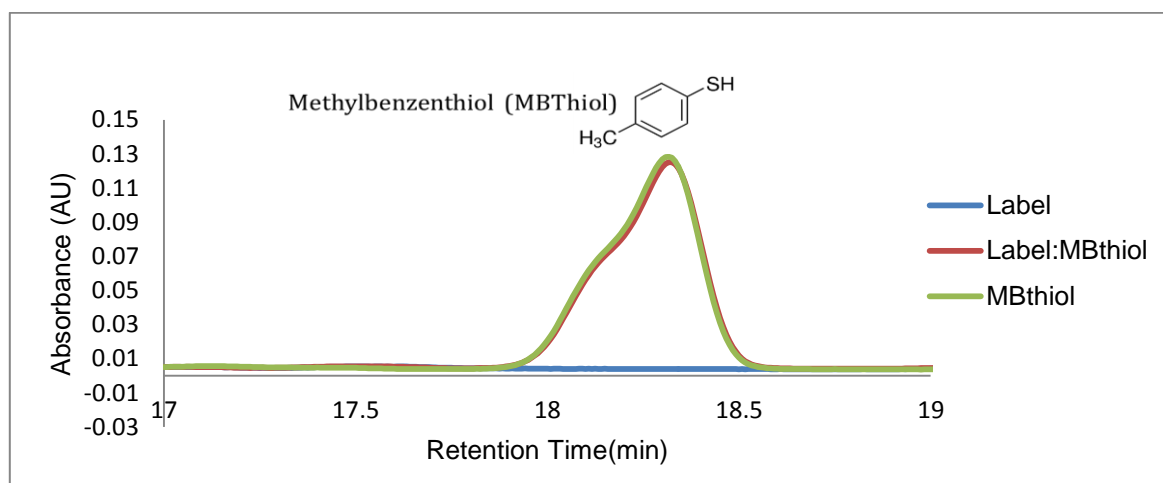
Figure 46- Peak height zooms from HPLC chromatogram before and after reaction of 2-(Methylsulfonyl)-5-phenyl-1,3,4-oxidiazole(linker) with MBT using a molar ratio of label : MBT (0.2:1). Analytical HPLC was employed using a Waters 2695 Separation Module, with a chromatographic column C18 ((YMC-pack ODS-AQ 5.0 µm, 15cm × 4.6 mm) Buffer A 10% ACN (0.1%) TFA pH1.7, Buffer B 90% ACN (0.1%) TFA pH 0.9

6.2 Reaction of HSA with N-Ethylmaleimide (NEM) Reagent

6.2.1 Backfround

N-Ethylmaleimide (NEM) is an alkylating compound derived from maleic acid (molecular structure shown in Figure 47).
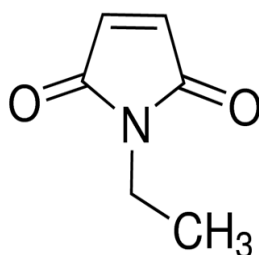
Figure 47- Molecular structure N-Ethylmaleimide

The functional group of NEM (maleimide) reacts with the sulfhydryl groups to modify cysteine residues in proteins and peptides by a nucleophilic attack of the thiolate anion. Thus the reagent has been used to label the free thiol. However it has also been shown to have reactivity towards amine groups under the pH conditions > 7.5 (140).

In this reaction, the thiol is added across the double bond of the maleimide to yield a thioether as illustrated in Figure 48.
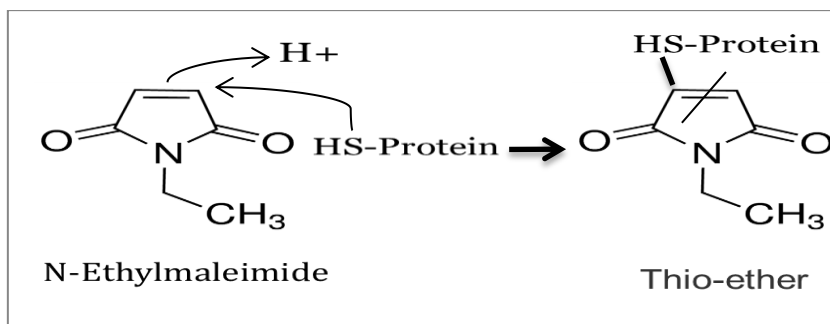
Figure 48- Reaction scheme for the N-Ethylmaleimide with thiol group.

NEM has been widely used to probe the functional role of thiol groups in enzymology and shows a high reactivity with sulfhydryl groups. NEM reaction is an irreversible inhibitor of all cysteine peptidases, with alkylation occurring at the active site thiol group (141).

NEM is excellent reagent for thiol-selective modification, quantitation and analysis to form succinimide conjugates, NEM reaction is an irreversible inhibitor of all Cysteine peptidases, the pH value (pH 6.0 - 7.0) is critical for the reaction, because outside this pH range NEM hydrolyses to N-Ethylmaleaminic acid (142)

6.2.2 Results and discussion

Characterization and identification of the NEM reaction with thiol was monitored following the experimental procedure described in paragraph (A) in section 2.5.1.2. Initially, Cysteine (Cys) was used to follow the reaction and the stability of the NEM compound and Thioether derivative at pH 7.

NEM showed good reactivity towards Cys-thiol and the reaction proceeded rapidly forming of stable thio-ether derivative which resulted in a decrease in the absorbance at 300nm (see Figure 49). The difference in the absorbance between blank NEM and the absorbance after reaction was divided by molar extinction coefficient of the NEM (620 M^{-1} cm^{-1}) (143), the quotient reflected the molar thiol concentration in the samples.
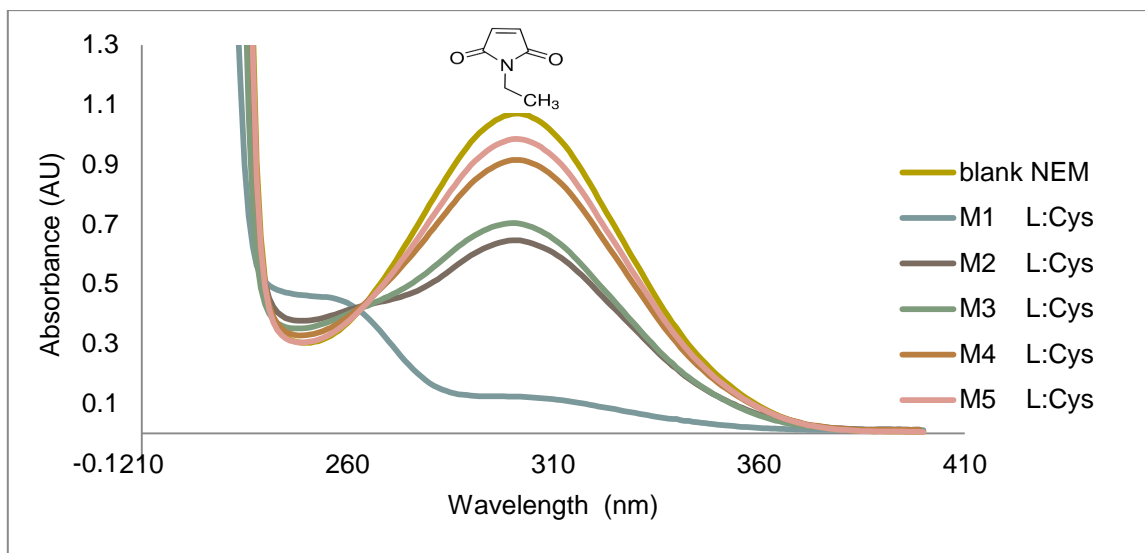
Figure 49 - Absorption Spectra of the reaction of the NEM & Cysteine using the concentrations – (M1) 1.65 x 10^{-3} M, (M2) 8.25 x 10^{-4} M, (M3) 6.6 x 10^{-4} M, (M4) 3.3 x 10^{-4} M, (M5) 1.6 x 10^{-4} M with 1.61 x 10^{-3}M N-Ethylmaleimide. Comparison of values of absorption maximum at the wavelength of 300, spectra measured in the interval form 200 to 500 nm.

Reactive groups have been characterized as a competitive test using for assessing the reactivity of NEM towards thiol by reacting with MBT. Reaction samples were prepared following the experimental procedure described in paragraph (B) in section 2.5.1.2

Experimentally, spectrophotometry proved to be an inefficient method to monitor the reaction due to the overlap of the absorbance in the wavelength of the reactant and product peaks at the wavelength 300nm.

All samples were analysed using a reversed-phase C18 column under the conditions established previously in Table 10. RP-HPLC successfully separated the thiol-ether derivative, MBT and NEM which showed differences in retention time (see Figure 50).

The chromatogram demonstrates the formation of the thioether derivative of the reaction of MBT and NEM at different molar ratios. In addition, a good separation was achieved by RP-HPLC.

Assessment of the reactivity of NEM towards protein-thiol was made using BSA to examine the amount of free thiol in the BSA. Samples were prepared following the experimental procedure described in paragraph (C) in section 2.5.1.2
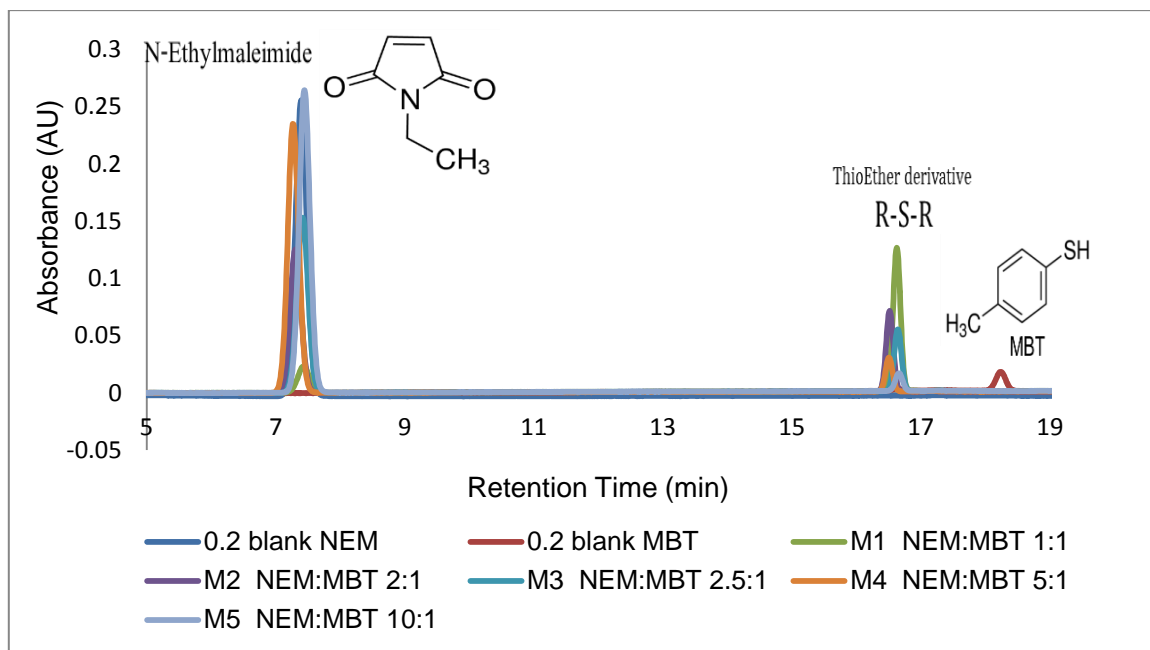
Figure 50- HPLC chromatogram of the reaction of NEM & MBT using the concentrations (M1) 1.61 x 10^{-3} M, (M2) 8.1 x 10^{-4} M, (M3) 6.4 x 10^{-4} M, (M4) 3.2 x 10^{-4} M, (M5) 1.61 x 10^{-4} M with 1.61 x 10^{-3} N-Ethylmaleimide and under the following conditions: chromatographic column C18 ((YMC-pack ODS-AQ 5.0 µm, 15cm × 4.6 mm) , solvent A was 10% v/v ACN containing (0.1%) TFA pH1.7 and solvent B 90% v/v ACN containing (0.1%) TFA pH 0.9

Limited reactivity of BSA toward NEM was found under these conditions. The data was analysed using the spectrophotometric absorbance at 300 nm. The slope of the linear regression between the amounts of bound NEM calculated using the extinction coefficient of NEM versus the amount of BSA represents the amount of free thiol present in the samples.

The reaction of NEM with thiol-BSA was much slower than the reaction with the thiol group of free amino acid cysteine. The slope of the regression showed that 94% of thiol groups of cysteine were derivatised compared to only 26% of thiols BSA. In addition the reaction of NEM with thiol-BSA illustrated a non-linearity in the relationship as shown in Figure 51.

The non-linearity was suspected to the limited amount of free thiol in the BSA which may represent a saturation state with the label (NEM).
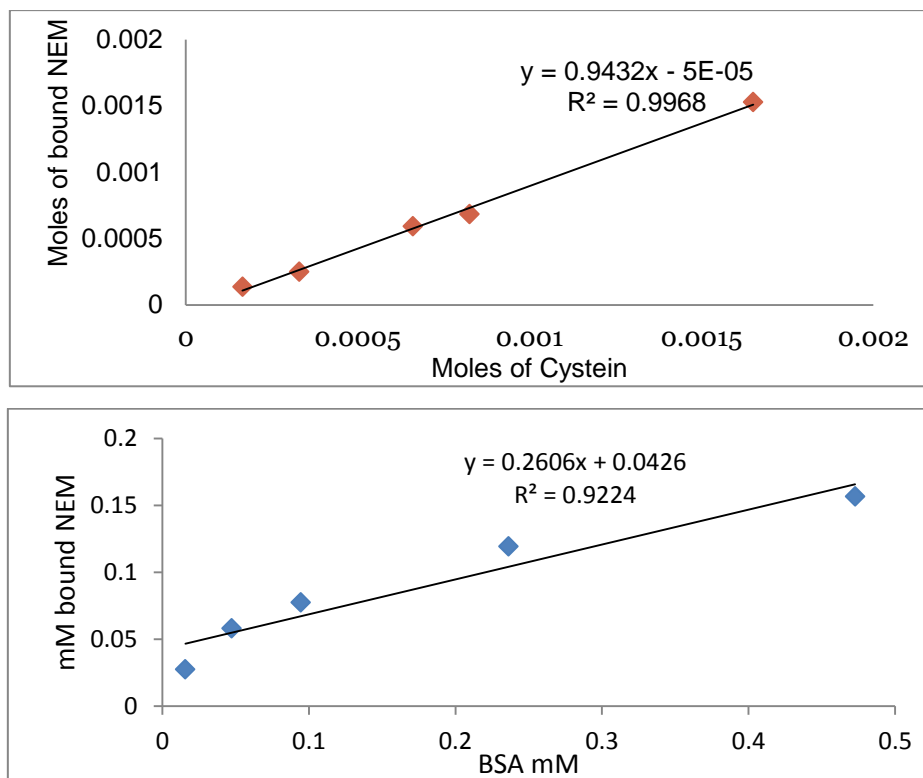
Figure 51- Reactivity of N-Ethylmaleimide toward Cysteine-thiol (♦) and BSA-thiol (♦) using reaction buffer 100mM phosphate pH 7 containing 150mM NaCl

It has been reported that the specificity of NEM towards free thiol can be maintained using a reaction pH below 7 (140). In an attempt to investigate this effect and to improve the reaction, the same procedure was repeated using phosphate buffer at pH6 to see whether the specificity of NEM was improved. The following concentrations of BSA were prepared: 1, 3, 6, 15, 21, 27, and 30 mg/mL using phosphate buffer 100mM pH 6 containing 150mM NaCl.

Under these conditions (pH 6), the specificity of NEM towards protein- thiol was limited either by the number of free thiols on the BSA surface or by the accessibility of the groups. Thus the same results were obtained with almost no change in the slope of the regression as shown in Figure 52.

These reaction conditions were further investigated by employing a reducing agent. The presence of a reducing agent has been employed in some cases to maintain the activity and stability of thiol in this reaction. Dithiothreitol (DTT) is a thiol-reducing agent which was used to reduce thiol groups of proteins and prevent disulfide bond formation. Thus reduction in the presence of DTT might improve and accelerate the reaction with NEM.

DTT inhibits maleimide attachment and must be removed before labelling; the reducing power of DTT is limited to pH values above 7. (144)
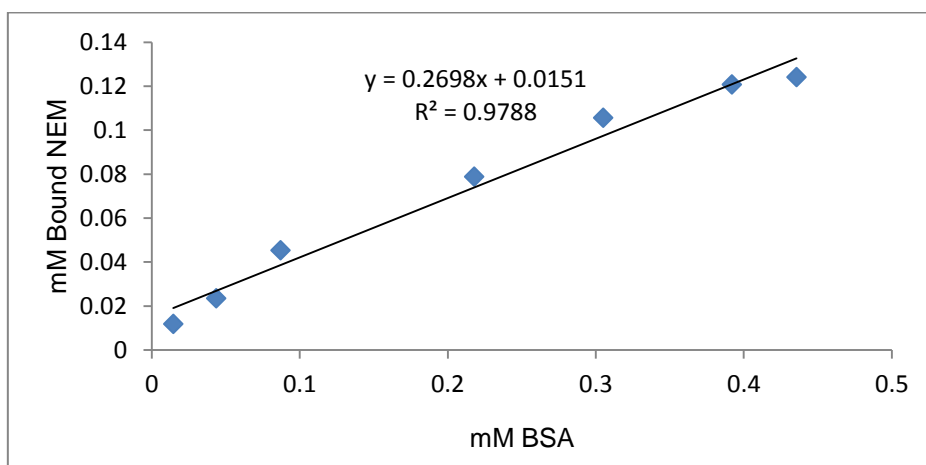
Figure 52- Reactivity of N-Ethylmaleimide toward BSA -thiol using reaction buffer 100mM phosphate pH 6 contain 150mM NaCl

The main aim of this experiment was to increase the reactivity of NEM towards thiol by increasing the amount of free thiols.

An initial test was made using Dextran as a high molecular weight compound which has no free thiols, thus any free thiols found are those of residual DTT. Dextran was mixed with an amount of DTT and Cys.

Cysteine has a molecular weight 121.5 g/mole and DTT has a molecular weight 154.25 g/mole and are expected to be eliminated as a result of the dialysis step. The aim of this step was to measure the dialysis time which would be sufficient to eliminate all the DTT and cysteine also to determine the efficiency of the dialysis.

Dextran, DTT, NEM and Cysteine stock solutions were prepared at a concentration of 30mg/mL, 1M, 2mg/mL and 40mg/mL respectively in the phosphate buffer 100mM pH 6 containing 150mM NaCl. The dialysis mixture consists of 10mL Dextran, 100 µL DTT and 100 µL cys.

Dry dialysis tubing was used for removal of unwanted small molecules of DTT and cysteine. The membrane was swollen by treating with warm water and the length of tubing necessary to contain the protein sample was calculated with an extra two inches on each side. One end of the tube was closed, and then 2mL of the mixture sample was pipetted into the tubing and the other end was closed off. The dialysis tubing was inserting into dialysis buffer (phosphate buffer 100mM pH 6 containing 150mM NaCl)

using a large beaker contain 3L of buffer and gently stirred. The Dialysis Buffer was discarded and replaced with the same volume of fresh Buffer after 6, 22 and 28 hours and each time one tube was removed and carefully pipetted into a fresh tube.

1mL of the dialyzed solution was mixed with 25 µL NEM to confirm the efficiency of the dialysis process to eliminate the DTT. After 28 hours the dialysis was found to be 100% complete with no presence of any DTT.

The same experiment was repeated using 30mg/mL BSA instead of Dextran to see whether this would improve the reaction with NEM. Three different concentration of BSA 1.5, 3, 6mg/mL were prepared from stock, 10mL of each concentration was mixed with 100 µL DTT (1M) and 2mL carefully aliquoted into the dialysis tube and the same procedure was carried out. An overnight incubation was found to be optimal for removal DTT molecules from the protein samples. However, the treated with DTT did not improve the reaction with NEM and that may be due to irreversible oxidation of the free thiol.

6.3 Reaction of albumin with 5, 5'-dithiobis (2-nitrobenzoate) Ellman's Reagent

6.3.1 Background:

Ellman's reagent (DTNB) has been used as a quantitative method for the determination of the sulfhydryl content of proteins. DTNB is a rapid and direct colorimetric assay for any free thiol (145). It has been widely used in analytical biochemistry to measure thiol content in proteins and for labelling cysteine residues (146). The reaction includes the formation of mixed disulphide with release of one equivalent of 2-nitro-5-thiobenzoic acid (TNB^{-2}) as shown in Figure 53 (147).

Figure 53- Reaction of Ellman's reagent (DTNB) with free thiol to form TNB^{2-} and a mixed disulphide.

The main aims of this section were to study the modification of protein using Ellman's reagent, study the details of the reaction mechanisms and to estimate the total protein thiols by monitoring the decrease of DTNB and the amount of TNB production during the reaction.

6.3.2 Results and discussion:

Ellman's reagent was used to calculate total thiol groups in a non-protein thiol (Cysteine) employing a spectrophotometric assay and following the experimental procedure in paragraph (A) section 2.5.1.3.

Initially the conjugation was calibrated under a specific reaction condition. The increase in the absorbance of TNB^{2-} ion was measured, the number of mmoles of TNB formed was calculated using an extinction coefficient of 14,150 $M^{-1}cm^{-1}$ at a λ_{max} of 412 nm (106); Figure 54 shows the UV/VIS spectra of the reaction between Cysteine and Ellman's reagent.

With increasing concentration of cysteine there was a progressive concentration dependent decrease in absorbance at 324nm and an increase in the amount of TNB^{2-} produced from the reaction as shown by the increase in absorbance at a wavelength 412nm.

Figure 54- Spectra of DTNB and Cysteine at concentrations from 0 to 1.5mM; (a) 1.5, (b) 1.25, (c) 1.0, (d) 0.75, (e) 0.5, (f) 0.25, (g) 0 Cysteine (blank Ellman's reagent), Comparison of values of absorption maximum at the wavelength of 324, 412 nm.

Reactivity of Ellman's reagent with the thiol of cysteine was investigated through the formation of TNB. The slope of regression represents the amount of released 2-nitro-5-thiobenzoate anion for each sulfhydryl group present resulting from reaction of each mole of Ellman's with a mole of cysteine as shown in Figure 55.

$$y = 0.9031x + 0.0092$$
$$R^2 = 0.9874$$
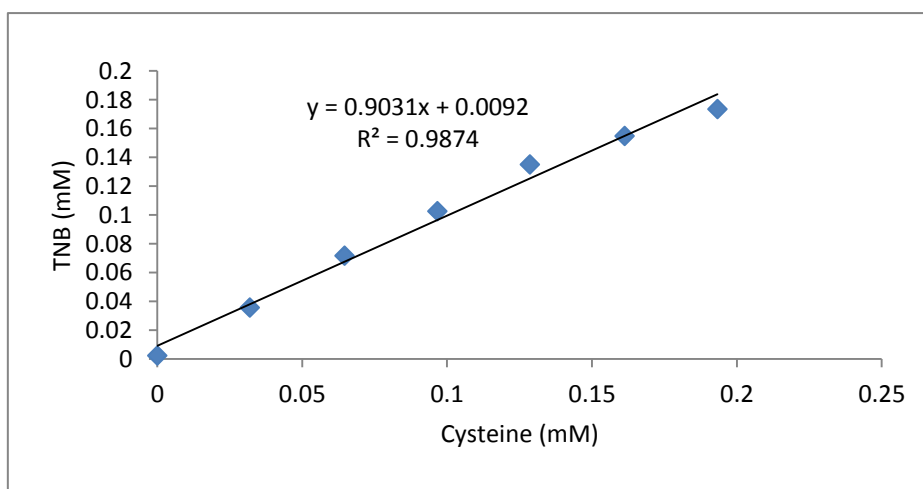
Figure 55- Reactivity of Ellman's reagent toward Cysteine-thiol derived from the amount of TNB^{2-} produced.

Following this reaction, Ellman's reagent was used in reaction with purified HSA to examine the reactivity of the label toward the protein thiol. DTNB reacts with the conjugate base (R—S-) of a free sulfhydryl group on the protein surface resulting in the production of a mixed disulphide linked to the thiol of the substrate (albumin) and 2-

nitro-5-thiobenzoate anion (TNB) , a yellow product having a maximum absorbance at 412 nm.

Reaction mixture samples of protein and Ellman's reagent were prepared following the experimental procedure in paragraph (B) and Table 14 in section 2.5.1.3

In spite of the intensive use of Ellman's reagent to quantify free thiol, no specific HPLC-analytical procedure was found in the literature. Samples were analysed by reversed phase-HPLC utilizing the method previously described in Table 12).

Based on the results obtained from HPLC, there was no change in the peak height of the either protein nor the Ellman's reagent after the reaction, as shown in Figure 56. The purified HSA seems to show a poor reactivity with Ellman's perhaps due to its limited thiol content.
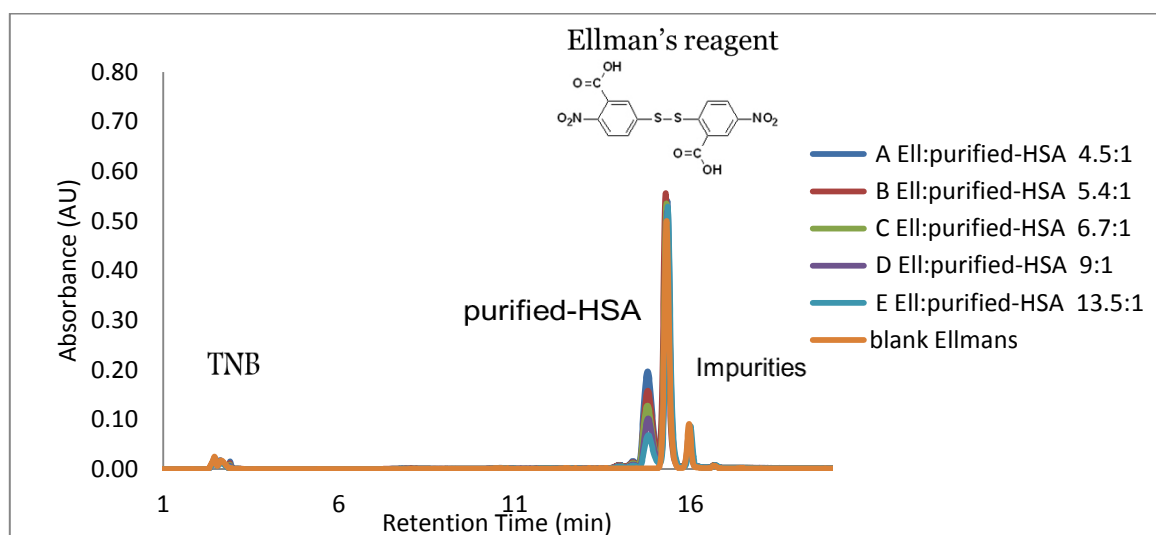
Figure 56- HPLC –chromatogram of the reaction of Ellman's reagent and purified-HSA at the concentration (A) 4.028 x 10^{-5}, (B) 3.357 x 10^{-5}, (C) 2.685 x 10^{-5}, (D) 2.014 x 10^{-5} and (E) 1.343 x 10^{-5}mM, the analysis was performed under the following conditions: chromatographic column C18 (YMC-pack ODS-AQ 5.0 µm, 15cm × 4.6 mm). solvent A was 10% v/v ACN containing (0.1%) TFA pH1.7 and solvent B 90% v/v ACN containing (0.1%) TFA pH 0.9

On the other hand, TNB has a weak signal at 412 nm by HPLC, thus samples were re-analysed by spectrophotometry using the absorbance at 412 nm the λ$_{max}$ of TNB.

By doing so, an estimate of the protein free-thiol concentration could be obtained according to the stoichiometry of the reaction. The concentration of TNB was estimated from its molar extinction coefficient and that was plotted against the molar concentration of the added cysteine or albumin.

TNB formation can be used to assess the number of thiols present, the slope of the regression represents the amount of free thiol derivative produced from reaction with

Ellman's reagent or the percent of the reaction through the Linear relationship for the reaction of Ellman's: Cys and Ellman's: purified-HSA this was determined by plotting the concentration of TNB calculated from its extinction coefficient (y) versus the corresponding concentration of cysteine or protein in the reaction mixture (x) resulting in an estimate of thiol reactivity for cysteine of about 90% (as shown in Figure 55) and only about 18% for purified HSA as shown in Figure 57.
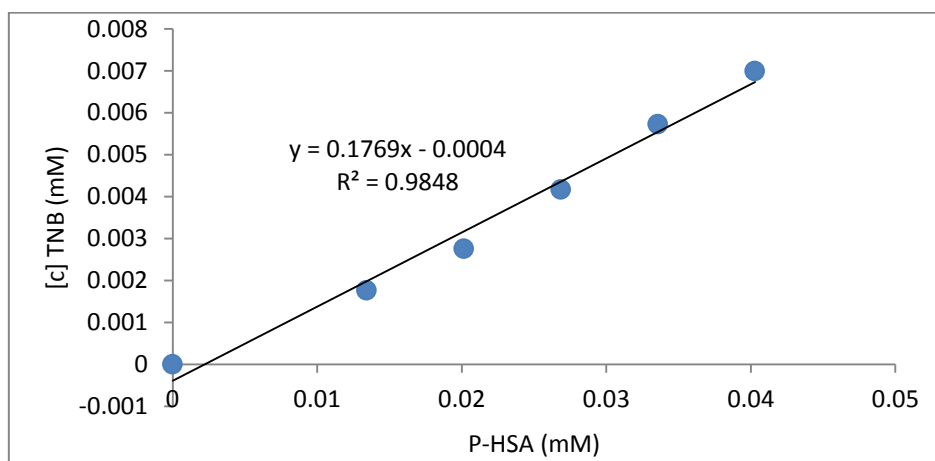
Figure 57- Reactivity of Ellman's reagent toward p-HSA thiol using phosphate reaction buffer of 100mM pH8 containing 1mM EDTA.

One important issue in the quantitation of thiol by UV/VIS spectrophotometry may be the contribution from compounds whose absorption spectra overlap that of the analyte resulting in contributions to the absorption at the wavelength used to measure the analyte.

Spectral results (see Figure 58 using one sample mixture as an example illustrated obvious interference peaks and indicate a potential contribution for the three compounds (protein, Ellman's and TNB) which could result in failure to accurately determine the concentration of derivative protein. Therefore, it was decided to examine the reaction components by HPLC and to develop a mumerical method using Mathcad to overcome the problem.
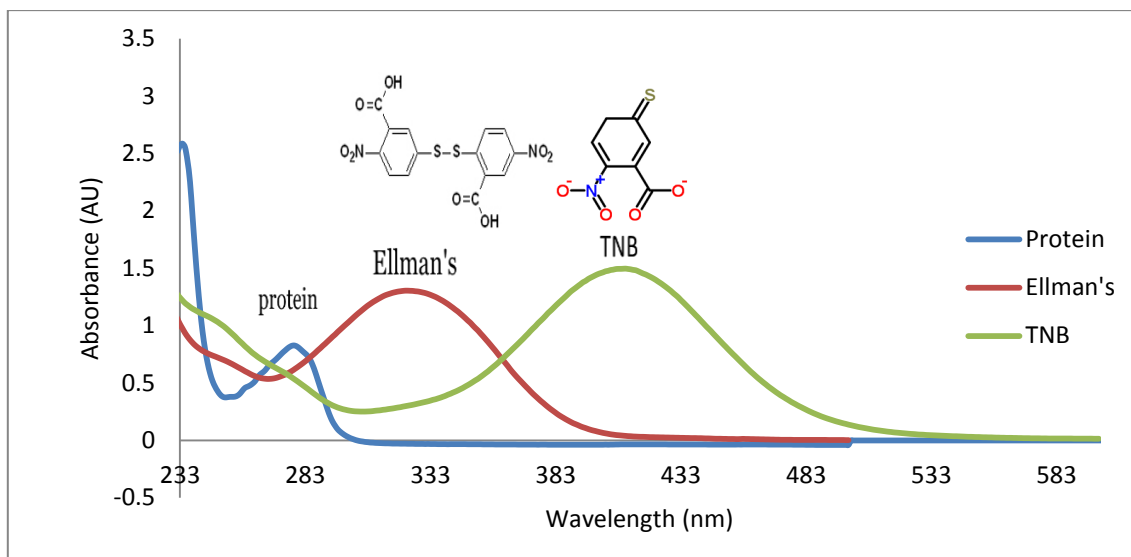
Figure 58- UV/VIS Spectra showing the contribution of the Ellman's reagent (red line) , protein HSA (blue line) and TNB (green line) peaks showing spectral overlap.

It was not possible to calculate the total free thiol in the purified HSA solutions using HPLC analysis due to their limited content of free thiol. Thus spectrophotometric relationships between the absorbance of protein, Ellman's reagent and TNB were used to determine the mixture compositions. The extinction coefficients (E) for the three compounds (Albumin, Ellman's reagent and TNB) are known from the literature at their λ_{max} (280nm, 324nm and 412nm respectively). By constructing a standard series of Ellman's reagent, the contribution of Ellman's reagent at 280nm (E280Ellmans) and at 412nm (E412 Ellman's) could be derived. In the same way, from a standard series of HSA the contribution of HSA at 324nm (E324 HSA) and at 412nm (E412 HSA) could be derived. Similarly, from the concentration of TNB using the cysteine reaction data the contribution to the total absorbance at each wavelength from TNB could be obtained.

However, the contribution of TNB to the absorbance at 280nm in the standard curve was effectively zero and was neglected. The contribution of TNB at 324nm was calculated using the same cysteine reaction data.

By numerical analysis and using a system of simultaneous equations employing the absorbance of the HSA, Ellman's reagent and TNB at each wavelength the concentration of each component in the mixture could be calculated as will illustrate in Appendix (C).

Subsequently, recombinant-HSA (rHSA) was used in reaction with Ellman's reagent. Single phase reaction samples were prepared following the experimental procedure in paragraph (C) and the partitioning experiment was performed following the procedure in paragraph (D) in section 2.5.1.3. Reaction mixtures of Ellman's reagent with recombinant-HSA (rHSA) were performed following Table 15 to prepare different molar ratios of Ellmans' reagent to protein. Single phase reaction was prepared to calculate the total free thiol in the protein samples, and then used in the partitioning experiment. The ATPS PEG3350 - Dextran500 phase system was used to study the partitioning of protein after reaction with Ellman's reagent.

The concentration of the protein, Ellman's reagent and TNB were calculated using the previously described numerical methods. The results indicated no change in the partition coefficient value of the protein after reaction (K was 0.54 for the native protein and 0.6 for the modified protein), but showed a different partitioning coefficient for Ellman's reagent before and after reaction (1.86, 1.24 respectively as shown in (Figure 59 Figure 60).
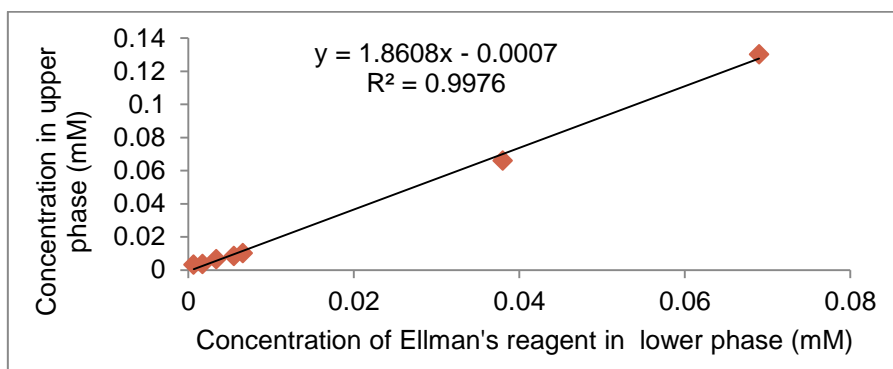
Figure 59- The partition coefficient of Ellman's reagent standard in PEG3350 - Dextran500 system at the TLL composition 8.4 % w/w PEG3350 and 8.4 % w/w Dextran500.
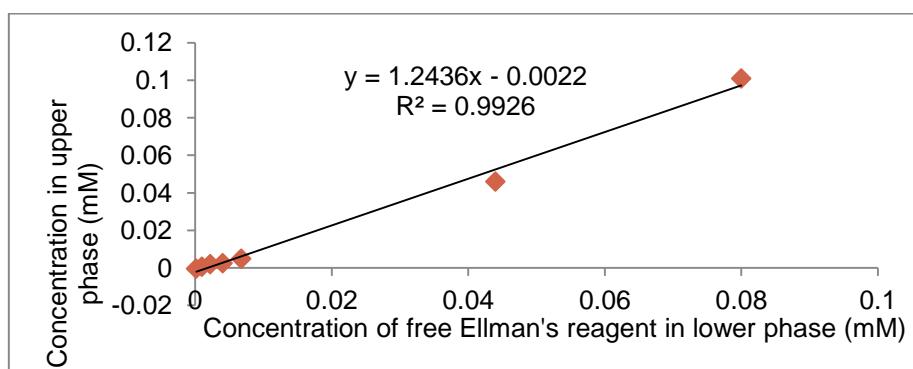
Figure 60- The partition coefficient of the free Ellman's reagent after reaction with rHSA using PEG3350-Dextran500 system at the TLL composition 8.4 % w/w PEG3350 and 8.4 % w/w Dextran500.

A 1:1 molar ratio was used to estimate the free thiol content of which was found to be 50% from the ratio of the mMoles of TNB released to the mMoles of protein used.

It has been reported that 5% of Ellman's reagent hydrolyses within 48 h when the pH reaches 8 and this becomes much more significant when the pH is increased (148). Hydrolysis of Ellman's reagent independently of its reaction with free thiol groups will result in production TNB which will affect the calculation of the real content of thiol in the protein solution since the amount of TNB produced is used to estimate the number of protein total free-thiols.

The ATPS phases were analysed by Size Exclusion Chromatography (SEC) to separate the unreacted DTNB, the reacted protein and TNB exploiting the differences in the molecular weight using a TSKgel G2000 SW column (5µm, 7.8 x 300 mm; Tosoh Bioscience purchased from HiChrom, Reading, UK) as shown in Figure 61. Potassium phosphate buffer (0.05 M) pH 7.0 containing 0.15M NaCl was used to equilibrate the column at a flow rate of 0.7 mL/min with UV detection at 280 & 324 nm. None of the analytes were observed to bind to the column during SEC and and consequently were eluted normally in the flow-through regime.
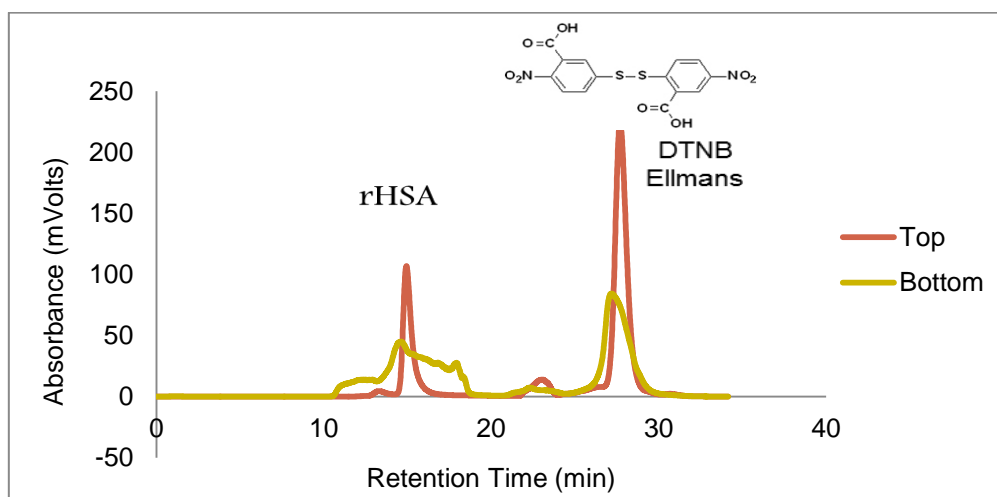
Figure 61- Size Exclusion chromatogram of the upper & lower phases of (sample A), Absorbance (mVolts) vs. retention time (min) obtained following the partitioning of rHSA & Ellman's in PEG3350-Dextran500 system using 50mM phosphate buffer pH7 containing 150mM NaCl as an elution buffer, Column TSKgel G2000SW 300 x 7.8 mm, Flow rate 0.4 mL/min,

As shown in Figure 61, it was difficult to achieve a good separation and quantitation for the components of the Ellman's reagent reaction with rHSA using PEG3350-Dextran500 system. The presence of Dextran reduced the resolution during the chromatographic

separation. Probably because the presence of the high molecular weight Dextran was excluded from the column and preventing the other solution components reaching equilibrium with the column.

A different ATPS was selected to avoid the problems of performing SEC in the presence of Dextran. PEG3350-K_2HPO_4 was selected from (149), the system composition was (10.08 % w/w K_2HPO_4, 10% w/w PEG3350) corresponding to a TLL of 34. Samples from the single phase were partitioned in the chosen system prepared following the experimental procedure in section 2.5.1.3 paragraph (E).

Samples from the equilibrium phases of the ATPS were withdrawn and following appropriate dilution were scanned photometrically (324nm and 412nm). From these results following the numerical procedure the concentrations of each component of the reaction mixture could be estimated. The results of the partitioning in the two phases indicated a very low partition coefficient (K_{HSA} 0.005) for the protein after reaction as shown in Figure 62. Protein preferred lower phase with almost zero concentration in the upper phase. Thus, the system was un-suitable for the quantitative calculations since the formation of the mixed disulphide is unable to influence the partition coefficient of the protein because of its strong lower phase preference.
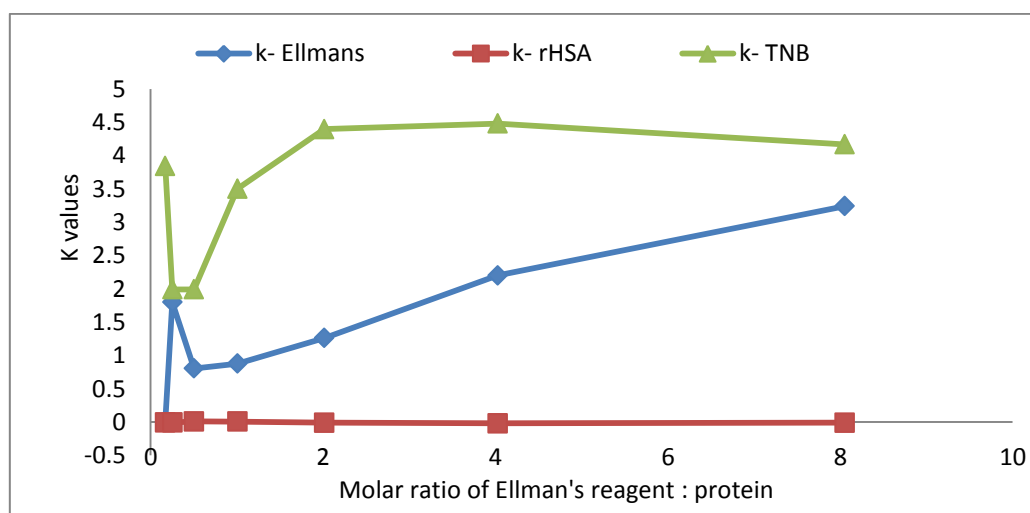
Figure 62- The partition trend for partitioning of rHSA and Ellman's reagent in PEG3350-K_2HPO_4 system at the TLL composition 10% w/w PEG3350 and 10.08 % w/w K_2HPO_4. The partitioning values were determined using the calculated concentration by the numerical method using Mathcad (see appendix C).

In order to increase the protein partition coefficient to make it more reliably quantitative and perhaps increase the influence of the formation of the mixed disulphide, the molecular weight of PEG was decreased by substituting PEG 1000 for PEG 3350 to increase the protein partition to the top phase, another system was chosen (149).

Thus a PEG1000- K_2HPO_4 system was used to partition the protein reaction mixture solution. Having the composition (14.7 % w/w PEG1000, 11.55 % w/w salt and TLL 31.296) the samples were prepared as in section 2.5.1.3 paragraph (F).

The concentrations of the protein, un-reacted Ellman's reagent and TNB in the single phase and ATPS phases were calculated using the numerical methods previously established.

The amount of free thiol in the single phase solutions was estimated from the amount of TNB released. Results indicated a high partitioning value for the protein, use of low molecular weight PEG 1000 resulted in an increase in the partition coefficient (2.97) with almost no difference between the partitioning coefficient before and after reaction (see Figure 63), secondly it was found that there was a discrepancy in the mass balance (see *Table 56*) between the amount of TNB recovered in the ATPS and that found under single phase conditions.

Table 56- Mass balance of TNB in the single phase and two phases of PEG1000- K_2HPO_4 system.

Samples No.	Concentration of TNB in single phase solutions (mM)	Concentration of total TNB in ATPS solutions (mM)
A	0.055	0.00
B	0.06	0.002
C	0.06	0.0178
D	0.055	0.050
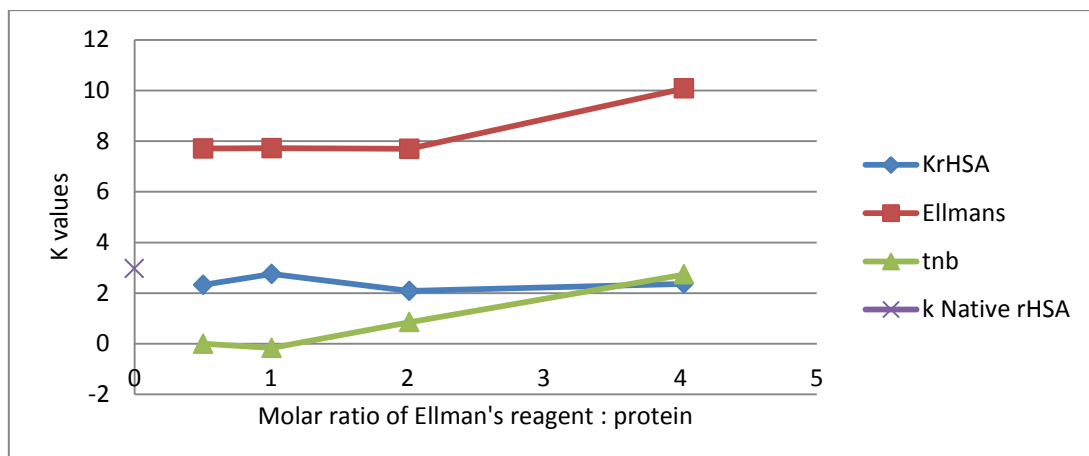
Figure 63- The partition trend for partitioning of rHSA & Ellman's in PEG1000- K_2HPO_4 system at the TLL composition 14.7 % w/w PEG1000, (0.72g) 11.55 % w/w salt. The partitioning values were determined using the calculated concentration by the numerical method using Mathcad. (see appendix C).

Final conclusion: Use of this reagent resulted in a very specific reaction with albumin which could be monitored from the decrease in the concentration of DTNB following the reaction, the decrease in the absorbance at 324nm and the increase at 412nm due to the production of the TNB ion could also be followed by spectrophotometric assay. A mathematical method employing simultaneous equations was developed to calculate the concentration of TNB produced from the spectrophotometric relationship between Ellman's reagent, the protein substrate and TNB.

Following the reaction of DTNB with protein the partitioning of the reaction mixture was examined in a variety of ATPS with the aim of developing a system in which production of TNB would indicate the total reactive free thiols present and the change in the partition coefficient of the mixed disulphide protein product compared to that of the un-derivatised protein would indicate the free thiol content due to albumin. The ATPS systems examined were; (1) PEG3350 - Dextran500 buffered with 10mM potassium phosphate pH9 containing 50mM potassium sulphate (2) PEG3350 – K_2HPO_4 (3) PEG 1000 - K_2HPO_4. However, neither of these systems showed any significant change in the partition coefficient of the native derivative protein following reaction with DTNB and formation of its mixed disulphide. In the PEG3350 - K_2HPO_4 system albumin partitioned strongly to the salt phase and there was no change in the partitioning coefficient on derivatisation. In the PEG1000 - K_2HPO_4 system the partition coefficient was higher with albumin showing a higher preference for the polymer phase but there was still no change to the native partition coefficient on derivatisation with Elman's reagent, also the

197

system showed significant and unaccountable reduction in the amount of TNB recoverd in the ATPS.

6.4 Reaction of HSA with N-pyrenylmaleimide (NPM) reagent

6.4.1 Background:

N-pyrenylmaleimide (NPM) is a reagent widely used in the reaction with reduced cysteine-thiols (molecular structure shown in Figure 64), but there are limited studies of the reaction with protein-thiols (150). NPM was selected as an alternative conjugate on the grounds that the additional aryl groups would have a more pronounced effect on the partition coefficient of the conjugate compared to and that the solvatochromic and fluorescent properties of pyrene could later be useful in increasing the sensitivity of any assay.
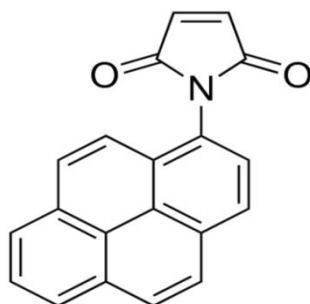
Figure 64- Molecular structure N-pyrenylmaleimide

6.4.2 Results and discussion:

Initial work concentrated on the determination of the molar extinction coefficient of NPM in DMSO due to its low solubility in aqueous solution. Since it has been reported that the molar extinction of NPM in Me-OH is 40,000 M^{-1} cm^{-1} (107), it could be used to calculate the extinction coefficient in DMSO. A series dilution of NPM was prepared from stock solution using Di-methyl sulphoxide (DMSO) and methanol (MeOH) as diluents following the experimental procedure describe in paragraph (A) in section 2.5.1.4. The UV/VIS spectra of N-pyrenylmaleimide in MeOH and DMSO are shown in Figure 65 and Figure 66.
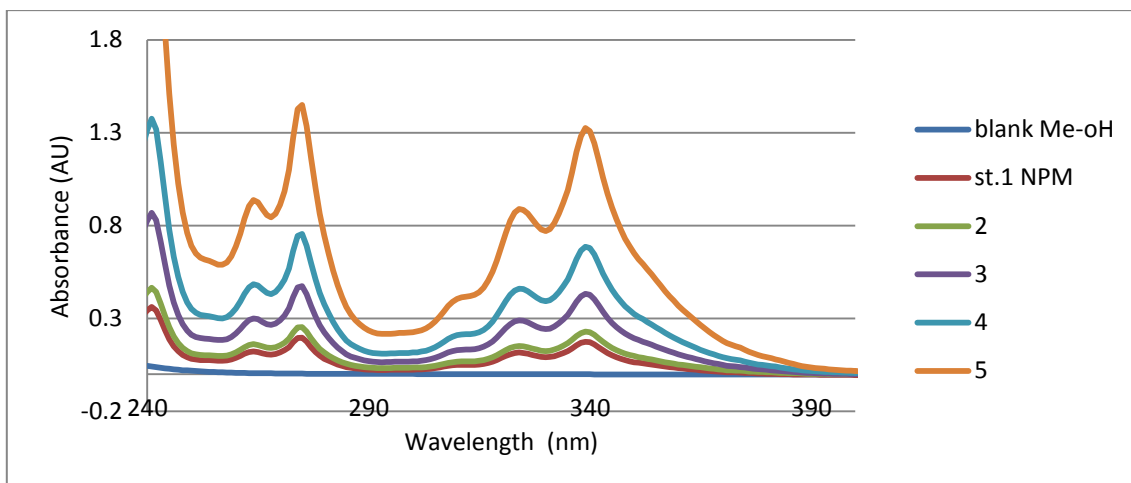
Figure 65- The UV/VIS spectra of N-pyrenylmaleimide in Methanol at a concentration of (1) $5x10^{-4}$, (2) $1x10^{-3}$, (3) $1.5x10^{-3}$, (4) $3x10^{-3}$ and (5) $5x10^{-3}$ mg/mL.
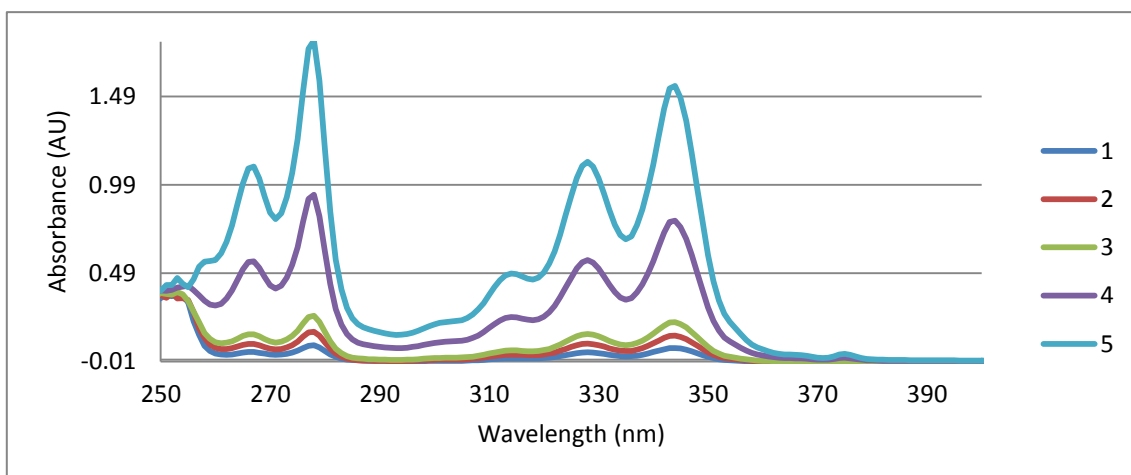
Figure 66- The UV/VIS spectra of N-pyrenylmaleimide in DMSO at a concentration of (1) $5x10^{-4}$, (2) $1x10^{-3}$, (3) $1.5x10^{-3}$, (4) $3x10^{-3}$ and (5) $5x10^{-3}$ mg/mL.
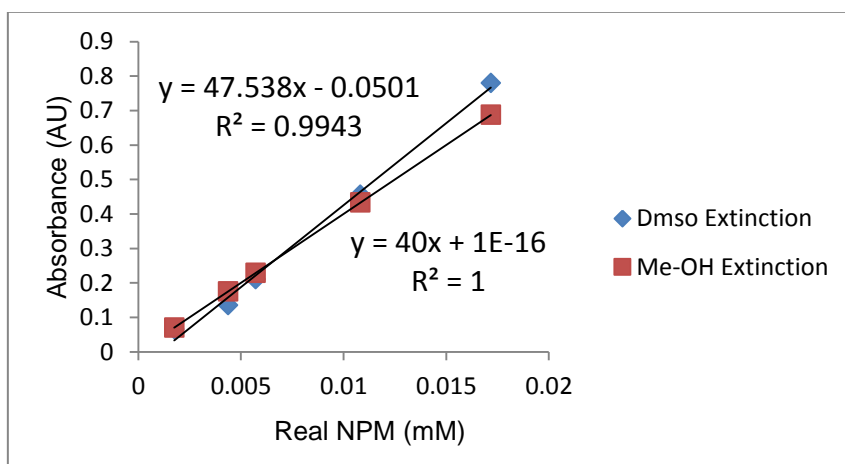
Figure 67- The regression of the absorbance of NPM vs. the real concentration (mM). The real concentrations were calculated using the extinction coefficient of NPM in MeOH.

The actual concentration of NPM was calculated using the extinction coefficient of NPM in MeOH, then the absorbance of NPM in DMSO was calibrated against this concentration; the slope of the regression represented the extinction coefficient of NPM in DMSO as shown in Figure 67.

Following this the solubility and reactivity of NPM was studied. The NPM was dissolved in a mixture of 60% v/v DMSO and water as a stock, since we cannot use pure DMSO with protein solutions since it may result in denaturation of the protein. The solutions were prepared following the paragraph (B) in the experimental procedure in section 2.5.1.4

The analysis of the samples was carried by spectrophotometry and RP-HPLC. The results indicated there was a poor solubility of NPM after adding the amount of protein dissolved in water which has been related to the degree of dissolution of NPM in water. It has been reported that the use of DMSO and water with compounds, which have a low solubility in aqueous solution, may result in a precipitation of the compounds and also a permutation of a certain reaction (151).

Table *57* shows the nominal concentration of NPM compared to the calculated concentration using the extinction coefficient. There was a significant decline in the solubility under these conditions but did not affect the reactivity of NPM.

Table 57- Concentration and reactivity percent of NPM in 60% v/v DMSO/water after reaction with rHSA-thiol.

Nominal mM NPM	real [c] mM-NPM	Nominal Molar ratio	real molar ratio	NPM % reacted
0.037	0.0010	2.80	0.07	87
0.030	0.0008	2.24	0.06	90
0.022	0.0005	1.68	0.04	89
0.015	0.0004	1.12	0.03	83
0.007	0.0002	0.56	0.02	84

The solvent DMSO in water itself results in a precipitation leading to degradation of NPM, since the hydrophobic compounds like NPM may be more soluble in solvents with a low cohesive energy density which affects the solubility but not the reactivity (152). Figure 68 shows that the amount in solution is proportional to the total amount added

reflecting equilibrium between solid and solution phases. When analysing the NPM standard, an unknown peak was observed affecting the mass balance calculation.
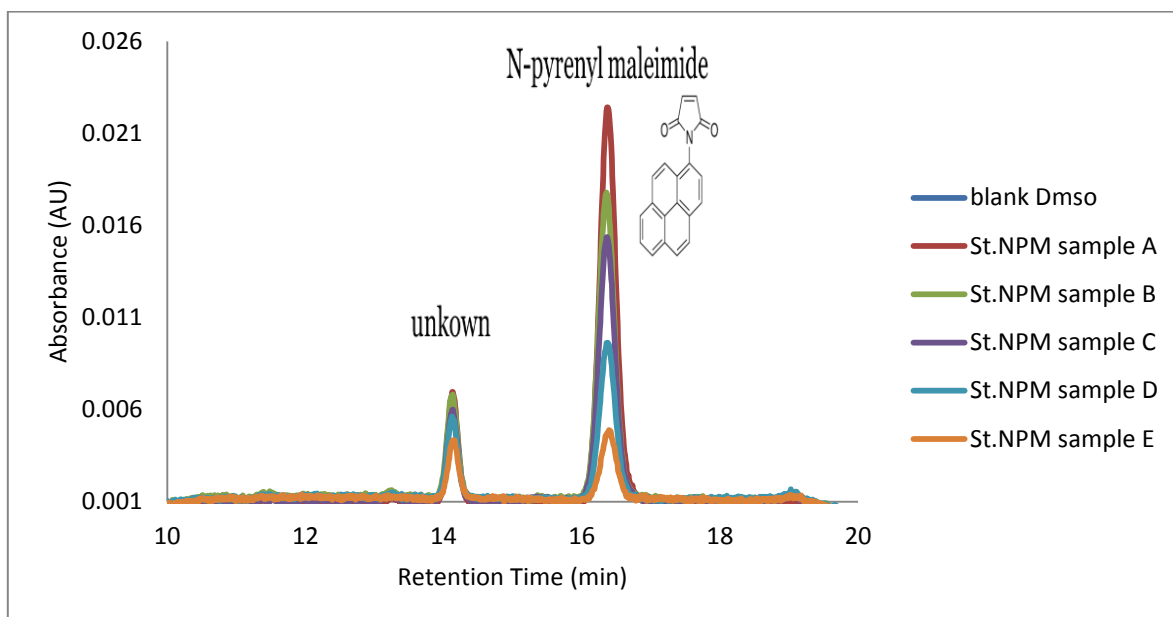
Figure 68- The HPLC chromatogram of the Standard NPM at the concentration (A) 1.8 x 10^{-4} M, (B) 1.49 x 10^{-4} M, (C) 1.12 x 10^{-4} M, (D) 7.47 x 10^{-5} M NPM and (E) 3.73 x 10^{-5} M , the solutions were prepared in %60 v/v DMSO/water. The analysis was performed under the following conditions: chromatographic column C18 ((YMC-pack ODS-AQ 5.0 µm, 15cm × 4.6 mm), solvent A was 10% v/v ACN containing (0.1%) TFA pH1.7 and solvent B 90% v/v ACN containing (0.1%) TFA pH 0.9

As a result of the insolubility of NPM in DMSO/water, the solubility was examined in DMSO / phosphate buffer 20mM pH 7.5. The solutions were prepared following paragraph (C) in the experimental procedure of section 2.5.1.4. Samples were analysed by spectrophotometry and RP-HPLC. Following a 20 fold dilution of all samples a rapid decrease in the NPM concentration was observed as shown in Table 5

Table 58- The decrease in the concentration of standard NPM in the 60% v/v DMSO/20mM phosphate buffer pH 7.5 as measured from spectra at 343nm.

Nominal NPM (mM)	Real [NPM] mM after diluted NPM in 60% v/v DMSO
0.168	0.062
0.135	0.058
0.067	0.035
0.034	0.018
0.017	0.009
0.008	0.004

Under these experimental conditions full solubility of the NPM could not be achieved using DMSO / buffer, but even so, following the reaction of NPM with protein it was important to examine the reactivity towards thiol under the new conditions. The reaction mixture samples were prepared following the paragraph (D) in the experimental procedure in section 2.5.1.4.

The extinction coefficient determined earlier in DMSO was used to calculate the concentration using the absorbance of the samples resulting from spectrophotometry. The calculated solution concentrations were used to calibrate the absorbance results from RP-HPLC chromatogram which are shown in *Figure 69*.
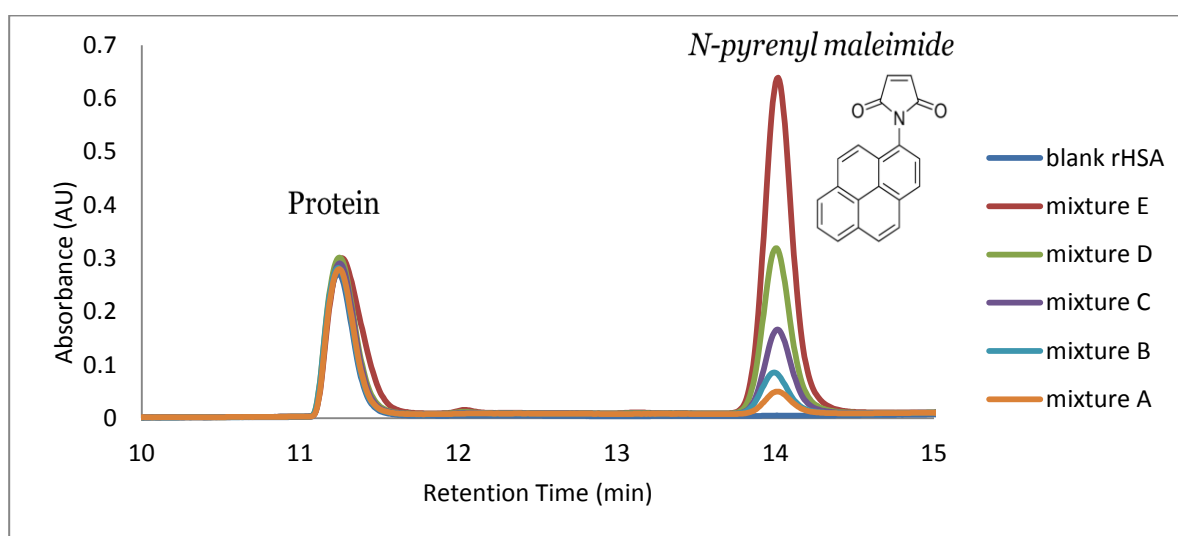
Figure 69- The HPLC chromatogram of the reaction mixture samples of NPM and protein (rHSA) in 60% v/v DMSO and phosphate reaction buffer of 20mM pH7.5 following Table 22 . The analysis was performed under the following conditions: chromatographic column C18 ((YMC-pack ODS-AQ 5.0 µm, 15cm × 4.6 mm), solvent A was 10% v/v ACN containing (0.1%) TFA pH1.7 and solvent B 90% v/v ACN containing (0.1%) TFA pH 0.9

The calibration of HPLC was used to calculate the amount bound, total and free NPM and also the real molar ratio related to the NPM solubility. The percent of NPM reacted to the free thiol of the protein was calculated form the percent ratio of the amount bound over the total, Table 59 shows the calculated results.

Calculations of the HPLC results for the NPM concentration after reaction indicated a low reactivity in presence of DMSO & buffer, inhibiting and reducing conjugation efficiency as demonstrated in Figure 70.

Table 59- The concentration and % reactivity of the reaction mixture of NPM with protein in the 60% v/v DMSO / 20mM phosphate buffer pH 7.5

Nominal Molar ratio	real molar ratio	NPM % reacted
0.28	0.13	4
0.56	0.27	15
1.12	0.57	18
2.24	1.12	19
4.47	2.24	18
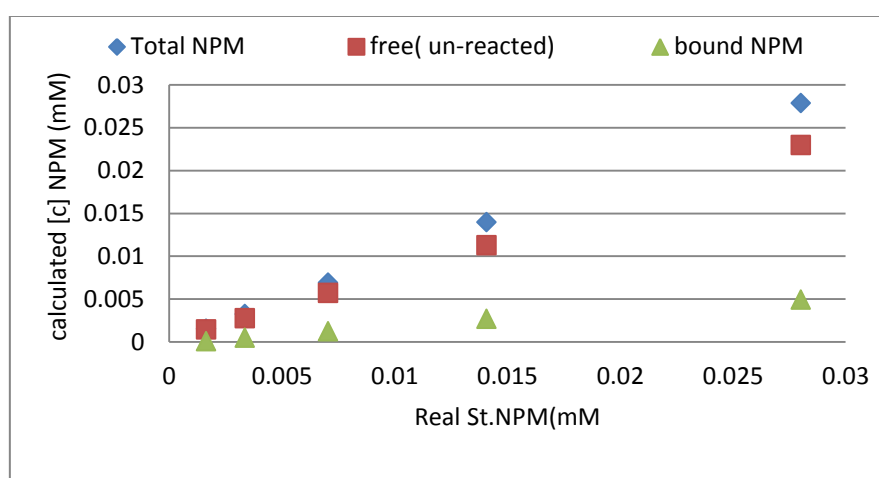
Figure 70- The concentration of the total NPM, free NPM and the amount of protein bound NPM (which was calculated from the difference of the standard NPM solution before reaction and the amount of free NPM after reaction with the protein) in the 60% DMSO / 20mM phosphate buffer pH 7.5.

Assuming that the pH of buffer was the reason behind the low reactivity since it has been reported that the pKa of all serum albumin give ~8.5 for their cys-thiol (153). An attempt was made to re-react NPM with protein using 20mM phosphate buffer pH 8.7. Using same basic reaction a quick experiment was performed to study the effect of buffer pH. Reaction mixture solutions in 1100 µL total volume were prepared following the Table 60.

No further improvement was achieved and the reactivity was almost the same, overall solubility of NPM was also low as in previous experiments, which is illustrated in Table 62.

Table 60- The volume composition of the reaction mixture samples of NPM and protein

Samples	rHSA µL (5mg/mL)	NPM µL (0.5mg/mL) in 60% DMSO	60% DMSO solution	Molar ratio NPM:rHSA
A	1000	25	75	0.56
B	1000	50	50	1.13
C	1000	100	0	2.26

Table 61- The concentration and % reactivity of the reaction mixture of NPM with protein in the 60% v/v DMSO / 20mM phosphate buffer pH 8.7

Nominal Molar ratio	real molar ratio	NPM % reacted
0.56	0.32	19.14
1.13	0.65	22.43
2.26	1.30	22.20

These observations led to new experiment designed to examine the low reactivity of NPM and re-study the solubility in different percent of DMSO.

Pure DMSO was used to prepare 5mg/mL NPM, which was diluted 10 fold to obtain 0.5 mg/mL at a different % composition of DMSO (60, 70, 80, and 90%) in 20mM phosphate buffer pH 8.7, glass tubes were used to eliminate the possibility of adsorption to plastic tubes.

It was immediately apparent that there was a distinct change in colour of the NPM solution in 90% DMSO (see Figure 71). Secondly, there was a gradually decrease in the absorbance of NPM solutions apparently correlated to the increasing amount of DMSO in the solutions. The solubility and stability of NPM in these solutions are shown in Table 62 which indicate a >50% decrease in the concentration under all conditions examined.

Table 62- The experimental solubility of NPM in different percent compositions of DMSO

Nominal calculations	Experimental calculations			
NPM mM	NPM in 60% DMSO	NPM in 70% DMSO	NPM in 80% DMSO	NPM in 90% DMSO
0.018	0.012	0.009	0.007	0.008
0.035	0.023	0.017	0.014	0.014
0.070	0.044	0.038	0.028	0.027
0.140	0.071	0.062	0.054	0.045
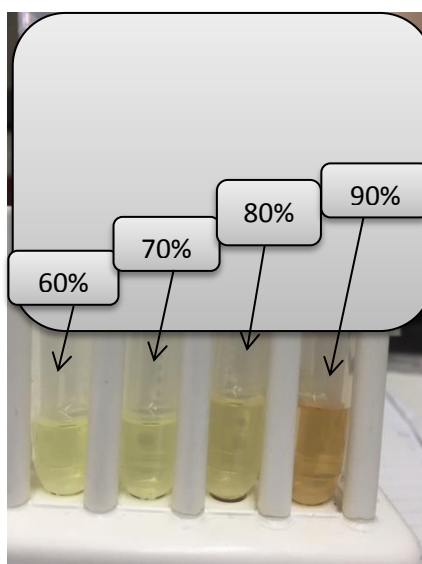
Figure 71- colour change with increase of DMSO concentration in NPM – buffer solutions.

The increasing concentration of DMSO in buffer seems to encourage a reaction between DMSO and the functional group of NPM (pyrenyl rings), which did not occur when the reaction was performed in un-buffered conditions (see the earlier experiment with water). This implies that the reaction with protein might be difficult to control. It also means that the pyrenyl ring does not attach to the free thiol of rHSA but just methyl group. Thus there is almost no difference in the HPLC chromatograms for the protein peak before and after the reaction (see *Figure 69*). This may be the reason for the low reactivity of NPM toward the protein, or it may be a competitive reaction between thiol and DMSO.

In general, solvents can affect the solubility and reactivity of any compound in several ways. Water might cause degradation in presence of DMSO, light could also induce a certain reactions for some compounds, buffer solutions may reduce the solubility of the compound and produce de-composition products which may lead to low reactivity resulting from the differences in stability (151).

Within this short survey examining the solubility and stability of NPM, the full-details about the physical properties could not be elucidated, thus several experiment modifications were made to improve the reaction. An assumption was made that the problem of DMSO could be resulting from the long-term storage time. Therefore, a new bottle was used for further experiments.

Using Acetonitrile (ACN) instead of DMSO was another option to examine whether it could improve the reactivity; the calculation of the extinction coefficient of NPM in ACN was performed in a similar way to that of DMSO by calibration with (MeOH).

Samples were prepared following the experimental procedure given in paragraph (E) in section 2.5.1.4. The real concentration of NPM was calculated using the extinction coefficient of NPM in MeOH, and the extinction coefficient of NPM in ACN was determined. The slope of regression represented the extinction coefficient of NPM in ACN. The extinction coefficient of NPM in ACN was estimated to be 37.09 M^{-1} cm^{-1} and was used in all subsequent calculations.

Following this calibration, the reactivity of NPM in ACN/buffer towards protein thiol was examined and the reaction mixtures were prepared following the experimental procedure paragraph **(F)** in section 2.5.1.4. Solutions were checked visually for signs of precipitation and a precipitate was observed in samples 4 and 5 (see Table 23). Thus no improvement in the solubility of NPM under these conditions was achieved.

In support of these findings, the maximum solubility of NPM in 20% v/v ACN/20mM phosphate buffer pH 7, containing 20mM NaCl and 5mM EDTA has been reported to be at a concentration of 50µM (154).

Further attempts were made to examine the effect of raising the percent of solvent in the protein mixture up to 20% and using a new buffer. The strategy included preparing a diluted stock of NPM at different concentrations in a pure solvent rather than using one

diluted stock at a defined % of a solvent, which means using more diluted NPM to avoid further dilution after adding the protein solution.

In this case the 20mM phosphate buffer pH 7 containing 20mM NaCl and 5mM EDTA, and 2mg/mL NPM in pure DMSO were used to prepare the following concentrations of NPM (0.4, 0.2, 0.1, 0.05 and 0.025 mg/mL) using pure DMSO as a diluent. Subsequently these concentrations were diluted fivefold with pure DMSO to give 0.08, 0.04, 0.02, 0.01 and 0.005 mg/mL. From each of these concentrations 250µL was mixed with 1mL buffer for the standard NPM solutions. The absorbance was measured over time by spectrophotometry and the results are shown in Figure 72. The results indicated that this procedure seemed to enable maintaining solubility of NPM in 20% v/v DMSO and buffer. As a result the concentration could be determined accurately up to about 0.01 mM.
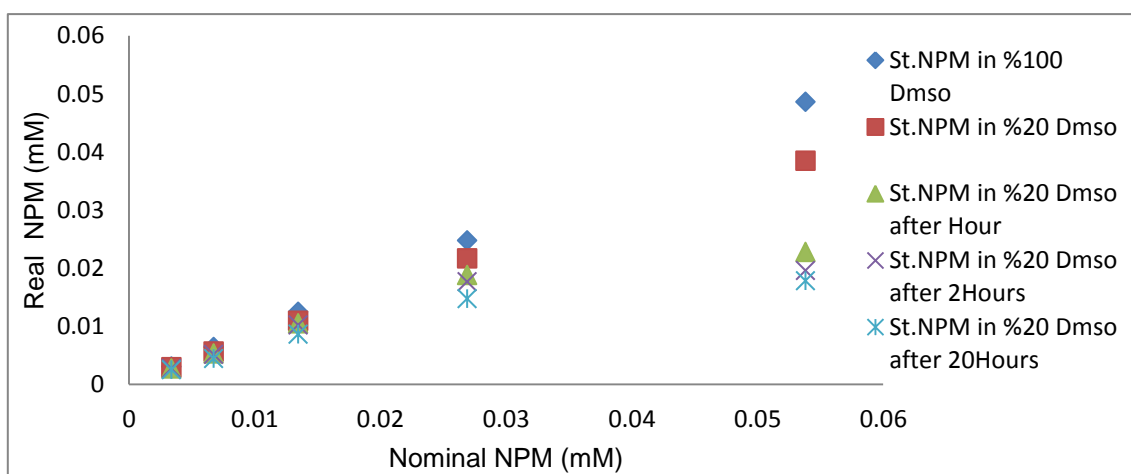
Figure 72- Stability of 0.016, 0.008, 0.004, 0.002 and 0.001 mg/mL of NPM dissolved in 20% DMSO and 20mM phosphate buffer pH 7 containing 20mM NaCl and 5mM EDTA, over 20H measured by the absorbance of UV/VIS spectra at 343nm . Nominal concentration of NPM is the theoretical number of mMoles in the reaction, while the real concentration is the actual concentration under the experiment conditions.

To examine the effect of raising the percent of solvent in the protein mixture up to 20% and using a new buffer, a further attempt was made exactly as in the previous experiment. Using Acetonitrile instead of DMSO gave essentially identical results. The instability and insolubility of NPM made it difficult to achieve a selective conjugation due to reducing of the performance of conjugation efficiency (see Figure 73).
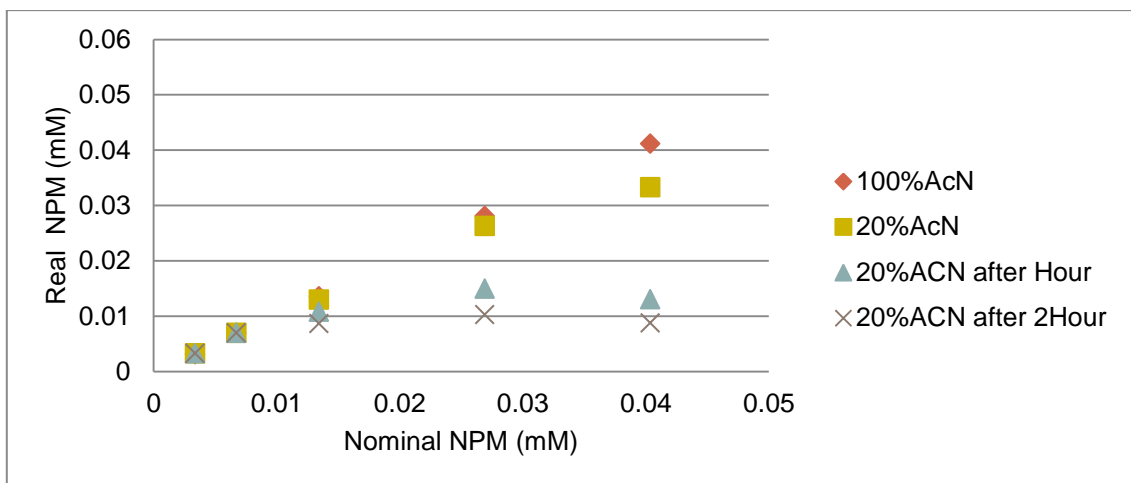
Figure 73- Stability of (0.012, 0.008, 0.004, 0.002, 0.001mg/mL) of NPM dissolved in 20% v/v ACN and 20mM phosphate buffer pH 7 containing 20mM NaCl and 5mM EDTA over 2H measured by the absorbance of UV/VIS spectra at 340nm.

Exactly the same experiment steps were repeated using rHSA to examine the conjugation performance of NPM under the new conditions. The standard and samples were analysed by RP-HPLC the standard solutions of NPM showed an unknown peak. The unknown form increases in peak height at the same rate as the reactive form. However, it did not show any reactivity towards protein-free thiol (see Figure 74, Figure 75
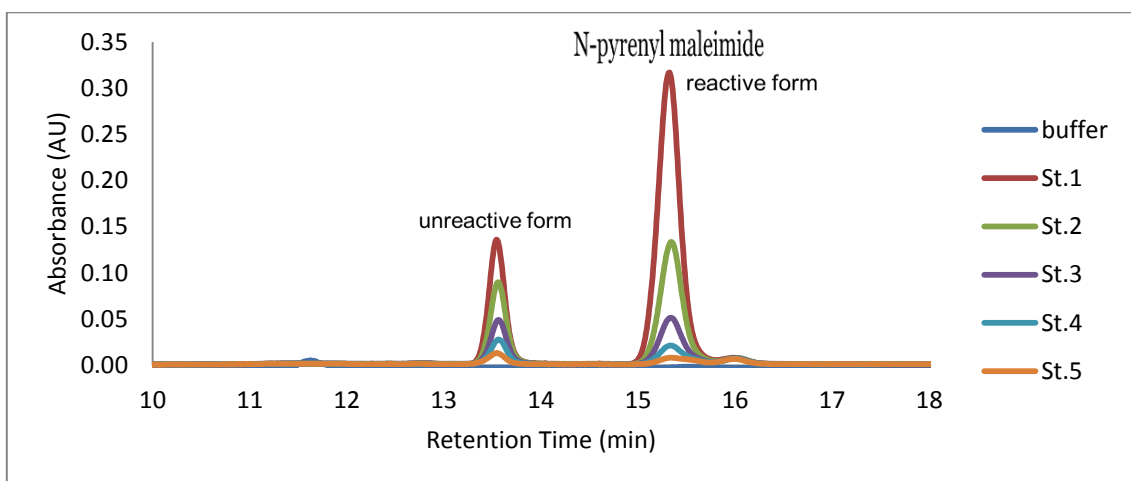
Figure 74- HPLC chromatogram of Standard NPM at 340nm dissolved in 20% v/v DMSO and 20mM phosphate buffer pH 7 containing 20mM NaCl and 5mM EDTA. Standard solutions were prepared following Table 24. The analysis was performed under the following conditions: chromatographic column C18 ((YMC-pack ODS-AQ 5.0 μm, 15cm × 4.6 mm), solvent A was 10% v/v ACN containing (0.1%) TFA pH1.7 and solvent B 90% v/v ACN containing (0.1%) TFA pH 0.9
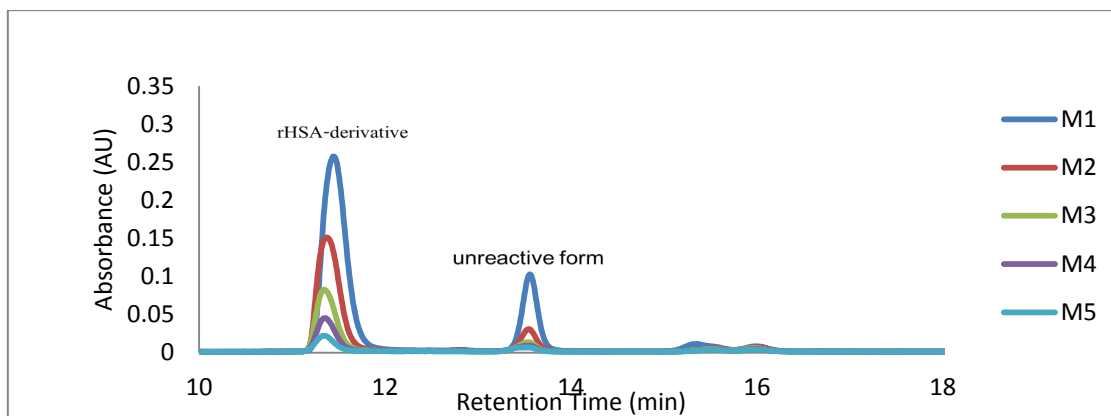
Figure 75- HPLC chromatogram of reaction mixture samples of NPM and protein at 340nm dissolved in 20% v/v DMSO and 20mM phosphate buffer pH 7 containing 20mM NaCl and 5mM EDTA. Mixture solutions were prepared following Table 23. The analysis was performed under the following conditions: chromatographic column C18 (YMC-pack ODS-AQ 5.0 μm, 15cm × 4.6 mm), solvent A was 10% v/v ACN containing (0.1%) TFA pH1.7 and solvent B 90% v/v ACN containing (0.1%) TFA pH 0.9

Presence of DMSO with sulfhydryl containing molecules may oxidize in solution and form disulphide bonds, which cannot react with maleimides as shown in the proposed reaction (Figure 76). As reported, the possibility of a selective and quantitative conversion of thiols to disulphides was effected by DMSO under mild conditions catalysed by dichlorodioxomolybdenum(VI) (155), which might be one reason for the low reactivity of NPM in presence of DMSO.
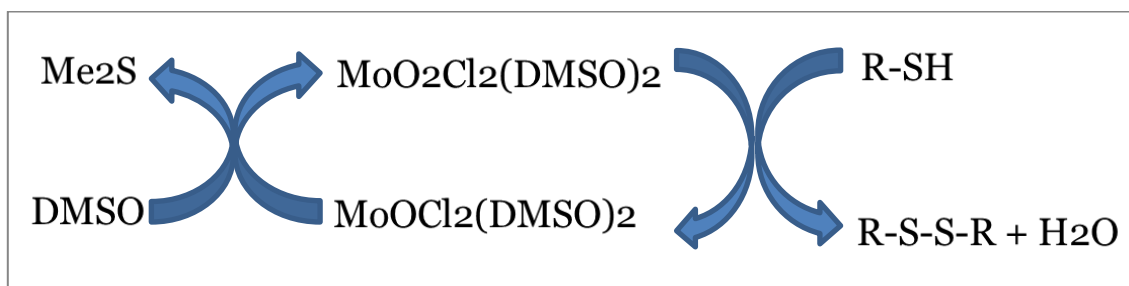
Figure 76- Proposed mechanism for the conversion of thiols to disulphide by DMSO under mild conditions and catalysed (155).

A conclusion has been made from the colour change with increasing the amount of organic solvent namely DMSO and the low reactivity of NPM that the presence of DMSO with buffer stimulated a reaction with the maleimide reagent, thereby inhibiting and reducing conjugation efficiency of the intended molecule. By monitoring the loss of the absorbance at 340nm, which could be confirmed that the maleimide NPM had a side-reaction with the DMSO in presence of buffer. In addition, increasing the pH above

7 could affect the reactivity toward primary amines, hydrolysis of the maleimide group can occur and a functional moiety can be attached to the nitrogen (142)

Reaction time was an important factor affecting the solubility of NPM. Sample stability was determined by analysis of a single standard concentration 0.016 mg/ml of NPM by HPLC over a time course of 120 min. The stability of each sample was compared with the first run which was processed immediately after preparation. The results showed a significant difference in the peak height of NPM in each run demonstrating the instability of NPM in the 20% v/v DMSO resulting in the production of unreactive form. The reaction is progressive over time and this might indicate that it is the DMSO which is the reactant since an impurity might be expected to be consumed during the course of the reaction. (See Figure 77)
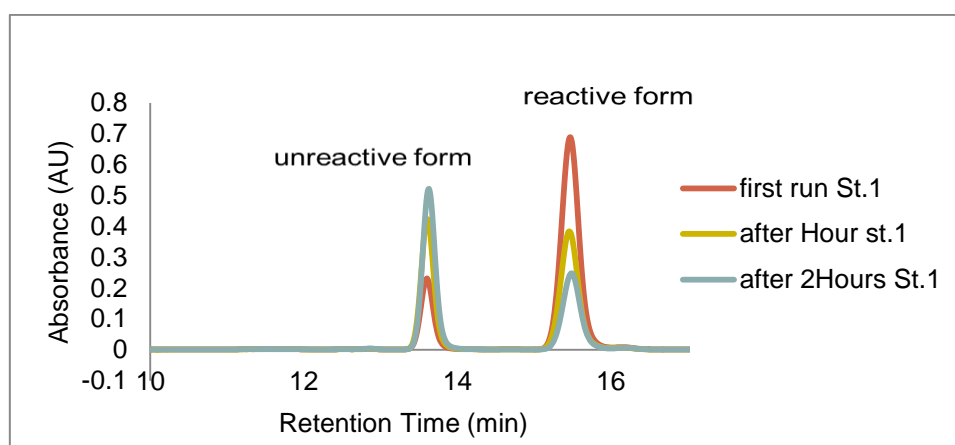
Figure 77- Stability of St.NPM in 20% v/v DMSO and 20mM phosphate buffer pH 7 containing 20mM NaCl and 5mM EDTA over a time course for 2H. The analysis was performed under the following conditions: chromatographic column C18 ((YMC-pack ODS-AQ 5.0 µm, 15cm × 4.6 mm), solvent A was 10% v/v ACN containing (0.1%) TFA pH1.7 and solvent B 90% v/v ACN containing (0.1%) TFA pH 0.9

To confirm that the maleimide NPM was involved a side-reaction in the presence of DMSO and buffer, the same procedure was repeated with a different maleimide, N-Ethylmaleimide (NEM) in 20mM phosphate pH 8.7, containing 10% v/v DMSO.

Pure DMSO was used to prepare 5mg/mL NEM which was then diluted 10 fold using 60% v/v DMSO with 20mM phosphate buffer pH 8.7 to obtain 0.5mg/mL (the phosphate buffer pH 8.7 and 10% v/v DMSO has been shown to be an un-stable condition due to their previous effect on NPM), Serial dilutions were prepared following Table 63.

Table 63- The volume composition of the NEM samples dissolved in two different buffers to probe the effect of DMSO on another type of Maleimide compound.

Samples	Buffer (µL)	NEM µL (0.5mg/mL)	60% v/v DMSO solution
A	1000	6	194
B	1000	12.5	187.5
C	1000	25	175
D	1000	50	150
E	1000	100	100

A further series was prepared in exactly the same way but using the normal reaction buffer for NEM consisting of 100mM phosphate buffer containing150mM NaCl pH6 (stable condition). Both sets contained a final concentration of 10% v/v DMSO in the reaction mixture. The extinction coefficient of NEM 620 M^{-1} cm^{-1} was used to calculate the concentration of NEM from the spectrophotometric absorbance. Once again the maleimide appeared to be converted to an unreactive form under these conditions as illustrated from the decrease in concentration shown in Figure 78.
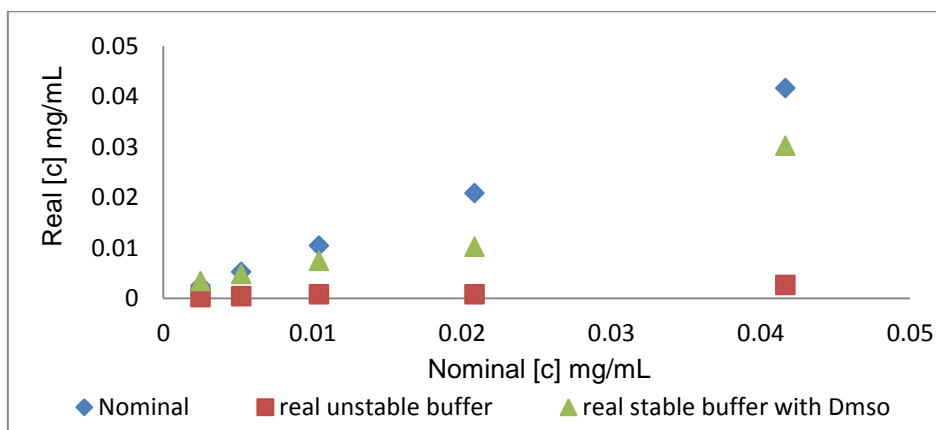
Figure 78- Stability of NEM in (▲) 20mM phosphate buffer pH 8.7 containing 1mM EDTA, 10% v/v DMSO and (■) 100mM phosphate buffer containing150mM NaCl pH6 ,10% v/v DMSO. The stability of the NEM was measured by the calculated concentration in different buffers as determined by spectroscopy at 300nm.

The results above were confirmed using a different approach, 1M KOH was used to raise the pH >8 for samples prepared under "stable" buffer conditions (100mM phosphate buffer pH 6 containing 150mM NaCl). NEM 5mg/mL in DI water was

prepared, and then diluted to give the concentrations of (1, 0.75, 0.5 and 0.25 mg/mL) using 100mM phosphate buffer pH 6 containing 150mM NaCl.

1M KOH was used to raise the pH > 8 making an identical series of solutions, and the pH was increased by mixing 500µL from each concentration with 500µL KOH which raised the pH to 8.35, and then 100µL of DMSO was added to each tube to give 10 % v/v DMSO in each solution, the results are shown in Figure 79.
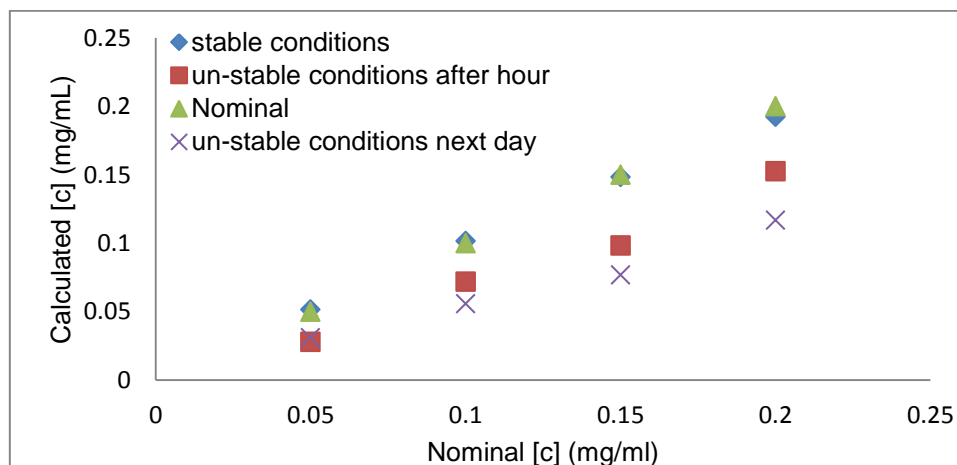
Figure 79- Stability of NEM in different conditions as determined by spectroscopy at 300nm. "Stable" buffer conditions was (100mM phosphate buffer pH 6 containing 150mM NaCl), while un stable conditions were increased the pH above 8 by 1M KOH and added 10% v/v DMSO to the solutions of NEM.

Under these experimental conditions, NEM appeared to be involved in a side reaction which could confirm the assumption of the reaction of the maleimide NPM and DMSO in the presence of buffer at a pH > 8. A quick test was done by which it was possible to visually see the changing in the colour of the solutions when using 90% v/v DMSO. Two samples were prepared at a concentration 0.5mg/mL using two different concentrations of DMSO, one containing 60% v/v DMSO with phosphate buffer pH 8.7 and another containing 90% v/v DMSO and phosphate buffer at pH 8.7, this resulted in a rapid change in colour of the solution that contained 90% v/v DMSO as shown in Figure 80.
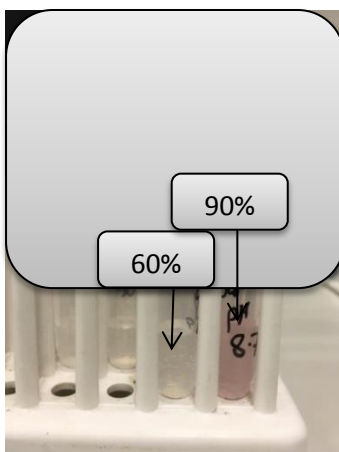
Figure 80- Colour change with increase of DMSO in NEM- buffer solutions.

These observations indicated the limitation of NPM for the purpose of rapid and site specific derivatisation of protein free-thiols, where instability reduces the conjugate performance and reactivity which results in low efficiency to achieve the conjugation concept and that makes the quantitative reaction difficult if not impossible to achieve.

6.5   Reaction of HSA with Fluorescein-5-maleimide (F-5-M) reagent

6.5.1 Background:

Fluorescein-5-maleimide (F-5-M) was used as a thiol specific conjugate because it again contains several aryl groups (molecular structure shown in Figure 81) which might be expected to give a large change to the partition coefficient of a conjugated protein and its fluorescent properties should convey added sensitivity in an analytical setting. The reaction solutions were prepared following the experimental procedure outlined in section **2.5.1.5**
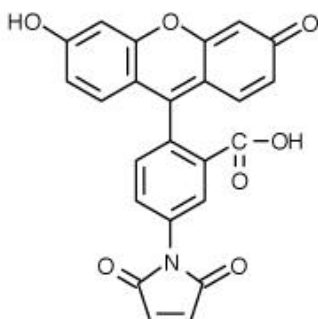
Figure 81- Molecular structure Fluorescein-5-maleimide

6.5.2 Results and discussion

The concentration of F-5-M was calculated using its extinction coefficient (68000 M^{-1} cm^{-1}) in DMF at 494nm (156). Standard solutions of F-5-M were prepared to examine the solubility after dilution with the phosphate reaction buffer 20mM pH 7.2 containing 150mM NaCl and 5mM EDTA. This step was made following the experience with preparation of NPM in DMSO. The study was carried out during a time course of 120min, the samples showed good solubility and stability in the buffer as illustrated in Figure 82.
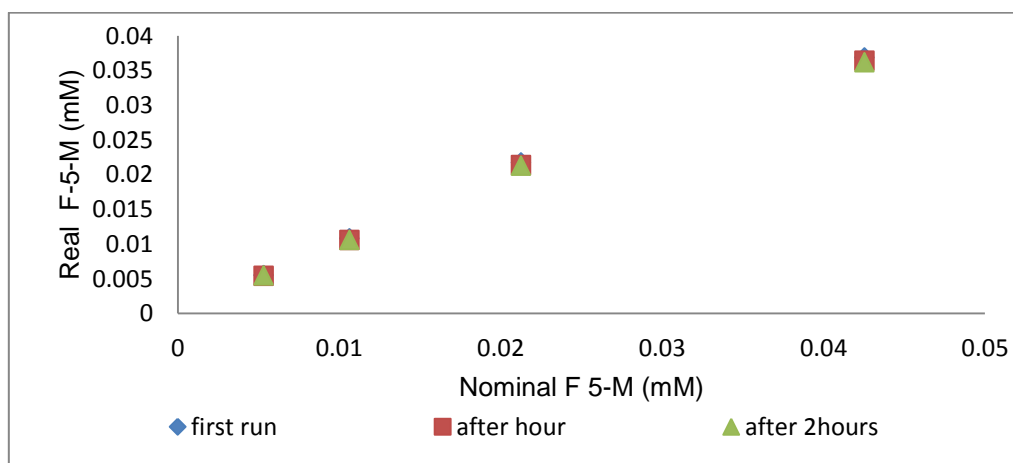
Figure 82- Spectroscopy results of the stability of F-5-M standard in 20% v/v DMSO and 20mM phosphate buffer pH 7 containing 20mM NaCl and 5mM EDTA through a time course for 2H.

The reaction of the F-5-M and protein was performed using 20mM phosphate reaction buffer pH 7.2 containing 150mM NaCl and 5mM EDTA. The analysis of the samples was carried out by spectrophotometry and RP-HPLC. Figure 83 shows the spectra for the reaction solutions of F-5-M and protein after subtracting the protein from the samples.
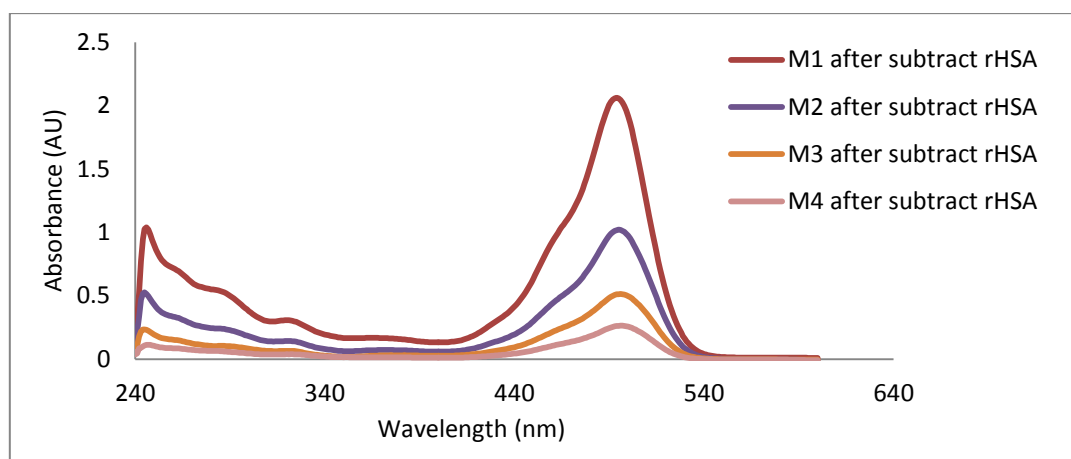
Figure 83- The UV/Vis spectra of F-5-M in phosphate buffer 20mM pH 7.2 containing 150mM NaCl and 5mM EDTA at a concentrations; (M1) $4.5x10^{-2}$, (M2) $2.13x10^{-2}$, (M3) $1.06x10^{-2}$ and (M4) $5.32x10^{-3}$ mM.

The difficulty of analysing data using spectrophotometry was inability to distinguish between the amount of free and bound F-5-M. Therefore, all samples were reanalysed by RP-HPLC (see *Figure 84*). The concentrations of the F-5-M standard covering the range (0.21, 0.11, 0.05 and 0.03mM) were determined by spectrophotometry using the extinction coefficient of F-5-M. This data was then used to calibrate the peak heights of the RP-HPLC results for the same samples. Separation of protein solutions after reaction with F-5-M showed an increase in the peak height of the unreacted protein comparing to the peak after reaction (Δ280nm) even with using a high molar ratio of F-5-M: rHSA (see *Figure 84*)
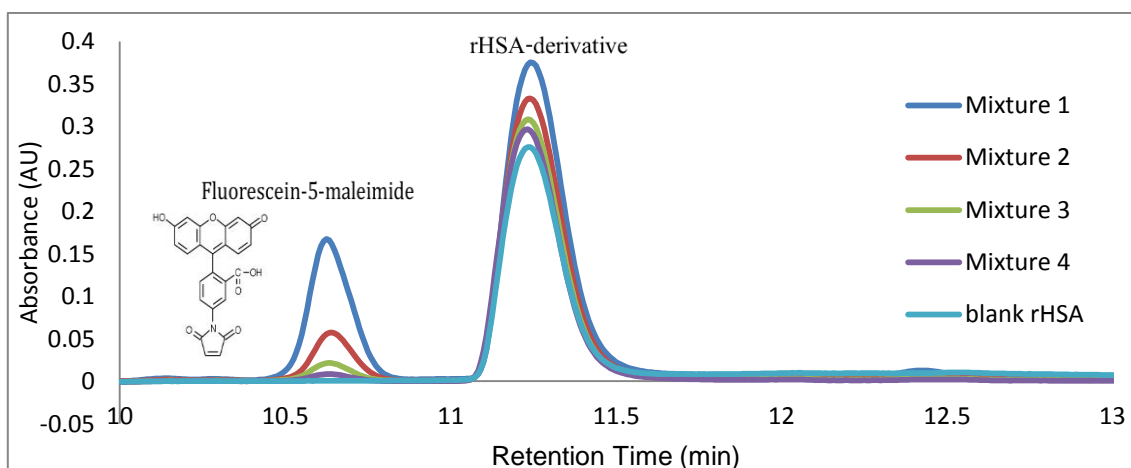
Figure 84- HPLC chromatogram of the reaction mixture samples of F-5-M and protein at a different molar ratios label: protein Mixture 1 (3.11), Mixture 2 (1.56), Mixture 3 (0.78), and Mixture 4 (0.39). The analysis was performed under the following conditions: chromatographic column C18 ((YMC-pack ODS-AQ 5.0 µm, 15cm × 4.6 mm), solvent A was 10% v/v ACN containing (0.1%) TFA pH1.7 and solvent B 90% v/v ACN containing (0.1%) TFA pH 0.9.

Table 64 shows the increasing amount of F-5-M binding to the protein with increasing concentration of the label in the samples, in addition the change in the absorbance peak height of the samples at increasing maleimide concentration compared to the original protein peak height ($\Delta 280$) shows a continual increase. The reaction between protein and F-5-M was performed using 0.068mM protein with different amount of F-5-M in each mixture (0.213, 0.106, 0.053 and 0.027mM in mixture 1, 2, 3 and 4 respectively), but the degree of conjugation exceeded the molar concentration of free thiol known to be present in that particular protein. It indicated that the Fluorescein-5-Maleimide compound reacted non-specifically with other reactive groups which may be surface lysine residues. However it was found that the reagent was not specific toward the free thiol of albumin since the degree of conjugation exceeded the molar concentration of free thiol known to be present.

Table 64- The amount of binding F-5-M after reacting with r-HSA and the changes in the peak height of the protein at 280nm.

Molar Ratio Fluorescein-5-Maleimide : protein	Increasing in the peak height compared to unreacted protein at the same concentration	Increasing in the amount of F-5-M bound to protein at a different molar ratios
3.1	0.099	0.207
1.6	0.057	0.149
0.8	0.033	0.086
0.4	0.021	0.049

The influence of the pH of the reaction buffer on the reactivity of F-5-M towards the protein free thiol was examined further to see whether more specificity could be achieved. Firstly, the reaction buffer was prepared at three different pH (6.5, 7.5 and 8.5) using 1M KOH to adjust the pH. Secondly, a molar ratio of 3:1 (F-5-M: protein) was prepared at these pH values using a mixture composition consisting of 2.12×10^{-4} M F-5-M with 6.83×10^{-5} M rHSA.

However, the specificity of the reaction towards the free thiol did not improve. Indeed the solution of F-5-M at pH 6.5 seems to be hydrolysing under these conditions resulting

in low reactivity. An unknown peak for the sample of F-5-M at pH 6.5 was observed in the HPLC chromatogram as illustrated in *Figure 85*
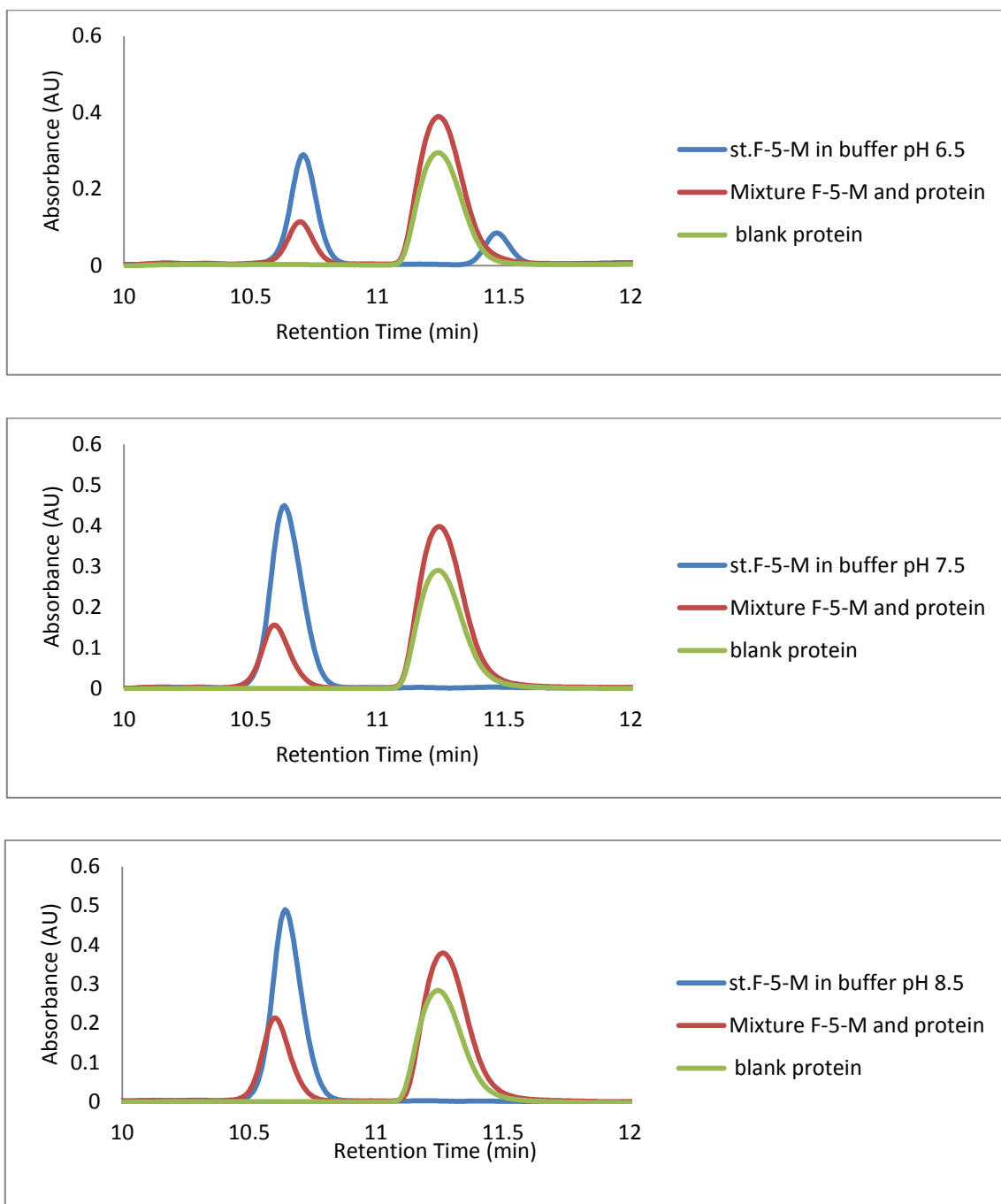
Figure 85- HPLC –Chromatograms for the F-5-M reaction with protein at different pH. The analysis was performed under the following conditions: chromatographic column C18 ((YMC-pack ODS-AQ 5.0 μm, 15cm × 4.6 mm), solvent A was 10% v/v ACN containing (0.1%) TFA pH1.7 and solvent B 90% v/v ACN containing (0.1%) TFA pH 0.9

In addition, the reactivity of F-5-M at each pH was calculated from the ratio of the F-5-M bound concentration to the concentration of the protein used. It can be seen that the lower pH shows lower reactivity (see Table 65)

Table 65- The amount of bound F-5-M after reaction with rHSA at a different pH

pH	[c] mM bound F-5-M	mM bound F-5-M /mM r-HSA
6.5	0.017	1.27
7.5	0.029	2.13
8.5	0.027	1.99

Conclusions:

A number of chemical labels were examined under a variety of conditions in order to develop a reliable method to prepare a stable and thiol specific conjugate which could be used as a probe for the determination of protein surface free thiols.

The solubility and the stability of the chemical labels and the protein conjugate were investigated and the reactivity of the labels towards the albumin free thiol was examined. The limitations of the selected labels can be summarized by the following points:

2-methylsulfonyl-5-phenyl -1,3,4 oxidiazole reagent (MSPO) was employed as a thiol specific ligand in reaction with free thiol groups of albumin, cysteine and methylbenzenthiol. However the reagent proved unreactive under all tested conditions.

N-Ethylmaleimide (NEM) showed limited modification of the Cysteine residue and protein thiol Specificity of NEM towards free thiol required maintaining the pH below 7, otherwise the reactivity towards the primary amine increased along with hydrolysis at pH greater than 7.5 - 8.

N-pyrenyl maleimide (NPM): showed low solubility in aqueous solution, and mass balance issues were found. DMSO with buffer appeared to stimulate a reaction with the maleimide reagent, thereby inhibiting and reducing the conjugation efficiency with the protein free thiol. In addition the reactivity toward primary amines was found to increase at pH more than 7.5.

Fluorescein-5-maleimide showed no specificity for the protein surface free thiol.

However, the main aims for this chapter were to find a highly specific label to estimate the free thiols groups on the protein and in the ATPS solutions, which could be used as an approach to examine an analytic problem by phase partitioning. These goals could not be achieved due to the reported problems such as the non-specificity of the label, instability, low conjugation efficiency and low reactivity.

Of all the thiol specific probes examined only DTNB showed a good specificity to the protein free thiol but the work need a further attempt to study the partitioning behaviour of the protein conjugate and Ellman's reagent.

Chapter 7

7   Attempt to exploit the specificity of DTNB toward protein free-thiols in a partitioning assay for free thiols.

Introduction:

In view of the chapter six results since Ellman's reagent had shown the best specificity in quantifying the number of protein free-thiol groups it seemed possible to take a different approach to the development of a quantitative partitioning assay for protein free-thiols despite the fact that the addition of this label did not significantly alter the protein partition coefficient as had ideally been anticipated (see section 6.3).

A novel recombinant Human Serum Albumin was kindly donated by Novozymes (now Albumedix) which was developed as a novel protein therapeutic agent and the manufacturer claims about 90% of its surface thiols are in the free thiol form. This novel protein was employed in this section and the results were compared with other albumins (BSA, purified-HSA and sigma recombinant –HSA).

Aims and Objectives

The aims and objectives of this chapter were:

1. To make further attempts to improve the method for the quantification of protein free thiol groups using ATPS partitioning.
2. To attempt to develop an ATPS partitioning strategy to distinguish and quantify protein free thiol in the presence of low molecular weight free thiol containing species.
3. To develop analytical and numerical methods in support of these objectives.

7.1   Study of the specificity of DTNB toward protein free-thiols in the development of a partitioning assay for free thiols

Initially three different batches of Albumin (BSA, p-HSA and N-rHSA) were compared using DTNB in order to estimate the amount of free thiol in each type. Samples were prepared following the experimental procedure in paragraph (A) in section 2.6
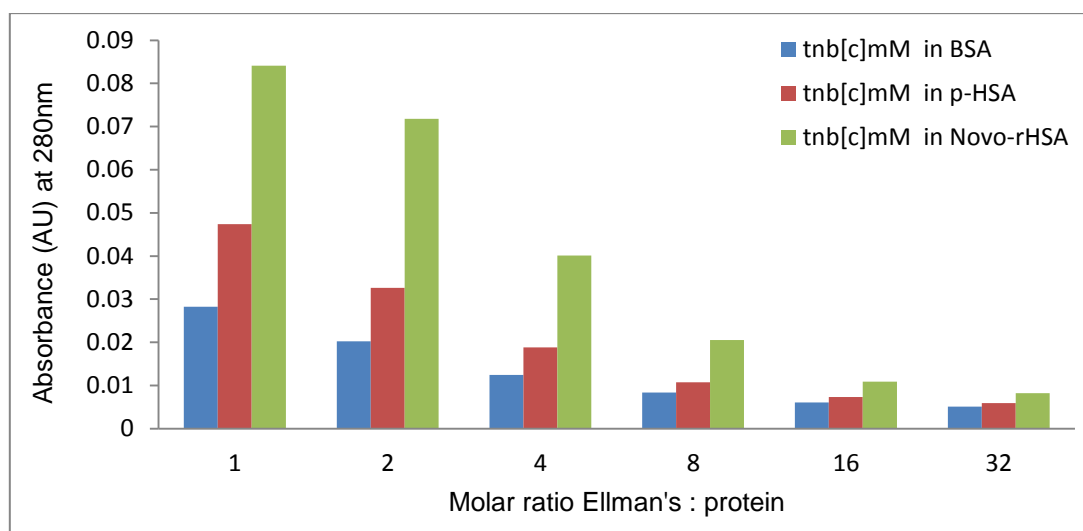
Figure 86- The amount of TNB released from different batches of albumin after reaction with different molar ratios of Ellman's reagent.

The experiment was performed by making different molar ratio mixtures containing a constant amount of DTNB and a range of proteins concentrations covering (0.134, 0.089, 0.045, 0.022, 0.011, 0.006mM).

The results shown in Figure 86 showed that the strongest reaction reflecting the highest free thiol content as shown by the amount of TNB released was consistently seen using N-rHSA at all molar ratios used. Having shown that there were quantifiable differences in the amount of free-thiols on these different batches of albumin an initial partitioning experiment was performed using the system PEG1400- K_2HPO_4. This particular system was chosen since the last system PEG1000 - K_2HPO_4 used in section 6.3 showing a higher protein preference for the polymer phase with almost no change in the partition coefficient of the protein derivative with Elman's reagent. An attempt was made to increase the molecular weight of PEG which could be expected to change the partitioning behaviour.

The partitioning experiment was performed using a set of four different molar ratio of DTNB: protein in a system having the same overall polymer/salt composition following the experimental procedure in the paragraph (B) in section 2.6. The pH of the lower phase was found to be about 10 which caused direct hydrolysis of the DTNB resulting in release of TNB and thus compromising the calculation of the thiol content of the protein solutions in the protein reaction mixtures since the pH causes hydrolysis of free DTNB in the solution. Figure 87 shows the amount of TNB calculated from the absorbance at

412nm of the standard Ellman's samples after partitioning in the PEG1400- K_2HPO_4 system
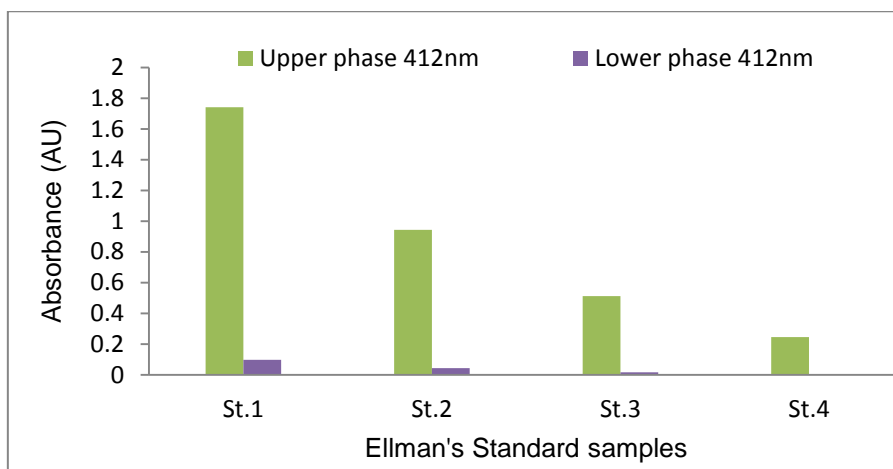
Figure 87- Standard Ellman's partitioning in PEG1400 - K_2HPO_4 system showing the direct hydrolyses of Ellman's reagent to TNB due to the pH of the system (pH10). The TLL composition was 11.125 % w/w PEG1400, 13.875 % w/w K_2HPO_4.

In a further experiment this was controlled by adjusting the pH to 8 and a similar experiment was performed, the results of partitioning were improved. The concentration of each component in upper and lower phases was calculated by the numerical methods. However, the partition coefficient for the native protein was found to be inconveniently low (ca. 0.006) and thus difficult to reliably measure.

The ATPS system required was further adjusted to increase the partitioning to the upper phase and this was achieved using a composition containing 50% PEG1400 and 50% PEG1000 in order to raise the protein partition coefficient, by decreasing the average molecular weight of the polymer in the system (157).

Stock solution of the polymer PEG was prepared at a concentration 25% w/w PEG consisting of (50% PEG1400/ 50% PEG1000) by weighing 6.25g of each molecular weight of PEG and dissolving this in 37.5g of 18.2 MΩ-cm DI water. The reaction of DTNB with protein was conducted under single phase conditions and subsequently subject to partition in the ATPS following the experimental procedure in paragraph (B) in section 2.6. N-rHSA was used because of its high thiol content to study the effect of the amount of TNB released and its behaviour in the partitioning process.

The calculated results of the amount of each component in the single phase reaction should show agreement with the amount recovered after partitioning. The partitioning

results of DTNB blank and protein show agreement with single phase results, but in the mixture of DTNB and protein where conversion of DTNB to TNB has occurred a discrepancy was found as illustrated in Table 66

There was found to be a striking decrease in the amount of TNB in the ATPS compared to the amount determined in the single phase reaction mixture prior to partitioning. In addition there was an apparent increase in the amount of DTNB following partitioning compared to the single phase results. However, in conducting this experiment it was not possible to get a mass balance.

The spectrophotometric results of this experiment raises some important questions in particular why failure to close the mass balance. Could the partitioning have brought this about?

This seemed to raise the possibility that some component of the reaction of DTNB to give TNB and mixed disulphides was not properly accounted for in the spectrophotometric numerical model for this reaction. Stoichiometrically it could be imagined that mixed disulphides represent ½ of the DTNB consumed but this did not coincide with a similar stoichiometry for the production of TNB regardless of whether the mixed disulphides are assumed to absorb at the same wavelength of DTNB or not.

Table 66- Comparison of the mass balance between (A) single phase reaction solutions and (B) the partitioning experiment. The TLL composition was 11.125 % w/w PEG1400, 13.875 % w/w K_2HPO_4.

-A- single phase solutions			
	HSA (mM)	DTNB (mM)	TNB (mM)
DTNB blank mM	0	1.16	0.006
N-rHSA blank	0.175	0	0
Mixture	0.19	0.96	0.172

-B- ATPS solutions	Upper phase		
DTNB blank	0	0.19	0
N-rHSA blank	0.003	0	0
Mixture	0.007	0.15	0.013
	Lower phase		

DTNB blank	0	0.035	0
N-rHSA blank	0.035	0	0
Mixture	0.04	0.095	0.0005
Total			
DTNB blank	0	1.14	0
N-rHSA blank	0.18	0	0
Mixture	0.2	1.23	0.068

To investigate this alarming, possibility HPLC was used to examine the stoichiometry of this reaction. The investigation was begun by monitoring a single phase reaction of a range of DTNB with protein which would release different amounts of TNB and the results were monitored by HPLC and spectrophotometric detection using the numerical modelling procedure

Thus an experiment was designed to react Novo-HSA (N-rHSA) and Ellman's reagent following the experimental procedure in paragraph (C) in section 2.6

Separation of the protein containing reaction mixture after treatment with DTNB was achieved by RP-HPLC using a C18 column following the method protocol in Table 12. The spectrophotometric results were used to calibrate the results of HPLC and thus to confirm the calculation by both methods.

The spectrophotometric absorbance at 280, 324, 412nm was used to calculate the concentration by numerical methods, and the resulting concentrations were used to calibrate the absorbance peak heights found by HPLC. The absorbance at 324 and 412nm from HPLC was calibrated with the real concentration of DTNB and TNB calculated using the numerical procedure. The calibration regression was used to calculate the concentration in the HPLC samples. The HPLC results are shown in the Figure 88.
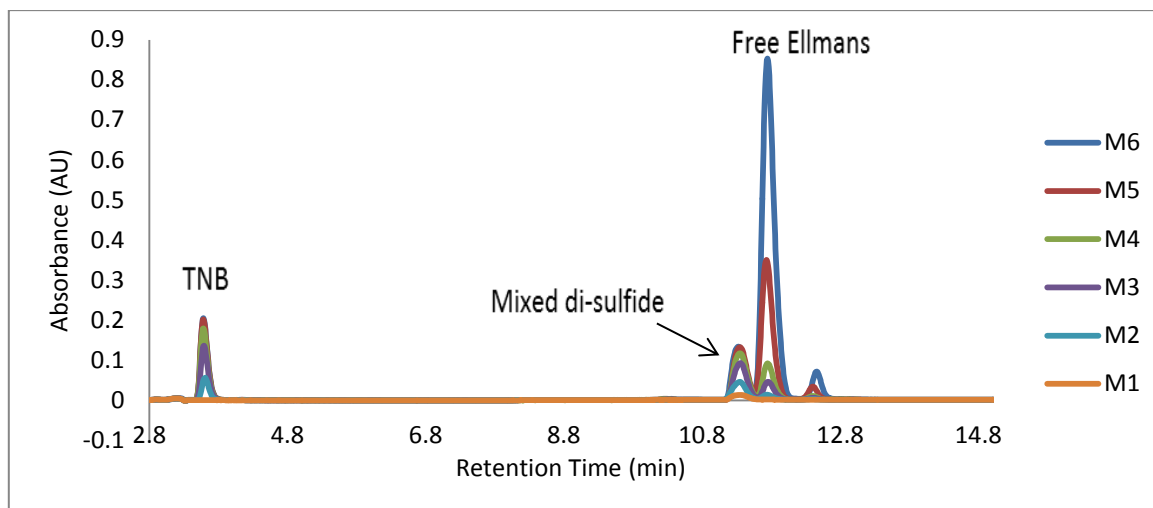
Figure 88- HPLC – chromatogram extracted for the single phase reaction for N-rHSA and Ellman's reagent at 324nm. The analysis was performed under the following conditions: chromatographic column C18 ((YMC-pack ODS-AQ 5.0 μm, 15cm × 4.6 mm), solvent A was 10% v/v ACN containing (0.1%) TFA pH1.7 and solvent B 90% v/v ACN containing (0.1%) TFA pH 0.9

The amounts of DTNB consumed calculated from the difference between the initial amount of DTNB and the free DTNB remaining at the retention time of the protein but monitored at 324nm was found to represent the DTNB reaction product as its mixed disulphide (this can be seen in column 3 of Table 67).

To validate this result, the calculation of mixed disulphide using this method should be equal to the amount of TNB released after the reaction (column 2 of Table 67) as demanded by the reaction stoichiometry, since each mole of Ellman's yields a 1mole of TNB and 1mole of mixed disulphide

Also as shown by the HPLC chromatogram in Figure 88 each increase in the absorbance of protein at 324nm (column 6 of Table 67) (reflecting the formation of the mixed disulphide) should be equal to half the decrease in the DTNB Ellman's peak (column 5 of Table 67).

Thus by calculating the total DTNB from TNB, Mixed disulphide and free DTNB as a (mM TNB+ mM Mixed disulphide)/2+ mM free DTNB) (column 4 of Table 67) yield the correct amount of DTNB that the reaction started with (column 1 in Table 67).

Table 67- Validate the HPLC calculation by the spectrophotometry results

[c] (mM) Standard DTNB	[c] TNB (mM)	[c] (mM) mixed disulphide	Total (mM) DTNB in mixture	Decrease in 324nm DTNB	Increased in A324 (nm) for Mixture
0	0	0	0	0	0
0.007	0.005	0.006	0.005	0.06	0.03
0.02	0.014	0.017	0.02	0.16	0.08
0.03	0.02	0.02	0.03	0.20	0.10
0.06	0.02	0.02	0.06	0.24	0.12
0.11	0.02	0.02	0.11	0.17	0.12

7.2 Application of TNB to study the effect of pH on the analysis conditions.

Having eliminated any difficulties with the implementation of the numerical methods used to quantify the components of this reaction a method was required to investigate the discrepancies in the mass balance of the reaction following ATPS partition.

To this end a method was applied to hydrolyse Ellman's reagent by alkaline solution (KOH) to produce TNB (158). The hydrolysis step could be performed and partitioned free from added protein and thus it could be considered to act as a standard for TNB to study the partitioning performance of TNB in the 50/50 PEG1000/PEG1400-K$_2$HSO$_4$ system enabling examination of the issue of the mass balance.

Several DTNB reagent samples were prepared from 4mg/mL stock solution using 100mM phosphate pH8 containing 1mM EDTA as a diluent as shown in Table 68, samples tubes were mixed by vortexing to give intense yellow coloured solutions.

Table 68- The volume composition of the Standard Ellman's samples

Samples	Ellman's µL (4mg/mL)	Reaction buffer (µL)	Ellman's mM
1	0	2800	0.00
2	28	2772	0.14
3	42	2758	0.20
4	84	2716	0.40
5	168	2632	0.81
6	336	2464	1.62

Similar samples were prepared using 50mM KOH instead of buffer to hydrolyse DTNB to TNB. Samples were diluted 10 fold with buffer and analysed by spectrophotometry (Figure 89) and HPLC Figure 90 and 91
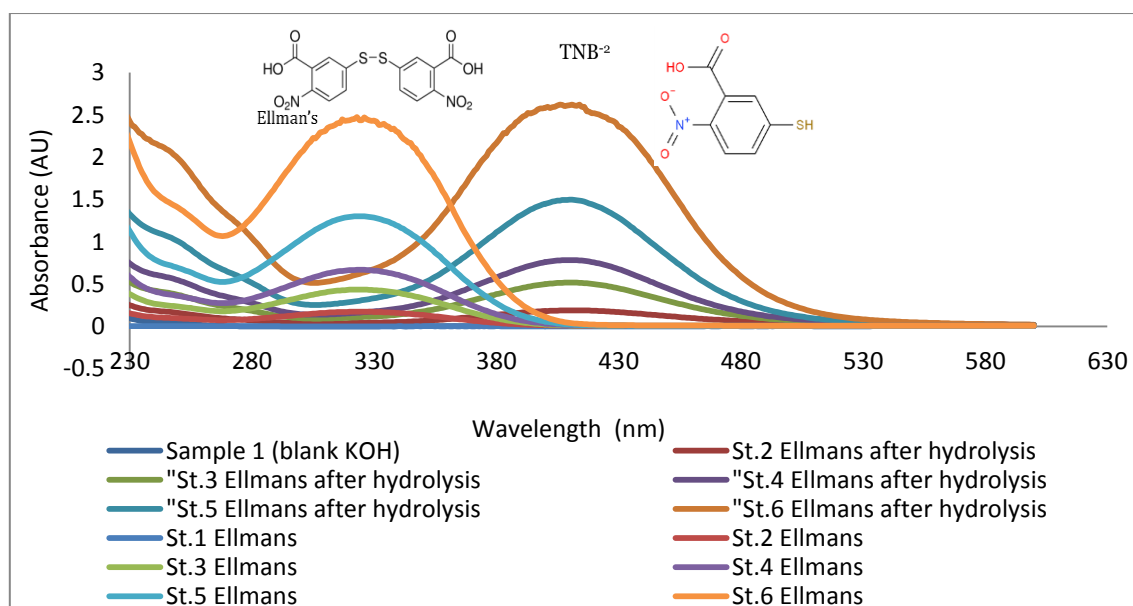
Figure 89- UV/Vis spectra at 324 and 412nm for the single phase hydrolysis of DTNB reagent by alkaline solution covering the following concentrations of DTNB St.1 (0mM), St.2 (0.14mM), St.3 (0.20mM), St.4 (0.40mM), St.5 (0.81mM) and St.6 (1.62mM).
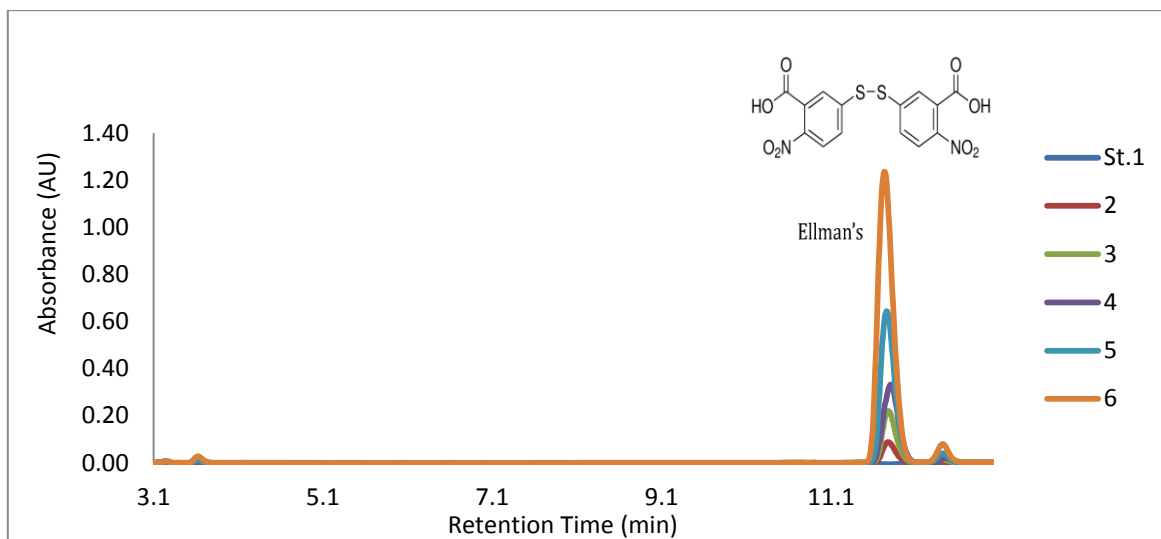
Figure 90- HPLC – chromatogram extracted for the single phase samples of Standard Ellman's reagent at 324nm, at the concentration (1) 0mM, (2) 0.14mM, (3)0.2mM, (4) 0.4mM, (5) 0.81mM and (6) 1.62mM. The analysis was performed under the following conditions: chromatographic column C18 ((YMC-pack ODS-AQ 5.0 µm, 15cm × 4.6 mm), solvent A was 10% v/v ACN containing (0.1%) TFA pH1.7 and solvent B 90% v/v ACN containing (0.1%) TFA pH 0.9
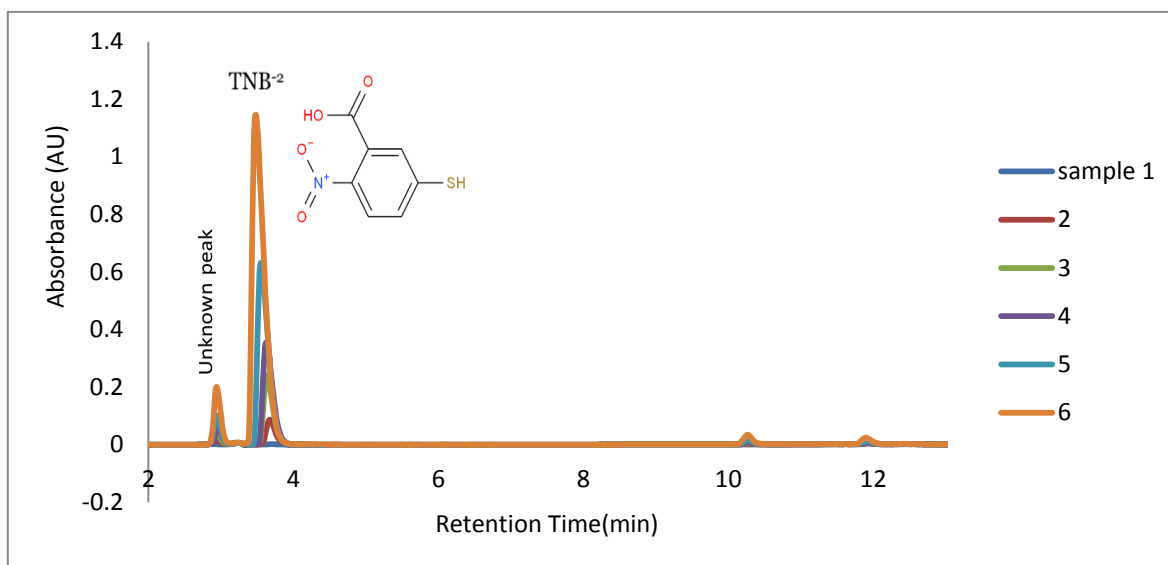
Figure 91- HPLC – chromatogram extracted from the single phase samples for Ellman's reagent after alkaline hydrolysis at 324nm. the DTNB concentrations were covered the range (1) 0mM, (2) 0.14mM, (3)0.2mM, (4) 0.4mM, (5) 0.81mM and (6) 1.62mM. The analysis was performed under the following conditions: chromatographic column C18 ((YMC-pack ODS-AQ 5.0 µm, 15cm × 4.6 mm), solvent A was 10% v/v ACN containing (0.1%) TFA pH1.7 and solvent B 90% v/v ACN containing (0.1%) TFA pH 0.9

The results of HPLC were extracted also as spectra at specific wavelengths from the diode array results and the TNB maximum absorption when using HPLC was found at 324nm. Therefore, extraction the HPLC-spectra at the retention time of TNB using the absorbance at 324nm was chosen as a detection wavelength as illustrated in Figure 92
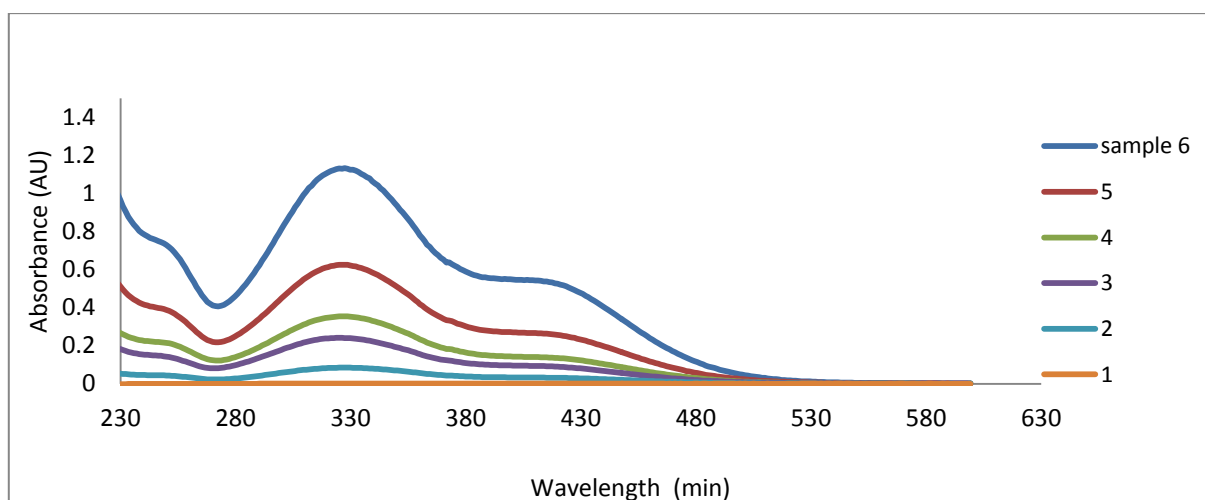
Figure 92- HPLC spectrum (see chromatogram shown in Figure 91) at the retention time of the TNB (3.6min) at 324nm, samples prepared according to table 68.

HPLC spectra at the retention time of TNB revealed a large peak at 324nm which is closely similar to the wavelength of maximal adsorption of DTNB despite the fact that all the DTNB has been converted to TNB. An assumption was made that it could be because of the difference in the pH of the elution buffer for the HPLC which was very acidic (buffer A was 10% ACN containing (0.1%) TFA pH1.7 and buffer B 90% ACN containing (0.1%) TFA pH 0.9) compared to 100mM phosphate pH8 containing 1mM EDTA, so that TNB could be halochromic resulting in a hypochromic shift in its wavelength of maximal absorption.

Freshly prepared samples of 300µL Ellman's reagent (4mg/mL) were mixed with 9.7 ml KOH (50mM) and used to examine the effect of changing the pH of the solution by adding a few microliters of 1M HCL to give solutions having a pH range from 3 to 11.5. Wavelength scans from 600 to 200nm were taken and the absorbance at 324 and 412nm was measured by spectrophotometer. The results are shown in *Figure 93* A and 93 B
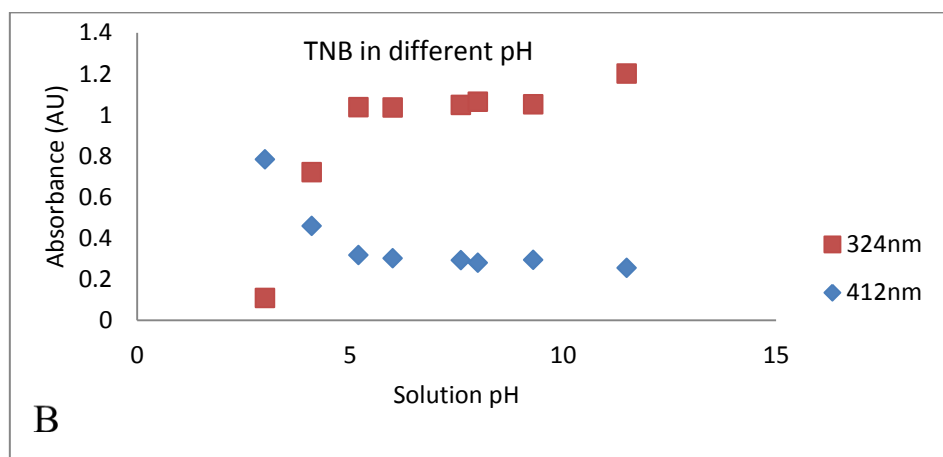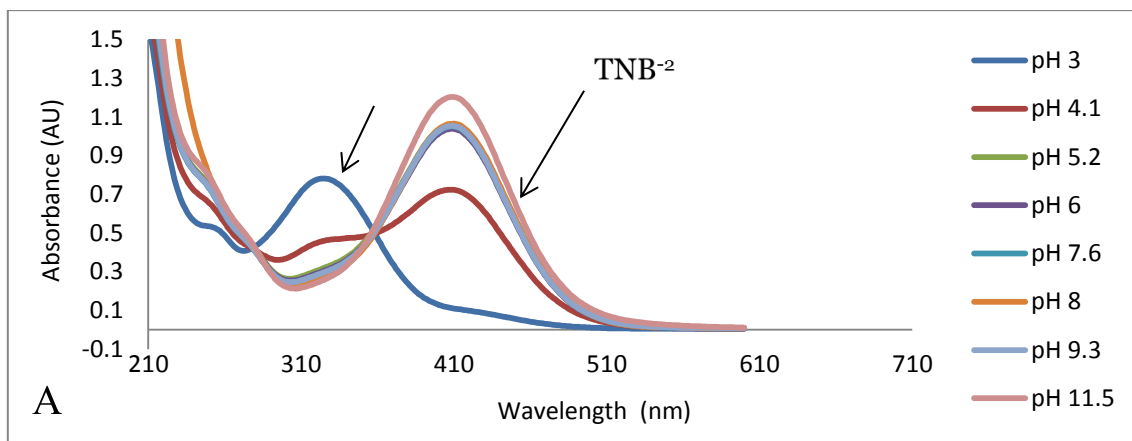
Figure 93- (A) UV/Vis spectra at 324 and 412nm for the solutions resulting from the hydrolysis of Ellman's reagent by alkaline solution at different pH and (B) the trend of the absorbance at 324 and 412nm as a function of the solution pH.

The results indicated that the pH has a significant effect on the hydrolysed DTNB and it may be anticipated that there was a reverse reaction at low pH which could explain the spectra obtained during HPLC using elution buffer with a low pH (containing TFA) thus explaining the difference between the spectrophotometric and the HPLC spectra. It has been reported that the pKa of TNB is 4.41 (159). At low pH TNB could be decomposed to the Thiosulfinate (R-SS (O) R) which may be converted to the sulfonic acid (R-SO3H) in a pH dependent manner as shown in Figure 94 (160).
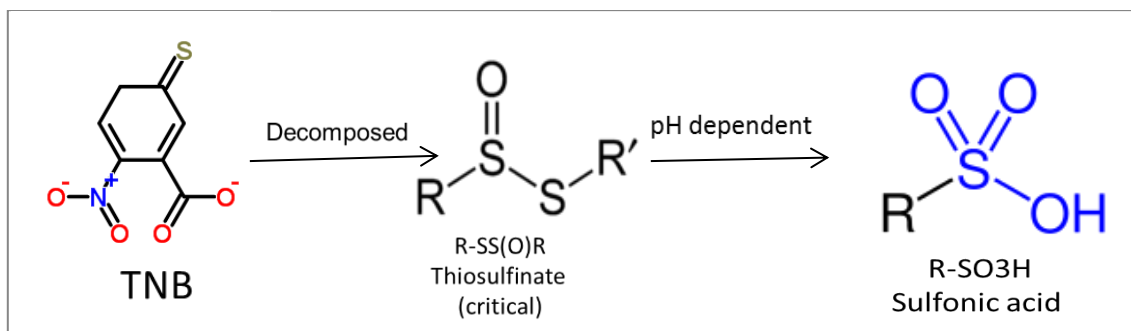
Figure 94- Proposed decomposition scheme of TNB under the effect of pH

7.3 Study of the partitioning behaviour of TNB in ATPS and the discovery of the oxidative power of PEG

Subsequently TNB standards solutions prepared by hydrolysis of DTNB using KOH were partitioned in a 50/50% PEG1000 / PEG 1400 - K_2HPO_4 system in order to examine the behaviour of TNB in such a system. Analysis of the samples was carried out spectrophotometry and RP-HPLC. The concentrations of TNB in the single phase and ATPS resulting from the UV/VIS spectral absorbance were calculated using the numerical methods previously outlined, and the calculated results are illustrated in Table 69. The results indicate that there is still a significant mass balance problem associated with the partitioning step even in the absence of both protein and DTNB. Therefore the failure to close the mass balance cannot be due to interference from these species or a failure in the numerical analysis.

Table 69- Comparison of the concentration of TNB in the single phase and following partition in an ATPS (TLL composition was 11.125 % w/w PEG1400, 13.875 % w/w K_2HPO_4) showing the recovery % in the ATPS

Single phase TNB (Mm)	Total TNB (mM) in ATPS	TNB ATPS Recovery %
0.000	0.000	-
0.128	0.040	31.08
0.203	0.063	30.92
0.418	0.161	38.49
0.795	0.494	62.11
1.491	1.328	89.04

By comparing the calculated amount of TNB in the single phase and the two phase system a significant difference was found with low recovery especially with samples having a lower concentration of TNB. In addition the mass balance could not be closed.

231

The spectrophotometric results of partitioning in the ATPS for the upper phase were very surprising (Figure 96), it appears that PEG is capable of oxidising TNB and that this occurs primarily in the PEG phase following partitioning thus a peak begins to develop at 324nm which is not found in the single phase reaction mixture (compare Figures 95 and 96). Now the story starts to become clear and the failure to close the mass balance in the ATPS for this reaction is due to the oxidative power of PEG which implies that the partitioning method cannot be made to work for this system unless the oxidative power of the PEG solutions can be controlled.
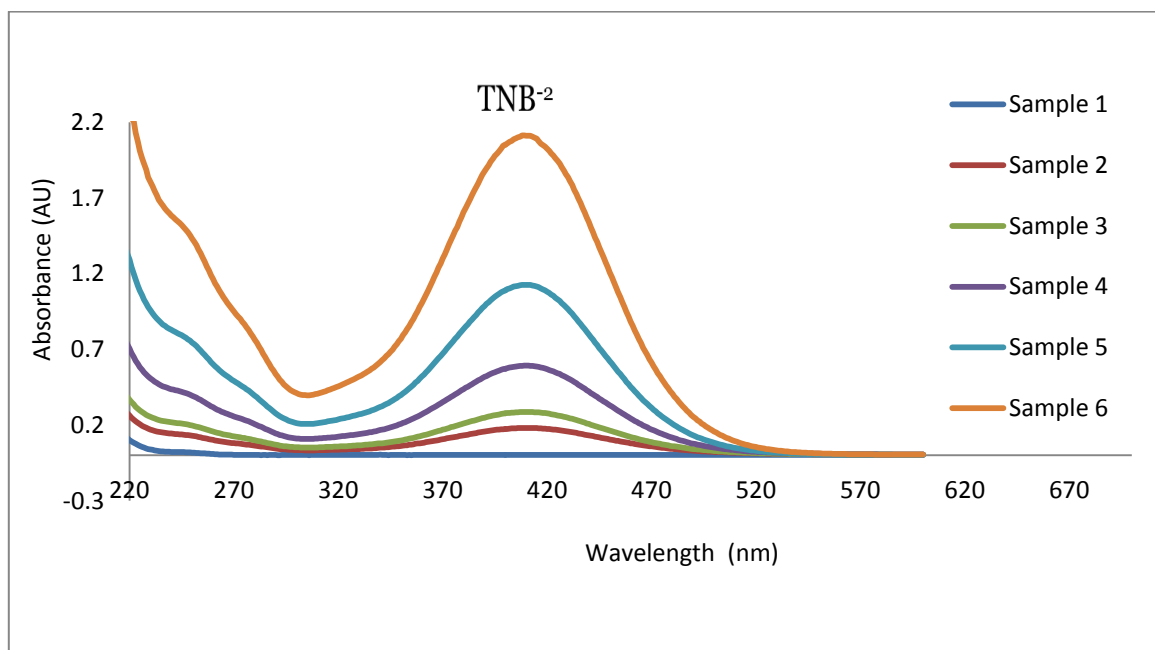
Figure 95- UV/Vis spectra at 412nm of the single phase hydrolysis of Ellman's reagent by alkaline solution at concentrations of Sample 1 (0), Sample 2 ($1.01x10^{-2}$), Sample 3 ($1.51x10^{-2}$), Sample 4 ($3.03x10^{-2}$), Sample 5 ($6.05x10^{-2}$) and Sample 6 ($1.21x10^{-1}$) mM.
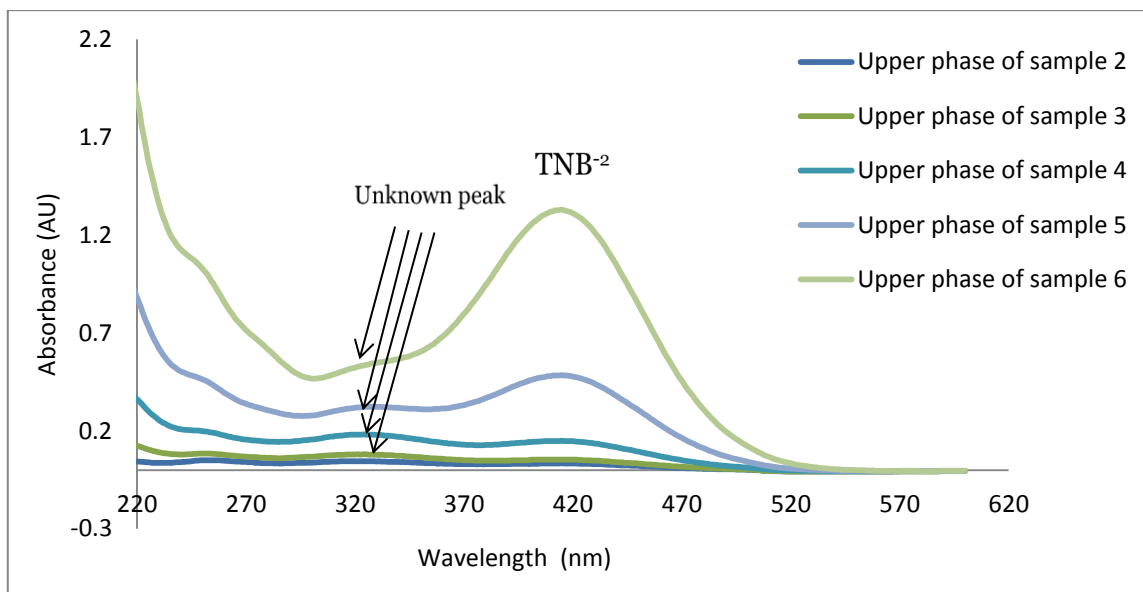
Figure 96- UV/Vis spectra for the TNB solutions in the upper phase of the 50/50 PEG1000 / PEG1400 - K_2HPO_4 system (TLL composition was 11.125 % w/w PEG1400, 13.875 % w/w K_2HPO_4) showing the unknown peaks at 324nm. The Upper phase hydrolysis of DTNB by alkaline solution at a concentrations of Sample 2 ($1.01x10^{-2}$), Sample 3 ($1.51x10^{-2}$), Sample 4 ($3.03x10^{-2}$), Sample 5 ($6.05x10^{-2}$) and Sample 6 ($1.21x10^{-1}$) mM as used in the partitioning experiment.

7.4 Investigation of the effect of the addition of reducing agents and / or antioxidants to control the oxidative effect of PEG.

The appearance of the unknown peak seems to be due to the oxidation power of PEG solution acting onto the TNB^{2-}. In addition the unknown peak (see Fig. 96) seems to explain the mass balance issue of the ATPS and the low recovery of the partitioning process by interconversion of the TNB.

This raises a number of questions; Can the oxidant be quantified using the loss of TNB? Can the oxidation due to PEG be saturated to make the phase system useful in this separation?

The investigation of methods to accomplish this by addition of reducing agents and / or antioxidants were examined since the commercial PEG (Mwt. 1000 and 1450) have been used as supplied by Sigma-Aldrich UK and Fisher UK do not contain any antioxidants (161).

7.4.1 Examination of the use of sodium borohydride as a reducing agent on the oxidative power of PEG 1000 and PEG 1400.

An initial attempt focussed on the addition of sodium borohydride ($NaBH_4$) reagent to the PEG solutions and investigating the response by repeating the partitioning experiment under the same conditions to monitor the oxidative effect.

A new short experiment was designed by partitioning one sample of TNB in the 50/50 PEG1000-PEG1400 - K_2HPO_4 system containing different amounts of $NaBH_4$ (0, 10, 50 and 100mM). The recovery of each system was calculated and the total amount of TNB from ATPS compared with the amount in the single phase.

A stock solution 100mM $NaBH_4$ was prepared by dissolving 0.378g in 100mL (18.2 MΩ-cm) DI water, the solution of 25 % w/w (12.5g) PEG 50/50 was dissolved in each $NaBH_4$ solution following the Table 70

Table 70- The volume composition of the 50/50 PEG1000/1400 samples containing different concentrations of $NaBH_4$.

PEG solutions	Amount of NaBH4(mL) from(100mM)	Amount of water (mL)
PEG contain 0mM $NaBH_4$	0	37.5
PEG contain 10mM $NaBH_4$	3.75	33.75
PEG contain 50mM $NaBH_4$	18.75	18.75
PEG contain 100mM $NaBH_4$	37.5	0

Sample No.5 in (Table 68) was used to repeat the experiment under these conditions. A single phase mixture was prepared by hydrolysis of Ellman's reagent (168µL Ellman's 4mg/mL) in (2632µL KOH 50mM) and the ATPS was prepared using 50/50 PEG1400/ PEG1000- K_2HPO_4 system and following the experimental procedure in paragraph (B) in section 2.6, all samples were analysed by spectrophotometry.

Use of $NaBH_4$ to stabilise PEG and eliminate the oxidation effect on the TNB was achieved, the results showed an absence of the oxidised TNB peak in the presence of PEG and in addition there is an increase in the total amount of TNB recovered from the

phases containing NaBH$_4$ compared to the single phase (as shown in *Table 71*), also there was a difficulty in estimating the correct amount of NaBH$_4$ to saturate the oxidative properties of PEG solution.

Table 71 - The TNB recovery percent under the effect of NaBrH$_4$ as an antioxidant.

ATPS contain		mM TNB	Total	TNB Recovery (%)
(0mM) NaBH$_4$	Top	0.10	0.565	65.89
	Bottom	0.012		
(10mM) NaBH$_4$	Top	0.163	0.919	107.18
	Bottom	0.020		
(50mM) NaBH$_4$	Top	0.167	0.936	109.14
	Bottom	0.019		
(100mM) NaBH$_4$	Top	0.177	0.987	115.11
	Bottom	0.019		
Single phase TNB		0.085	0.857	100

Further investigation was made looking for the effect and stability of NaBH$_4$ on the partitioning of the whole reaction of protein, Ellman's and TNB. The same procedure for the preparation of the solution following (Table 68) was repeated, samples of the protein reaction with Ellman's and standard DTNB were partitioned in the 50/50 PEG1000-PEG1400 - K$_2$HPO$_4$ system, The stock solution of 25 % w/w PEG contained 10mM NaBH$_4$. Stock protein (N-rHSA), and stock DTNB were prepared using Ellman's reaction buffer 100mM phosphate pH8 containing 1mM EDTA.

The 50/50 PEG1000-PEG1400 solution containing sodium borohydride (10mM NaBH$_4$) which was used to prepare the ATPS for partitioning of the reaction mixture of protein with DTNB resulted in a direct reduction of the Ellman's reagent to TNB. This reduction will affect the real amount of TNB in the solution since it does not reflect the amount of thiol in the protein. Figure 97 shows the amount of TNB in the standard Ellman's after partitioning in the 50/50 PEG1000/PEG 1400 - K$_2$HPO$_4$ system containing 10mM NaBH$_4$.
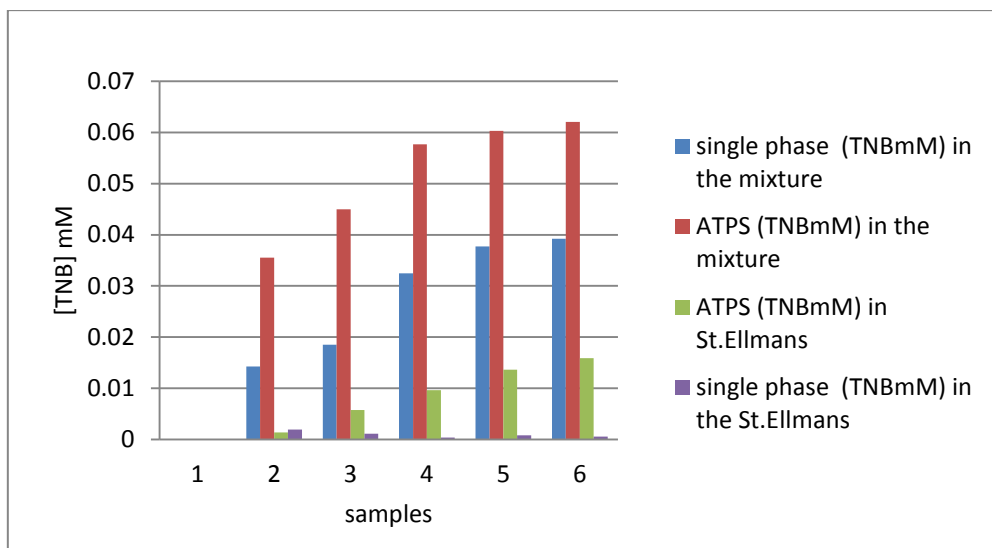
Figure 97- Hydrolysis of standard Ellman's reagent in the 50/50 PEG1000/PEG1400 - K_2HPO_4 system (TLL composition was 11.125 % w/w PEG1000/1400, 13.875 % w/w K_2HPO_4) containing 10mM $NaBH_4$.

7.4.2 Examination of the use of Vitamin C as an antioxidant with PEG 1000 and PEG 1400.

An alternative approach employing an antioxidant was examined. Antioxidants act as a stabilizer added to hydrocarbons that are susceptible to oxidation. When the antioxidants donate an electron or hydrogen atom to a radical derivative it is termed a primary antioxidant. These antioxidants are usually hindered amines (light stabilizers inhibit the photo oxidation) or substituted phenolic compounds with one or more bulky functional groups Butylated hydroxytoluene (BHT) is a common example of a hindered phenolic antioxidant. Primary antioxidants are free radical scavengers which combine with peroxy radicals and break the autocatalytic cycle. On the other hand there are secondary antioxidants; their activity is implemented by the removal of an oxidative catalyst and the consequent prevention of the initiation of oxidation.

Vitamin C ($C_6H_8O_6$) was used as a safe antioxidant stabiliser and the amount to be added to the PEG solution could be calculated easily after measuring its absorbance under the experimental conditions. In this experiment the same procedure was followed, a stock solution of 100mM Vitamin C (1.76g) was dissolved in 100mL (18.2 MΩ-cm) DI water and used to prepare PEG solution following Table 70. The proposed action of the antioxidant could be assumed by the reaction scheme shown in *Figure 98*.

236
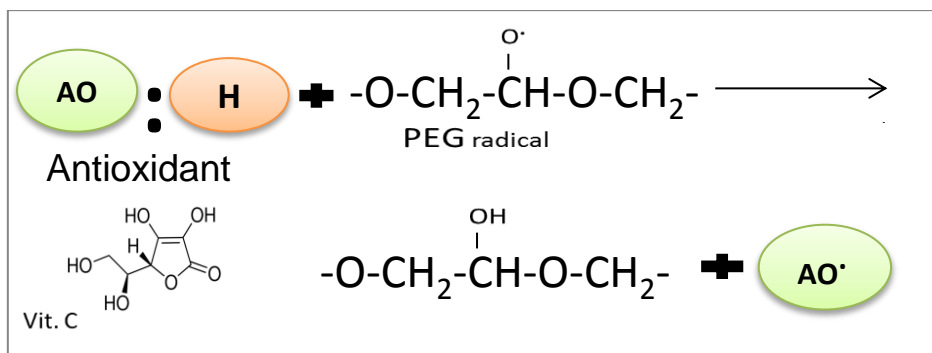
Figure 98- Proposed reaction scheme of the antioxidant and the degradation products of PEG.

The absorbance of vitamin C and the oxidation product of the Vitamin C interfere with the spectrophotometric determination of TNB which will inevitably complicate the calculation of the TNB concentration due to the contribution of the antioxidant reagent (as shown in *Figure 99*) and the maximum % recovery achieved was only was 90 as illustrated in Table 72.

Table 72 - The TNB recovery percent in the 50/50 PEG1000/PEG1400 - K₂HPO₄ system (TLL composition was 11.125 % w/w PEG1000/1400, 13.875 % w/w K₂HPO₄) under the effect of Vitamin C as an antioxidant.

ATPS contain		TNB (mM)	Total (mM)	Recovery %
Vit. C (0mM)	Top	0.148	0.779	74.3
	Bottom	0.008		
Vit. C (10mM)	Top	0.153		
	Bottom	0.018	0.857	81.8
Vit. C (50mM)	Top	0.169		
	Bottom	0.019	0.943	89.9
Vit. C (100mM)	Top	0.167		89.9
	Bottom	0.022	0.942	
Single phase			1.048	100
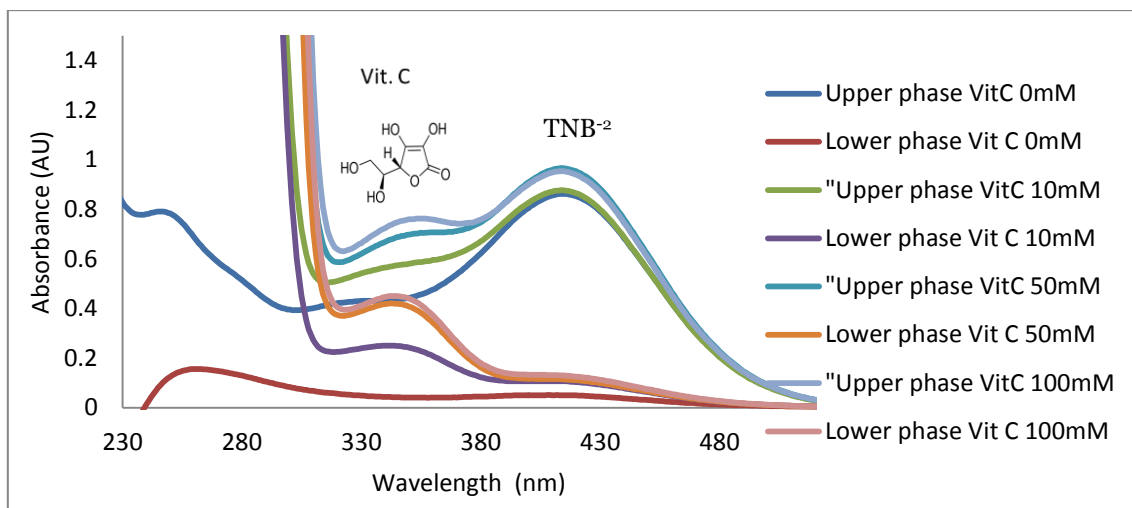
Figure 99- UV/Vis spectroscopy of the partitioning of TNB in 50/50 PEG1000/PEG1400 - K$_2$HPO$_4$ system (TLL composition was 11.125 % w/w PEG1000/1400, 13.875 % w/w K$_2$HPO$_4$) containing different amounts of Vitamin C (0, 10, 50 and100mM).

Further attempts were made to study the stability of TNB in a simplified ATPS containing only freshly sourced PEG 1400 on the assumption that the storage age of PEG1000 might have been the reason behind the strong oxidative effect. Sample No.5 in (Table 68) was used to repeat the last experiment under the new conditions with partitioning into a 25% w/w PEG1400-K$_2$HPO$_4$. The samples were analysed as before and the results indicated no-improvement in the stability of TNB since TNB which was still consumed and the TNB-derived oxidation product was still present as demonstrated in

Figure *100*.
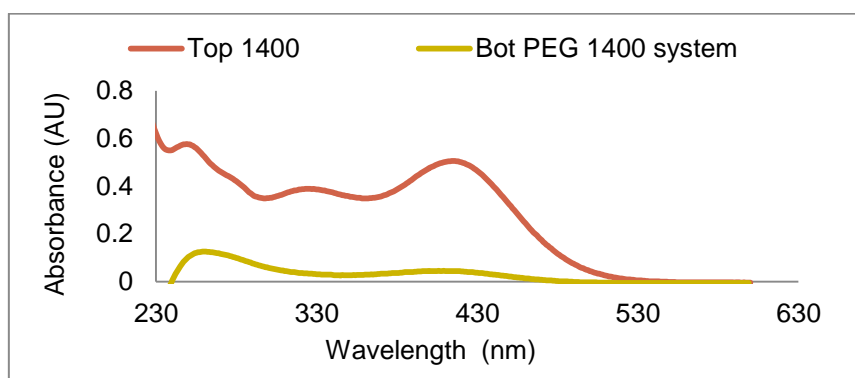
Figure 100- Scanning spectrophotometry of the TNB in a PEG1400-Potassium phosphate (pH 8) system (TLL composition was 11.125 % w/w PEG1400, 13.875 % w/w K$_2$HPO$_4$) showing a TNB derived reaction product with maximum absorbance at about 320nm.

7.4.3 Examination of the use of Sodium metabisulphite as an antioxidant with PEG 1000 and PEG 1400.

As an alternative the effectiveness of another antioxidant Sodium metabisulphite ($Na_2O_5S_2$) was studied and the same procedure was followed. A stock solution of 100mM Sodium metabisulphite was prepared by dissolving 1.9 g in 100mL (18.2 MΩ-cm) DI water and this was used to prepare PEG solutions following Table 70. TNB sample No.5 in (Table 68) was used to repeat the experiment under the new conditions. The effect of Sodium metabisulphite on PEG was monitored by spectrophotometry to follow the oxidation effect of PEG on TNB in the presence of the new antioxidant reagent

The spectra of the TNB obtained from the partitioning in 50/50 PEG1000/1400- K_2HPO_4 ATPS containing Sodium metabisulphite were analysed and the recovery was calculated as shown in Table 73.

Table 73- The TNB recovery percent in the 50/50 PEG1000/PEG1400 - K_2HPO_4 system (TLL composition was 11.125 % w/w PEG1000/1400, 13.875 % w/w K_2HPO_4) under the effect of Sodium metabisulphite as an antioxidant

ATPS contain	Total (mM)	Recovery %	Next day Recovery%
$Na_2O_5S_2$ (0mM)	0.406	59.4	54.2
$Na_2O_5S_2$ (10mM)	0.595	86.9	81.9
$Na_2O_5S_2$ (50mM)	0.452	66.12	42.2
$Na_2O_5S_2$ (100mM)	0.244	35.64	1.2
single phase	0.684	100	-

The recovery of TNB was not very high and fluctuated with the amount of sodium metabisulphite in the solutions. Samples containing high concentrations of Sodium metabisulphite showed a very low recovery (1.2%) and no TNB was detected even in the Lower phase. This indicates that an additional reaction had occurred and eliminated TNB from this phase. Additionally after 24 hours there was a change in the colour of the samples especially in the sample containing the highest concentration of Sodium metabisulphite (100mM). The absorbance measurements were repeated and a decrease in the absorbance was found with complete disappearance of the yellow colour from the samples containing Sodium metabisulphite after 2 days (see Figure

102), the colourless product may be TNB-derived sulfenic acid as reported in (160) and Figure 101 shows the reaction scheme.
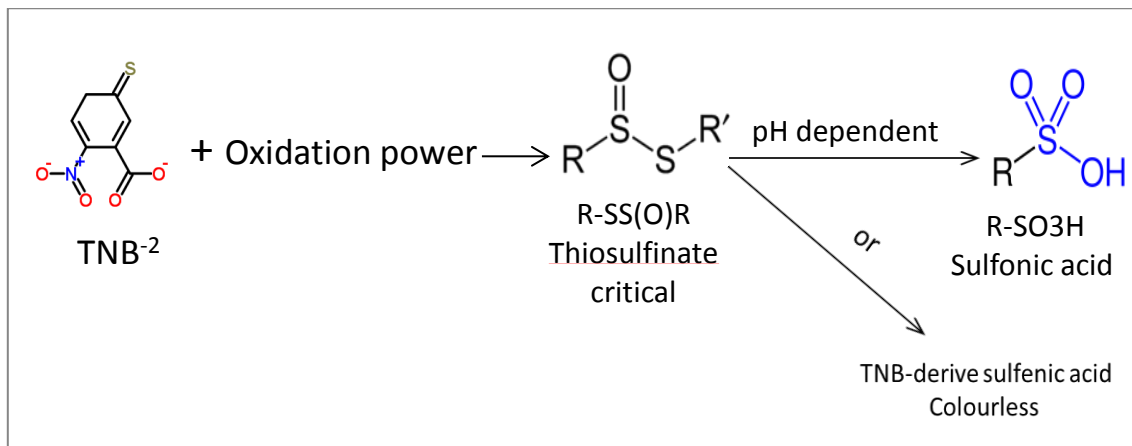
Figure 101- Proposed reaction scheme of TNB in the presence of an oxidant
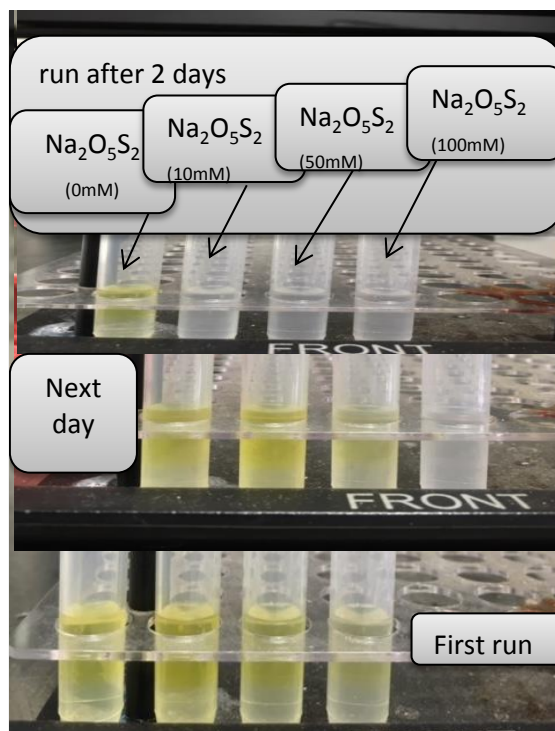
Figure 102- Experimental samples of TNB in the 50/50 PEG1000/1400- K_2HPO_4 ATPS containing different amounts of sodium metabisulphite showing initial colouration, and colouration after 24 and 48 hours.

7.4.4 Examination of the use of 2,2'-methylene-bis(4-methyl-6-tert-butyphenol) and Butylated hydroxytoluene as an antioxidant with PEG 1000 and PEG 1400.

A survey of the literature was made to find other means to overcome the issue of PEG derived oxidation, one report concerned the successful stabilization of the oxidation power of PEG (Mw. 6000) following thermal degradation by using a phenolic antioxidant 2,2'-methylene-bis(4-methyl-6-tert-butylphenol (MPM-TBP) whose molecular structure is shown in Figure 103. The reaction resulted in an inhibition of the peroxide radical action (commonly known as peroxide decomposer antioxidant) (162).
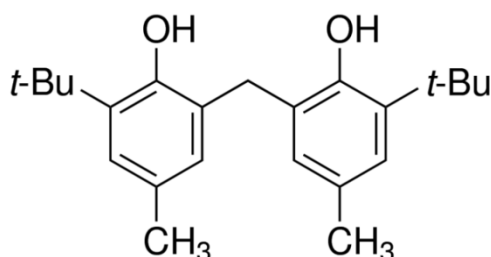
Figure 103- Molecular structure 2,2'-methylene-bis(4-methyl-6-tert-butyphenol)

A stock solution of (MPM-TBP) was prepared at a concentration 0.025g/mL in Ethanol. Standard TNB in single phase was prepared by mixing 168µL Ellman's (4mg/mL) with 2632µL (50mM KOH), 50/50 PEG1000/1400 was prepared by dissolving 2.5g PEG 1000 and 2.5g PEG 1400 in 15g (18.2 MΩ-cm) DI water to which 12µL (stock MPMTBP 25mg/mL) was added. The study in the ATPS was carried out by preparing a system which was almost a single phase. In other words the stability study of TNB was undertaken in a PEG phase by using half the amount of salt thus making the system a PEG-rich phase and in a similar way a salt-rich phase was prepared.

A blank sample was prepared consisting of 0.3g salt, 1.47g Blank PEG (without adding any antioxidants), 0.25g standard TNB or DTNB and 0.478g buffer.

As above samples containing TNB in PEG (with added MPM-TBP) was prepared by mixing 0.3g salt, 1.47g PEG+ MPMTBP, 0.25g standard TNB and 0.478g buffer.

Similarly TNB in salt rich phases was prepared by mixing 0.72g salt, 1.47g buffer and 0.25g TNB solution. The stability of the TNB absorbance for all samples was measured by spectrophotometer over a time course. UV/Vis spectra of the effect of PEG

containing 2,2'-methylene-bis(4-methyl-6-tert-butylphenol) as an antioxidant on the recovery of TNB in the PEG rich and salt-rich phases are shown in *Figure 104Figure 105*.
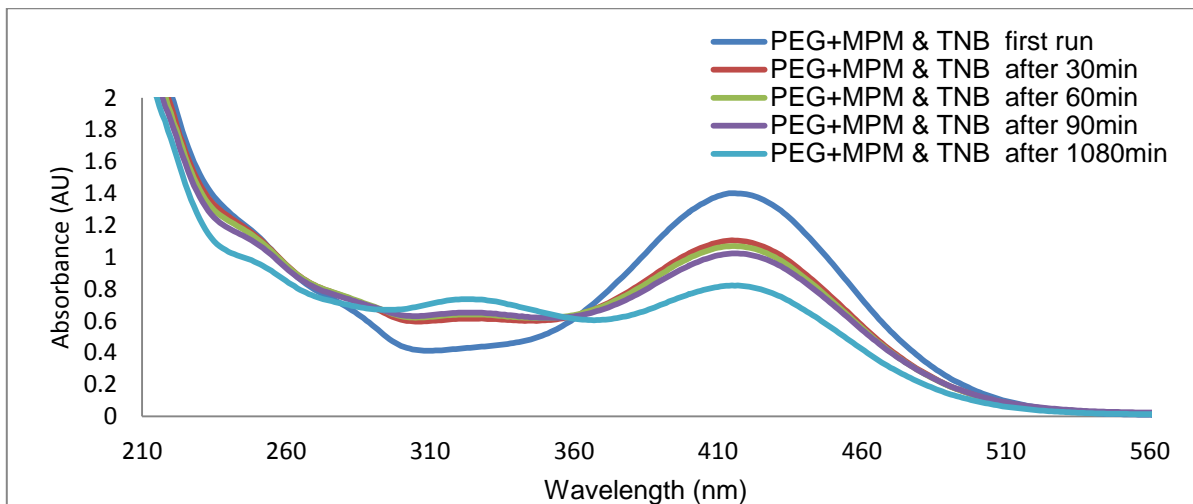
Figure 104- UV/Vis spectra of the effect of using 2,2'-methylene-bis(4-methyl-6-tert-butylphenol) as an antioxidant in the 50/50% PEG1000/1400 rich phase (0.3g K_2HPO_4, 1.47g PEG 1000/1400) on the recovery of TNB over a time course of 18 hours.
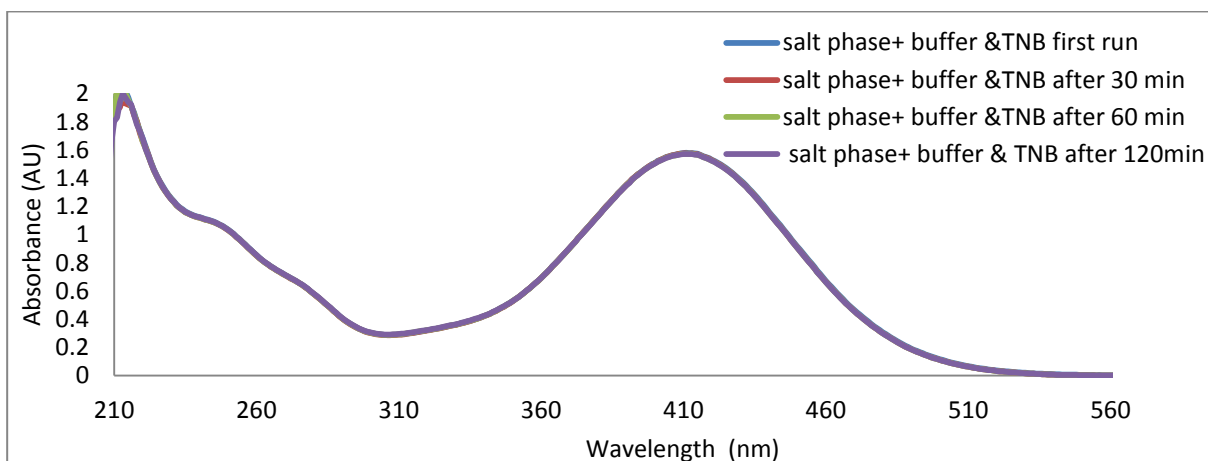
Figure 105- UV/Vis spectra at 412nm of TNB in the salt-rich solution (0.72g K_2HPO_4) of the two phase system showing the recovery of TNB over a time course of 2 hours.

The results indicated poor control by the antioxidant towards the oxidation power of PEG and due to its limited solubility in aqueous solution its concentration could not be increased. The same experiment confirmed that the oxidative phase is the PEG phase.

Dow Technical Data Sheets reveals the use of BHT as an antioxidant, it has been reported that the optimum amount of BHT lies in a range 0.1- 2% w/w (163). PEG solutions were thus made containing100 ppm BHT as a stabilizer.

Stock BHT was prepared at a concentration of 25mg/mL in Ethanol. PEG solution contain 100ppm BHT was prepared by mixing 2.5g PEG 1000 and 2.5g PEG 1400 in 15g (18.2 MΩ-cm) DI water to which 60µL (Stock BHT 25mg/mL) was added. Exactly the same solutions of TNB as in the previous experiment were prepared using PEG with the new antioxidant. However, no improvement was achieved as shown in Table 74

Table 74- Comparison of the amount of missing TNB in the presence of different antioxidants (BHT and MPMTBP) as stabilisers of the PEG solution (0.3g K_2HPO_4, 1.47g PEG 1000/1400).

PEG Oxidation power as judged by missing TNB (%)			
(Initial TNB/Final TNB in PEG)*100			
Time (min)	Blank PEG	PEG& MPMTBP	PEG & BHT
10	26.07	11.77	28.97
30	-	30.33	-
60	35.95	32.48	36.25
90	-	35.52	-
120	38.11	-	42.49
180	41.23	-	44.50
240	42.57	-	49.25
1080	50.07	48.65	58.25

7.4.5 Examination of the effect of using freeze dried PEG in combination with anitioxidants on the oxidative power of PEG 1000 and PEG 1400.

Vacuum drying has been reported as an effective method to remove peroxide residues, which appears to take advantage of the volatility of formic acid and/or formaldehyde. On the other hand, Pyrgallol (Py) has been found to be a high effective antioxidant which has been used to improve the oxidative stability of Jatropha oil (164).
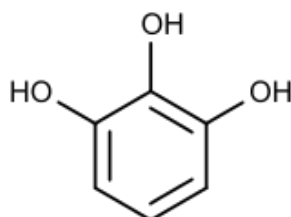
Figure 106- Molecular structure Pyrogallol

Pyrogallol was found to have the ability to delay the oxidation reaction by the following suggested mechanism: an alcoholic solvent could be effective as a proton donor; the three hydroxyl groups in Pyrogallol could be involved in releasing hydrogen atoms and effectively preventing oxidation. This suggested the use of Dextran with the PEG solution since it has a large number of hydroxyl groups and thus might be a good alternative to Pyrogallol. This further suggested that a combined approach might be effective in controlling PEG autoxidation; freeze drying of PEG solutions, use of Dextran phase systems and the inclusion of an antioxidant.
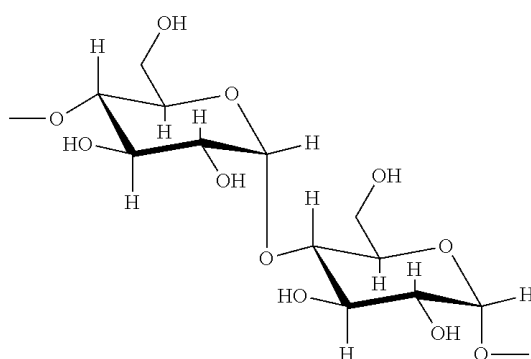
Figure 107- Molecular structure of Dextran

A 25 % w/w 50/50 PEG1000/1400 solution was prepared, which was frozen at -20 ^{o}C and freeze dried for 24 h. This was followed by re-dissolving the PEG in nitrogen saturated water with added antioxidant to increase the efficiency of the elimination of the oxidative effect.

The freeze dried PEG was used to re-prepare 25 % w/w PEG solution with an inhibitor (12 µL MPM-TBP (25mg/mL)) and 60 µL BHT(25mg/mL) separately, and by using both of them in the same solution. The solution of using Dextran500 as a stabiliser was prepared by dissolving the lyophilised PEG in 15mL degassed water and adding 50µL Dextran500 of (30% w/w) and 60µL BHT (25mg/mL)

The partitioning of TNB in each type of PEG (freeze dried PEG alone, Freeze dried PEG with MPM, with MPM + BHT, with BHT + Dextran) was performed and the reaction was monitored for the effectiveness of lyophilised PEG with and without additives to control the TNB oxidation by scanning spectrophotometry over a time course of 3 hours with a final point at 18 hours.

The method outlined above was used to study the effectiveness of freeze drying in removing contaminants and the mixtures of 50/50 PEG1000/1400 treated with antioxidants to inhibit or reduce oxidative effects. By spectroscopy the loss of TNB was calculated for each solution and used to assess the effectiveness of each treatment regime.

The amount of TNB in each system was calculated from its extinction coefficient and then the amount of missing TNB was computed by the difference in the amount of TNB in the single phase (1mM) compared to the amount found in the PEG solutions. The loss or reduction in TNB was then compared to each other to examine the effect of freeze drying and the stabilizers on the method. The effect of freeze drying PEG combined with the addition of antioxidants and Dextran only showed limited effectiveness in reducing the oxidative properties of PEG as judged by the amount of missing TNB in each system (see Table 75), thus this approach could have only limited utility since the chain scission of PEG is slow but continuous and the PEG will over time continue to degrade.

Table 75- Comparison of the amount of missing TNB in a PEG rich phase solution containing 1mM TNB in the presence of different stabilisers of the lyophilised PEG solution.

Time (min)	missing TNB(mM) in Blank Freeze dried PEG	missing TNB(mM) in Freeze dried PEG + MPM	missing TNB(mM) in Freeze dried PEG +BHT+ MPM	missing TNB (mM) in Freeze dried PEG + BHT+Dextran
60	0.32	0.29	0.26	0.27
90	0.35	0.29	0.26	0.28
120	0.36	0.29	0.27	0.29
150	0.37	0.30	0.28	0.29
180	-	-	0.30	0.300
1080	0.45	0.35	-	-
1260	-	-	0.44	0.34

Low molecular weight PEG seems to possess considerable oxidative power often exceeding the ability to control this by addition of antioxidant and PEG degradation seems difficult to prevent even in the presence of stabilisers. The repeated removal of the contaminants could result in change in the physico-chemical properties of the PEG

which consequently will affect the apparent molecular weight and other physical properties.

A further attempt was made to overcome these problems by returning to the PEG3350 - Dextran500 system since the presence of Dextran had shown some utility in controlling the loss of TNB (Table 75). A single phase mixture was prepared by hydrolysis of Ellman's reagent (168µL Ellman's 4mg/mL) in (2632µL KOH 50mM) and the ATPS was prepared using PEG3350 -Dextran500 system following the experimental procedure in paragraph (D) section 2.5.1.3. The analysis of the upper and lower phases showed a stable peak for TNB at 412nm (see *Figure 108*). The result was much better than the previous system (50/50 PEG1000/PEG1400 - $K_2HPO_{4)}$ and showed an improvement in the mass balance, It is possible that the increasing the molecular weight of PEG and using a polymer/polymer system could be more stable and the degradation of long polyether chains much slower than shorter chains. The reason may be due to the physico-chemical state of the high molecular weight PEG3350 which is normally more crystalline and not liquid or waxy compared to lower molecular weight of PEG thus the mobility of reactive oxygen species if present may be much reduced and could perhaps be further reduced when used in combination with Dextran.
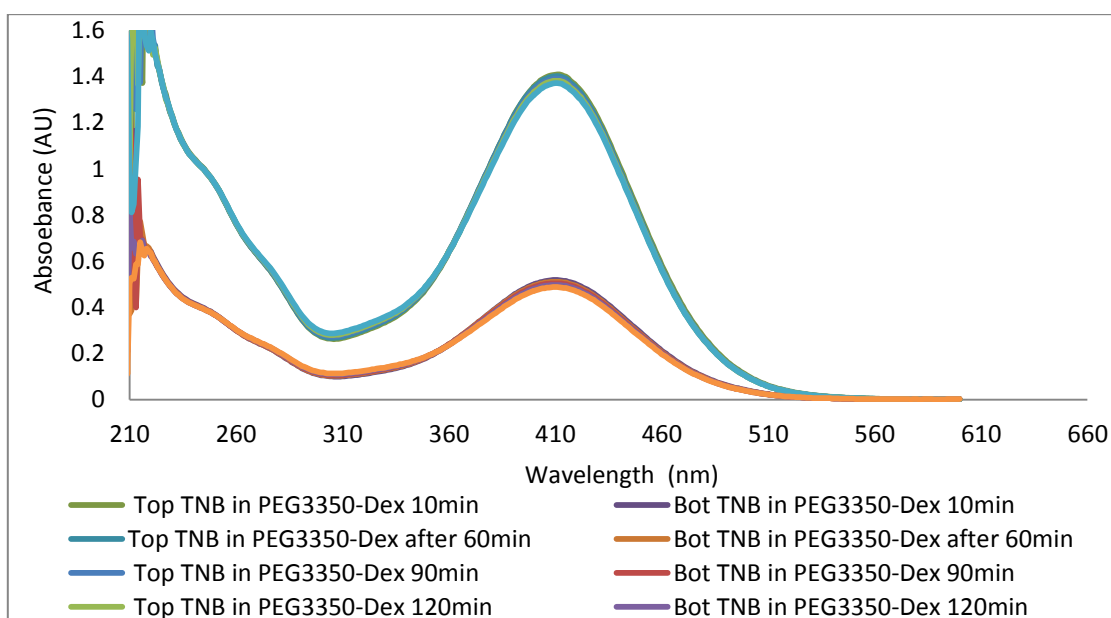
Figure 108- UV/Vis spectra at 412nm for the partitioning of TNB in a PEG3350 -Dextran500 system (the TLL composition was 8.4% w/w PEG3350, 8.4 % w/w Dextran500) over a time course of 150min.

7.5 Development of a partitioning assay to distinguish and quantify protein free thiols and total free thiols in the presence of low molecular weight (LMW) free thiols.

Since the PEG3350 -Dextran500 system has been shown to be reasonably safe to use in this application in terms of the presence of unwanted oxidative reactions a partitioning experiment using protein samples was performed. The preparation of the samples was prepared exactly as in the previously reported experiment following Table 17. N-rHSA protein was used and in order to examine different amounts of TNB, three different solutions varying in thiol content were prepared. A previous experiment (Figure 86) showed that the albumin sourced from Novozymes (N-rHSA) had high free thiol content and the commercial bovine serum albumin had the lowest content thus an albumin sample may be constructed which will show an intermediate free-thiol content by mixing each in suitable proportions for example a 50:50 mixture

An experiment was designed to examine the reaction of DTNB with albumin samples having different amounts of free-thiol and to study the partitioning of the reaction products following the reaction. The reaction was conducted using different molar ratios of DTNB: protein and samples were prepared following the protocol of Table 68 for the samples 4, 5 and 6 shown in that table.

The amount of TNB determined by spectroscopy in the single phase reaction mixture and following partition in the system (PEG3350 -Dextran500) gave results which showed close agreement in terms of closing the mass balance. The numerical methods were used to calculate the concentration of protein, DTNB and TNB in the samples then the partition coefficient of the protein DTNB and TNB were calculated by the ratio of the upper phase concentration over the lower phase concentration. ΔK_{324nm} (which is the difference between the partitioning of DTNB before and after reaction with protein) in the N-rHSA sample was the highest value indicating greater consumption of DTNB due to its higher content of free thiol (see Figure 109). BSA consumed the lowest amount of DTNB and thus ΔK_{324nm} was lower. This experiment confirmed that the thiol content of the protein had an effect on ΔK_{324nm} and suggested that it might be possible to employ it to calculate the free thiol content.

Also the experiment gave an indication that the using of the molar ratio 2:1 was the more sensitive to the calculation of ΔK_{324nm} (see Figure 109) and that because it reflects

the change in DTNB concentration due to reaction with the protein thiol while the ratio 8:1 mostly represented the free un-reacted DTNB in the solution and not the TNB bound to protein as a mixed disulphide.
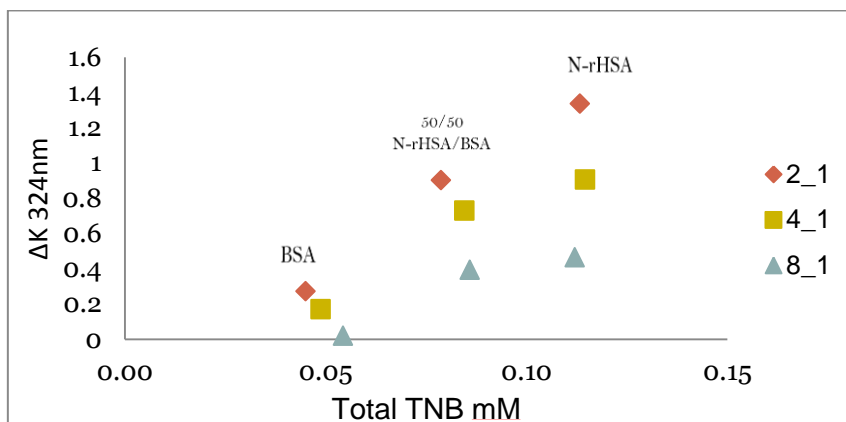
Figure 109- Partitioning of DTNB in a PEG3350 -Dextran500 system (the TLL composition was 8.4% w/w PEG3350, 8.4 % w/w Dextran500) showing the relation between ΔK324 vs the total TNB concentration following reaction of protein mixtures having different thiol content with Ellman's reagent at a different molar ratios of Ellman's : protein where 2:1 ratio consists of 0.150mM protein and 0.30mM Ellman's reagent, 4:1 ratio consists of 0.150mM protein and 0.60mM Ellman's reagent and 8:1 ratio consists of 0.150mM protein and 1.2mM Ellman's reagent.

Free thiol in protein samples could be calculated simply from a single phase reaction with Ellman's reagent, but one of the challenges set in chapters six & seven was to measure the degree of conjugation of protein by ATPS as an alternative method. Many studies have shown successful modification of protein thiols using some of the labels that have been used in the chapter six because they were interesting in the derivative product only. Here, the study sought the modification and calculation of the free thiol content without any prior purification process of the derivatives by the application of a phase partitioning method.

The final experiment reported above found a relationship between the amount of free thiol in the protein and ΔK for the bound TNB as the mixed dsulphide. This raises some important practical questions; in a real blood sample non-protein thiols such as glutathione (GSH) or free cysteine residues will be present as well as protein free thiols present on the albumin. In this case both the non-protein thiol and protein thiol will react with DTNB, and thus the TNB product will be produced as a result of reaction with total free thiols and not just the free thiols associated with the albumin alone. Approximately

two-thirds of serum albumin contains the thiol group of Cys-34 in the reduced form, which correspond to about 80 % of all serum thiol groups also corresponds to more than 50 % of all serum proteins (98).

Analysis by HPLC could provide information about the total amount of mixed-disulphide from the non-protein thiol (GSH-TNB) and protein thiol (Pro-TNB). The important issue here is to distinguish the mixed disulphide which is specific to protein from the other mixed disulphides (GSH-TNB) which might be present in the sample.

From the single phase reaction experiments the amount of free thiol content of the protein affects the amount of protein disulphides produced and the cleavage of DTNB which in turn may lead to ΔK_{324nm} being different. ΔK_{324nm} is the difference in K_{324nm} in the absence of protein free thiols and in the presence of protein free thiols. In addition ΔK_{324nm} is proportional to the total free thiol in the sample.

 ΔK_{324nm} will be determined by the total free thiols, including LMW free thiols and protein free thiols and so it was necessary to understand how the source of the free thiol affected ΔK_{324nm}.

Thus an experiment was designed consisting of protein samples having different free thiol contents combined with different levels of addition of cysteine considered as a representative LMW free thiol. The experiment thus examines the relationship between different amounts of protein free thiol and total free thiol on ΔK_{324nm}.

Three different sets having 3 levels of cysteine addition containing 5 different protein free thiol contents were prepared following Table 76. In addition a standard series of cysteine was prepared as shown in Table 77 and each series was reacted with DTNB following the single phase method as shown in the tables.

 All samples were subsequently partitioned in a PEG3350 -Dextran500 system following the experimental procedure in paragraph (D) section 2.5.1.3. For the single phase reaction all samples were diluted 5 fold and the spectrophotometry was used to measure the absorbance at the target wavelengths of 280, 324 and 412nm. The numerical method previously outlined was used to calculate the concentration of the protein, Ellman's reagent and TNB in the samples.

Table 76- The compositions of the reaction mixture samples of DTNB containing protein differing in free thiol content prepared from mixtures of N-rHSA and BSA; set 1 represents samples containing different protein mixtures and DTNB without added cysteine, set 2 represents samples containing different protein mixtures, DTNB but with the addition of 0.02mM Cysteine while set 3 represents samples containing different protein mixtures, DTNB with 0.05mM Cysteine.

Set 1	Proteins +DTNB				
	Novo (µL) (50mg/mL)	BSA (µL) (50mg/mL)	DTNB(µL) (4mg/mL)	(0.5mg/mL) Cys. (µL)	buffer (mL)
N-rHSA	280	0	38.5	0	2481.5
BSA	0	280			
50 N-rHSA /50 BSA	140	140			
75 N-rHSA /25 BSA	210	70			
25 N-rHSA /75 BSA	70	210			
Blank Ellmans	0	0	38.5		2761.5

Set 2	Proteins +DTNB+ 0.02mMCys				
	Novo (µL) (50mg/mL)	BSA (µL) (50mg/mL)	DTNB(µL) (4mg/mL)	(0.5mg/mL) Cys. (µL)	buffer (mL)
N-rHSA	280	0	38.5	14.5	2467
BSA	0	280			
50 N-rHSA /50 BSA	140	140			
75 N-rHSA /25 BSA	210	70			
25 N-rHSA /75 BSA	70	210			

Set 3	Proteins +DTNB+ 0.05mMCys				
	Novo (µL) (50mg/mL)	BSA (µL) (50mg/mL)	DTNB(µL) (4mg/mL)	(0.5mg/mL) Cys.(µL)	buffer (mL)
N-rHSA	280	0	38.5	34	2447.5
BSA	0	280			
50 N-rHSA /50 BSA	140	140			
75 N-rHSA /25 BSA	210	70			
25 N-rHSA /75 BSA	70	210			

Table 77- The compositions of the reaction mixture samples of DTNB and Cysteine.

Standard reaction mixture of cysteine and DTNB		
Ellman's μL (4mg/mL)	Cys μL (0.5mg/mL)	Buffer μL
38.5	14.5	2747
	34	2727.58
	56	2705.50
	84	2677.50

The reaction mixtures containing only protein and DTNB (set 1) were used to calculate the percent of free thiol in each case using the equation:

$$\% \textbf{ Thiol} = \frac{\textbf{mM of TNB}}{\textbf{mM of protein}} * \textbf{100}\% \qquad \text{Equ. 38}$$

Where mMoles of protein indicates the nominal amount added. Also the theoretical amount of total free thiol was calculated as

$$\textbf{Thiol mM} = \textbf{protein mM} * \% \textbf{ Thiol} \qquad \text{Equ. 39}$$

Calculations of the experimental total free thiol in each sample were estimated from the amount of TNB released as measured by absorbance at 412nm in each case. The partition coefficient of the free DTNB was calculated by the ratio of the upper phase concentration over the lower phase concentration. In addition, the ΔK_{324nm} was calculated from the difference of K_{324nm} for standard DTNB and K_{324nm} for the sample after reaction.

Numerical methods were used to calculate the protein free thiol and cysteine free thiol in each mixture from spectrophotometric measurements of DTNB partitioning. For each set of samples, a plot of ΔK_{324nm} vs total free thiol estimated from the single phase reaction was constructed and a linear regression ΔK_{324nm} vs total free thiol was computed. The slope of the regression was assumed to describe the relation of ΔK_{324nm} to the concentration of free thiol in the sample as shown in Figure 110.

The average slope of the three sets of regressions was calculated. From this limited data it is not absolutely clear that (a) the slope of this regression is strictly linear and (b)

that the slopes are truly invariant. In the absence of clear evidence either way as a "first approximation" or as a simplifying assumption the slopes of these regressions were treated as linear and invariant.

Each protein series is distinguished by a discrete regression with slopes of x y z and each slope is shifted right depending on the amount of cysteine added. The regression of free cysteine is quite distinct having a slop of z. In addition the slopes of the protein samples regressions intersect the cysteine regression at a characteristic value apparently the cysteine addition. Each of these slopes is characterised by a line having the simple relationship Y=mX+c, thus for any point in the ΔK_{324nm} vs total thiol graphic space, it seems to be possible to distinguish the amount of protein free thiol and cysteine free thiol.
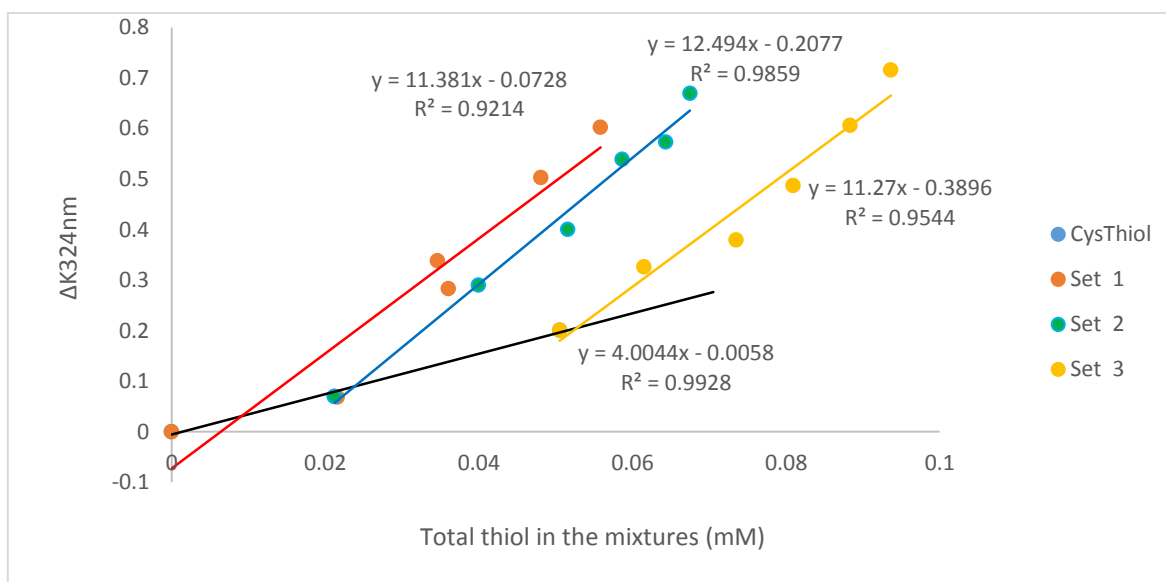
Figure 110- ΔK_{324nm} vs total thiol content for five different protein mixtures having three levels of cysteine addition (0, 0.02 and 0.05mM) also showing the ΔK_{324nm} for simple serial additions of cysteine. ΔK_{324nm} for Ellman's reagent was calculated after partitioning in a PEG3350 - Dextran500 system (the TLL composition was 8.4% w/w PEG3350, 8.4 % w/w Dextran500)

Taking any point representing a discrete protein cysteine mixture the intercept of the average slope through that point is given by the following equation

$$Cp = Yp - m.Xp \qquad \text{Equ. 40}$$

Where Cp is the constant of the regression (intercept), m is the average slope; Xp & Yp are the total free thiol and ΔK324nm respectively. A pair of equations represents the cysteine and protein regressions which can be solved by numerical methods to yield the

intercept of the average slope applied to each point with the cysteine regression yielding a unique value representing the cysteine content of the sample

$$Y1 = Cp + m.X1 \qquad \text{Equ. 41}$$

$$Y1 = Ccys + mcys.X1 \qquad \text{Equ. 42}$$

Where X1 represents the amount total thiol and Y1 represents the response of ΔK_{324nm} for this amount of thiol, Ccys and mcys represent the regression data (intercept and slope for the set of data containing no cysteine). Consequently, since the amount of total free thiol is known from the single phase reaction and the simultaneous equations give the specific amount of low molecular weight thiol (from cysteine); the amount of free thiol due to the protein may be calculated from equation 43, the predictive value of this approach comparing the calculated amount of protein free thiol from partitioning to that found from the single phase reaction as shown in *Table 78* and the regression data for each set shown in Table 79.

$$\text{Protein thiol} = \text{Total free thiol} - \text{Cysteine thiol} \qquad \text{Equ. 43}$$

Table 78- Comparison of the calculated protein free thiol content derived from the ΔK_{324nm} (equations 41-43) for each point in the three sets of partitioning data (Table 76 and Figure 110) to a determination made in a single phase reaction without added cysteine.

	Protein free thiol (mM) in single phase samples	Calculated protein free thiol (mM) in set 1 Proteins +DTNB	Calculated protein free thiol (mM) in set 2 Proteins +DTNB+ 0.02mM Cys	Calculated protein free thiol (mM) in set 3 Proteins +DTNB+0.05mM Cys
N-rHSA	0.048	0.041	0.052	0.045
BSA	0.022	-0.002	0.018	0.011
50 N-rHSA /50 BSA	0.036	0.019	0.041	0.022
75 N-rHSA /25 BSA	0.056	0.05	0.041	0.033
25 N-rHSA /75 BSA	0.035	0.027	0.026	0.011
	0	0.0007	-0.0007	0.00053

Table 79- Regression data for the calculated protein free thiol content derived from the ΔK_{324nm} (equations 41-43) for each of the three sets of partitioning data (Table 78 and Figure 110) to a determination made in a single phase reaction without added cysteine.

Regression data	Set 1	Set 2	Set 3
intercept	-8.608x10^{-3}	2.052x10^{-4}	-2.693x10^{-3}
slope	0.956	0.897	0.712
R2	0.834	0.857	0.765

The regression data has shown that the amount of protein thiols could be estimated from a mixture by partitioning in ATPS. The slopes were close to one and the R^2 showed a reasonable correlation with free thiol content of the added proteins. However it could be seen that there was some error associated with individual determinations.

An argument needs to be made about the difference in the ΔK_{324nm} of the protein reaction and that of the cysteine reaction with DTNB, the rate of increase in ΔK_{324nm} with the amount of free thiol in each case is quite different. The cysteine free thiol leads to a slow increase of ΔK_{324nm} while increasing the thiol of protein leads to a greater increase of ΔK_{324nm}. The reason may be attributed to the fact that the increase in the ΔK_{324nm} does not represent the difference in the distribution of free DTNB only but also reflects the contribution of mixed disulphides which results in a difference in distribution between the phases of the mixed disulphides arising from the low molecular weight thiol (cysteine in this case) and the high molecular weight thiol (protein).

Conclusions

A notable discovery arising from the work in this chapter concerned the discovery of the oxidative power of PEG solutions during the attempts to exploit the reduction of DTNB to TNB to develop a quantitative assay for serum albumin free-thiols. This appeared to be particularly prominent in LMW PEG systems containing phase forming salts. Many recent papers and patents focus on the application of PEG/salt systems in large scale applications especially for the recovery and fractionation of proteins see for example surveys such as that conducted by Anna Glyk et al. (2015) which contain a comprehensive summary table (165).

Furthermore other studies investigating PEG/salt systems have been carried out in the context of many other applications for example in medical treatments and

bioremediation, quality control of food, paper, detergent industry and pharmaceutical products safety (166).

Other studies (28) (167) have examined PEG/salt systems with the recycling of the phase-forming components, and waste disposal cost regarding the consumption of chemicals but seem to have completely ignored the presence of contaminants in the form of auto-oxidative products in PEG.This is the more surprising because the problem has long been noted with the use of PEG as a conservation medium for ancient wooden artefacts, in the use of polysorbates as excipients and in protein crystallization (168).

Extraction by PEG/salt systems is often performed using low molecular weight of PEG; however it seems that experimentally, such systems have ability to chain scission faster than the higher molecular weight. It has been found that the oxidative power of PEG (1000, 1400) is largely uncontrollable. The process continues at a variable rate over long periods of time and it appears that the generation of the complex series of breakdown products is very difficult to control.

Evidence presented in this study suggests that Ellman's reagent and it's adduct with protein could represent an ideal technique capable of detecting small changes in the structure and to detect the presence of oxidative impurities in ATPS.

The oxidative power of PEG seems to oxidise the fully negatively charged TNB ion and it could also be involved in a competitive oxidation reaction with the thiol and Ellman's reagent. The application of several antioxidants and combinations of antioxidants seemed unable to prevent PEG oxidation either due to their low solubility in water or through having insufficient power to reduce reactive oxygen species in the presence of PEG

The present results suggest that TNB could be used for monitoring PEG oxidative ability to form Sulfenic acid under the experimental conditions used. This may have important implications in the partitioning of protein in PEG containing phase systems. TNB revealed the role of reactive oxygen species in PEG and suggested the importance of thiols as one target of oxidative attack. Whether other amino acids could also be oxidative modified seems likely from studies on polysorbates (169). Applications of ATPS containing PEG need to be carefully assessed for the effects of contaminants on the process and stocks need to be regularly monitored for aldehyde and peroxide

content to avoid unexpected and deleterious effects on assays products and recovery processes.

In terms of the initial aims and objectives of this chapter and despite the oxidative problem already highlighted, a promising method for the determination of protein free thiol in the presence of additional LMW free thiols by partitioning was discovered.

In this method the degree of conjugation with DTNB showed a correlation between the amount of free thiol and ΔK_{324nm}. It was shown that there were differences in ΔK_{324nm} for high molecular weight thiol (protein) and low molecular weight thiol (cysteine) which could be exploited in an assay to distinguish protein free thiol from cysteine free thiol.

Numerical methods were used to calculate the protein free thiol and cysteine free thiol in a mixture. The partitioning experiment represents the first step to understand how the source of the free thiol could affect the ΔK_{324nm} and the development of a working partitioning assay for the oxidative status of biological samples such as serum. Such an assay might find utility in monitoring a variety of disease processes.

Chapter 8

8   Final conclusions and future work

Final conclusions and main achievements of this work

1-   Application of the linear partition isotherm.

The application of the partitioning isotherm was examined as a tool to characterise the partition of analytes in ATPS. The experiment was valuable in confirming the linear partition isotherm in all cases. It was amenable to statistical analysis by ACNOVA and thereby revealed the difference in partition of ovalbumin with and without aggregated material.

1.1 The application of the linear partition isotherm can be recommended in all future work since little additional effort is required over running identical sample replicates and additional valuable information is obtained on the linearity of the relationship. It might be interesting to extend application of this technique to productive applications of ATPS to study the nature of the isotherm in relation to, for sample concentration, and variations in phase ratio and to consider its impact on process modelling of partitioning processes.

2-   Analysis and partitioning of ovalbumin isoforms.

Ovalbumin was selected as a model protein to begin this study since it is widely and cheaply available and consists of a number of different isoforms with differing glycosylation patterns and degrees of phosphorylation.

Dephosphorylated ovalbumin was produced enzymatically by the action of alkaline phosphatase. Methods of analysis were successfully developed based on Strong anion exchange chromatography. Dephosphorylated ovalbumin showed distinct differences in behaviour in ATPS.

De-glycosylation of ovalbumin and removal of neuraminic acid residues proved impossible to achieve using neuraminidase and Endo-glycosidase. Apparently, this was due to the inaccessibility of the linking residues to the enzymes used. It is possible this could have been achieved by alternative methods such as denaturation followed by refolding but native refolding would have been difficult to verify.

Analytical methods based on ion-exchange chromatography were developed successfully and applied to the separation of the ovalbumin isoforms after partitioning in

ATPS. In several PEG salt systems a clear difference was demonstrated between the behaviour of the protein isoforms. The detection of the modified protein isoforms was achieved by showing differences in the partition coefficient in the ATPS and confirmed by specific detection methods such as the spectrophotometry and Size exclusion chromatography. Separation of protein by ATPS according to changes in their surface properties generated very complex changes in the system and the protein such as the salting out, the mass balance, the instability and the recovery of the system. All these issues have been explored in the investigation of the partitioning of the protein before and after the modifications.

The best separation was achieved by using PEG3350-Dextran500 system which showed a significant difference in partition when comparing ALP treated (dephosphorylated) and non-treated (native) ovalbumin. This might be ascribed to the addition of inorganic salt (K_2SO_4) changing the hydrophobic character and the ionic composition of the phases. On the other hand the effect of the pH on the partitioning by altering the surface net charge of the protein resulted in an increasing difference in the behaviour of the ovalbumin isoforms. Analysis of covariance (ANCOVA) illustrated a significant different in the regression coefficients of the respective partition isotherms of native and dephosphorylated ovalbumin (p value < 0.05).

2.1 Future work on the partitioning protein isoforms. An alternative approach to the partitioning of glycoforms could be developed such as the use of Lectins or carbohydrate binders (e.g boronates). Additionally synthetic biology derived binding proteins or aptamers might be employed to influence the partitioning of protein glycoforms. A great deal of work is required before ATPS can be validated for the analysis of protein isoforms whether in bioprocessing or clinical chemistry. Perhaps a large scale separation of different isoforms could be attempted (see for example the SAX separation of ovalbumin isoforms) in order to validate a partitioning analysis. Such an approach relies on charge doifference and it seems more challenging to separate the glycoforms based on differences in their carbohydrate composition as opposed to charge differences. Recently a synthetic biology approach has been used to produce model PTMs which might be adapted to the study of their phase partitioning and analytical separation (171).

3- Robotic methods

LHSP methods for the dispensing of ATPS were successfully developed and it was shown that major determinants of successful preparation were attention to the aspiration and dispensing of the viscous solutions involved (see chapter 5).

A twostep calibration procedure was developed to control accurate targeting of the desired system composition through the optimization of the aspiration and dispensing of the phases (See chapter 5). In addition great care was required to avoid phase cross-contamination which was solved by a twostep sampling procedure (see chapter 5).

Whilst the aspiration of the system components could be accurately achieved by the LHSP an unexpected finding was the way in which the accuracy of the final system composition depended on the form of the phase diagram.

The developed LHSP methods were used to examine the partition of the model protein ovalbumin and revealed that the geometrical form of the phase diagram co-existence curve was of crucial importance since this directly affected the accuracy with which the system could be constructed in terms of TLL and MR. For systems with a very low degree of curvature, PEG -salt systems in this example, increases in bias (accuracy) are appreciable at relatively long tie line lengths (> 5% bias). Where the degree of curvature is more pronounced, PEG-Dextran systems here, closer approach to the critical point is possible without major effect on % bias (accuracy) and such a system could be dispensed with good accuracy (< 5% error) much closer to the critical point than for the PEG-salt systems. (See chapter 5)

3.1 As future work for the robotic approach much can still be done to enhance the performance and particularly the speed of delivery. In addition more could be done to extend the range of systems for which performance parameters have been determined so that the approach could be adopted for surveying a wider range of ATPS. Such procedures are inevitably time consuming to develop.

4- Protein labelling

A number of attempts to label the free-thiol of serum albumin with a wide variety of molecular probes were largely unsuccessful. Probes used were 2-methylsulfonyl-5-phenyl -1,3,4 oxidiazole (MSPO), N-pyrenylmaleimide (NPM) and Fluorescein-5-maleimide (F-5-M). Reasons for failure were; non-reactivity of the probe 2-

methylsulfonyl-5-phenyl -1,3,4 oxidiazole; insolubility of the probe N-pyrenylmaleimide (NPM); and off target reactions of the probe Fluorescein-5-maleimide (F-5-M).

Only DTNB was found to be successful in specifically labelling the serum albumin free-thiol. However, although this probe resulted in conjugation of the free thiol groups but they did not significantly influence the partitioning of the serum albumin (See chapter 6).

4.1 The use of carbonylacrylic reagents (172) might represent an alternative approach to the serum albumin labelling procedure.

5-   PEG oxidation

A significant discovery while attempting to develop a partitioning assay for protein free thiols (chapter 7) was the strong oxidative properties of PEG which was based on the failure of the DTNB free thiol assay (reduction) and on the oxidation of the reduced TNB reaction product.

In addition it seemed to be very difficult to control this oxidation using antioxidants. Use of high MW PEG combined with Dextran did seem to overcome this effect however. Nevertheless high molecular weight PEG (6000) has been noted in the literature and reported to show strong autoxidation which was sufficient to compromise the development of a clinical assay for macroprolactin (170). This is a perplexing finding the effects of which on process and analytical applications are currently difficult to assess. Monitoring of PEG chain scission or degradation products (e.g peroxide or formaldehyde) on a regular basis where PEG is used seems mandatory especially in critical applications such as bioprocessing or in the formulation of clinical products.

5.1 PEG- oxidation is quite disturbing and requires further research. In practice stocks must be monitored for autoxidation. The present results suggest that pre-prepared TNB solution (from DTNB by alkaline hydrolysis) could be used for monitoring PEG oxidative ability through the formation of the sulfenic acid derivative of TNB under the experimental conditions used. Work could be done to discover to what extent and which residues of proteins become modified and oxidised by contact with PEG. What are the implications for protein crystallography which makes extensive use of PEG for crystal growth? Reactive oxygen species are now receiving considerable attention in the formulation of therapeutic biomolecules. TNB revealed the role of reactive oxygen species in PEG here, but PEG and derivatives thereof are widely used in the preparation of biopharmaceuticals and this work highlighted the importance of thiols as

one target of oxidative attack. Whether other amino acids could also be oxidatively modified seems likely from studies on polysorbates (ref). The effect of aqueous PEG solutions on the surface chemistry and activity of model proteins could be studied in order to estimate the consequences of this autoxidation for protein integrity. Bromelain, a cysteine-protease from pineapple, has a free-thiol in the active site and thus its activity may be expected to be progressively lost under oxidising conditions. α-amylase, an enzyme which breaks down polysaccharides to yield glucose and maltose, possesses surface tryptophan residues essential for activity and oxidation of these should lead to loss of activity and alterations in UV-absorption and fluorescence.

6-   Protein thiol assay

An assay for the determination of serum albumin free thiols in the presence of LMW free thiols was developed and shown to be able to distinguish between these two forms.

6.1 The protein thiol assay requires much further work before it could be validated as a clinical assay for the oxidative state of plasma which is a feature of numerous disease conditions. The study could initially be extended to the study of model blood formulations replicating as many serum components as possible at realistic concentrations to discover the most stable and sensitive partitioning conditions. This could be followed up with a clinical study.

References

1. Walsh C. T. (2006) Posttreanslation modification of proteins: expanding nature's inventory. Roberts and Company Publisher, Colorado.

2. Karve T. M., Cheema A. K. (2011) Small changes huge impact: the role of protein posttranslational modifications in cellular homeostasis and disease. Journal of Amino Acids, 2011, Article ID 207691.

3. Jenkins N., Murphy L., Tyther R. (2008) Posttranslational modifications of recombinant proteins: significance for biopharmaceuticals. Molecular Biotechnology, 39(2), 133-118.

4. Kinoshita-Kikuta E., Kinoshita E., Koike T. (2009) Mobility shift detection of phosphorylation on large proteins using a Phos-tag SDS-PAGE gel strengthened with agarose. Proteomics, 9(16), 4098-4101.

5. Dionex Corporation (2013) Accelerated solvent extraction techniques for in-line selective removal of interferences. Application Note 210. Thermo Fisher Scientific, Sunnyvale, CA, Sunnyvale, CA.

6. Wang P. G., Giesel R.W. (1995) Phosphate-specific fluorescence labeling of pepsin by BO-IMI. Analalytical Biochemistry, 230, 329-332.

7. Wang X., Ni M., Niu C., Zhu X., Zhao T., Zhu Z., Xuan Y., Cong W. (2014) Simple detection of phosphoproteins in SDS-PAGE by quercetin. EuPA Open Proteomics, 4, 156–164.

8. Liu S. (2013) Bioprocess engineering: kinetics, biosystems, sustainability, and reactor design. Newnes, USA.

9. Nawale R. B., Mourya V. K., Bhise S. B. (2006) Non-enzymatic glycation of protein: A cause for complication in diabetes. Indian Journal of Biochemistry & Biophysics, 43, 337-344.

10. Higel F., Seide A., Sorgel F., Friess W. (2016) N-glycosylation heterogeneity and the influence on structure, function and pharmacokinetics of monoclonal antibodies and Fc fusion proteins. European Journal of Pharmaceutics and Biopharmaceutics, 100, 94-100.

11. Roth Z., Yehezkel G., Khalaila I. (2012) Identification and quantification of protein glycosylation. International Journal of Carbohydrate Chemistry, 2012, Artical ID 640923.

12. Lodish H., Berk A., Zipursky S. L., Matsudaira P., Baltimore D., Darnell J. (2000) Molecular Cell Biology. Section 3.5: Purifying, Detecting, and Characterizing Proteins 4th edition. New York: W. H. Freeman.

13. Grilo A. L., Aires-Barros M. R., Azevedo A. M. (2016) Partitioning in aqueous two-phase systems: fundamentals, applications and trends. Separation & Purification Revews, 45, 68–80.

14. Rosa P. A. J., Ferreira I. F., Azevedo A. M., Aires-Barros M. R. (2010) Aqueous two phase systems : a viable platform in the manufacturing of biopharmaceuticals. Journal of Chromatography A, 1217(16), 2296-2305.

15. Zaslavsky A., Madeira P., Breydo L., Uversky V. N., Chait A., Zaslavsky B. (2013) High throughput characterization of structural differences between closely related proteins in solution, Biochimica et Biophysica Acta - General Subjects, 1834(2), 583-592.

16. Albertsson, P.-A. (1986) Partition of cell particles and macromolecules. Separation and purification of biomolecules, cell organelles, membranes, and cells in aqueous polymer two-phase systems and their use in biochemical analysis and biotechnology, 3rd edition. Wiley-Interscience, New York.

17. Beijerinck M. W. (1896) Ueber eine Eigentümlichkeit der löslichen Stärk. Zweite Abteilung, 2, 697-699.

18. Hartman A., Johansson G., Albertsson P.-A. (1974) Partition of proteins in a three phase system. European Journal of Biochemistry, 46, 75-81.

19. Hatti-Kaul R. (2000) Methods in Biotechnology. Vol 11. Aqueous two-phase systems; methods and protocols. New Jersey, Humana Press Inc.

20. Fisher D. (1981) The separation of cells and organelles by partitioning in two-polymer aqueous phases. Biochemical Journal, 196, 1-10.

21. Kula MR, Kroner KH, Hustedt H. (1982) Purification of enzymes by liquid-liquid extraction; in: Reaction engineering. Advances in biochemical engineering/biotechnology, 24, 73-118. Springer, Berlin Heidelberg.

22. Walter H., Brooks D. E., Fisher D. (1985) Partitioning in aqueous two-phase systems: Theory, methods, uses and applications to biotechnology. Academic Press, New York.

23. Zaslavasky B.Y. (1995) Aqueous two-phase partitioning: Physical chemistry and bioanalytical applications. Marcel Dekker Inc, New York.

24. Walter H. (1977) Partition of cells in two-polymer aqueous phases: a surface affinity method for cell separation; in: Methods Cell Separation. Ed. Catsimpoolas N, 307-354. Springer, Berlin Heidelberg.

25. Albertsson P. A. (1986) Aqueous polymer-phase systems. Wiley, New York.

26. Walter H., Johansson G. (1994) Aqueous two-phase systems; in: Methods in enzymology. Academic Press, London. Vol. 228, 725 pp.

27. Hustedt H., Kroner K. H., Kula M.-R. (1985) Applications of phase partitioning in biotechnology; in: Partitioning in aqueous two-phase systems: Theory, methods, uses and applications to biotechnology, 529–587. Eds: Walter H., Brooks D. E., Fisher D. Academic Press, New York.

28. Kula M.-R., Selber K. (1999) Protein purification, aqueous liquid extraction; in: Encyclopedia of Bioprocess Technology:Fermentation, Biocatalysis, and Bioseparation, 2179–2191. John Wiley and Sons ,New York.

29. Tjerneld, F., Berner, S., Cajarville, A., Johansson, G. (1986) New aqueous two-phase system based on hydroxypropyl starch useful in enzyme purification. Enzyme and Microbial Technology, 8(7), 417-423.

30. Vernau J., Kula M.-R. (1990) Extraction of proteins from biological raw material using aqueous polyethylene glycol-citrate phase systems. Biotechnology and Applied Biochemistry, 12(4), 397-404.

31. Tjerneld, F., Persson, I., Albertsson, P.Å. and Hahn-Hägerdal, B. (1985) Enzymatic hydrolysis of cellulose in aqueous two-phase systems. I. partition of cellulases from Trichoderma reesei. Biotechnology and Bioengineering, 27(7), 1036-1043.

32. Sikdar S. K., Cole K. D., Stewart R. M., Szlag D. C., Todd P., Cabezas Jr, H. (1991) Aqueous two-phase extraction in bioseparations: an assessment. Bio/technology (Nature Publishing Company), 9(3), 252-254.

33. Dissing U., Mattiasson B. (1994) Partition of proteins in polyelectrolyte-neutral polymer aqueous two-phase systems. Bioseparation, 4(6), 335-342.

34. Planas J., Ra P., Tjerneld F., Hahn-Hägerdal B. (1996) Enhanced production of lactic acid through the use of a novel aqueous two-phase system as an extractive fermentation system. Applied Microbiology and Biotechnology, 45(6), 737-743.

35. Walter H., Johansson G., Brooks D. E. (1991) Partitioning in aqueous two-phase systems: recent results. Analytical Biochemistry, 197(1), 1-18.

36. Eriksson E., Albertsson P. Å., Johansson G. (1976) Hydrophobic surface properties of erythrocytes studied by affinity partition in aqueous two-phase systems. Molecular and Cellular Biochemistry, 10(2), 123-128.

37. Mistry S.L., Kaul A., Merchuk J.C., Asenjo J.A. (1996) Mathematical modelling and computer simulation of aqueous two phase continuous protein extraction. Journal of Chromatography A. 741(2) 151-163.

38. Asenjo J.A., Andrews B.A. (2012) Aqueous two-phase systems for protein separation: phase separation and applications. Journal of Chromatography A, 1238, 1-10.

39. Zaslavsky B. Y., Massimov E. A., Miheeva L. M., Rogozhin S. V., Hasaev D.P. (1981) Doklady Acad. Nauk USSR (Rus), 261, 669.

40. Willauer H.D., Huddleston J.G., Rogers R.D. (2002) Solvent properties of aqueous biphasic systems composed of polyethylene glycol and salt characterized by the free energy of transfer of a methylene group between the phases and by a linear solvation energy relationship. Industrial & engineering chemistry research, 41(11), 2591-2601.

41. Huggins M.L., Lewis D. J., Daly W. H., Mosqueira F.G., Dunnill P., Lilly M. D. (1978) Theory of solutions of high polymers. Biotechnology and Bioengineering, 20(2), 159.

42. Mohamadi H., Omidinia E., Dinarvand R. (2007) Evaluation of recombinant phenylalanine dehydrogenase behavior in aqueous two-phase partitioning. Process Biochemistry, 42(9), 1296-1301.

43. González-González M., Mayolo-Deloisa K., Rito-Palomares M., Winkler R. (2011) Colorimetric protein quantification in aqueous two-phase systems. Process Biochemistry, 46(1), 413-417.

44. Chait A., Zaslavsky B.Y. (2006) U.S.Patent No. 0269946 A1.

45. Chait A., Zaslavsky B.Y. (2007) U.S.Patent No. 0128618 A1.

46. Chait A., Zaslavsky B.Y. (2012) U.S.Patent No. 8,099242 B2.

47. Chait A., Zaslavsky B.Y. (2011) U.S.Patent No.7,968,350 B2.

48. Chait A., Zaslavsky B.Y. (2012) U.S.Patent No. 8,211,714 B2.

49. Zaslavsky B.Y. (1998) U.S.Patent 5,734,024.

50. Chait A., Zaslavsky B.Y. (2000) U.S.Patent 6,136,960.

51. Zaslavsky B.Y., (1992) Bioanalytical applications of partitioning in aqueous polymer two-phase systems. Analitical Chemitry, 64, 765A-773A.

52. Johansson G.(1985) Partitioning of proteins; in: Partitioning in aqueous two-phase systems: Theory, methods, uses and applications to biotechnology, 161-226. Eds: Walter H., Brooks D. E., Fisher D. Academic Press, New York.

53. Walter H., Johansson G., Brooks D.E. (1991) Partitioning in aqueous two-phase systems: recent results. Analytical Biochemistry, 197(1), 1-18.

54. Chait A., Zaslavsky B.Y. (2011) U.S.Patent No. 8,041,513B2.

55. Zaslavsky B.Y. (2003) U.S.Patent 0162224A1.

56. Iqbal M., Tao Y., Xie S., Zhu Y., Chen D., Wang X., Huang L., Peng D., Sattar A., Shabbir M.A.B., Hussain H.I. (2016) Aqueous two-phase system (ATPS): an overview and advances in its applications. Biological Procedures Online, 18(1), 18.

57. Zaslavsky B.Y., Uversky V.N., Chait A. (2016) Analytical applications of partitioning in aqueous two-phase systems: Exploring protein structural changes and protein–partner interactions in vitro and in vivo by solvent interaction analysis method. Biochimica et Biophysica Acta (BBA)-Proteins and Proteomics, 1864(5), 622-644.

58. Raymond F.D., Moss D.W., Fisher D. (1993) Phase partitioning detects differences between phospholipase-released forms of alkaline phosphatase — a GPI-linked protein. Biochimica et Biophysica Acta (BBA)-General Subjects, 1156(2), 117–122.

59. Zaslavsky A., Gulyaeva N., Chait A., Zaslavsky B. (2001) A new method for analysis of components in mixture without preseparation: evaluation of the concentration ratio and protein-protein interaction. Analytical Biochemistry 296(2), 262-269.

60. Albertsson P.-A. (1983) Interaction between the biomolecules studies by phase partition. Method of Biochemical Analysis, Vol. 29, 1-24. John Wiley & Sons.Inc., New York.

61. Huntington J. A., Stein P. E. (2001) Structure and properties of ovalbumin. Journal of Chromatography B: Biomedical Sciences and Applications, 756 (1-2), 189–198.

62. Baynes J., Dominiczak M. (2004) Medical Biochemistry. 2d edition. Elsevier.

63. Kelly J. F., Locke S. J., Ramaley L., Thibault P. (1996) Development of electrophoretic conditions for the characterization of protein glycoforms by capillary electrophoresis-electrospray mass spectrometry. Journal of Chromatography A, 720, 409-427.

64. Chakel J. A., Pungor E. Jr., Hancock W. S., Swedberg S. A. (1997) Analysis of recombinant DNA-derived glycoproteins via high-performance capillary electrophoresis coupled with off-line matrix-assisted. Journal of Chromatography B: Biomedical Sciences and Applications, 689(1), 215-220.

65. Holen E., Elsayed S. (1990) Characterization of four major allergens of hen-egg white by IEF/-SDS-PAGE combined with electrophoretic transfer, International Archives of Allergy and Immunology, 91(2), 136-141.

66. Nisbet A. D., Saundry R. H., Moir A. J., Fothergill L. A., Fothergill J. E. (1981) The complete amino-acid sequence of hen ovalbumin. European Journal of Biochemistry, 115(2), 335-45.

67. Weintraub M. S., Schlamowitz M. (1970) Comparison of three avian ovalbumins: physical and chemical properties. Comparative biochemistry and physiology, 37(1), 49-58.

68. Elwood P.C., Reid W.K., Marcell P.D., Allen R. H., Kolhouse J. F. (1988) Determination of the carbohydrate composition of mammalian glycoproteins by capillary gas chromatography/mass spectrometry. Analytical biochemistry, 175(1), 202-211.

69. Henderson J. Y., Moir A. J., Fothergill L. A., Fothergill J. E. (1981) Sequences of sixteen phosphoserine peptides from ovalbumins of eight species. European Journal of Biochemistry, 114(2), 439-50.

70. Yamashita K., Tachibana Y., Hitoi A., Kobata A. (1984) Sialic acid-containing sugar chains of hen ovalbumin and ovomucoid. Carbohydrate Research, 130, 271-288.

71. Chen L. M., Yet M. G., Shao M.C. (1988) New methods for rapid separation and detection of oligosaccharides from glycoproteins. The FASEB Journal, 2(12), 2819-24.

72. Rago R.P., Ramirez-Soto D., Poretz R.D. (1992) Two-dimensional poly (acrylamide) electrophoresis of fluoresceinated glycopeptides. Resolution and structural characterization of ovalbumin glycans. Carbohydrate Research, 236, 1-8.

73. Ekman P., Jäger O. (1993) Quantification of subnanomolar amounts of phosphate bound to seryl and threonyl residues in phosphoproteines using alkaline hydroysis and malachite green. Analytical Biochemistry, 214(1), 138-141.

74. Suzuki T., Kitajima K., Emori Y., Inoue Y., Inoue S. (1997) Site-specific de-N-glycosylation of diglycosylated ovalbumin in hen oviduct by endogenous peptide: N-glycanase as a quality control system for newly synthesized proteins. Proceedings of the National Academy of Sciences, 94(12), 6244-6249.

75. Wei J., Yang L., Harrata A. K., Lee C. S. (1998) High resolution analysis of protein phosphorylation using capillary isoelectric focusing - electrospray ionization - mass spectrometry. Electrophoresis, 19(13), 2356-2360.

76. Chamow S.M., Hedrick J.L. (1988) A micromethod for the estimation of oligosaccharides containing glycosidically linked sialic acid or hexoses, or both, in glycoproteins. Carbohydrate research, 176(2), 195-203.

77. Lee Y. C., Montgomery R. (1961) The carbohydrate of ovalbumin. Archives of Biochemistry and Biophysics, 95(2), 263-270.

78. Iwase H., Kato Y., Hotta K. (1984) Comparative study of the carbohydrate chain of ovalbumin from various avian species by high pressure liquid chromatography. Comparative Biochemistry and Physiology Part B: Comparative Biochemistry, 77(4), 743-747.

79. Kato Y., Iwase H., Hotta K. (1988) Comparative study of chicken ovalbumin subfractions having different carbohydrate chain from each other by high performance anion exchange chromatography. Comparative Biochemistry and Physiology Part B: Comparative Biochemistry, 90(1), 37-39.

80. Lattova E., Perreault H., Krokhin O. (2004) Matrix-assisted laser desorption/ionization tandem mass spectrometry and post-source decay fragmentation

study of phenylhydrazones of N-linked oligosaccharides from ovalbumin. Journal of American Society for Mass Spectrometry 15, 725-735.

81. Matsuno K., Suzuki S. (2008) Simple fluorimetric method for quantification of sialic acids in glycoproteins. Analytical Biochemistry, 375, 53–59.

82. Yamamoto S., Shinohara C., Fukushima E., Kakehi K., Hayakawa T., Suzuki S. (2011) Partial-filling affinity capillary electrophoresis of glycoprotein oligosaccharides derivatized with 8-aminopyrene-1, 3, 6-trisulfonic acid. Journal of Chromatography A, 1218, 4772– 4778.

83. Matsuno K., Suzuki S. (2008) Simple fluorimetric method for quantification of sialic acids in glycoproteins. Analytical Biochemistry, 375, 53–59.

84. Burley R. W., Vadehra D. V. (1989) The avian egg: chemistry and biology. John Wiley & Sons, New York.

85. Ellmerer M., Schaupp L., Brunner G. A., Sendlhofer G., Wutte A., Wach P., Pieber T. R. (2000) Measurement of interstitial albumin in human skeletal muscle and adipose tissue by open-flow microperfusion. American Journal of Physiology-Endocrinology and Metabolism, 278(2), E352-E356.

86. Francis G. L. (2010) Albumin and mammalian cell culture: implications for biotechnology applications. Cytotechnology, 62(1), 1-16.

87. Meijer D. K., van der Sluijs P. (1989) Covelant and noncovelant binding of drugs:implications for hepatic clearnce, storage and cell-specific drug delivery. Pharmaceutical research, 6, 105-118.

88. Ishima Y., Maruyama T. (2016) Human Serum Albumin as Carrier in Drug Delivery Systems, Yakugaku zasshi: Journal of the Pharmaceutical Society of Japan, 136(1), 39-47.

89. Masuoka J., Saltman P. (1994) Zinc(II) and copper (II) binding to serum albumin. Journal of Biological Chemistry, 269, 25557-25561.

90. Takikawa H., Sugiyama Y., Hanano M., Kurita M., Yoshida H., Sugimoto, T. (1987) A novel binding site for bile acids on human serum albumin. Biochimica et Biophysica Acta (BBA)-General Subjects, 926(2),145-153.

91. Kosaka N., Ogawa M., Choyke P. L., Karassina N., Corona C., McDougall M., Lynch D. T., Hoyt C. C., Levenson R. M., Los, G. V., Kobayashi H. (2009) In vivo stable tumour-specific painting in various colours using dehalogenase-based protein-tag fluorescent ligands. Bioconjugate chemistry, 20(7), 1367-1374.

92. Atkinson S. F., Bettinger T., Seymour L. W., Behr J. P., Ward C. M. (2001) Conjugation of folate via gelonin carbohydrate residues retains ribosomal-inactivating properties of the toxin and permits targeting to folate receptor positive cells. Journal of Biological Chemistry, 276(30), 27930-27935.

93. Meng W., Guo X., Qin M., Pan H., Cao Y., Wang W. (2012) Mechanistic Insights into the Stabilization of srcSH3 by PEGylation. Langmuir, 28(46), 16133−16140.

94. Rodríguez-Martínez J. A., Solá R. J., Castillo B., Cintrón- Colón H. R., Rivera-Rivera I., Barletta G., Griebenow K. (2008) Stabilization of α-Chymotrypsin upon PEGylation Correlates with Reduced Structural Dynamics. Biotechnology and Bioengineering, 101(6), 1142-1149.

95. Mehtala J.G., Kulczar C., Lavan M., Knipp G., Wei A. (2015) Cys34-PEGylated human serum albumin for drug binding and delivery. Bioconjugate chemistry, 26(5), 941-949.

96. Ghuman J., Zunszain P. A., Petitpas I., Bhattacharya A. A., Otagiri M., Curry S. (2005) Structural basic of the drug-binding specific of human serum albumin. Journal of Molecular Biology, 353, 38-52.

97. Willcox J. K., Ash S. L., Catignani G. L. (2004) Antioxidants and Prevention of Chronic Disease. Critical reviews in food science and nutrition, 44(4), 275-95.

98. Bracht A., Silveira S.S., Castro-Ghizoni C.V., Sá-Nakanishi A.B., Oliveira M.R.N., Bersani-Amado C.A., Peralta R.M., Comar J.F. (2016) Oxidative changes in the blood and serum albumin differentiate rats with monoarthritis and polyarthritis. SpringerPlus, 5(1), 1.

99. Merchuk J.C., Andrews B.A., Asenjo J.A. (1998) Aqueous two-phase systems for protein separation: Studies on phase inversion. Journal of Chromatography B: Biomedical Sciences and Applications, 711(1), 285–293.

100. MathCad 15.0, PTC Inc.2013.

101. Worthington K., and Worthington V. (2011). Worthington Biochemical Corporation. Worthington Enzyme Manual. Date of access 29/01/2016 (http://www.worthington-biochem.com/OA/default.html).

102. Smith P.K., Krohn R.I., Hermanson G.T., Mallia A.K., Gartner F.H., Provenzano M.D., Fujimoto E.K., Goeke N.M., Olson B.J., Klenk D.C. (1985) Measurement of protein using bicinchoninic acid. Analalytical Biochemistry, 150, 76-85.

103. Wiechelman K., Braun R., Fitzpatrick J. (1988) Investigation of the bicinchoninic acid protein assay: Identification of the groups responsible for color formation. Analalytical Biochemistry, 175, 231-237.

104. BCA Protein assay kit, Pierce Biotecknology, Inc., 10/2003 USA.

105. Al-Rimawi F. (2014) Development and Validation of HPLC-UV Method for Determination of Bovine Serum Albumin and Myoglobin Proteins. International Research Journal of Pure & Applied Chemistry 4(6): 585-593.

106. Han J.C., Han G.Y. (1994) A procedure for quantitative determination of Tris(2-Carboxyethyl)phosphine, an odorless reducing agent more stable and effective than Dithiothreitol. Analytical Biochemistry, 220(1), 5-10.

107. Sabnis R. W. (2015) Handbook of Fluorescent Dyes and Probes. John Wiley & Sons, New York.

108. Ozlem B. A. (2013) Ion-Exchange chromatography and its applications; in Column Chromatography. Eds. Martin D. F., Martin B. B., InTech.

109. Tomimatsu Y. (1965) A light-scattering study of the aggregation of ovalbumin near its isoelectric pH. Biochimica et Biophysica Acta (BBA) - Biophysics including Photosynthesis, 94(2), 525–534.

110. Doebler R., Başaran N., Goldston H., Holloway P. W. (1999) Effect of protein aggregation in the aqueous phase on the binding of membrane proteins to membranes. Biophysical Journal, 76(2), 928–936.

111. Berkowitz S. A., Engen J. R., Mazzeo J. R., Jones G. B. (2012) Analytical tools for characterizing biopharmaceuticals and the implications for biosimilars, Nature Reviews Drug Discovery, 11(7), 527-540.

112. Bensch M., Selbach B., Hubbuck J. (2007) High throiughput secreening techniques in downstream processing: preparation, characterization and optimization of aqueous two phase systems. Chemical Engineering Science, 62, 2011-2021.

113. Yamashita K., Tachibana Y., Kobata A. (1978) The structure of the galactose-containing sugar chains of ovalbumin. Journal of Biological Chemistry, 253, 3862-3869.

114. Harvey D. J., Wing D. R., Küster B., Wilson I. B. H. (2000) Composition of N-linked carbohydrates from ovalbumin and co-purified glycoproteins. Journal of the American Society for Mass Spectrometry, 11(6), 564-571.

115. Pezennec S., Gauthier F., Alonso C., Graner F., Croguennec T., Brule G., Renault A. (2000) The protein net electric charge determines the surface rheological properties of ovalbumin adsorbed at the air-water interface. Food Hydrocolloids, 14(5), 463-47.

116. Landers J.P.; Oda R.P., Madden B.J., Spelsberg, T.C. (1992) High Performance Capillary Electrophoresis of Glycoproteins: The Use of Modifiers of Electroosmotic Flow for Analysis of Microheterogeneity. Anal. Bioch., 205, 115–124.

117. Stein, P.E., Leslie, A.G., Finch, J.T., Carrell, R.W. Crystal structure of uncleaved ovalbumin at 1.95 A resolution, J.Mol.Biol. 221(1991): 941-959.

118. U.S. Public Health Service (Nos. GM-10374 and 1-K3-GM32, 160).

119. Kobata A. (2013) Exo- and endoglycosidases revisited. Proceedings of the Japan Academy, Series B, 89(3), 97-117.

120. Larsen M.R., Sørensen G.L., Fey S.J., Larsen P.M., Roepstorff P. (2001) Phospho-proteomics: evaluation of the use of enzymatic de-phosphorylation and differential mass spectrometric peptide mass mapping for site specific phosphorylation assignment in proteins separated by gel electrophoresis. Proteomics, 1(2), 223–238.

121. Dionex Corporation (2010) Background Currents and Baseline Noise. Application Note 99. Thermo Fisher Scientific, Sunnyvale, CA, Sunnyvale, CA.

122. Krishna R. G., Wold, F. (1993) Post- translational modification of proteins. Advances in Enzymology and Related Areas of Molecular Biology, 67, 265-298.

123. Berman H.M., Westbrook J., Feng Z., Gilliland G., Bhat T.N., Weissig H., Shindyalov I.N., Bourne P.E. (2000) The Protein Data Bank. Nucleic Acids Research, 28(1), 235-242.

124. Goja A. M., Yang H., Cui M., Li C. (2014) Aqueous two-phase extraction advances for bioseparation. Journal of Bioprocessing & Biotechniques, 2, 1.

125. Wiendahl M., Volker C., Husemann I., Krarup J., Staby A., Scholl S., Hubbuch J. (2009) A novel method to evaluate protein solubility using a high throughput screening approach, Chemical Engineering Science, 64, 3778 – 3788.

126. Albert K. J., Bradshaw J. T.(2007) Importance of Integrating a volume verification method for liquid handlers: Applications in learning performance behavior. Journal of the Association for Laboratory Automation, 12(3), 172-180.

127. Curtis R. H., Rundell A. E. Artel, Inc. (1993) Reagent system for calibration of pipettes and other volumetric measuring devices. Patent US 5, 492,673.

128. McGown E. L., Schroeder K., Hafeman D. G. (1998) Verification of multichannel liquid dispenser performance in the 4e30 mL range by using optical pathlength measurements in microplates. Clinical Chemistry, 44, 2206-2208.

129. McGown E. L., Hafeman, D. G. (1998) Multi-channel pipettor performance verified by measuring pathlength of reagent dispersed into a microplate. Analytical Biochemistry, 258, 155-157.

130. Taylor P.B., Ashman S., Baddeley S.M., Bartram S.L., Battle C.D., Bond B.C., Clements Y.M., Gaul N.J., McAllister W.E., Mostacero J.A., Ramon, F. (2002) A standard operating procedure for assessing liquid handler performance in high-throughput screening. Journal of Biomolecular Screening, 7(6), 554-569.

131. Croarkin C., Guthrie W. (2013) NIST/SEMATECH e-Handbook of Statistical Methods. URL Available at: http://www.itl.nist.gov/div898/handbook/, 2013.

132. Chai S.C., Goktug A.N., Cui J., Low J., Chen T. (2013). Practical considerations of liquid handling devices in drug discovery; in: Drug Discovery., 177-200. Ed. El-Shemy H.A. INTECH Open Access Publisher.

133. Hong P., Koza S., Bouvier E.S. (2012) A review size exclusion chromatography for the analysis of protein biotherapeutics and their aggregates. Journal of Liquid Chromatography & Related Technologies, 35(20), 2923–2950.

134. Kline M. (1998) Calculus: an intuitive and physical approach, 457-461. Courier Corporation, Dover.

135. Walash M.I., Metwally M.E.-S., El-Brashy A.M., Abdelal A.A. (2003) Kinetic spectrophotometric determination of some sulfur containing compounds in pharmaceutical preparations and human serum. Il Farmaco, 58(12), 1325-1332.

136. Desai, N. (2007) Nab Technology: A Drug Delivery Platform Utilizing Endothelial gp60 Receptor-Based Transport and Tumour-Derived SPARC for Targeting; in Drug Delivery Report, 16th ed., PharmaVentures, Ltd.: Oxford and Winter 2007/2008, pp 37−41.

137. Sulkowska A. (2002) Interaction of drugswith bovin and human serume albumin. Journal of Molecular structure, 614, 227-232.

138. Kim Y., Ho S. O., Gassman N. R., Korlann Y., Landorf E. V., Collart F. R., Weiss S. (2008) Efficient Site-Specific Labeling of Proteins via Cysteines. Bioconjugate Chemistry, 19(3), 786–791.

139. Toda N., Asano S., Barbas C. F. (2013) Rapid, stable, chemoselective labeling of thiols with julia–kocien´ skilike reagents: a serum-stable alternative to maleimide-based protein conjugation. Angewandte Chemie International Edition, 52, 12592 –12596.

140. Smyth D. G. (1964) Reaction of N-Ethylmaleimide with peptides and amino acids. Biochemical Journal, 91(3), 589-595.

141. Nelson D. L., Cox M. M. (2000) Lehninger principles of biochemistry. 3rd Ed. Worth Publishing, New York.

142. Riordan J.F., Vallee B. L. (1972) Reactions with N-Ethylmaleimide and p-Mercuribenzoate. Methods in Enzymology, 25, 449-456.

143. Gregory J.D. (1955) The Stability of N-Ethylmaleimide and its reaction with sulfhydryl groups. Journal of the American Chemical Society, 77(14), 3922–3923.

144. Getz E.B., Xiao M., Chakrabarty T., Cooke R., Selvin P.R. (1999) A comparison between the sulfhydryl reductants tris(2-carboxyethy)phosphine and dithiothreitol for use in protein biochemistry. Analytical Biochemistry, 273, 73-80.

145. Ellman G.L. (1958) A colorimetric method for determining low concentrations of mercaptans. Archives of Biochemistry and Biophysics, 74, 443-450.

146. Riddles P. W., Blakeley R. L., Zerner B. (1983) Reassessment of Ellman's reagent. Methods in Enzymology, 91, 49-60.

147. Riddles P.W., Blakeley R.L., Zerner B. (1979) Ellman's reagent: 5, 5´-dithiobis(2-nitrobenzoic acid) - a re-examination. Analytical Biochemistry, 94, 75-81.

148. Riener C. K., Kada G., Gruber H. J. (2002) Quick measurement of protein sulfhydryls with Ellman's reagent and with 4,4'-dithiodipyridine. Analytical and Bioanalytical Chemistry, 373(4-5), 266-276.

149. Huddleston J.G. (1995) Polymer- salt aqueous two phase systems in biochemical recovery. PhD thesis, University of Birmingham, UK.

150. Niwayama S., Kassar A.S., Zhao T., Sutton R.B., Altenberg G.A. (2011) A pyrene maleimide with a flexible linker for sampling of longer inter-thiol distances by excimer formation. PLoS one, 6(10), e26691.

151. Cheng X., Hochlowski J., Tang H., Hepp D., Beckner C., Kantor S., Schmitt R. (2003) Studies on repository compound stability in DMSO under various conditions. Journal of Biomolecular Screening, 8(3), 292-304.

152. Alves N., Bai G., Bastos M. (2006) Enthalpies of solution of paraceteamol and sodium diclofenac in phosphate buffer and DMSO at 298.15K. ThermoChimica Acta 441,16-19.

153. Tong C. C. (2003) Characterization of cysteine -34 in serum albumin. PhD thesis, The Ohio State University, USA.

154. Peterson J.R., Smith T.A., Thordarson P. (2010) Synthesis and room temperture photo-induced electron transfer in biologically active bis(terpyridine) ruthenium (II)-cytochrome c biocinjugates and the effect of solvents on the bioconjugation of cytochrome c. Organic and Biomolecular Chemistry, 8, 151-162.

155. Sanz R., Aguado R., Pedrosa M. R., Arnáiz F. (2002) Simple and selective oxidation of thiols to disulfides with dimethylsulfoxide catalyzed by dichlorodioxomolybdenum(vi). Synthesis, 2002, 856-858.

156. Thermo scientific (2007) Fluorescein-5-maleimide. Instruction No.46130.

157. Albertsson P.-A., Cajarvill A., Brooks D. E., Tjerneld F. (1987) Partition of proteins in aqueous polymer two-phase systems and the effect of molecular weight of the polymer. Biochimica Et Biophysica Acta (BBA)-General Subjects, 926, 87-93.

158. Hawkins C. L., Morgan P. E., Davies M. J. (2009) Quantification of protein modefication by oxidants. Free Radical Biology & Medicine, 46, 965-988.

159. Brocklehurst K., Little G. (1973) Reactions of papain and of low-molecular-weight thiols with some aromatic disulphides. 2, 2′-Dipyridyl disulphide as a convenient active-site titrant for papain even in the presence of other thiols. Biochemical Journal, 133, 67-80.

160. Landion L. M., Mall C. B., Nicklay J. J., Dutcher S. K., Moynihan K. L. (2008) Oxidation of 5-thio-2-nitrobenzoic acid by the biologically relevent oxidanys peroxynitrite anion, hydrogen peroxide and hypochlorous acid. Nitric Oxide. 18, 11-18.

161. Personal Communication (2016), Sigma-Aldrich European Technical Services and Fisher Scientific UK Product Support.

162. Han S., Kim C., Kwon D. (1997) Thermal/Oxidative degredation and stabilization of polyethylene glycol. Polymer, 38(2), 317-323.

163. Puz M. J., Johnson B. A., Murphy B. J. (2005) Use of the antioxidant BHT in asymmetric membrane tablet coatings to stabilize the core to the acid catalyzed peroxide oxidation of a thioether drug. Pharmaceutical Development and Technology, 1, 115–125.

164. Subroto E., Manurung R., Heeres H. J., Broekhuis A. A. (2013) Screening of antioxident as stabiliser for Jatropha curcas L. oil. European Journal of Lipid Science and Technology, 115, 909-920.

165. Glyk A., Scheper T., Beutel S. (2015) PEG–salt aqueous two-phase systems: an attractive and versatile liquid–liquid extraction technology for the downstream processing of proteins and enzymes. Applied Microbiology and Biotechnology. 99, 6599-6616.

166. Benavides J., Rito-Palomares M., Asenjo J. A. (2011) Aqueous two-phase systems; in: Comprehensive biotechnology. Principles and practices in industry, agriculture, medicine and the environment. Ed. Moo-Young M, 2nd edn. Academic Press, Burlington, pp 697–713.

167. Rito-Palomares M., Lyddiatt A. (2000) Practical implementation of aqueous two-phase processes for protein recovery from yeast. Journal of Chemical Technology and Biotechnology, 75(7), 632–638.

168. Almkvist G. (2008) The Chemistry of the Vasa - iron, acids and degradation. Doctoral Thesis, Swedish University of Agricultural Sciences, Uppsala, Sweden.

169. Kumar V., Kalonia D. S. (2006) Removal of peroxides in polyethylene glycols by vacuum drying: implications in the stability of biotech and pharmaceutical formulations. AAPS PharmSciTech, 7(3), Article 62.

170. Ellis G. (2006) Degradation of crystalline polyethylene glycol 6000 and its effect on assays for macroprolactin and other analytes. Clinical Biochemistry, 39(10), 1035-40.

171. van Kasteren S. I., Kramer H. B., Jensen H.H., Campbell S. J., Kirkpatrick J., Oldham N. J., Anthony D. C., Davis B. G. (2007) Expanding the diversity of chemical protein modification allows post-translational mimicry. Nature, 446, 1105-1109.

172. Bernardim B., Cal P. M.S.D., Matos M. J., Oliveira B. L., Martı́nez-Sa´ez N., Albuquerque I. S., Perkins E., Corzana F., Burtoloso A. C. B., Jime´nez-Ose´s G., Bernardes G. J. L. (2016) Stoichiometric and irreversible cysteine-selective protein modification using carbonylacrylic reagents. Nature Communications, 7, 13128.

APPENDIX - A. The performance files for dispensing each component and step of ATPS after optimization the robotic system.

| PEG8000 performance file (slope :1.041   offset :-3.943) | | | | | | | | | | |
Volume (µL)	Asp. speed (µL/s)	Asp. Delay msec	Dis. speed (µL/s)	Dis. Delay msec	Waste volume µL	Waste volume% (%of Asp.)	Blowout Volume µL	Blowout Delay msec	Transport Air Gap µL	System AirGap µL
5	1.7	300	500	300	5	100	0	0	3	8
30	2.5	300	500	300	15	50	0	0	3	8
50	5	300	400	300	25	50	0	0	3	8
100	8	300	400	300	30	30	0	0	3	8
250	10	300	300	300	75	30	0	0	3	8
400	10	300	300	300	120	30	0	0	3	8
900	10	300	300	300	270	30	0	0	3	8
2000	10	300	300	300	600	30	0	0	3	8

Dextran performance file (slope :1.0731 offset :5.3867)										
Volume (µL)	Asp. speed (µL/s)	Asp. Delay msec	Dis. speed (µL/s)	Dis. Delay msec	Waste volume µL	Waste volume% (%of Asp.)	Blowout Volume µL	Blowout Delay msec	Transport Air Gap µL	System AirGap µL
5	2.5	800	125	800	5	100	0	0	8	10
30	2.5	800	125	800	15	50	0	0	8	10
50	2.5	800	100	800	25	50	0	0	8	10
100	5	800	100	800	50	50	0	0	8	10
250	10	800	50	800	100	40	0	0	8	10
400	12.5	800	30	800	120	30	0	0	8	10
900	15	800	30	800	225	25	0	0	8	10
2000	15	800	30	800	400	20	0	0	8	10

Phosphate buffer performance file(slope :0.99288 offset :0.17881)										
Volume (µL)	Asp. speed (µL/s)	Asp. Delay msec	Dis. speed (µL/s)	Dis. Delay msec	Waste volume µL	Waste volume% (%of Asp.)	Blowout Volume µL	Blowout Delay msec	Transport Air Gap µL	System AirGap µL
5	1.7	500	100	300	5	100	0	0	3	8
30	2	500	100	300	15	50	0	0	3	8
50	4	500	100	300	25	50	0	0	3	8
100	6	500	100	300	30	30	0	0	3	8
250	10	500	100	300	75	30	0	0	3	8
400	20	500	100	300	120	30	0	0	3	8
900	25	500	100	300	270	30	0	0	3	8
2000	30	500	100	300	600	30	0	0	3	8

Ovalbumin performance file(slope :0.99288 offset :0.17881)										
Volume (µL)	Asp. speed (µL/s)	Asp. Delay msec	Dis. speed (µL/s)	Dis. Delay msec	Waste volume µL	Waste volume% (%of Asp.)	Blowout Volume µL	Blowout Delay msec	Transport Air Gap µL	System AirGap µL
5	1.7	300	500	300	5	100	0	0	3	8
30	2.5	300	500	300	15	50	0	0	3	8
50	5	300	500	300	25	50	0	0	3	8
100	8	300	500	300	30	30	0	0	3	8
250	10	300	500	300	75	30	0	0	3	8
400	10	300	500	300	120	30	0	0	3	8
900	10	300	500	300	270	30	0	0	3	8
2000	10	300	500	300	600	30	0	0	3	8

Sampling Top phase performance file(slope :1.041 offset :1.5574)										
Volume (µL)	Asp. speed (µL/s)	Asp. Delay msec	Dis. speed (µL/s)	Dis. Delay msec	Waste volume µL	Waste volume% (%of Asp.)	Blowout Volume µL	Blowout Delay msec	Transport Air Gap µL	System AirGap µL
5	1.7	300	500	300	5	100	0	0	3	8
30	2.5	300	500	300	15	50	0	0	3	8
50	5	300	400	300	25	50	0	0	3	8
100	8	300	400	300	30	30	0	0	3	8
250	10	300	300	300	75	30	0	0	3	8
400	10	300	300	300	120	30	0	0	3	8
900	10	300	300	300	270	30	0	0	3	8
2000	10	300	300	300	600	30	0	0	3	8

Sampling Bottom phase performance file(slope: 1.0731 offset:-6.521)										
Volume µL	Asp. speed (µL/s)	Asp. Delay msec	Dis. speed (µL/s)	Dis. Delay msec	Waste volume µL	Waste volume% (%of Asp.)	Blowout Volume µL	Blowout Delay msec	Transport Air Gap µL	System AirGap µL
5	2.5	800	125	800	5	100	0	0	8	10
30	2.5	800	125	800	15	50	0	0	8	10
50	2.5	800	100	800	25	50	0	0	8	10
100	5	800	100	800	50	50	0	0	8	10
250	10	800	50	800	100	40	0	0	8	10
400	12.5	800	30	800	120	30	0	0	8	10
900	15	800	30	800	225	25	0	0	8	10
2000	15	800	30	800	400	20	0	0	8	10

Dil.top Transfer performance file(slope :1.0068 offset :1.9031)										
Volume µL	Asp. speed (µL/s)	Asp. Delay msec	Dis. speed (µL/s)	Dis. Delay msec	Waste volume µL	Waste volume% (%of Asp.)	Blowout Volume µL	Blowout Delay msec	Transport Air Gap µL	System AirGap µL
5	1.7	300	500	300	5	100	0	0	3	8
30	2.5	300	500	300	15	50	0	0	3	8
50	5	300	400	300	25	50	0	0	3	8
100	8	300	400	300	30	30	0	0	3	8
250	10	300	300	300	75	30	0	0	3	8
400	10	300	200	300	120	30	0	0	3	8
900	10	300	200	300	270	30	0	0	3	8
2000	10	300	200	300	600	30	0	0	3	8

Dil.bottom Transfer performance file(slope: 0.98889 offset:0.70436)										
Volume µL	Asp. speed (µL/s)	Asp. Delay msec	Dis. speed (µL/s)	Dis. Delay msec	Waste volume µL	Waste volume% (%of Asp.)	Blowout Volume µL	Blowout Delay msec	Transport Air Gap µL	System AirGap µL
5	2.5	800	125	800	5	100	0	0	8	10
30	2.5	800	125	800	15	50	0	0	8	10
50	2.5	800	100	800	25	50	0	0	8	10
100	5	800	100	800	50	50	0	0	8	10
250	10	800	50	800	100	40	0	0	8	10
400	12.5	800	30	800	120	30	0	0	8	10
900	15	800	30	800	225	25	0	0	8	10
2000	15	800	30	800	400	20	0	0	8	10

PEG600 (50%) performance file(slope 1.0909 offset -1.3036)										
Volume µL	Asp. speed (µL/s)	Asp. Delay msec	Dis. speed (µL/s)	Dis. Delay msec	Waste volume µL	Waste volume% (%of Asp.)	Blowout Volume µL	Blowout Delay msec	Transport Air Gap µL	System AirGap µL
5	1.7	200	15	300	5	100	0	0	3	8
30	2.5	200	15	300	15	50	0	0	3	8
50	5	200	15	300	25	50	0	0	3	8
100	5	200	15	300	30	40	0	0	3	8
250	5	200	15	300	75	40	0	0	3	8
400	5	200	15	300	120	40	0	0	3	8
900	5	300	15	300	270	40	0	0	3	8
2000	5	300	15	300	600	40	0	0	3	8

Sampling 200 μl Bottom performance file(slope: 1.0282 offset:1.35)										
Volume μL	Asp. speed (μL/s)	Asp. Delay msec	Dis. speed (μL/s)	Dis. Delay msec	Waste volume μL	Waste volume% (%of Asp.)	Blowout Volume μL	Blowout Delay msec	Transport Air Gap μL	System AirGap μL
5	2.5	800	125	800	5	100	0	0	8	10
30	2.5	800	125	800	15	50	0	0	8	10
50	2.5	800	100	800	25	50	0	0	8	10
100	5	800	100	800	50	50	0	0	8	10
250	10	800	50	800	100	40	0	0	8	10
400	12.5	800	30	800	120	30	0	0	8	10
900	15	800	30	800	225	25	0	0	8	10
2000	15	800	30	800	400	20	0	0	8	10

(NH$_4$)$_2$SO$_4$ performance file (slope 1.1741 offset -3.9036)										
Volume µL	Asp. speed (µL/s)	Asp. Delay msec	Dis. speed (µL/s)	Dis. Delay msec	Waste volume µL	Waste volume% (%of Asp.)	Blowout Volume µL	Blowout Delay msec	Transport Air Gap µL	System AirGap µL
5	1.7	200	100	300	5	100	0	0	3	8
30	2	200	100	300	15	50	0	0	3	8
50	4	300	100	300	25	50	0	0	3	8
100	6	200	100	300	30	30	0	0	3	8
250	10	200	100	300	75	30	0	0	3	8
400	10	200	100	300	120	30	0	0	3	8
900	10	300	100	300	270	30	0	0	3	8
2000	30	200	100	300	600	30	0	0	3	8

Phosphate buffer 0.15M performance file(slope 1.0349 offset -7.6107)										
Volume μL	Asp. speed (μL/s)	Asp. Delay msec	Dis. speed (μL/s)	Dis. Delay msec	Waste volume μL	Waste volume% (%of Asp.)	Blowout Volume μL	Blowout Delay msec	Transport Air Gap μL	System AirGap μL
5	1.7	500	100	300	5	100	0	0	3	8
30	2	500	100	300	15	50	0	0	3	8
50	4	500	100	300	25	50	0	0	3	8
100	6	500	100	300	30	30	0	0	3	8
250	10	500	100	300	75	30	0	0	3	8
400	10	500	100	300	120	30	0	0	3	8
900	10	500	100	300	270	30	0	0	3	8
2000	30	500	100	300	600	30	0	0	3	8

PEG600 (100%) performance file(slope 1.0976 offset -5.225)										
Volume µL	Asp. speed (µL/s)	Asp. Delay msec	Dis. speed (µL/s)	Dis. Delay msec	Waste volume µL	Waste volume% (%of Asp.)	Blowout Volume µL	Blowout Delay msec	Transpo rt Air Gap µL	System AirGap µL
5	1.7	200	15	300	5	100	0	0	3	8
30	2.5	200	15	300	15	50	0	0	3	8
50	5	300	15	300	25	50	0	0	3	8
100	5	200	15	300	30	40	0	0	3	8
250	5	200	15	300	75	40	0	0	3	8
400	5	200	15	300	120	40	0	0	3	8
900	5	300	15	300	270	40	0	0	3	8
2000	5	200	15	300	600	40	0	0	3	8

APPENDIX - B. Dispensing files and Statistical analysis to describe the accuracy of the experiments.

Table [1A] Dispensing of PEG Stock Solution [PEG performance file slope 1, offset 0]

Dispensing of PEG Solution (PEG performance file slope 1 offset 0)					
Tubes No.	Mass of Empty Tubes[g]	Mass Tubes + PEG[g]	Mass of PEG[g]	Volume Demanded[µL]	Weight delivered[µg]
1	2.3761	2.4764	0.1003	100	100.3
2	2.3349	2.5403	0.2054	200	205.4
3	2.3614	2.6668	0.3054	300	305.4
4	2.3256	2.7399	0.4143	400	414.3
5	2.3425	2.8578	0.5153	500	515.3
6	2.3363	2.9586	0.6223	600	622.3
7	2.3664	3.0913	0.7249	700	724.9
8	2.3977	3.2259	0.8282	800	828.2

Table [1B] Statistical regression analysis using Excel for dispensing stock PEG Solution

Residuals	Std. Dev.	Mean	CV	RSD %	%Bias Accuracy
-0.3	0.255	0.4645	0.549	54.8962	0.3
-5.4					2.7
-5.4					1.8
-14.3					3.58
-15.3					3.06
-22.3					3.72
-24.9					3.56
-28.2					3.53
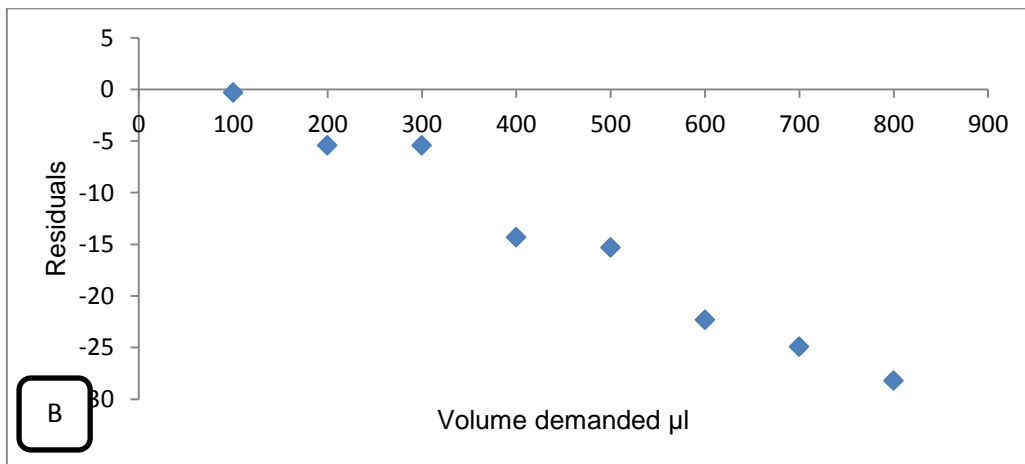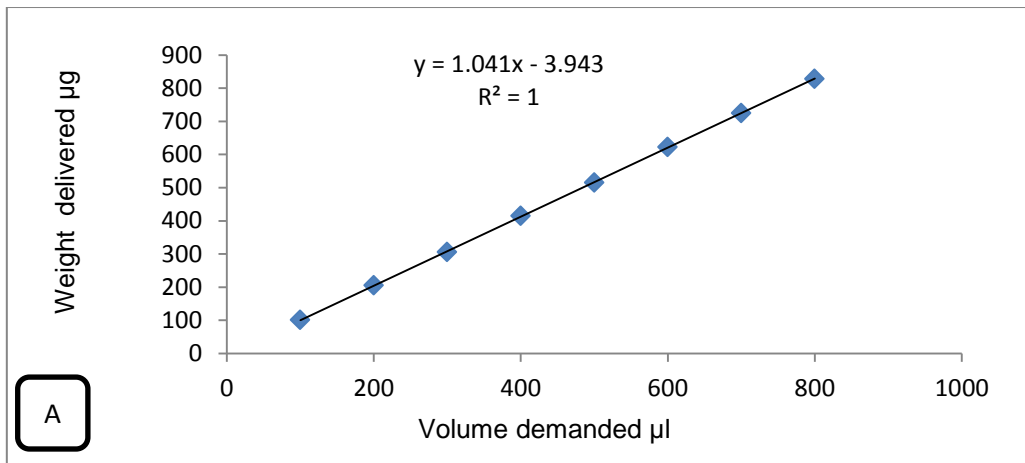
Figure [1] (A) Regression plot for dispensing stock PEG Solution (B) Residuals of regression for handling PEG stock solution [slope 1,offset 0) by Robotics system

Table [2A] Dispensing of PEG Stock Solution range of volumes using PEG performance file slope 1.041,offset -3.943]

Dispensing of PEG Stock Solution (PEG performance file slope 1.04 , offset -3.943)					
Tubes No.	Mass of Empty Tubes[g]	Mass Tubes + PEG[g]	Mass of PEG[g]	Volume Demanded[μL]	Weight delivered[μg]
1	2.4764	2.5745	0.0981	100	98.1
2	2.5403	2.7384	0.1981	200	198.1
3	2.6668	2.9629	0.2961	300	296.1
4	2.7399	3.1413	0.4014	400	401.4
5	2.8578	3.3575	0.4997	500	499.7
6	2.9586	3.559	0.6004	600	600.4
7	3.0913	3.7901	0.6988	700	698.8
8	3.2259	4.0236	0.7977	800	797.7

Table [2B] Statistical regression analysis using Excel for dispensing stock PEG Solution [slope 1.041,offset -3.943]

Residuals	Std. Dev.	Mean	CV	RSD %	%Bias Accuracy
1.9	0.2453	0.4488	0.5466	54.659	-1.9
1.9					-0.95
3.9					-1.3
-1.4					0.35
0.3					-0.06
-0.4					0.067
1.2					-0.17
2.3					-0.29

A Graph showing y-axis "Weight delivered µg" (0 to 900) versus x-axis "Volume demanded µl" (0 to 1000), with data points and regression line.

$y = 1.0014x - 1.85$

$R^2 = 1$

B Graph showing y-axis "Residuals" (-30 to 5) versus x-axis "Volume demanded µl" (0 to 1000), with scattered data points.

Figure [2] (A) Regression plot for dispensing stock PEG Solution (B) Residuals of regression for handling PEG stock solution [slope 1.041,offset -3.943)by Robotics system

Table [3A] Dispensing of PEG Stock Solution specific volume using PEG performance file slope 1.041, offset -3.943)

Dispensing of PEG Stock Solution (PEG performance file slope 1.041 offset -3.943)					
Tubes No.	Mass of Empty Tubes[g]	Mass Tubes + PEG[g]	Mass of PEG[µg]	Volume Demanded[µL]	Weight delivered[µg]
1	2.432	2.9363	0.5043	502.7	504.3
2	2.3404	2.8432	0.5028	502.7	502.8
3	2.3508	2.8558	0.505	502.7	505
4	2.3556	2.8595	0.5039	502.7	503.9
5	2.3964	2.9001	0.5037	502.7	503.7
6	2.3765	2.8819	0.5054	502.7	505.4
7	2.3583	2.863	0.5047	502.7	504.7
8	2.3251	2.8289	0.5038	502.7	503.8

Table [3B] Statistical regression analysis using Excel for dispensing stock PEG Solution specific volume (slope 1.041, offset -3.943)

Residuals	Std. Dev.	Mean	CV	RSD %	%Bias Accuracy
-1.6	0.000828	0.5042	0.001642	0.164236	0.32
-0.1					0.02
-2.3					0.45
-1.2					0.24
-1					0.20
-2.7					0.54
-2					0.39
-1.1					0.22

Table [4A] Dispensing of Dextran Stock Solution (viscous performance file slope 1 offset 0)

Dispensing of Dextran Stock Solution (viscous performance file slope 1 offset 0)					
Tubes No.	Mass of Empty Tubes[g]	Mass Tubes + Dex[g]	Mass of Dex[g]	Volume Demanded[µL]	Weight delivered[µg]
1	2.3357	2.4405	0.1048	100	104.8
2	2.3715	2.5842	0.2127	200	212.7
3	2.3529	2.6793	0.3264	300	326.4
4	2.3896	2.8279	0.4383	400	438.3
5	2.3333	2.8803	0.547	500	547
6	2.3778	3.0313	0.6535	600	653.5
7	2.3586	3.127	0.7684	700	768.4
8	2.343	3.222	0.879	800	879
9	2.3648	3.346	0.9812	900	981.2
10	2.3665	3.4132	1.0467	1000	1046.7

Table [4B] Statistical regression analysis for dispensing stock Dextran Solution (viscous performance file slope 1   offset

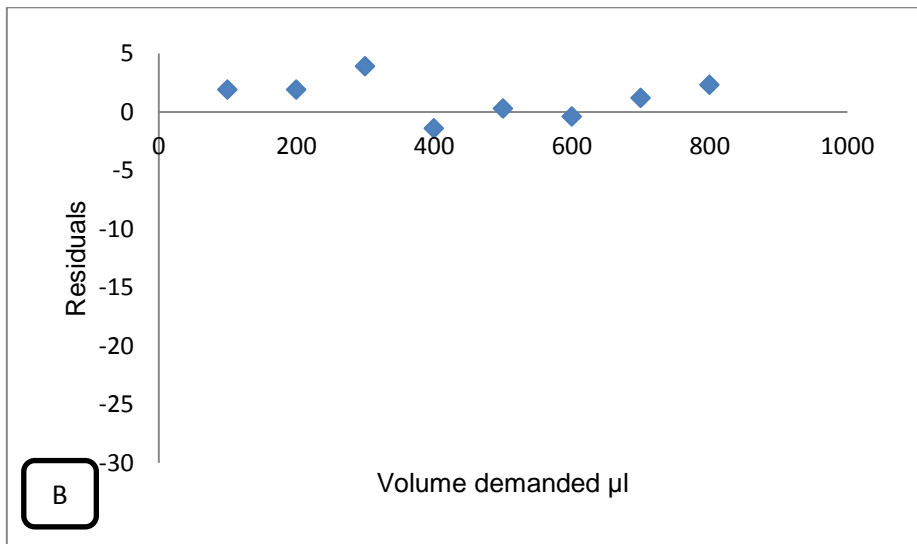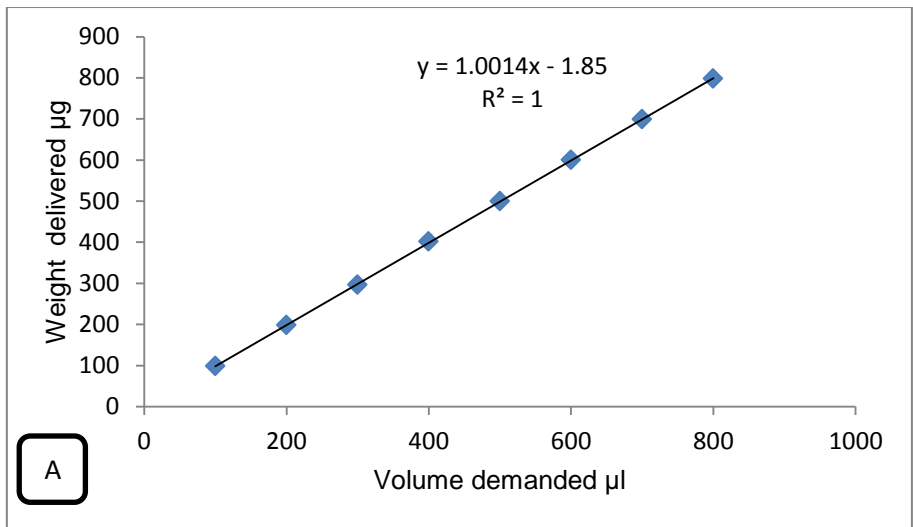| Residuals	Std. Dev.	Mean	CV	RSD %	%Bias Accuracy
-4.8	0.33	0.59	0.54	54.61	4.8
-12.7					6.35
-26.4					8.8
-38.3					9.575
-47					9.4
-53.5					8.91
-68.4					9.77
-79					9.875
-81.2					9.02
-46.7					4.67
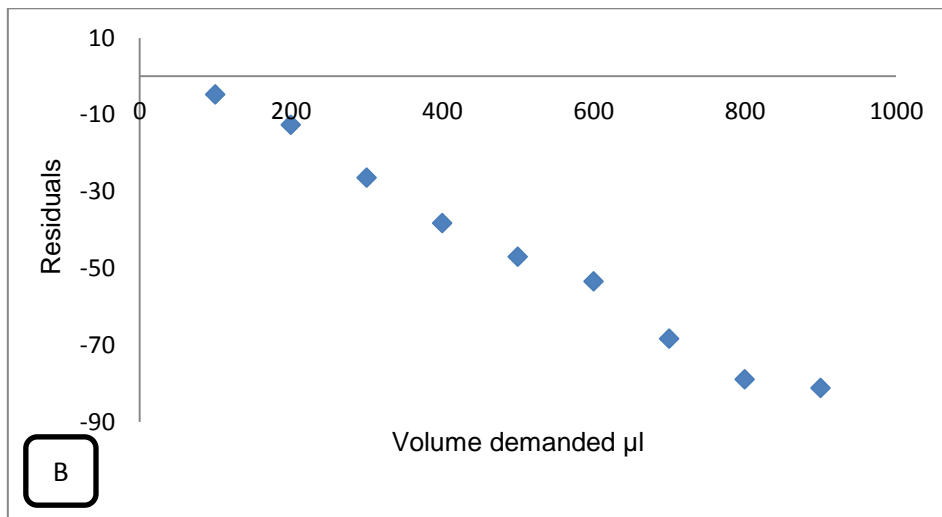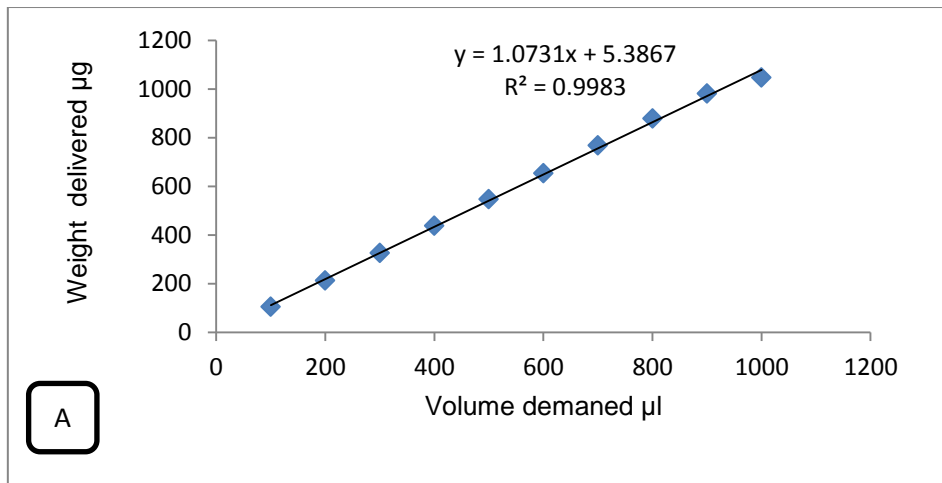
Figure [4] (A) Regression plot for dispensing stock DEX solution (B) Residuals of regression for handling DEX stock solution [slope 1, offset 0) by Robotics system

Table [5A] Dispensing of Dextran Stock Solution (viscous performance file slope 1.0731 offset 5.3867)

Dispensing of Dextran Stock Solution (viscous performance file slope 1.0731 offset 5.3867)					
Tubes No.	Mass of Empty Tubes[g]	Mass Tubes + Dex[g]	Mass of Dex[g]	Volume Demanded[µL]	Weight delivered[µg]
1	2.364	2.4549	0.0909	100	90.9
2	2.375	2.5686	0.1936	200	193.6
3	2.3536	2.6481	0.2945	300	294.5
4	2.3222	2.7211	0.3989	400	398.9
5	2.3443	2.8455	0.5012	500	501.2
6	2.3656	2.9628	0.5972	600	597.2
7	2.3512	3.0568	0.7056	700	705.6
8	2.3606	3.1688	0.8082	800	808.2
9	2.3695	3.2718	0.9023	900	902.3
10	2.3553	3.3373	0.982	1000	982

Table [5B] Statistical regression analysis for dispensing stock Dextran Solution (viscous performance file slope1.073 , offset 5.3867)

| Residuals	Std. Dev.	Mean	CV	RSD %	%Bias Accuracy
9.1	0.30406	0.5474	0.5554	55.542	-9.1
6.4					-3.2
5.5					-1.83
1.1					-0.275
-1.2					0.24
2.8					-0.46
-5.6					0.8
-8.2					1.025
-2.3					0.25
18					-1.8
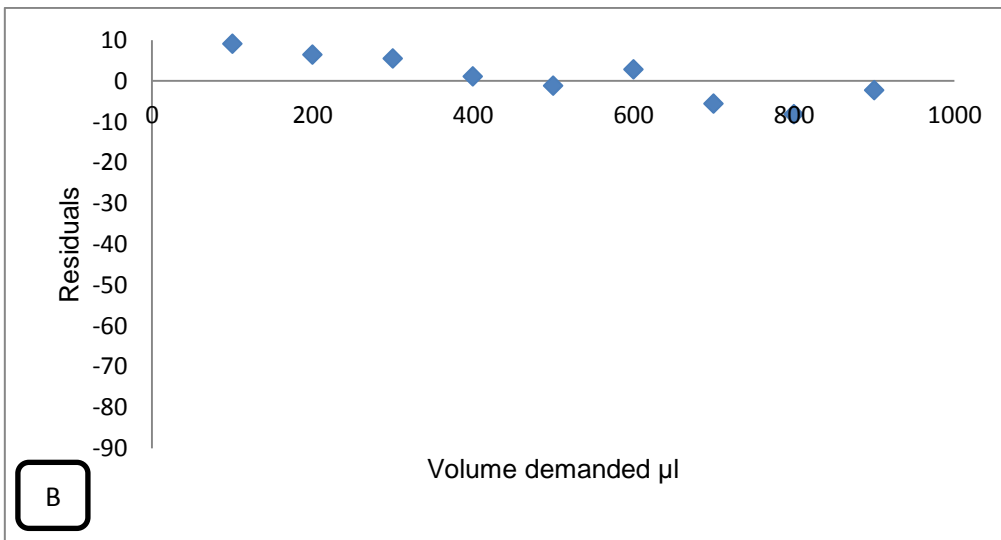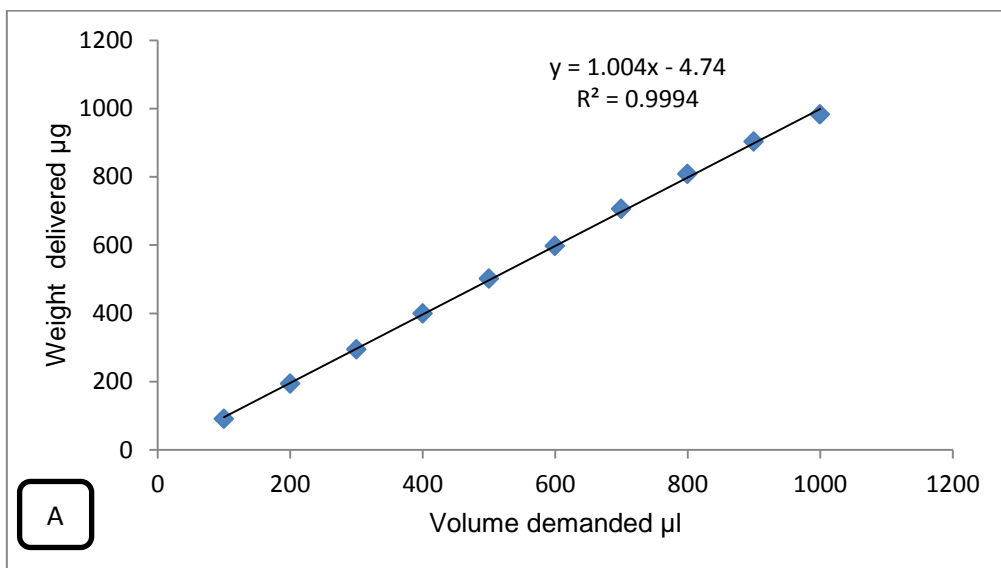
Figure [5] (A) Regression plot for dispensing stock DEX Solution (B) Residuals of regression for handling DEX stock solution slope 1.0731 , offset 5.3867)

Table [6A] Dispensing of Dextran Stock Solution specific volume (viscous performance file slope 1.0731   offset 5.3867)

Tubes No.	Mass of Empty Tubes[g]	Mass Tubes + Dex[g]	Mass of Dex[g]	Volume Demanded[µL]	Weight delivered[µg]
1	2.9363	3.911	0.9747	973.44	974.7
2	2.8432	3.8154	0.9722	973.44	972.2
3	2.8558	3.8309	0.9751	973.44	975.1
4	2.8595	3.8341	0.9746	973.44	974.6
5	2.9001	3.8759	0.9758	973.44	975.8
6	2.8819	3.8555	0.9736	973.44	973.6
7	2.863	3.8424	0.9794	973.44	979.4
8	2.8289	3.8125	0.9836	973.44	983.6

The header of the above table reads: "Dispensing of Dextran Stock Solution (viscous performance file slope 1.0731   offset 5.3867)"

Table [6B] Statistical regression analysis for dispensing stock Dextran Solution specific volume (slope1.0731, offset 5.3867)

Residuals	Std. Dev.	Mean	CV	RSD %	%Bias Accuracy
-1.26	0.003662	0.976125	0.003752	0.375203	0.13
1.24					-0.13
-1.66					0.17
-1.16					0.12
-2.36					0.24
-0.16					0.016
-5.96					0.61
-10.16					1.04

Table [7A] Dispensing of Ovalbumin and Buffer Stock Solution (ovalbumin or buffer performance file (slope 1 offset 0)

Tubes No.	Mass of Empty Tubes[g]	Mass Tubes + Ova. or Buffer[g]	Mass of Ova. or Buffer [g]	Volume Demanded[μL]	Weight delivered[μg]
1	2.3558	2.3554	2.3554	0	0
2	2.3553	2.4067	0.0514	50	51.4
3	2.3575	2.4578	0.1003	100	100.3
4	2.4288	2.6301	0.2013	200	201.3
5	2.3614	2.657	0.2956	300	295.6
6	2.3517	2.7461	0.3944	400	394.4
7	2.3721	2.8668	0.4947	500	494.7
8	2.3718	2.9702	0.5984	600	598.4
9	2.3526	3.0442	0.6916	700	691.6
10	2.3553	3.1538	0.7985	800	798.5

Table [7B] Statistical regression analysis for Dispensing of Ovalbumin and Buffer Stock Solution (ovalbumin or buffer performance file (slope 1 offset 0)

Residuals	Std. Dev.	Mean	CV	RSD %	%Bias Accuracy
0	0.665402	0.5982	1.1124	111.241	0
-1.4					2.8
-0.3					0.3
-1.3					0.65
4.4					-1.47
5.6					-1.4
5.3					-1.06
1.6					-0.27
8.4					-1.2
1.5					-0.19
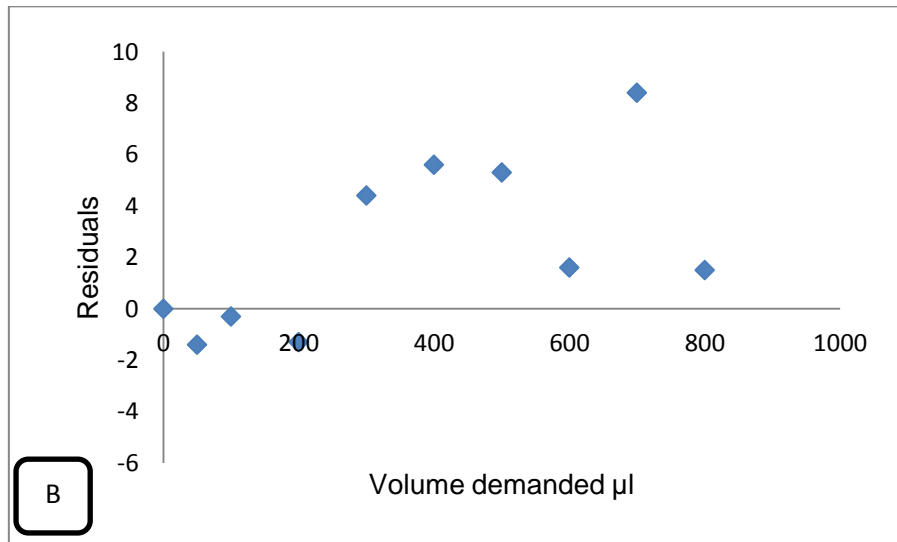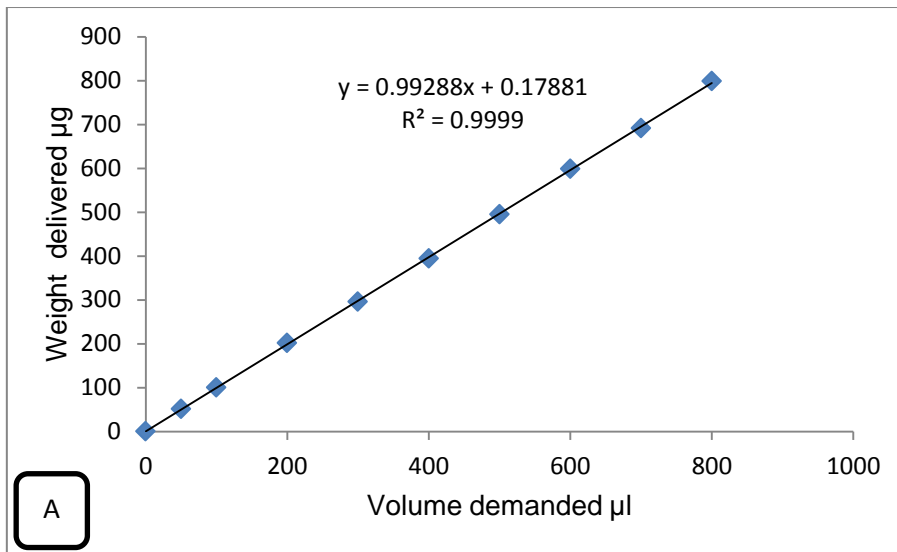
Figure [7] (A) Regression plot for dispensing stock Ovalbumin and Buffer Solution (B) Residuals of regression for handling Ovalbumin and Buffer Solution (slope 1 offset 0)

Table [8A] Dispensing of Ovalbumin and Buffer Stock Solution (slope 0.99288, offset 0.17881)

Tubes No.	Mass of Empty Tubes[g]	Mass Tubes + Ova. or Buffer[g]	Mass of Ova. or Buffer [g]	Volume Demanded[μL]	Weight delivered[μg]
1	2.3418	2.3418	0	0	0
2	2.366	2.4186	0.0526	50	52.6
3	2.3301	2.4311	0.101	100	101
4	2.3804	2.5834	0.203	200	203
5	2.3725	2.6701	0.2976	300	297.6
6	2.3718	2.7689	0.3971	400	397.1
7	2.33	2.8272	0.4972	500	497.2
8	2.3325	2.9353	0.6028	600	602.8
9	2.3385	3.0359	0.6974	700	697.4
10	2.3586	3.1627	0.8041	800	804.1

Table [8B] Statistical regression analysis for Dispensing stock Ovalbumin and Buffer Solution (ovalbumin or buffer performance file slope 0.99288, offset 0.17881)

| Residuals	Std. Dev.	Mean	CV	RSD %	%Bias Accuracy
0	0.2808	0.3653	0.7687	76.873	0
-2.6					5.2
-1					1
-3					1.5
2.4					-0.8
2.9					-0.73
2.8					-0.56
-2.8					0.47
2.6					-0.37
-4.1					0.51
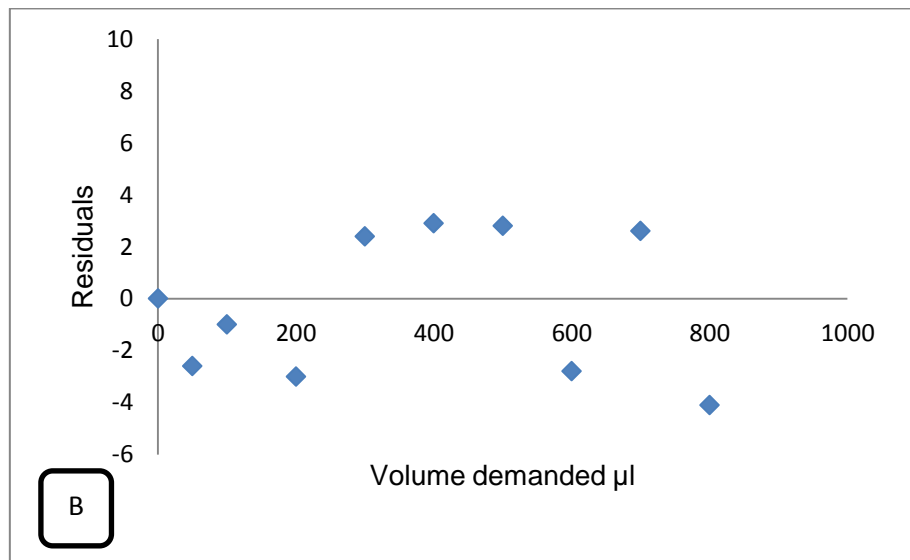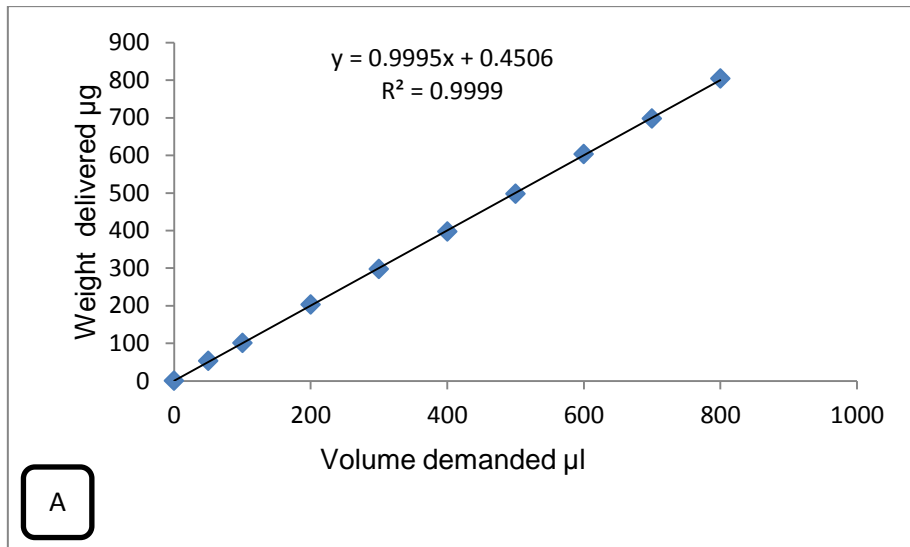
Figure [8] (A) Regression plot for dispensing stock Ovalbumin and Buffer Solution (B) Residuals of regression for handling Ovalbumin and Buffer Solution (slope 0.99288 , offset 0.17881)

Table [9A] Dispensing of Buffer Stock Solution (slope 0.99288, offset 0.17881)

Dispensing of Buffer Stock Solution (		slope 0.99288	offset 0.17881)		
Tubes No.	Mass of Empty Tubes[g]	Mass Tubes + Buffer[g]	Mass of Buffer [g]	Volume Demanded[µL]	Weight delivered[µg]
1	3.911	4.4387	0.5277	524	527.7
2	3.8154	4.2433	0.4279	424	427.9
3	3.8309	4.2077	0.3768	374	376.8
4	3.8341	4.1609	0.3268	324	326.8
5	3.8759	4.1526	0.2767	274	276.7
6	3.8555	4.0812	0.2257	224	225.7
7	3.8424	4.0178	0.1754	174	175.4
8	3.8125	3.9378	0.1253	124	125.3

Table [9B] Statistical regression analysis for dispensing stock Buffer specific volume slope 0.99288 offset 0.17881)

Residuals	Std. Dev.	Mean	CV	RSD %	%Bias Accuracy
-3.7	0.134401	0.307788	0.436669	43.66686	0.71
-3.9					0.921
-2.8					0.75
-2.8					0.86
-2.7					0.99
-1.7					0.76
-1.4					0.81
-1.3					1.05

Table [10A] Dispensing of Ovalbumin Stock Solution (slope 0.99288, offset 0.17881)

Dispensing of Ovalbumin Stock Solution (slope 0.99288 offset 0.17881)					
Tubes No.	Mass of Empty Tubes[g]	Mass Tubes + Ovalbumin[g]	Mass of Ovalbumin [g]	Volume Demanded[µL]	Weight delivered[µg]
1	4.4387	4.4387	0	0	0
2	4.2433	4.3467	0.1034	100	103.4
3	4.2077	4.3611	0.1534	150	153.4
4	4.1609	4.3652	0.2043	200	204.3
5	4.1526	4.4074	0.2548	250	254.8
6	4.0812	4.3864	0.3052	300	305.2
7	4.0178	4.3728	0.355	350	355
8	3.9378	4.3434	0.4056	400	405.6

Table [10B] Statistical regression analysis for dispensing of Ovalbumin Stock Solution (slope 0.99288, offset 0.17881)

Residuals	Std. Dev.	Mean	CV	RSD %	%Bias Accuracy
0.9	0.135311	0.2226	0.607864	60.78645	0
-3.4					3.4
-3.4					2.27
-4.3					2.15
-4.8					1.92
-5.2					1.73
-5					1.43
-5.6					1.4

Table [11A] Dispensing of Top phase [Sampling top phase performance file slope 1 offset 0]

Sampling top phase performance file			slope 1 offset 0		
Tubes No.	Mass of Empty Tubes[g]	Mass Tubes + Top[g]	Mass of Top [g]	Volume Demanded[μL]	Weight delivered[μg]
1	0.9949	1.0215	0.0266	25	26.6
2	0.9921	1.0454	0.0533	50	53.3
3	0.9934	1.0953	0.1019	100	101.9
4	1.0024	1.1561	0.1537	150	153.7
5	0.9929	1.1975	0.2046	200	204.6
6	0.9879	1.2432	0.2553	250	255.3
7	0.9954	1.3012	0.3058	300	305.8
8	0.9926	1.349	0.3564	350	356.4

Table [11B] Statistical regression analysis for dispensing of Top phase [Sampling top phase performance file slope 1 offset 0]

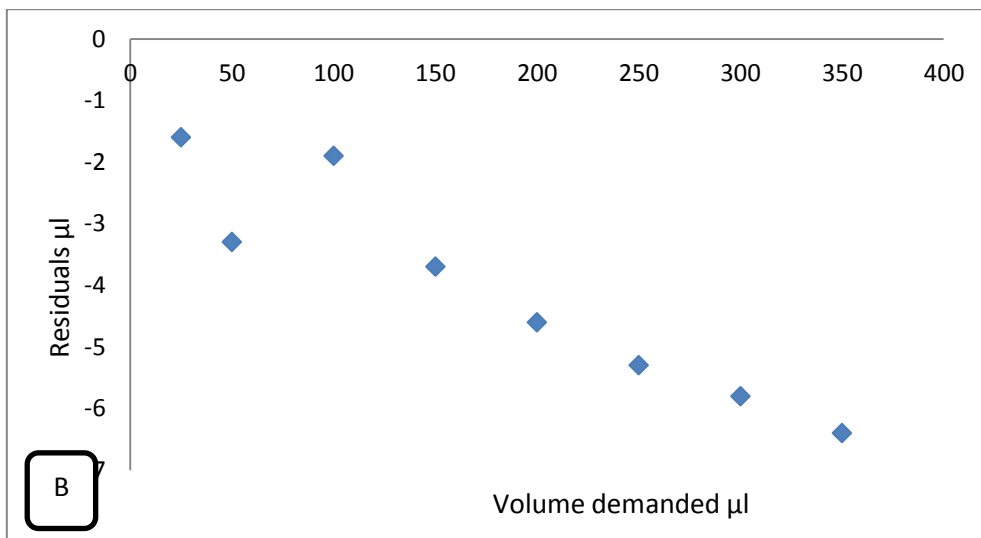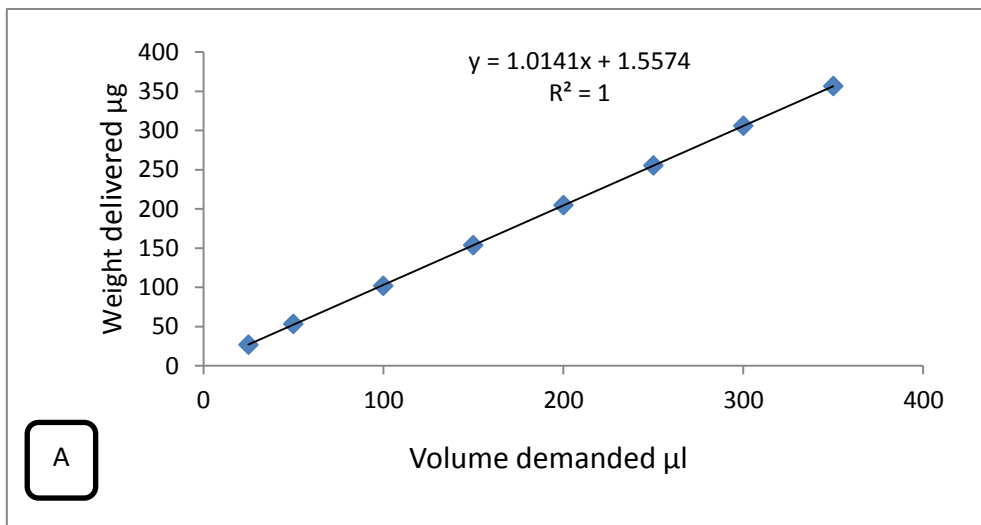| Residuals	Std. Dev.	Mean	CV	RSD %	%Bias Accuracy
-1.6	0.12	0.18	0.654	65.45	6.4
-3.3					6.6
-1.9					1.9
-3.7					2. 7
-4.6					2.3
-5.3					2.12
-5.8					1.93
-6.4					1.82

Figure [11] (A) Regression plot for dispensing stock Top phase Solution (B) Residuals of regression for handling Top phase Solution (slope 1, offset 0)

Table [12A] Dispensing of Bottom phase [sampling Bottom phase performance file slope 1, offset 0]

sampling Bottom phase performance file slope 1 offset 0					
Tubes No.	Mass of Empty Tubes[g]	Mass Tubes + Bottom[g]	Mass of Bottom [g]	Volume Demanded[µL]	Weight delivered[µg]
1	0.9966	1.0125	0.0159	25	15.9
2	1.0014	1.0509	0.0495	50	49.5
3	0.9917	1.0942	0.1025	100	102.5
4	1.0015	1.158	0.1565	150	156.5
5	0.9997	1.2111	0.2114	200	211.4
6	0.9969	1.2518	0.2549	250	254.9
7	0.9878	1.2976	0.3098	300	309.8
8	0.997	1.3702	0.3732	350	373.2

Table [12B] Statistical regression analysis for dispensing of Bottom phase [slope 1, offset 0] using Excel

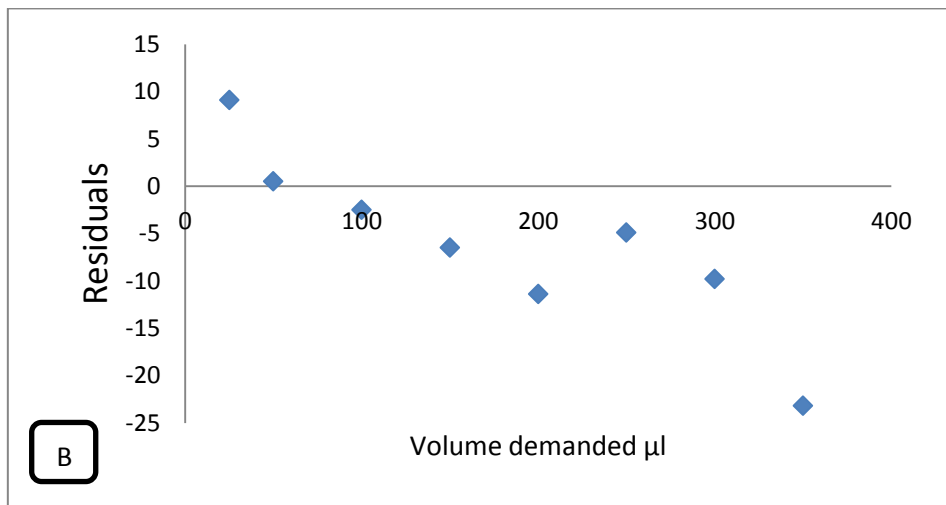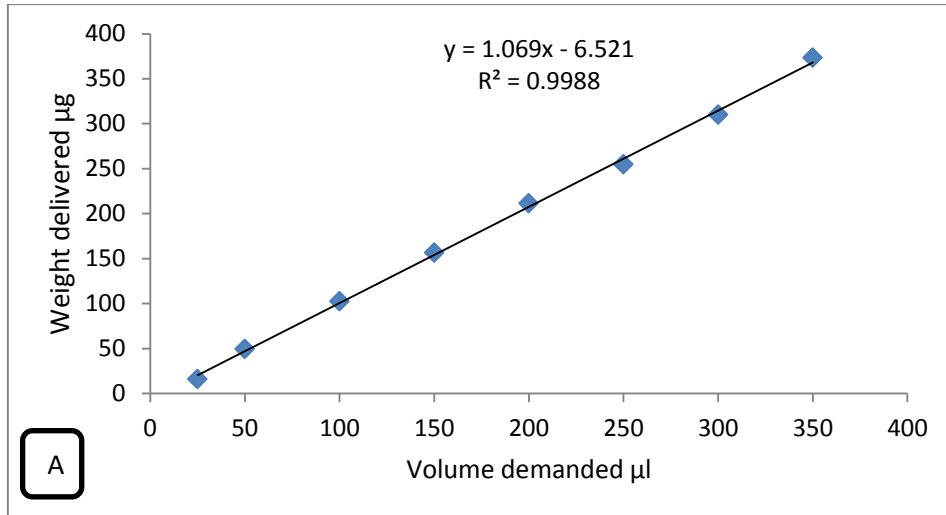| Residuals	Std. Dev.	Mean	CV	RSD %	%Bias Accuracy
9.1	0.1260079	0.1842125	0.6840353	68.40353	-36.4
0.5					-1
-2.5					2.5
-6.5					4.3
-11.4					5.7
-4.9					1.96
-9.8					3.27
-23.2					6.62

Figure [12] (A) Regression plot for dispensing stock Bottom phase Solution (B) Residuals of regression for handling Bottom phase Solution (slope 1 , offset 0)

Table [13A] Dispensing of Top phase [sampling Top phase performance file slope 1.041 offset 1.5574]

Sampling top phase performance file			(slope 1.041 offset 1.5574		
Tubes No.	Mass of Empty Tubes[g]	Mass Tubes + Top[g]	Mass of Top [g]	Volume Demanded[µL]	Weight delivered[µg]
1	0.9931	1.0173	0.0242	25	24.2
2	0.991	1.0402	0.0492	50	49.2
3	0.9878	1.0847	0.0969	100	96.9
4	0.9934	1.1394	0.146	150	146
5	0.9883	1.1829	0.1946	200	194.6
6	0.9928	1.2365	0.2437	250	243.7
7	0.9987	1.2907	0.292	300	292
8	0.9991	1.3402	0.3411	350	341.1

Table [13B] Statistical regression analysis for dispensing of Top phase [slope 1.041, offset 1.5574] using Excel

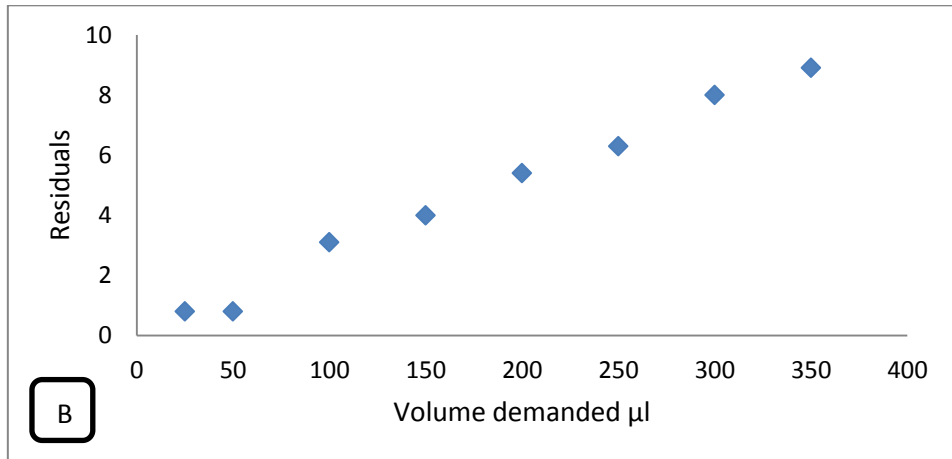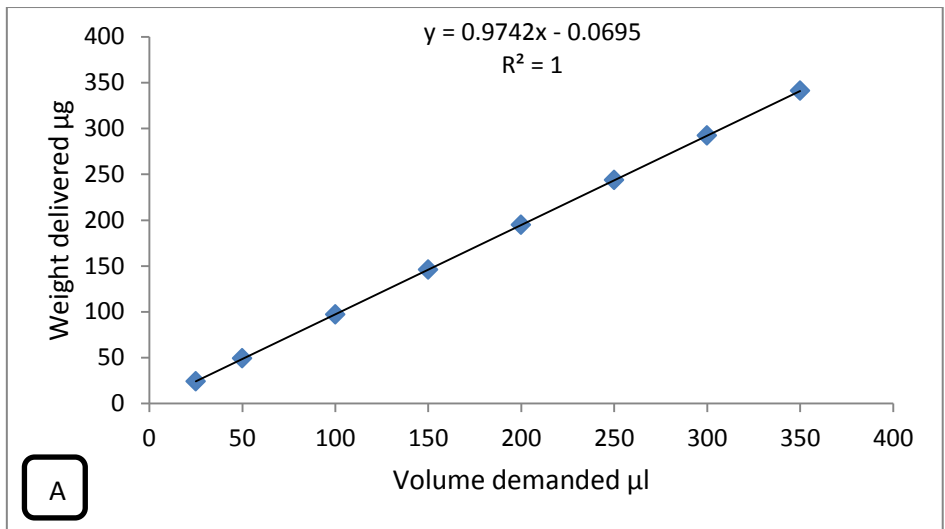| Residuals	Std. Dev.	Mean	CV	RSD %	%Bias Accuracy
0.8	0.114561	0.173463	0.66044	66.0438	-3.2
0.8					-1.6
3.1					-3.1
4					-2.67
5.4					-2.7
6.3					-2.52
8					-2.67
8.9					-2.55

Figure [13] (A) Regression plot for dispensing stock Top phase Solution (B) Residuals of regression for handling Top phase Solution (slope 1.041, offset 1.5574)

Table [14A] Dispensing of Bottom phase [sampling Bottom phase performance file slope 1.0731   offset -6.521]

Sampling Bottom phase performance file slope 1.0731 offset -6.521					
Tubes No.	Mass of Empty Tubes[g]	Mass Tubes + Bottom[g]	Mass of Bottom [g]	Volume Demanded[µL]	Weight delivered[µg]
1	0.9945	1.0166	0.0221	25	22.1
2	0.9936	1.0455	0.0519	50	51.9
3	0.9889	1.09	0.1011	100	101.1
4	0.9941	1.1398	0.1457	150	145.7
5	0.998	1.2034	0.2054	200	205.4
6	1.0001	1.2466	0.2465	250	246.5
7	0.9923	1.2924	0.3001	300	300.1
8	0.9961	1.3471	0.351	350	351

Table [14B] Statistical regression analysis for dispensing of Bottom phase [slope 1.0731   offset -6.521]

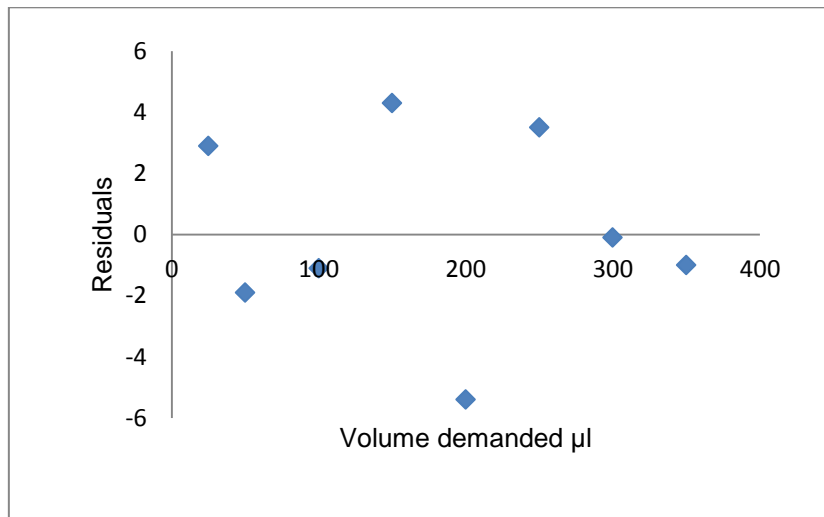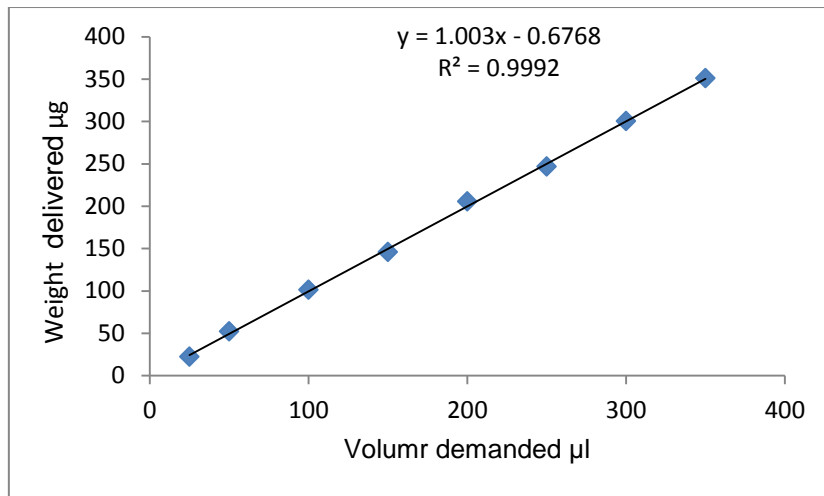| Residuals	Std. Dev.	Mean	CV	RSD %	%Bias Accuracy
2.9	0.117985	0.177975	0.66293	66.2931	-11.6
-1.9					3.8
-1.1					1.1
4.3					-2.87
-5.4					2.7
3.5					-1.4
-0.1					0.033
-1					0.29

Figure [14] (A) Regression plot for dispensing stock Bottom phase Solution (B)
Residuals of regression for handling Bottom phase Solution 1.0731   offset -6.521)

Table [15A] Dispensing of Top phase specific volume [sampling Top phase performance file slope 1.041 offset 1.5574]

Sampling top phase performance file			slope 1.041 offset 1.5574	
Tubes No.	Mass of Empty Tubes[g]	Mass Tubes + Top[g]	Mass of Top [g]	Volume Demanded[μL]	Weight delivered[μg]
1	0.9998	1.1959	0.1961	200	196.1
2	0.9877	1.1825	0.1948	200	194.8
3	0.9934	1.1882	0.1948	200	194.8
4	0.9997	1.1942	0.1945	200	194.5
5	0.9938	1.1891	0.1953	200	195.3
6	0.9995	1.1902	0.1907	200	190.7
7	1.0025	1.1971	0.1946	200	194.6
8	0.9963	1.1917	0.1954	200	195.4

Table [15B] Statistical regression analysis for dispensing of Top phase specific volume [slope 1.041 offset 1.5574]

Residuals	Std. Dev.	Mean	CV	RSD %	%Bias Accuracy
3.9	0.00163	0.19453	0.0084	0.838765	-1.95
5.2					-2.6
5.2					-2.6
5.5					-2.75
4.7					-2.35
9.3					-4.65
5.4					-2.7
4.6					-2.3

Table [16A] Dispensing of Bottom phase specific volume [sampling Bottom phase performance file slope 1.0731   offset -6.521]

Sampling Bottom phase performance file slope 1.0731 offset -6.521					
Tubes No.	Mass of Empty Tubes[g]	Mass Tubes + Bottom[g]	Mass of Bottom [g]	Volume Demanded[µL]	Weight delivered[µg]
1	0.9988	1.203	0.2042	200	204.2
2	1.0054	1.2096	0.2042	200	204.2
3	0.993	1.1962	0.2032	200	203.2
4	0.9988	1.2023	0.2035	200	203.5
5	0.995	1.1992	0.2042	200	204.2
6	0.9932	1.19966	0.20646	200	206.46
7	1.0077	1.212	0.2043	200	204.3
8	0.9959	1.1986	0.2027	200	202.7

Table [16B] Statistical regression analysis for dispensing of bottom phase specific volume [slope 1.0731   offset -6.521

Residuals	Std. Dev.	Mean	CV	RSD %	%Bias Accuracy
-4.2	0.00112	0.2041	0.0055	0.548408	2.1
-4.2					2.1
-3.2					1.6
-3.5					1.75
-4.2					2.1
-6.46					3.23
-4.3					2.15
-2.7					1.35

Table [17A] Dispensing of diluent Top [dil. Top transfer performance file slope 1, offset 0]

Tubes No.	Mass of Empty Tubes[g]	Mass Tubes + dil.Top[g]	Mass of dil.Top [g]	Volume Demanded[µL]	Weight delivered[µg]
	Dil. Top transfer performance file slope 1 offest 0				
1	1.0055	1.0318	0.0263	25	26.3
2	0.994	1.0468	0.0528	50	52.8
3	0.9947	1.0971	0.1024	100	102.4
4	0.9908	1.1441	0.1533	150	153.3
5	0.9995	1.2028	0.2033	200	203.3
6	0.9931	1.248	0.2549	250	254.9
7	0.9945	1.2968	0.3023	300	302.3
8	1.0078	1.3624	0.3546	350	354.6

Table [17B] Statistical regression analysis for dispensing of diluent top [slope 1, offset 0]

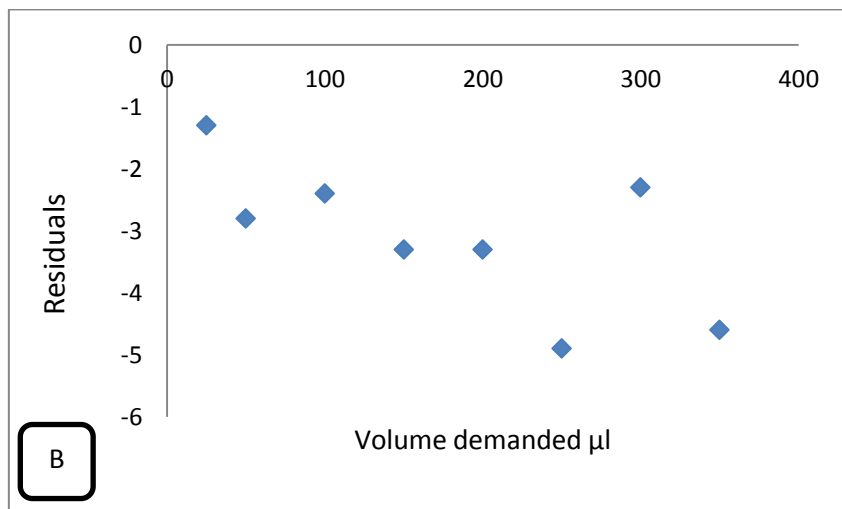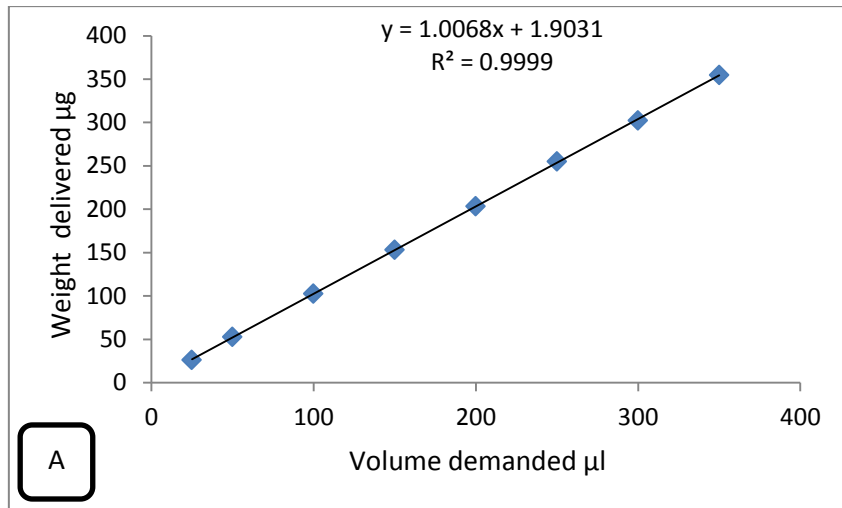| Residuals	Std. Dev.	Mean	CV	RSD %	%Bias Accuracy
-1.3	0.118395	0.181238	0.653258	65.32577	5.2
-2.8					5.6
-2.4					2.4
-3.3					2.2
-3.3					1.65
-4.9					1.96
-2.3					0.77
-4.6					1.31

Figure [17] (A) Regression plot for dispensing diluent top phase Solution (B) Residuals of regression for handling diluent top phase Solution[slope 1, offset 0]

Table [18A] Dispensing of diluent top phase solution [dil. Top transfer performance slope 1.0068 offset 1.9031]

Dil. Top transfer performance file slope 1.0068 offset 1.9031					
Tubes No.	Mass of Empty Tubes[g]	Mass Tubes + dil.Top[g]	Mass of dil.Top [g]	Volume Demanded[μL]	Weight delivered[μg]
1	1.0318	1.0573	0.0255	25	25.5
2	1.0468	1.0961	0.0493	50	49.3
3	1.0971	1.1953	0.0982	100	98.2
4	1.1441	1.2922	0.1481	150	148.1
5	1.2028	1.4017	0.1989	200	198.9
6	1.248	1.4943	0.2463	250	246.3
7	1.2968	1.5931	0.2963	300	296.3
8	1.3624	1.7103	0.3479	350	347.9

Table [18B] Statistical regression analysis for dispensing diluent top phase solution [slope 1.0068 offset 1.9031]

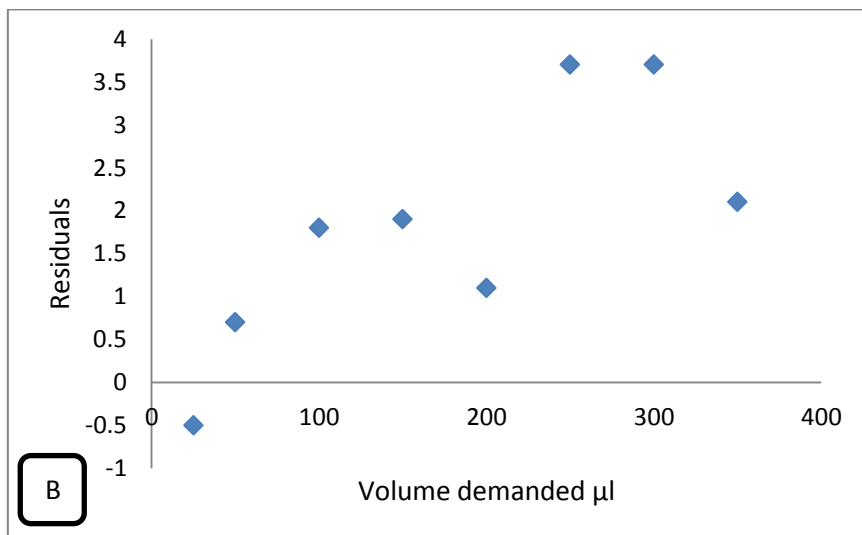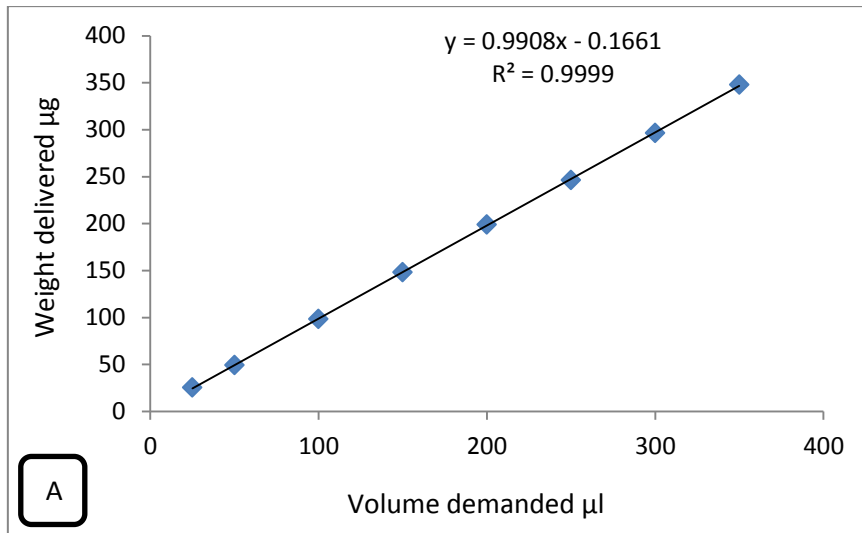| Residuals	Std. Dev.	Mean	CV	RSD %	%Bias Accuracy
-0.5	0.11651	0.176313	0.660814	66.08144	2
0.7					-1.4
1.8					-1.8
1.9					-1.27
1.1					-0.55
3.7					-1.48
3.7					-1.2
2.1					-0.6

Figure [18] (A) Regression plot for dispensing diluent top phase Solution (B) Residuals of regression for handling diluent top phase Solution[slope 1.0068 offset 1.9031]

Table [19A] Dispensing of diluent bottom phase solution [dil. bottom transfer performance file [slope 1 offset 0]

Dil. bottom transfer performance file slope 1 offest 0					
Tubes No.	Mass of Empty Tubes[g]	Mass Tubes + dil.Bottom [g]	Mass of dil.Bottom [g]	Volume Demanded[µL]	Weight delivered[µg]
1	1.0028	1.0279	0.0251	25	25.1
2	0.995	1.0466	0.0516	50	51.6
3	0.9957	1.0902	0.0945	100	94.5
4	0.9989	1.1506	0.1517	150	151.7
5	0.9966	1.1996	0.203	200	203
6	0.9959	1.238	0.2421	250	242.1
7	0.9881	1.2918	0.3037	300	303.7
8	1.0012	1.3443	0.3431	350	343.1

Table [19B] Statistical regression analysis for dispensing diluent bottom phase solution [slope 1 offset 0]

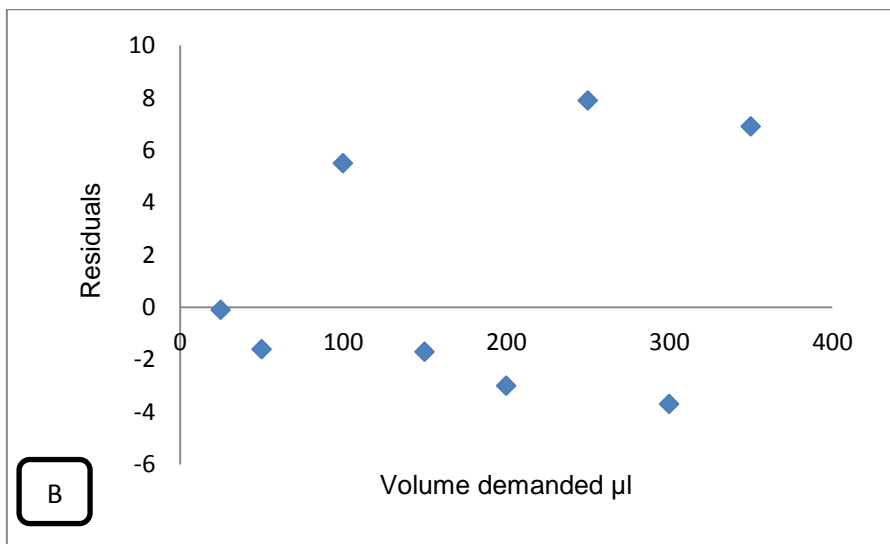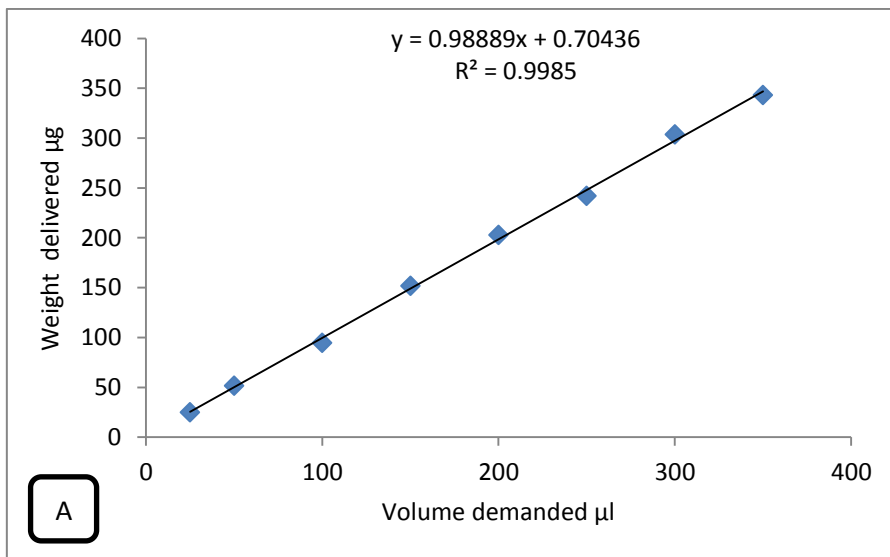| Residuals	Std. Dev.	Mean	CV	RSD %	%Bias Accuracy
-0.1	0.116374	0.17685	0.65804	65.80403	0.4
-1.6					3.2
5.5					-5.5
-1.7					1.13
-3					1.5
7.9					-3.16
-3.7					1.2
6.9					-1.97

Figure [19] (A) Regression plot for dispensing diluent bottom phase Solution (B) Residuals of regression for handling diluent bottom phase Solution [slope 1 offset 0]

Table [20A] Dispensing of diluent bottom phase solution [dil. bottom transfer performance file slope 0.98889, offset 0.70436]

Dil. bottom transfer performance file slope 0.98889 offset 0.70436					
Tubes No.	Mass of Empty Tubes[g]	Mass Tubes + dil.Bottom [g]	Mass of dil.Bottom [g]	Volume Demanded[μL]	Weight delivered[μg]
1	1.0279	1.0526	0.0247	25	24.7
2	1.0466	1.0966	0.05	50	50
3	1.0902	1.1919	0.1017	100	101.7
4	1.1506	1.3043	0.1537	150	153.7
5	1.1996	1.4038	0.2042	200	204.2
6	1.238	1.4932	0.2552	250	255.2
7	1.2918	1.592	0.3002	300	300.2
8	1.3443	1.693	0.3487	350	348.7

Table [20B] Statistical regression analysis for dispensing diluent bottom phase solution [slope 0.98889, offset 0.70436]

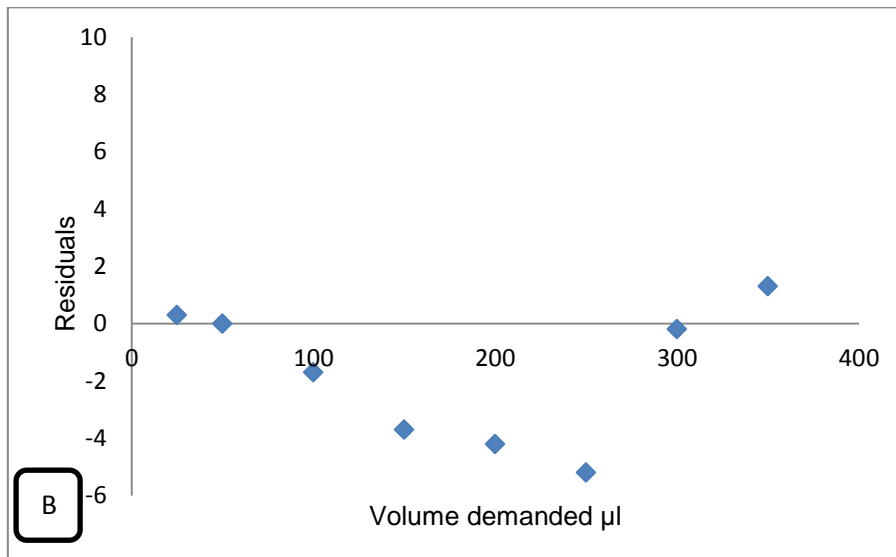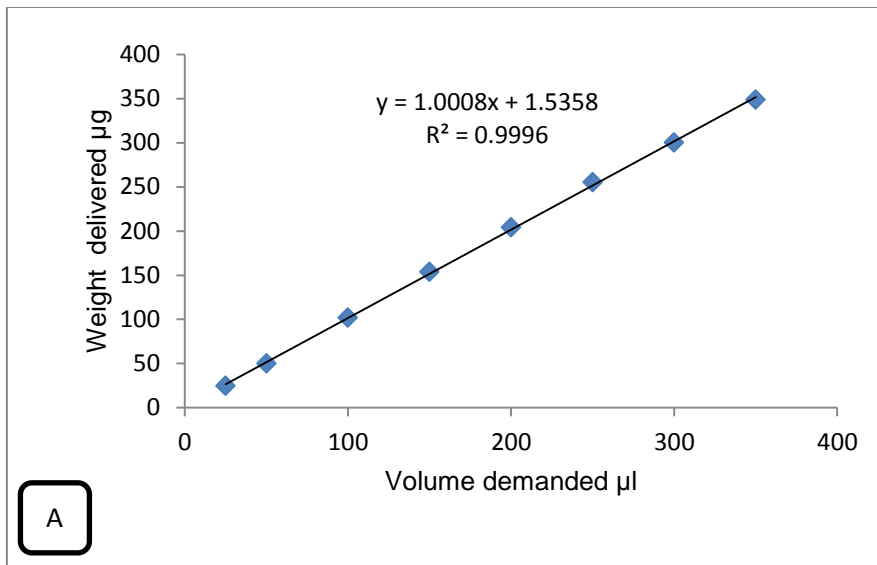| Residuals	Std. Dev.	Mean	CV	RSD %	%Bias Accuracy
0.3	0.11771	0.1798	0.654669	65.46693	-1.2
0					8.5E-14
-1.7					1.7
-3.7					2.467
-4.2					2.1
-5.2					2.08
-0.2					0.067
1.3					-0.37

Figure [20] (A) Regression plot for dispensing diluent bottom phase Solution (B) Residuals of regression for handling diluent bottom phase Solution [slope 0.98889, offset 0.70436]

Table [21A] Dispensing of 200µl bottom phase solution[sampling 200ul bottom performance file [slope 1 offset 0]

Sampling 200ul bottom performance file slope 1 offset 0					
Tubes No.	Mass of Empty Tubes[g]	Mass Tubes +Bottom [g]	Mass of Bottom [g]	Volume Demanded[µL]	Weight delivered[µg]
1	1.0022	1.0546	0.0524	50	52.4
2	0.9948	1.1005	0.1057	100	105.7
3	0.9944	1.1502	0.1558	150	155.8
4	0.9936	1.206	0.2124	200	212.4
5	0.9972	1.2485	0.2513	250	251.3
6	0.987	1.2945	0.3075	300	307.5
7	0.9917	1.3493	0.3576	350	357.6
8	0.9923	1.4111	0.4188	400	418.8

Table [21B] Statistical regression analysis for dispensing200µl bottom phase solution [slope 1 offset 0]

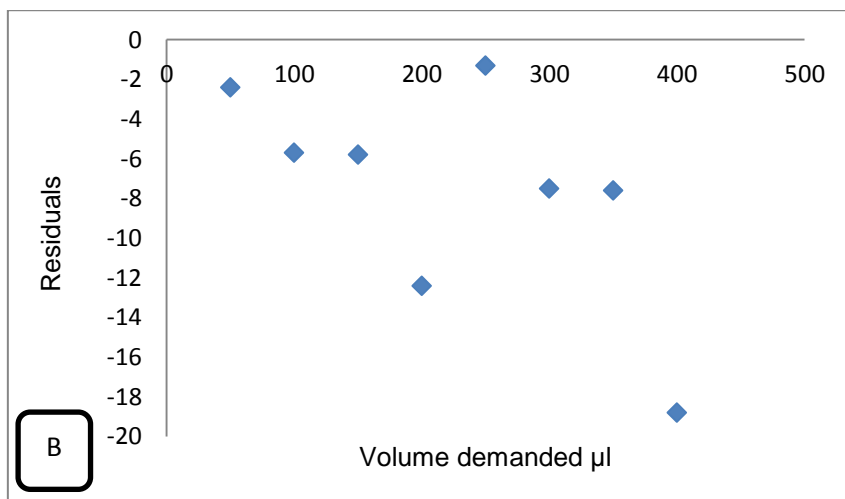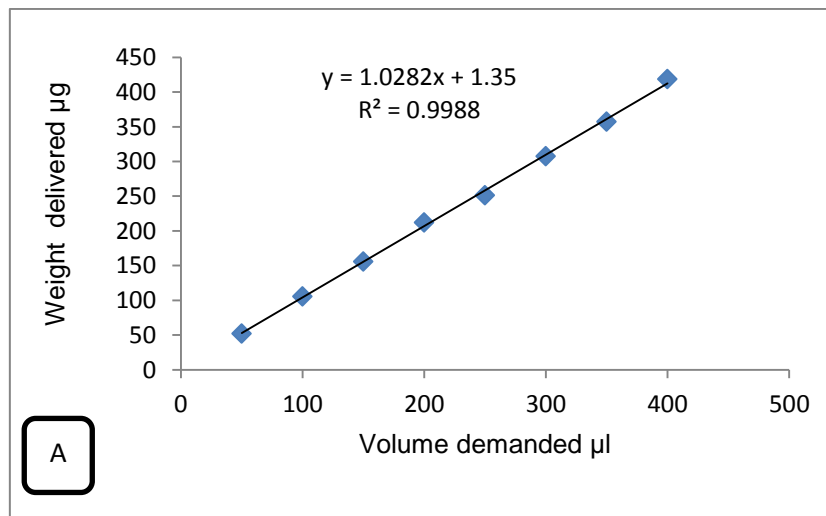| Residuals	Std. Dev.	Mean	CV	RSD %	%Bias Accuracy
-2.4	0.126003	0.232688	0.541511	54.1511	4.8
-5.7					5.7
-5.8					3.87
-12.4					6.2
-1.3					0.52
-7.5					2.5
-7.6					2.17
-18.8					4.7

Figure [21] (A) Regression plot for dispensing 200μl bottom phase Solution (B) Residuals of regression for handling 200μl bottom phase Solution [slope 1 offset 0]

Table [22A] Dispensing of 200µl bottom phase solution [sampling 200ul bottom performance file [slope 1.0282, offset 1.35]

Sampling 200ul bottom performance file		slope 1.0282		offset 1.35	
Tubes No.	Mass of Empty Tubes[g]	Mass Tubes +Bottom [g]	Mass of Bottom [g]	Volume Demanded[µL]	Weight delivered[µg]
1	0.9978	1.1983	0.2005	200	200.5
2	0.9975	1.1996	0.2021	200	202.1
3	0.9936	1.1968	0.2032	200	203.2
4	0.999	1.2002	0.2012	200	201.2
5	0.9956	1.2026	0.207	200	207
6	0.9813	1.1963	0.215	200	215
7	0.9999	1.2037	0.2038	200	203.8
8	0.9969	1.2016	0.2047	200	204.7

Table [22B] Statistical regression analysis for dispensing200µl bottom phase solution [Slope 1.0282, offset 1.35]

Residuals	Std. Dev.	Mean	CV	RSD %	%Bias Accuracy
-0.5	0.004646	0.204688	0.022697	2.269738	0.25
-2.1					1.05
-3.2					1.6
-1.2					0.6
-7					3.5
-15					7.5
-3.8					1.9
-4.7					2.35

Appendix (C)

Specrophotometric Relationships between HSA Ellman's reagent and TNB

$E280hsa := 44.555$ — 1 mMolar extinction coefficient of HSA at A 280 from literature

$E324ell := 17.78$ — 1 mMolar extinction coefficient of Ellman's reagent at A 324 from litera

$E412tnb := 14.150$ — 1 mMolar extinction coefficient of TNB at A 412 from literature

Absorbance at 324nm for Ellman's Standard curve to give concentration of Ellmans

$$A324EllStdCurve := \begin{pmatrix} 0.049 \\ 0.094 \\ 0.131 \\ 0.172 \\ 0.269 \\ 1.305 \\ 2.554 \end{pmatrix}$$

Calculate milli molar concentration of Ellmans from Extinction

$$Ellmmolar := \frac{A324EllStdCurve}{E324ell}$$

$$Ellmmolar = \begin{pmatrix} 2.756 \times 10^{-3} \\ 5.287 \times 10^{-3} \\ 7.368 \times 10^{-3} \\ 9.674 \times 10^{-3} \\ 0.015 \\ 0.073 \\ 0.144 \end{pmatrix}$$

Absorbance at 412 nm for Ellmans Stsndard Curve

$$A412EllStdCurve := \begin{pmatrix} 0.014 \\ 0.014 \\ 0.016 \\ 0.017 \\ 0.017 \\ 0.038 \\ 0.062 \end{pmatrix}$$

Perform regression of A412 on mmolar Ellmans concentration
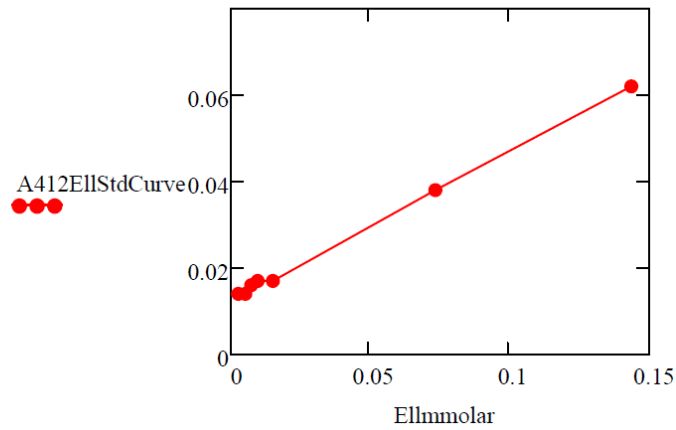
$$\text{Ellregress} := \text{line}(\text{Ellmmolar}, \text{A412EllStdCurve})$$

$$\text{Ellregress} = \begin{pmatrix} 0.013 \\ 0.342 \end{pmatrix}$$

$$\text{R2} := \text{corr}(\text{Ellmmolar}, \text{A412EllStdCurve})^2 \qquad \text{R2} = 0.999$$

Extinction Coefficient for Ellmans at 412 nm

$\text{E412ell} := \text{Ellregress}_1$

$\text{E412ell} = 0.342$

$\text{E280hsa} = 44.555$

$\text{E324ell} = 17.78$

$\text{E412tnb} = 14.15$

Calculate Extinction coefficient for HSA at 324 nm

HSA Absorbance at 280nm of Standard Curve to give HSA concentration

$$\text{A280hsa} := \begin{pmatrix} 0.666 \\ 0.509 \\ 0.337 \\ 0.182 \\ 0 \end{pmatrix}$$

Calculate mmolar concentration of HSA from extinction coefficient

$$\text{HSAmmolar} := \frac{\text{A280hsa}}{\text{E280hsa}}$$

mmol/litre

$$\text{HSAmmolar} = \begin{pmatrix} 0.015 \\ 0.011 \\ 7.564 \times 10^{-3} \\ 4.085 \times 10^{-3} \\ 0 \end{pmatrix}$$

$$\text{hsaconc} := \left(\frac{1}{66500} \right) \cdot 1000$$

$$\text{hsaconc} = 0.015$$

Absorbance of albumin standard curve at 324nm

$$\text{A324hsaStdCurve} := \begin{pmatrix} 0.062 \\ 0.051 \\ 0.037 \\ 0.024 \\ 0 \end{pmatrix}$$
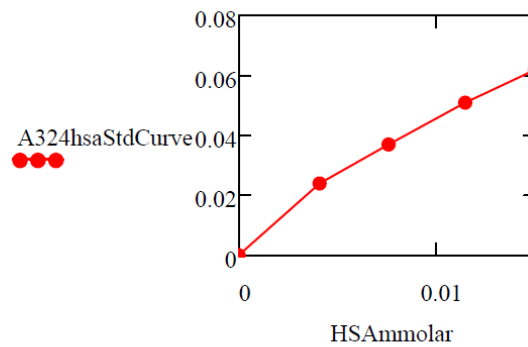
E324hsa extinction coefficient = slope of regression of A324 vs HSA mmolar

$$\text{HSAregress} := \text{line}(\text{HSAmmolar}, \text{A324hsaStdCurve})$$

$$\text{HSAregress} = \begin{pmatrix} 3.877 \times 10^{-3} \\ 4.067 \end{pmatrix}$$

$$\text{R2} := \text{corr}(\text{HSAmmolar}, \text{A324hsaStdCurve})^2 \qquad \text{R2} = 0.983$$

$$\text{E324hsa} := \text{HSAregress}_1$$

Extinction coefficient for HSA at 324 nm

$E324hsa = 4.067$

Calculate Extinction coefficient for HSA at 412 nm

Absorbance of albumin standard curve at 412 nm

$$A412hsaStdCurve := \begin{pmatrix} 0.029 \\ 0.026 \\ 0.019 \\ 0.014 \\ 0 \end{pmatrix}$$

A412hsaStdCurve
●●●
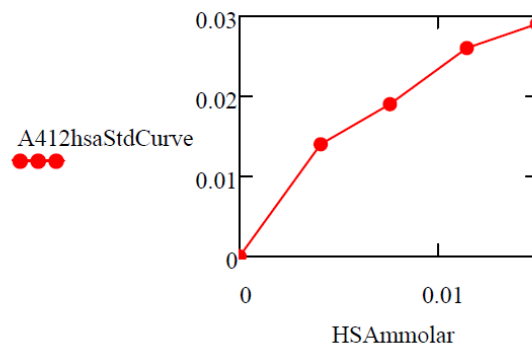
HSAmmolar

E412hsa extinction coefficient = slope of regression of A412 vs HSA mmolar

$$HSAregress412 := line(HSAmmolar, A412hsaStdCurve)$$

$$HSAregress412 = \begin{pmatrix} 3.226 \times 10^{-3} \\ 1.89 \end{pmatrix}$$

$$R2 := corr(HSAmmolar, A412hsaStdCurve)^2 \qquad R2 = 0.944$$

$$E412hsa := HSAregress412_1$$

Extinction coefficient for HSA at 412 nm

$E412hsa = 1.89$

Calculate Extinction coefficient for Ellmans reagent at 280 nm

Absorbance of Ellmans standard curve at 280 nm

$$A280ellStdCurve := \begin{pmatrix} 0.028 \\ 0.051 \\ 0.068 \\ 0.088 \\ 0.135 \\ 0.64 \\ 1.311 \end{pmatrix} \qquad Ellmmolar = \begin{pmatrix} 2.756 \times 10^{-3} \\ 5.287 \times 10^{-3} \\ 7.368 \times 10^{-3} \\ 9.674 \times 10^{-3} \\ 0.015 \\ 0.073 \\ 0.144 \end{pmatrix}$$
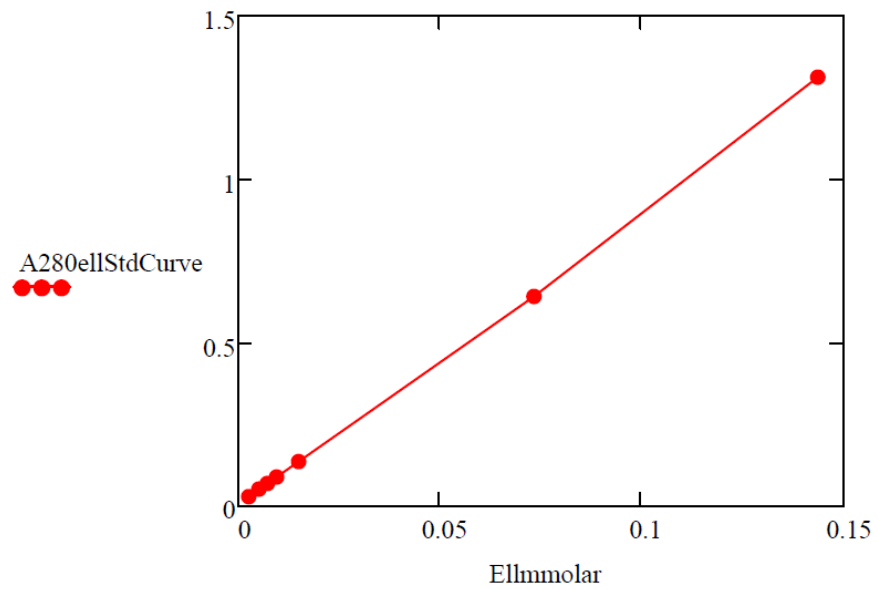
E280ell extinction coefficient = slope of regression of AA280 vs Ellmans mmolar

$$Ellregress280 := line(Ellmmolar, A280ellStdCurve)$$

$$Ellregress280 = \begin{pmatrix} -1.188 \times 10^{-3} \\ 9.055 \end{pmatrix}$$

$$R2 := corr(Ellmmolar, A280ellStdCurve)^2 \qquad R2 = 0.999$$

$$E280ell := Ellregress280_1$$

Extinction coefficient for Ellmans at 280 nm

$$E280ell = 9.055$$

To get the contribution of TNB at 280nm we use the cysteine reaction data where we can calculate the contribution of Ellmans, cysteine to the total absorbance and derive the contribution of TNB by difference. However the contribution of cysteine to the absorbance at 280 nm in a standard curve was effectively zero and has been neglected

thus for the Cys Ellmans experiment

A280 ellmans = concEllmans *E280ell + ConcTNB*E280tnb

$$\text{concEllmans} := \begin{pmatrix} 4.485 \times 10^{-3} \\ 0.014 \\ 0.024 \\ 0.04 \\ 0.056 \\ 0.074 \\ 0.091 \end{pmatrix} \qquad \text{ConcTNB} := \begin{pmatrix} 0.173 \\ 0.154 \\ 0.134 \\ 0.102 \\ 0.07 \\ 0.034 \\ 0 \end{pmatrix}$$

This concentration data is from the Cys Ellmans experiment by Simulataneous equations

$$\overrightarrow{\text{A280ell} := (\text{concEllmans} \cdot \text{E280ell})}$$

from Mix

$$\text{A280ell} = \begin{pmatrix} 0.041 \\ 0.127 \\ 0.217 \\ 0.362 \\ 0.507 \\ 0.67 \\ 0.824 \end{pmatrix} \qquad \text{RealA280} := \begin{pmatrix} 0.501 \\ 0.545 \\ 0.588 \\ 0.652 \\ 0.688 \\ 0.747 \\ 0.84 \end{pmatrix}$$

$$\text{A280tnb} := \text{RealA280} - \text{A280ell}$$

$$\text{A280tnb} = \begin{pmatrix} 0.46 \\ 0.418 \\ 0.371 \\ 0.29 \\ 0.181 \\ 0.077 \\ 0.016 \end{pmatrix}$$
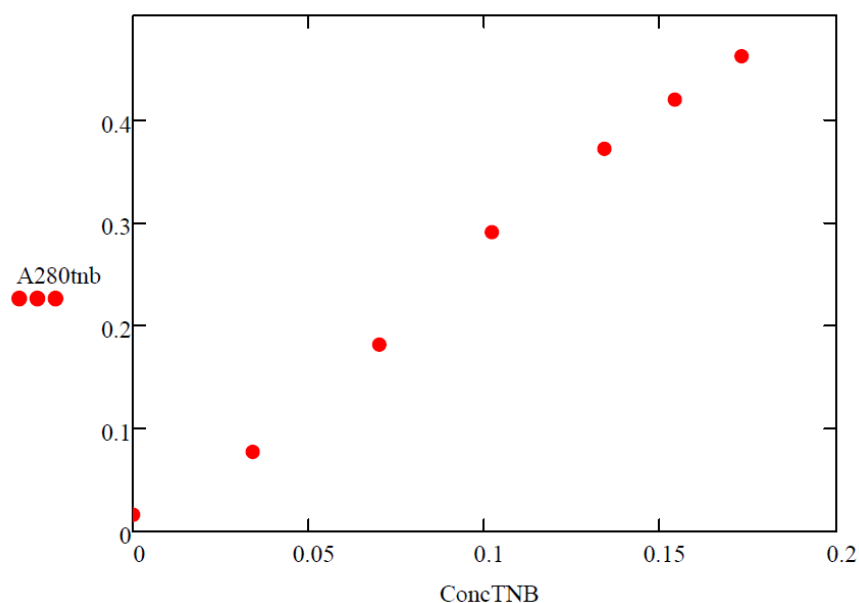
E280tnb extinction coefficient = slope of regression of A280 vs TNB mmolar

$$TNBregress280 := line(ConcTNB, A280tnb)$$

$$TNBregress280 = \begin{pmatrix} 3.115 \times 10^{-3} \\ 2.686 \end{pmatrix}$$

$$R2 := corr(ConcTNB, A280tnb)^2 \qquad\qquad R2 = 0.995$$

$$E280tnb := TNBregress280_1$$

Extinction coefficient for TNB at 280 nm

$$E280tnb = 2.686$$

To get the contribution of TNB at 324nm we use the cysteine reaction data where we can calculate the contribution of Ellmans, cysteine to the total absorbance and derive the contribution of TNB by difference. However the contribution cysteine to the absorbance at 324 nm in a standard curve was effectively zero and has been neglected

thus for the Cys Ellmans experiment

$$A324 = \text{concEllmans} * E324ell + \text{ConcTNB} * E324tnb$$

$$\text{concEllmans} := \begin{pmatrix} 4.485 \times 10^{-3} \\ 0.014 \\ 0.024 \\ 0.04 \\ 0.056 \\ 0.074 \\ 0.091 \end{pmatrix} \qquad \text{ConcTNB} := \begin{pmatrix} 0.173 \\ 0.154 \\ 0.134 \\ 0.102 \\ 0.07 \\ 0.034 \\ 0 \end{pmatrix}$$

This concentration data is from the Cys Ellmans experiment by Simulataneous equations

$$\overrightarrow{A324ell := (\text{concEllmans} \cdot E324ell)}$$

$$A324ell = \begin{pmatrix} 0.08 \\ 0.249 \\ 0.427 \\ 0.711 \\ 0.996 \\ 1.316 \\ 1.618 \end{pmatrix} \qquad \text{RealA324} := \begin{pmatrix} 0.404 \\ 0.602 \\ 0.785 \\ 1.048 \\ 1.227 \\ 1.453 \\ 1.709 \end{pmatrix}$$
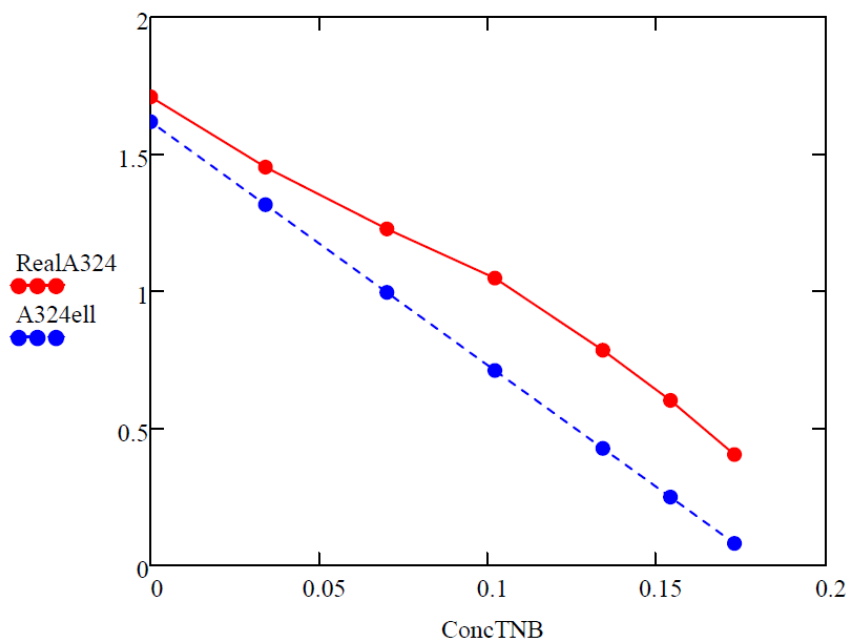
Calculate the regression for Real A324 vs Conc TNB

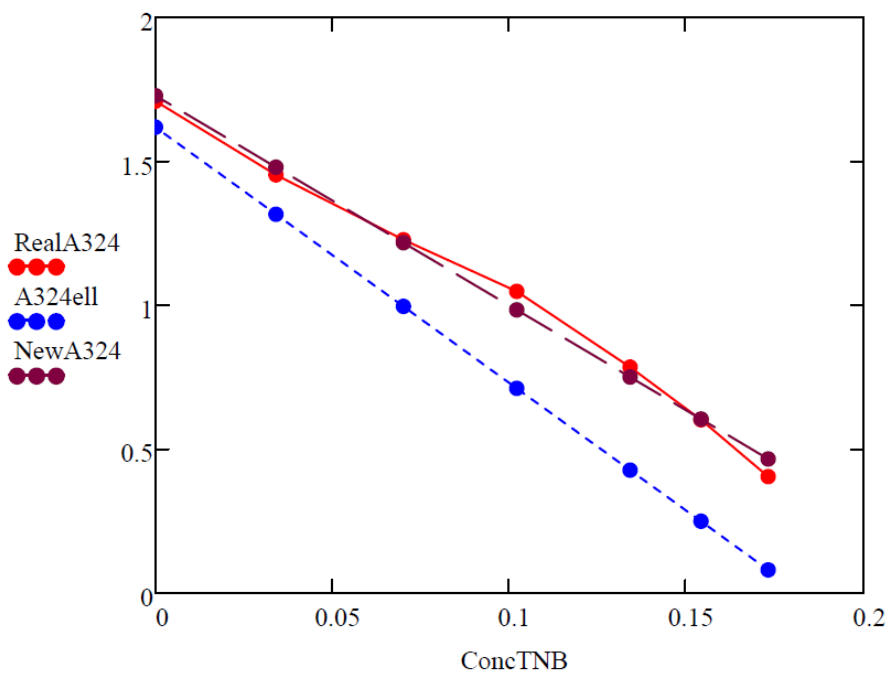Real A324 = a * concTNB + constant

A324tnb = (a * concTNB + constant) - A324ell

$$A324\text{regress} := \text{line}(\text{ConcTNB}, \text{RealA324})$$

$$A324regress = \begin{pmatrix} 1.728 \\ -7.294 \end{pmatrix}$$

$$R2 := \text{corr}(ConcTNB, RealA324)^2 \qquad R2 = 0.992$$

$$NewA324 := A324regress_1 \cdot ConcTNB + A324regress_0$$

$$NewA324 = \begin{pmatrix} 0.466 \\ 0.604 \\ 0.75 \\ 0.984 \\ 1.217 \\ 1.48 \\ 1.728 \end{pmatrix}$$


There is an error in the above determination of A324 since by definition the A324 due to TNB at zero TNB concentration is zero and here there is a constant value

The absorbance of TNB at 324 nm is now the difference between the regression for

336

Ellmans and the regression for Real A324

$$A324tnb := \left(A324regress_1 \cdot ConcTNB + A324regress_0 - A324ell \right)$$

$$A324tnb = \begin{pmatrix} 0.386 \\ 0.355 \\ 0.323 \\ 0.272 \\ 0.221 \\ 0.164 \\ 0.11 \end{pmatrix}$$
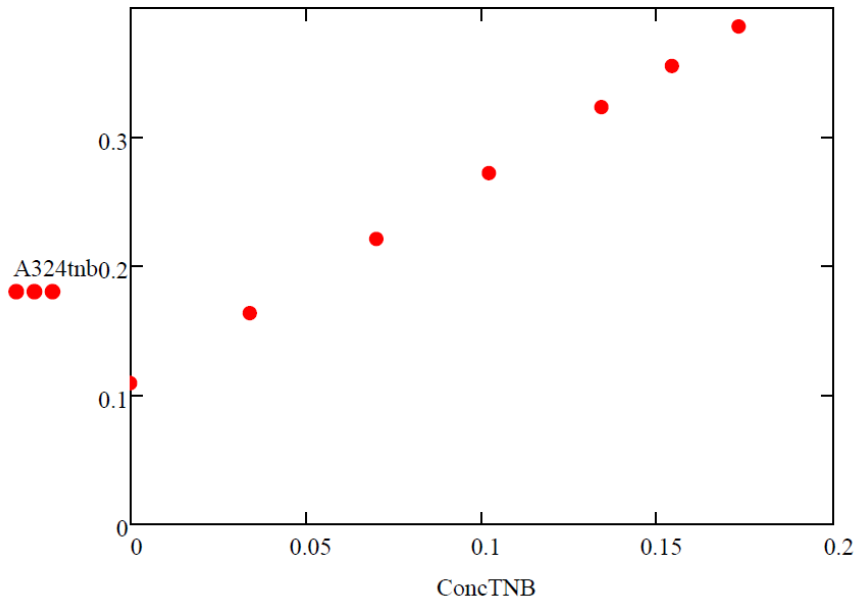
The error in A324 is clear from the above figure

$$TNBregress324 := line(ConcTNB, A324tnb)$$

$$TNBregress324 = \begin{pmatrix} 0.11 \\ 1.597 \end{pmatrix}$$

$$R2 := corr(ConcTNB, A324tnb)^2 \qquad R2 = 1$$

337

E324tnb extinction coefficient = slope of regression of A324 vs TNB mmolar

$E324tnb := TNBregress324_1$

Extinction coefficient for TNB at 324 nm

$E324tnb = 1.597$

The Extinction Coefficients are :-

$E280hsa = 44.555$

$E324ell = 17.78$

$E412tnb = 14.15$

$E412ell = 0.342$

$E324hsa = 4.067$

$E412hsa = 1.89$

$E280ell = 9.055$

$E280tnb = 2.686$ $\qquad E324tnb = 1.597$

A280 = concHSA * E280hsa + concEllmans * E280ell + concTNB * E280tnb

A324 = concHSA * E324hsa + concEllmans * E324ell + concTNB * E324tnb

A412 = concHSA * E412hsa + concEllmans * E412ell + concTNB * E412tnb

Enter the absorbance values below obtained from an experiment involving St. Ellmans or HSA with Ellman's Reagent after subtracting any blank values

Then

Enter initial guess values for the unknown concentrations if necessary. The numerical analysis can be dependent on the initial guess values causing it to fail to converge.

For example if the absorbance of on sample reaction has:

$$A280 = 0.874 \qquad A324 = 1.015 \qquad A412 = 0.042$$

Given

$$\frac{[A280 - (concEll \cdot E280ell + concTNB \cdot E280tnb)]}{E280hsa} = concHSA$$

$$\frac{[A324 - (concHSA \cdot E324hsa + concTNB \cdot E324tnb)]}{E324ell} = concEll$$

$$\frac{[A412 - (concHSA \cdot E412hsa + concEll \cdot E412ell)]}{E412tnb} = concTNB$$

$$vec := Find(concHSA, concEll, concTNB)$$

$$vec_0 = 8.383 \times 10^{-3} \qquad vec_1 = 0.055 \qquad vec_2 = 5.163 \times 10^{-4}$$

$$concHSA := vec_0 \qquad concEll := vec_1 \qquad concTNB := vec_2$$

$A280HSA := concHSA \cdot E280hsa$ $\qquad$ $\boxed{A280HSA = 0.374}$

$A280ELL := concEll \cdot E280ell$ $\qquad$ $\boxed{A280ELL = 0.499}$

$A280TNB := concTNB \cdot E280tnb$ $\qquad$ $\boxed{A280TNB = 1.386 \times 10^{-3}}$

$A280 := concHSA \cdot E280hsa + concEll \cdot E280ell + concTNB \cdot E280tnb$ $\qquad$ $\boxed{A280 = 0.874}$

$A324HSA := concHSA \cdot E324hsa$ $\qquad$ $\boxed{A324HSA = 0.034}$

$A324ELL := concEll \cdot E324ell$ $\qquad$ $\boxed{A324ELL = 0.98}$

$A324TNB := concTNB \cdot E324tnb$ $\qquad$ $\boxed{A324TNB = 8.243 \times 10^{-4}}$

$A324 := concHSA \cdot E324hsa + concEll \cdot E324ell + concTNB \cdot E324tnb$ $\qquad$ $\boxed{A324 = 1.015}$

$A412HSA := concHSA \cdot E412hsa$ $\qquad$ $\boxed{A412HSA = 0.016}$

$A412ELL := concEll \cdot E412ell$ $\qquad$ $\boxed{A412ELL = 0.019}$

$$A412TNB := concTNB \cdot E412tnb$$

$$A412TNB = 7.305 \times 10^{-3}$$

$$A412 := concHSA \cdot E412hsa + concEll \cdot E412ell + concTNB \cdot E412tnb$$

$$A412 = 0.042$$

Component concentrations

mmolar   mg/ml

$$concHSA = 8.383 \times 10^{-3}$$

$$concEll = 0.055$$

$$concTNB = 5.163 \times 10^{-4}$$

$$HSAmgml = 0.557$$

$$Ellmanmgml = 0.022$$

$$TNBmgml = 8.628 \times 10^{-5}$$